# Effects of metal-induced oxidative stress on endothelial cells in vitro

# Auswirkung von Metall induziertem oxidativen Stress auf Endothelzellen in vitro

Dissertation

Zur Erlangung des Grades

Doktor der Naturwissenschaften

Am Fachbereich Biologie

der Johannes Gutenberg-Universität Mainz

Roman Tsaryk

geb. am 09.06.1981 in Lviv

Mainz, 2009

Tag der mündliche Prüfung:12.03.2010

## Contents

## Abbreviations

| | |
|---|---|
| °C | Degree Celcius |
| µg | Microgram |
| µl | Microliter |
| µm | Micrometre |
| 8-oxoG | 8-oxodeoxyguanine |
| A | Adenine |
| ad | Adjust |
| Al | Aluminium |
| AM | Acetoxymethylesther |
| Ang1 | Angiopoietin1 |
| AP-1 | Activator protein-1 |
| APE | AP-endonuclease |
| APS | Ammonium persulfate |
| AP-sites | Apurinic/apyrimidinic sites |
| ARP | Aldehyde Reactive Probe |
| ASPP | Apoptosis stimulating proteins of p53 |
| ASTM | American Society for Testing and Materials |
| ATF2 | Activating transcription factor 2 |
| ATM | Ataxia telangiectasia mutated |
| ATR | Ataxia telangiectasia and Rad3 related |
| BCA | Bicinchoninic acid |
| BER | Base excision repair |
| bFGF | Basic fibroblast growth factor |
| BNip3 | Bcl-2/E1B 19 kDa interacting protein 3 |
| BSA | Bovine serum albumine |
| C | Cytosine |
| ca. | circa |
| $CaCl_2$ | Calcium chloride |
| CBP | CREB binding protein |
| CDK | Cyclin-dependent kinase |
| cDNA | Complementary DNA |
| $CH_3COOH$ | Acetic acid |
| CHK1 | Checkpoint kinase 1 |
| cm | Centimetre |
| Co | Cobalt |
| CO | Carbon monoxide |
| $CO_2$ | Carbon dioxide |
| $CoCl_2$ | Cobalt cloride |
| COX II | Cyclooxygenase II |
| cpTi | Commercially pure titanium |
| Cr | Chromium |
| CREB | cAMP response element-binding protein |

| | |
|---|---|
| CS-buffer | Cytoskeleton buffer |
| Cu | Copper |
| CV | Coefficient of variation |
| DCDHF-DA | 2´,7´-dichlorodihydrofluoresceine-diacetate |
| DMSO | Dimethyl sulfoxide |
| DMTU | Dimethylthiourea |
| DNA | Deoxyribonucleic acid |
| DNAJ | DNAJ homolog |
| dNTP | Deoxynucleotide triphosphate |
| DTT | Dithiothreitol |
| e.g. | Exempli gratia |
| ECM | Extracellular matrix |
| EDTA | Ethylenediamine-N,N,N',N'-tetraacetic acid |
| EGTA | Ethylene glycol-bis(2-aminoethyl ether)-N,N,N',N'-tetraacetic acid |
| EIA | Enzyme immunoassay |
| ELISA | Enzyme-linked immunosorbent assay |
| eNOS | Endothelial NO-synthase |
| ERK2 | Extracellular signal receptor regulated kinase 2 |
| EtOH | Ethanol |
| FBS | Fetal bovine serum |
| FGFRL1 | Fibroblast growth factor receptor like 1 |
| Fig. | Figure |
| FIH | Factor inhibiting HIF |
| G | Guanine |
| GADD45 | Growth Arrest and DNA Damage protein 45 |
| GPX | Glutathione peroxidase |
| GR | Glutathione reductase |
| GRP78 | Glucose-regulated protein 78 |
| GSH | Reduced glutathione |
| GSH-MEE | Reduced glutathione monoethyl ester |
| GST | Glutathione-S-transferase |
| h | Hour |
| $H_2O$ | Water |
| $H_2O_2$ | Hydrogen peroxide |
| $H_2SO_4$ | Sulfuric acid |
| $H_3PO_4$ | ortho-Phosphoric acid |
| HCl | Hydrocloric acid |
| HIF-1α | Hypoxia inducible factor-1α |
| HMDS | Hexamethyldisilizane |
| hMTH1 | human MutT homologue 1 |
| HNE | 4-hydroxy-2-nonenal |
| HO-1 | Heme oxygenase-1 |
| HRP | Horseradish peroxidase |
| HSP | Heat shock protein |

| | |
|---|---|
| i.e. | id est |
| ICAM-1 | Intercellular adhesion molecule-1 |
| Ig | Immunoglobulin |
| IKK | Inhibitor of NF-κB (I-κB) kinase |
| IL | Interleukin |
| IMDM | Iscove's Modified Dulbecco's Medium |
| I-κB | Inhibitor of NF-κB |
| KOH | Potassium hydroxyde |
| l | Liter |
| LDH | Lactate dehydrogenase |
| LPS | Lipopolysaccharide |
| mA | Milliamper |
| MAPK | Mitogen-activated protein kinase |
| mC | Millicoulomb |
| MCP-1 | Monocyte chemoattractant protein-1 |
| MDA | Malondialdehyde |
| MetOH | Methanol |
| $MgCl_2$ | Magnesium chloride |
| min | Minute |
| miRNA | Micro RNA |
| ml | Millilitre |
| mln | Million |
| mln | Million |
| mM | Millimolar |
| mm | Millimetre |
| MMP9 | Matrix metalloproteinase 9 |
| MMS | Methyl methanesulfonate |
| Mn | Manganese |
| mRNA | Messenger RNA |
| MTS | 3-(4,5-dimethylthiazol-2-yl)-5-(3-carboxymethoxyphenyl)-2-(4-sulfophenyl)-2H-tetrazolium |
| N | Normal concentration |
| $Na_2HPO_4$ | Sodium hydrogen phosphate |
| NAC | N-acetyl-L-cysteine |
| NaCl | Sodium chloride |
| NADPH | Nicotinamide adenine dinucleotide phosphate |
| NaOH | Sodium hydroxide |
| Nb | Niobium |
| NF-κB | Nuclear factor kappa-light-chain-enhancer of activated B-cells |
| ng | Nanogram |
| Ni | Nickel |
| nm | Nanometre |
| nM | Nanomolar |
| NO | Nitric oxide |
| NP-40 | Nonidet P-40 |

| | |
|---|---|
| $O_2$ | Oxygen |
| ODDD | Oxygen-dependent degradation domain |
| OGG1 | 8-oxoguanine-DNA glycosylase 1 |
| oPD | o-Phenylenediamine dihydrochloride |
| OPG | Osteoprotegerin |
| PAA | Polyacrylamide |
| PBS | Phosphate buffered saline |
| PCAF | p300/CBP-associated factor |
| PCNA | Proliferating cell nuclear antigen |
| PDGF | Platelet-derived growth factor |
| PDTC | Pyrrolidine dithiocarbamate |
| PECAM-1 | Platelet endothelial cell adhesion molecule-1 |
| PEG | Polyethylenglycol |
| Pen/Strep | Penicillin/streptomycin mix |
| PFA | Paraformaldehyde |
| PGE2 | Prostaglandin E2 |
| PHD | Prolyl hydroxylase domain-containing protein |
| PIPES | Piperazine-N,N'-bis(2-ethanesulfonic acid) |
| pmol | Picomole |
| PMSF | Phenylmethansulfonyl fluoride |
| Polβ | DNA polymerase β |
| Prx | Peroxiredoxin |
| PS | Polystyrene |
| PTP | Protein tyrosine phosphatase |
| pVHL | von Hippel-Landau protein |
| $R_a$ | Arithmetic average of absolute roughness values |
| RANKL | Receptor activator of nuclear factor kappa B ligand |
| Rb | Retinoblastoma protein |
| RCF | Replication factor C |
| RIPA buffer | Radioimmunoprecipitation assay buffer |
| RNA | Ribonucleic acid |
| RPA | Replication protein A |
| rpm | Revolutions per minute |
| $R_{RMS}$ | Root mean squared roughness |
| RT | Room temperature |
| s | Second |
| SDS | Sodium dodecylsulphate |
| SEM | Scanning electron microscopy |
| siRNA | Small interfering RNA |
| SOD | Superoxide dismutase |
| STAT3 | Signal transducer and activator of transcription 3 |
| T | Thymine |
| TBS | Tris buffered saline |
| TE | Tris-EDTA Buffer |

| | |
|---|---|
| TEMED | N,N,N‘,N‘-Tetramethylethylendiamine |
| TGFβ | Transforming growth factor β |
| Ti | Titanium |
| $TiO_2$ | Titanium oxide |
| TNF-α | Tumour necrosis factor-α |
| Tris | Tris-(hydroxymethyl)-aminoethane |
| Trx | Thioredoxin |
| U | Unit |
| uPAR | Urokinase-type plasminogen activator receptor |
| UPR | Unfolded protein response |
| V | Vanadium |
| v/v | Volume per volume |
| VCAM-1 | Vascular cell adhesion molecule-1 |
| VEGF | Vascular endothelial growth factor |
| VEZF1 | Vascular endothelial zinc finger 1 |
| XBP1 | X box binding protein-1 |
| Zn | Zinc |

# 1. Introduction

## 1.1. Metallic materials, implant integration and aseptic loosening of implants

### 1.1.1. Metallic materials for implantation

Metallic biomaterials have been used for many decades in the production of various devices for medical application. Due to their excellent mechanical properties metallic materials are used in orthopaedic prostheses for bone and joint replacement. They are, for instance, utilised in total hip and knee arthroplasty, spine surgery, in craniofacial and maxillofacial treatments and as load bearing parts of bone implants, such as pins and plates, for the fixation of fractured bones. Apart from bone- and joint-related applications dental implants and cardiovascular devices (pacemakers, intra-vascular stents, etc.) are produced from metals and their alloys.

The most common metallic materials used in implantology are stainless steel, CoCr-based alloys, commercially pure Ti (cpTi) and titanium alloys, such as Ti6Al4V, Ti6Al7Nb, Ti5Al2.5Fe and others. In joint replacement metallic materials are used either alone or in combination with other materials, such as ceramics, ultrahigh molecular weight polyethylene, polyurethane, cement etc. Different metals and their alloys are used for different applications based on their properties. While stainless steel and CoCr-based alloys are known for their mechanical strength and stiffness and high wear resistance (Marti 2000), Ti-based alloys usually display higher biocompatibility (Pohler 2000). Other advantages of Ti-containing alloys is their relative lightness (high strength to weight ratio), higher flexibility, fatigue resistance, capacity for joining with bone (osseointegration) and corrosion resistance (Disegi 2000, Long & Rack 1998). The latter is attributed to the fact that the surface of titanium(-alloy) implant is covered with a titanium oxide ($TiO_2$) film which reduces the corrosion potential of the metal (Williams 1981). It is known, however, that Ti-based materials exert a high mechanical friction effect that might lead to rupture or weakening of the $TiO_2$-layer, thus leading to a corrosion processes and the formation of wear debris in such regions. Therefore, the good mechanical properties of metals and their alloys regarding manufacture and stability of metal implants are often overshadowed by the cases of adverse biological reactions that might lead to implant failure and the requirement for revision surgery.

### 1.1.2. Integration of metal implants and the role of endothelial cells

Integration of an implant and a wound healing process in the peri-implant tissue proceeds by means of a number of physiological reactions that can be divided conveniently into three phases – inflammatory, proliferating and remodelling or maturation phase (Gurtner et al 2008, Li et al 2003, Martin & Leibovich 2005, Midwood et al 2004). Immediately after implantation blood coagulation is initiated at the damaged blood vessels, with platelets aggregating in the newly formed fibrin clot. Upon activation platelets release growth factors, such as platelet-derived growth factor (PDGF) and transforming growth factor β (TGFβ), which initiate an inflammatory response in the wound region by attracting inflammatory cells, e.g. neutrophils and monocytes, which differentiate into macrophages at the sites of inflammation (Fig. 1.1) (Werner & Grose 2003). Neutrophils are the first inflammatory cells to appear at the site of wound healing. Their function is mainly to remove cellular debris and to fight infective agents. An important part of their function is mediated by phagocytosis as well as by releasing high amounts of toxic reactive oxygen species (ROS) (Martin & Leibovich 2005). In the later stages of the inflammatory phase macrophages are the most

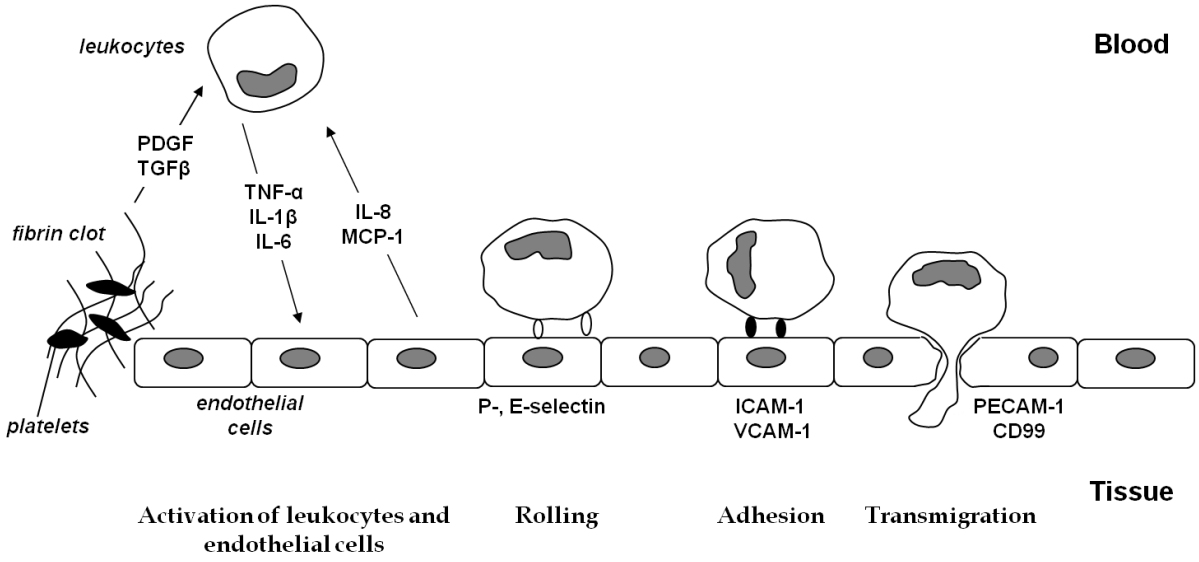


Fig.1.1. *Schematic depicture of the inflammatory phase of wound healing.*

abundant inflammatory cells in the wound region. Macrophages phagocytose damaged cells and extracellular matrix (ECM) debris and are also known to produce ROS. Activated inflammatory cells secrete pro-inflammatory cytokines, such as tumour necrosis factor-α (TNF-α), interleukin-1β (IL-1β), and IL-6, which can attract and activate neutrophils and monocytes, amplifying therefore the inflammatory response (Werner & Grose 2003). At first,

inflammatory cells are attracted from the tissues adjacent to the wound, while later on cell recruitment from blood is the main source of the inflammatory cells (Martin & Leibovich 2005). In the latter process the interaction of leukocytes with endothelial cells lining the vessel walls is decisive. This interaction is mediated by expression of cell adhesion molecules on the surface of endothelial cells that bind to integrins on the surface of leukocytes and can be up-regulated by pro-inflammatory cytokines. The interaction starts with the weak adhesion mediated by P- and E-selectin, called leukocyte rolling, and is followed by firm adhesion mediated, for example, by intercellular adhesion molecule-1 (ICAM-1) and vascular cell adhesion molecule-1 (VCAM-1) on endothelial cells (Ley et al 2007). Transmigration of leukocytes across the endothelial lining proceeds mainly through intercellular contacts of endothelial cells; proteins located at these contacts, such as platelet endothelial cell adhesion molecule-1 (PECAM-1 or CD31) and CD99 are important for this process (Johnson-Leger et al 2000, Peters et al 2003). The migration of leukocytes directly through endothelial cells has also been shown, with ICAM-1 being critical for such extravasation (Millan et al 2006). It is known that pro-inflammatory cytokines can increase permeability of capillaries. This is achieved through reorganisation of the endothelial cell actin cytoskeleton. Under normal conditions actin is concentrated at the edges of endothelial cells in the form of a so-called peripheral actin ring. Upon pro-inflammatory stimulation actin forms stress fibres, which can influence cell shape and intercellular contacts, thus elevating vessel permeability (Fig. 1.2) (Lum & Roebuck 2001). Endothelial cells can also amplify the inflammatory response by

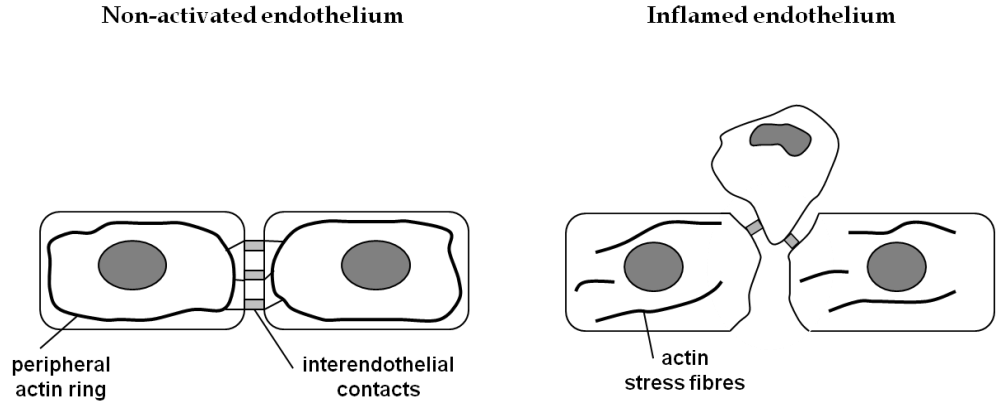


Fig. 1.2. *Cytoskeleton reorganisation in endothelial cells taking place during inflammation and transmigration of leukocytes.*

releasing cytokines, such as IL-8 and monocyte chemoattractant protein-1 (MCP-1), that can induce chemotaxis of neutrophils and monocytes respectively (Peters et al 2003). Expression of cell adhesion molecules and pro-inflammatory cytokines in endothelial cells as well as in

macrophages have been shown to be regulated by the transcription factors NF-κB (nuclear factor kappa-light-chain-enhancer of activated B-cells) and AP-1 (activator protein-1). NF-κB is a family of proteins, consisting of NF-κB1 (p50), NF-κB (p52), RELA (p65), REL and RELB that form dimers and are regulated by eight I-κB (inhibitor of NF-κB) family members (Ghosh & Hayden 2008). Under resting conditions inhibitory proteins I-κB sequester NF-κB in the cytoplasm. Upon inflammatory stimuli I-κB is phosphorylated by IKK (inhibitor of NF-κB (I-κB) kinase) and targeted to proteasomal degradation. NF-κB is released from this complex, translocates to the nuclei and induces gene expression of proteins involved in the inflammatory response (Gilmore 2006). AP-1 is a large family of transcriptional factors consisting of two subfamilies, Jun (c-Jun, JunB and JunD) and Fos (c-Fos, FosB, Fra1 and Fra2). AP-1 is active as a Jun homodimer or more stable Jun/Fos heterodimer (Lum & Roebuck 2001). Jun and Fos proteins can also form heterodimers with cAMP response element-binding protein/activating transcription factor (CREB/ATF) transcription factor family (Lum & Roebuck 2001).

The proliferative phase of wound healing is characterized by the formation of a granulation tissue that consists of inflammatory cells, fibroblasts and newly formed blood vessels. Recruitment of the cells involved in the proliferative phase to the site of wound healing is initiated mostly by growth factors released by activated inflammatory cells. It is known that macrophages are able to secrete PDGF and TGFβ that induce migration and proliferation of fibroblasts at the site of wound healing (Diegelmann & Evans 2004).

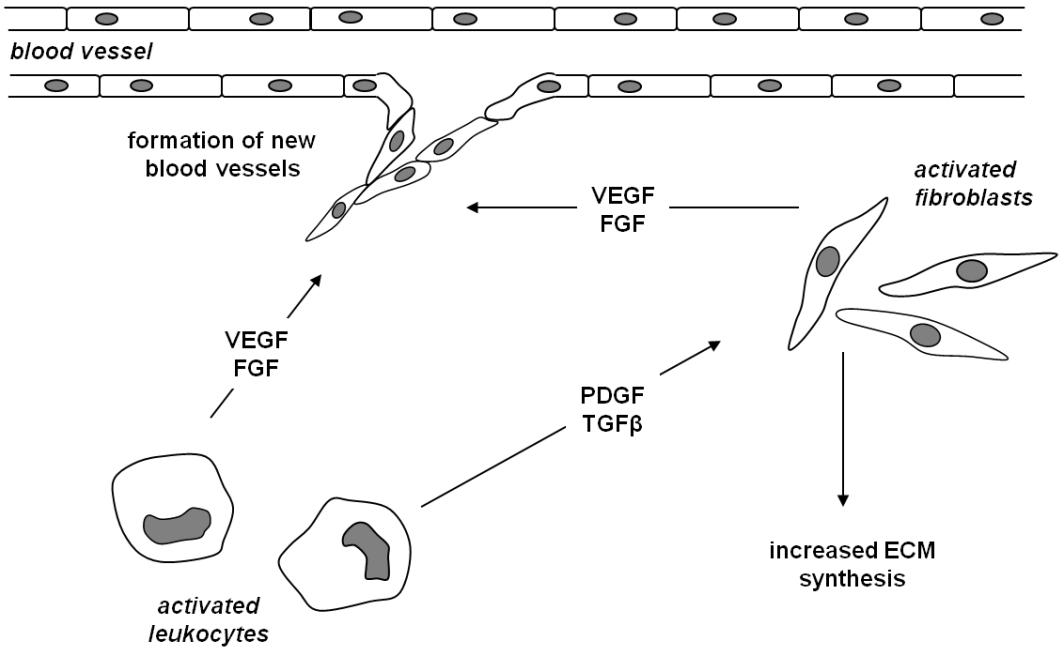


Fig. 1.3. *The main events occurring during the proliferative phase of wound healing.*

Fibroblasts take part in the production of ECM by releasing collagen type III and other ECM proteins (Midwood et al 2004). In addition, the formation of granulation tissue around the implant requires new blood vessels to supply oxygen and nutrients. The process of new blood vessel formation, called angiogenesis, is driven mainly by endothelial cells. Endothelial cells respond to angiogenic growth factors, such as vascular endothelial growth factor (VEGF) and basic fibroblast growth factor (bFGF), which can be released by e.g. macrophages and fibroblasts (Diegelmann & Evans 2004). This response involves increased vessel permeability, migration and elevated proliferation of endothelial cells that contribute to the formation of new blood vessels (Fig. 1.3) (Adams & Alitalo 2007, Li et al 2003). Angiogenesis is also triggered by oxygen deficiency (called hypoxia) in the region of wound healing (Fraisl et al 2009, Li et al 2003), since the expression of VEGF by diverse cell types is induced by hypoxia (Loboda et al 2005, Steinbrech et al 2000, Trompezinski et al 2000). This is mediated by stabilisation and activation of the transcription factor, hypoxia-inducible factor-1α (HIF-1α) (Albina et al 2001). In the final stage of wound healing, called the maturation or remodelling phase, type III collagen is replaced by a stronger type I collagen, other rearrangements of ECM components take place and cell density is decreased by controlled cell death in a process termed apoptosis (Midwood et al 2004) .

### 1.1.3. Aseptic loosening and metal corrosion

Aseptic loosening is one of the main reasons for the failure of orthopaedic implants. In fact, over 25% of all orthopaedic implants show features of aseptic loosening (Wooley & Schwarz 2004). It is characterised by the bone loss (osteolysis) around the prosthesis and appearance of a synovial peri-prosthetic membrane reminiscent of a foreign body reaction, which leads to the implant loosening that often requires revision surgery (Harris et al 1976). The failure of metal implants is attributed mainly to the formation of wear debris and corrosion of the implant materials, though cyclic loading, stress shielding and hydrodynamic pressure around the implant also play their role (Bauer & Schils 1999, Doorn et al 1996, Jacobs et al 1998a, Jacobs et al 2003, Konttinen et al 2005, MacDonald 2004, Sundfeldt et al 2006). As soon as load is applied to metal devices, they are permanently exposed to the action of mechanical forces and chemical attack. Micromotions and the friction between components of the implant and the implant and surrounding tissues are believed to be the main cause of the particulate wear debris generation (Goodman 1994, Jacobs et al 1998a, Sundfeldt et al

2006). The effects of the metal particles can be augmented by polyethylene particles in the case of metal-on-polyethylene implants and cement wear debris, originating from materials used for implant fixation (Bauer & Schils 1999, Sundfeldt et al 2006). Particles can often be detected in the peri-implant tissues as well as in remote locations. CoCr particles can be found in local and distant lymph nodes, bone marrow, liver and spleen of subjects with hip implants with higher particle amounts detected in subjects with loosened implants (Case et al 1994).

Metal degradation products can induce an inflammatory response in the peri-implant regions (Jacobs et al 1998a). This can occur during the initial phase of implant integration but also happens over the lifetime of the implant if wear and corrosion products are continuously developing. Such chronic inflammation may lead to metal surface modifications due to the interactions with soluble mediators, mainly ROS, extensive formation of granulation tissue and fibrous capsule, peri-prosthetic bone resorption due to osteoclast activation by inflammatory stimuli and finally aseptic loosening of the implant. The important role in bone resorption is played by the TNF-related cytokine RANKL (receptor activator of nuclear factor kappa B ligand). Interaction of RANK-positive monocytes with RANKL-positive fibroblasts or osteoblasts is known to lead to the multi-nuclear giant-cell formation and osteoclast differentiation of progenitor macrophages (Konttinen et al 2005). RANKL interaction with its receptor is inhibited by osteoprotegerin (OPG). Endothelial cells are the main producers of OPG, however in case of synovial membrane formation they are located remotely from bone resorption sites, further pointing to the important role of endothelial cells in aseptic loosening (Mandelin et al 2003). TNF-α and IL1β are believed to regulate RANKL system, although the direct influence of metal degradation products on osteoclastogenesis has also been reported. Thus, macrophages that phagocytosed metal and polymer particles where shown to differentiate into osteoclasts capable of bone resorption (Sabokbar et al 1998). Furthermore, metals undergo electrochemical corrosion, which can lead to release of metal ions (Jacobs et al 1998a). Metal particles are also a source of metal ions, therefore amplifying tissue responses to metal degradation products. This response can include local and remote toxicity, induction of chronic inflammation, bone resorption, loosening and failure of implants (Bauer

| **Anodic reaction** | **Cathodic reaction** |
|---|---|
| Metal dissolution<br>$Me \rightarrow Me^{z+} + ze^{-}$ | Hydrogen development (pH<4)<br>$2H_3O^{+} + 2e^{-} \rightarrow H_2 \uparrow + 2H_2O$ |
| Oxide formation<br>$Me^{z+} + 3/2zH_2O \rightarrow MeO_{z/2} + zH_3O^{+}$ | Oxygen reduction (pH>4)<br>$O_2 + 2H_2O + 4e^{-} \rightarrow 4OH^{-}$ |

Fig. 1.4. *Anodic and cathodic half-reactions of corrosion.*

& Schils 1999, MacDonald 2004, Sundfeldt et al 2006). Although considerable information has been collected since the onset of metal implant use, the cellular reactions induced by implant degradation products that can finally lead to implant failure are not yet well studied.

Metal corrosion is an electrochemical process occurring at the interface of metal and its environment. It consists of anodic and cathodic half-reactions (Zumdahl 2007). Two half-reactions are separated spatially. Metal oxidation takes place in the anodic region, and the electrons released in this process flow to the cathodic region, where they take part in the oxygen reduction in aqueous solutions with neutral pH. In acidic pH cathodic half-reaction leads to hydrogen development (Fig. 1.4.). While anodic half-reaction usually takes place at the sites of metal structure irregularities or mechanical damage, cathodic half-reaction can occur almost anywhere due to the conductor properties of metals.

As a result of anodic half-reaction metal ions are released into solution. This process also occurs *in vivo* as increased concentration of metal ions in the serum of patients with metal implants is a well known fact (Hallab et al 2000). In contrast, cathodic partial reaction and the effects of its products on biological processes, are rarely taken into consideration in experimental studies. Importantly, however, cathodic oxygen reduction proceeds through several partial reactions (Bockris et al 1998), resulting in oxygen radicals and hydrogen peroxide as intermediate products as indicated in equations (1 – 4):

$$O_2 + H_2O + e^- \rightarrow HO^{\cdot}_2 + OH^- \quad (1)$$

$$HO^{\cdot}_2 + H_2O \rightarrow H_2O_2 + {}^{\cdot}OH \quad (1a)$$

$${}^{\cdot}OH + e^- \rightarrow OH^- \quad (2)$$

$$H_2O_2 + e^- \rightarrow {}^{\cdot}OH + OH^- \quad (3)$$

$${}^{\cdot}OH + e^- \rightarrow OH^- \quad (4).$$

Formation of ROS and $H_2O_2$ on the metal implant surface during cathodic half-reaction of corrosion may have detrimental effects on surrounding tissues and contribute to the complex processes eventually leading to aseptic loosening.

Formation of metal oxide on the interface of metal with the environment is another important result of anodic half-reaction. This usually terminates the metal corrosion process. Oxide formation is especially important for Ti and Ti-based alloys. Titanium oxide layer (mainly consisting of $TiO_2$) is known to be relatively thick and stable, and this is believed to be the reason for inactivity of Ti-based materials and their biocompatibility. Experimental thickening of $TiO_2$ layer led to the decreased release of Ti ions (Lee et al 2000). However,

disruption of the $TiO_2$ layer immediately renews the corrosion process resulting in further metal ion release and ROS formation. Such $TiO_2$ layer disruption happens when the implant is exposed to friction with other implant parts or surrounding tissues, especially with bone tissue. Metal debris induces abrasive wear, causing further $TiO_2$ layer breakdown on the implant surface amplifying corrosion process (Long & Rack 1998). Although $TiO_2$ is considered to be inactive, ROS and $H_2O_2$, formed in high quantities by activated inflammatory cells, can modify the $TiO_2$-layer, since $H_2O_2$ in a phosphate-buffered solution leads to pronounced thickening of the $TiO_2$-layer (Pan et al 1998). Activated macrophages that produced high levels of ROS accelerated Ti ion release from cpTi, pointing to ROS-induced corrosion (Mu et al 2000). All this indicates the possibility of metal corrosion occurring even on materials considered to be relatively inactive.

## 1.2. Oxidative stress

### 1.2.1. ROS formation and antioxidant defence mechanisms

Molecular oxygen possesses two unpaired electrons with the same spin in the external $\pi^*$ orbital that is responsible for the ease with which $O_2$ forms radicals, or ROS (Galli et al 2005). ROS, such as singlet oxygen ($^1O_2$), hydroxyl radical ($^{\cdot}OH$ ) and superoxide radical ($^{\cdot}O_2$-), are a group of free radicals with high reactivity (D'Autreaux & Toledano 2007). $H_2O_2$ is another non-radical product of incomplete oxygen reduction. ROS and $H_2O_2$ are products of normal cell metabolism and are important for cell signalling but can also be toxic to cells by causing damage to nearly all macromolecules (Dhalla et al 2000). Cells possess enzymatic and non-enzymatic antioxidants involved in ROS elimination (Droge 2002). However, when production of ROS is increased upon certain stimuli, the balance of ROS formation and degradation may be distorted. Such a state is called oxidative stress.

ROS can be formed in the cell as by-products of electron transfer by a chain of cytochromes in mitochondrial respiration; cytochromes of the P450 family, involved in detoxification of various compounds, also produce ROS. Cellular oxidases, such as NADPH oxidase, myeloperoxidase, glucose oxidase, cyclooxygenase and xanthine oxidase are another potent ROS source (Winterbourn 2008). Oxidative stress can result in damage to most biological molecules. Lipid peroxidation is one of the best known markers of oxidative stress (Senderowicz 2003). It is comprised of a set of chain reactions in which lipid peroxyl radicals

are formed from unsaturated fatty acids and induce similar reactions in other fatty acid molecules. Peroxyl radicals can be rearranged via a cyclisation reaction to endoperoxides, which decompose to aldehydes, such as malondialdehyde (MDA) and 4-hydroxy-2-nonenal (HNE) (Davies 2000, Valko et al 2006). Other lipids, such as cholesterol, can also undergo oxidation reactions (Murphy & Johnson 2008). ROS can also oxidise proteins. The changes in amino acid residue side chains caused by ROS can induce conformational changes in protein structure that eventually can lead to loss of activity and protein misfolding (Valko et al 2006). Cells possess the mechanism to cope with unfolded and misfolded proteins called unfolded protein response (UPR) (Schroder & Kaufman 2005). UPR inhibits general translation, but induces gene expression and protein translation of chaperones, such as heat shock proteins (HSP) (Ni & Lee 2007). Although there are reports connecting oxidative stress to UPR (Malhotra et al 2008) the link between those two processes is poorly studied.

Cells possess mechanisms to defend themselves against ROS. Natural compounds present in the cell, such as vitamin E, vitamin C, carotenoids, polyphenols, bioflavonoids, selenium, copper, zinc and manganese, can function as non-enzymatic antioxidants (Droge 2002). On the other hand, antioxidant enzymes catalyse highly specific reactions which detoxify ROS and organic peroxides (Fig. 1.5). These include antioxidant enzymes, such as superoxide dismutase (SOD), catalase and glutathione peroxidise (GPX), which determine the response of cells to oxidative stress (Cai 2005). Two isoforms of SOD, cytosolic and nuclear (in endothelial cells) Cu/Zn-SOD (SOD1) and mitochondrial Mn-SOD (SOD2) catalyse the dismutation of superoxide radicals into $H_2O_2$ and $O_2$ by successive oxidation and reduction of the transition metal ion in the active site (equation 5) (Harris 1992). Interestingly, $^{\cdot}O_2^-$ can interact with nitric oxide (NO), forming another highly reactive compound peroxinitrite ($ONOO^-$) (Valko et al 2006). $H_2O_2$ can be degraded by both catalase and GPX. Catalase is a heme-containing enzyme that catalyses hydrolysis of $H_2O_2$ (equation 6); it is localised in peroxisomes and protects cells from $H_2O_2$ formed during β-oxidation of long-chain fatty acids (Davies 2000). GPX, which is mostly a cytosolic enzyme, can catalytically reduce $H_2O_2$ (equation 7) as well as lipid peroxides (equation 8) (Veal et al 2007). GPX requires glutathione (γ-glutamyl-cysteinyl-glycine, GSH) for these reactions. GSH, in turn, can react with $H_2O_2$ directly or through GPX-catalysed reaction. As a result, two GSH molecules are oxidised to form GSSH, which is then reduced by NADPH-dependent glutathione reductase (GR) (Wu et al 2004). GSH is also involved in the reactions catalysed by glutathione-S-transferases (GST), which conjugate GSH to various cellular metabolites and xenobiotics that are eventually converted to mercapturic acids for excretion (Jefferies et al 2003).

$$2^{\cdot}O_2^- + 2H^+ \rightarrow H_2O_2 + O_2 \quad (5)$$

$$2H_2O_2 \rightarrow 2\,H_2O + O_2 \quad (6)$$

$$H_2O_2 + 2GSH \rightarrow 2H_2O + GSSG \quad (7)$$

$$ROOH + 2GSH \rightarrow ROH + H_2O + GSSH \quad (8)$$

In the presence of heavy metal ions $H_2O_2$ can be converted into highly toxic $^{\cdot}OH$ via the Fenton (equation 9) and Haber-Weiss reactions (equations 10-11).

$$Me^{n+} + H_2O_2 \rightarrow Me^{(n+1)+} + {}^{\cdot}OH + OH^- \quad (9)$$

$$^{\cdot}O_2^- + H_2O_2 \rightarrow O_2 + {}^{\cdot}OH + OH^- \quad (10)$$

$$Me^{(n+1)+} + {}^{\cdot}O_2^- \rightarrow Me^{n+} + O_2 \quad (11)$$

Peroxiredoxins (Prx) form another family of proteins (consisting of six members in mammalian cells) capable of reducing $H_2O_2$ and alkylhydroperoxides with the use of thioredoxin (Trx). Prx exist as homodimers with one cysteine residue per active centre. Upon interaction with $H_2O_2$ cysteine sulfenic acid (Cys-SOH) is formed in the active site of one subunit, which subsequently forms disulfide bond with an additional cysteine residue of another subunit. The disulfide bond is then reduced by Trx, a protein that has two cysteine groups that form disulfide bonds upon oxidation. Trx, in turn, is reduced by the NADPH-

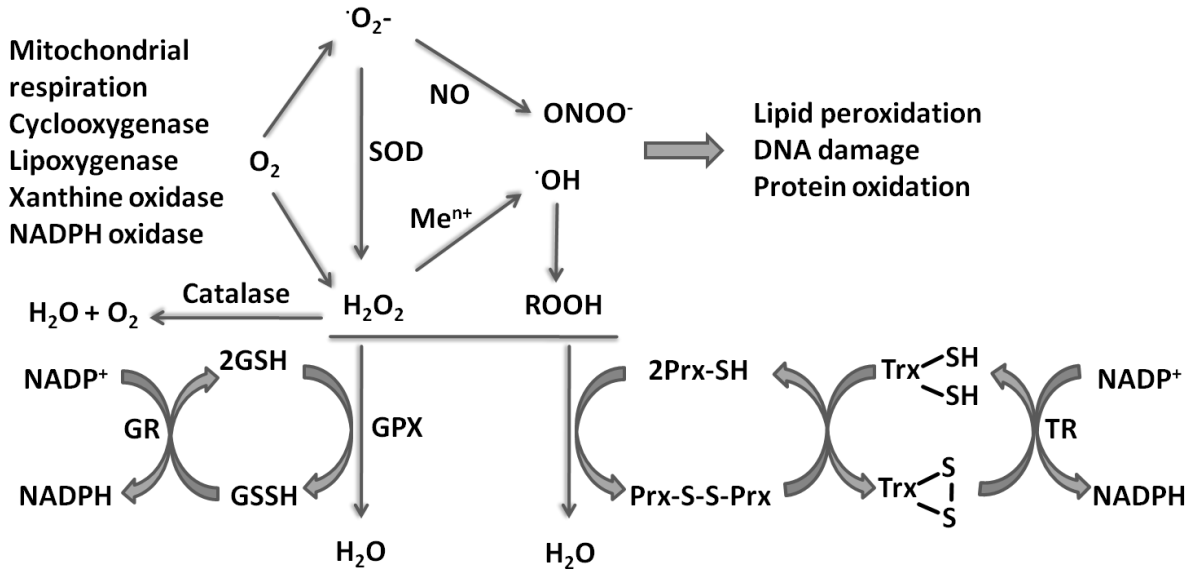


Fig. 1.5. *ROS formation and degradation pathways.*

dependent enzyme thioredoxin reductase (Forman & Torres 2002, Holmgren 1995, Rhee et al 2003).

Physiological concentrations of ROS are involved in cell signalling. Among others, insulin, VEGF, PDGF, TNF-α-induced signalling are ROS-dependent (Finkel 2003, Rhee et al 2003). Protein tyrosine phosphatases (PTP) have been shown to be one of the specific targets of ROS in cell signalling; their activity is reduced upon ROS oxidation of cysteine residues essential for PTP catalysis and can be restored by cellular thiols. PTP activity regulate, in turn, the signalling cascades induced by receptor tyrosine kinases (Forman & Torres 2002, Lee et al 1998).

ROS play an important role in endothelial cell functions. Vascular NADPH oxidase and endothelial NO-synthase (eNOS) are the important sources of ROS in endothelial cells. ROS can regulate among others inflammatory and angiogenic responses of endothelial cells, thus contributing to wound healing (Lum & Roebuck 2001, Ushio-Fukai & Alexander 2004). Oxidative stress has also been shown to be involved in the pathogenesis of cardiovascular diseases, such as atherosclerosis, hypertension, ischemia-reperfusion injury (Dhalla et al 2000).

### 1.2.2. Oxidative DNA damage and repair

ROS can induce the formation of different types of DNA damage, such as single- and double-strand breaks, purine, pyrimidine, or deoxyribose modifications, and DNA cross-links (Valko et al 2006). Lipid peroxidation products are also known to form DNA adducts (Blair 2008). More than 20 different types of DNA damage of aminobases induced by oxidative stress were detected. One of the main base modifications induced by ROS is 8-hydroxyguanine, which through keto-enol tautomerism can exist in the form of 8-oxoguanine (8-oxoG, Fig. 1.6). This DNA lesion is mutagenic and cancerogenic because it can pair with adenine apart from cytosine. It occurs even in normal cells at a frequency of approximately one in $10^5$ guanine residues. This modification can also occur in guanosine and such nucleotides can be incorporated by DNA polymerases into the nascent DNA strand opposite to adenine in the template strand (David et al 2007, Mitra et al 2001). The main ROS-induced modification of pyrimidines is thymine glycol. Apart from base modifications ROS can induce the formation of DNA single strand breaks and apurinic/apyrimidinic (AP) sites, areas in DNA that lack aminobase residues. All these lesions are repaired predominantly by the base excision repair pathway (BER, Fig. 1.7). BER is initiated by a spontaneous base loss or by DNA glycosylases. Each of 12 known DNA glycosylases is specific for a particular type of

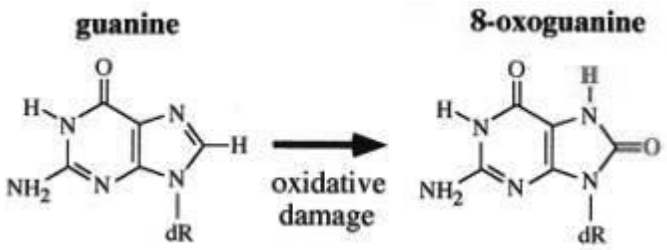


Fig. 1.6. *8-oxoguanine structure.*

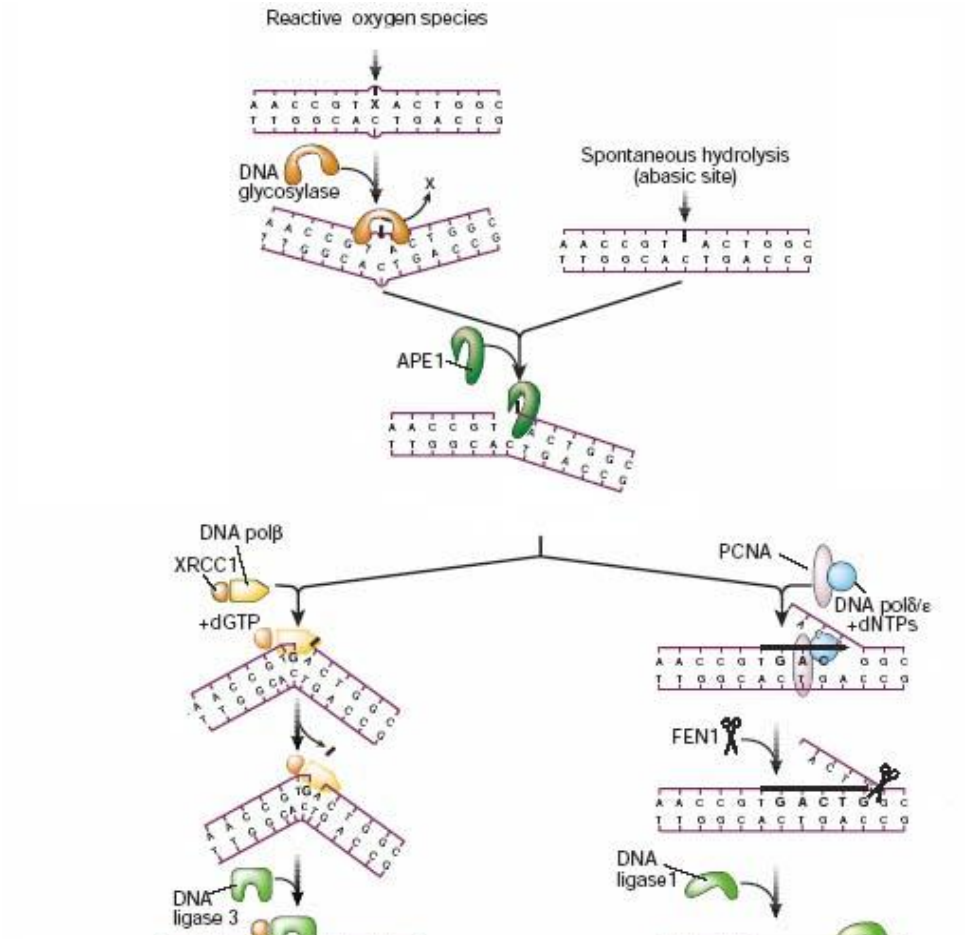


Fig. 1.7. *Schematic depicture of base excision DNA repair pathway.*

base modification. These enzymes are either monofunctional, removing the modified base only and leaving the resulting AP site intact, or bifunctional, possessing additional lyase activity that cleaves DNA 3' of the AP site. In the case of monofunctional DNA glycosylases AP sites are subsequently cleaved by AP-endonuclease (APE). 8-oxoguanine-DNA glycosylases (OGG), the enzymes responsible for the removal of 8-oxoG, are examples of bifunctional DNA glycosylases (Slupphaug et al 2003). Two distinct glycosylases exist,

OGG1 and OGG2. The first one is responsible for the removal of 8-oxoG induced by ROS in DNA. The second enzyme removes 8-oxoG incorporated into DNA opposite adenine from the 8-oxoGTP. 8-oxoGTP can be removed from the nucleotide pool by the enzyme human MutT homologue 1 (hMTH1) (Fujikawa et al 1999).

Depending on the size of the gap formed after base removal (which is determined by the nature of the DNA glycosylase as well as other factors) (Hazra et al 1998) repair proceeds through short-patch (1 nucleotide gap) or long-patch BER (10-12 nucleotides gap) (Christmann et al 2003). Most of 8-oxoG lesions are removed by short-patch repair, but some (up to 25%) are repaired by long-patch BER (Dianov et al 1998). 8-oxoG has also been shown to be removed by a combination of short- and long-patch repair (Hashimoto et al 2004). Briefly, in short-patch BER DNA polymerase β (Polβ) removes 5'-deoxyribose-5-phosphate formed after AP site cleavage (lyase activity) and inserts a new nucleotide (polymerase activity) (Sobol et al 1996, Sobol et al 2000), which is ligated by DNA ligase III–XRCC1 complex. In long-patch repair Polβ dissociates after incorporation of the first nucleotide and DNA polymerase ε or δ in complex with PCNA (proliferating cell nuclear antigen) and RFC (replication factor C) further incorporate new nucleotides (Stucki et al 1998) with simultaneous displacement of damaged DNA strand (so called "flap"). This nucleotide overhang is cleaved by Fen1, which is activated by PCNA (Dianova et al 2001). PCNA is also required for the activity of ligase I that ligates newly synthesised oligonucleotide with DNA strand finishing, therefore, long patch BER (Tomkinson et al 2001).

### 1.2.3. p53 pathway and cell cycle regulation

Many types of DNA damage are known to cause activation of the transcriptional factor, p53. However, the direct connection between oxidative DNA damage and p53 induction has not yet been established. As a result of p53 activation growth arrest or apoptosis is induced in the cells.

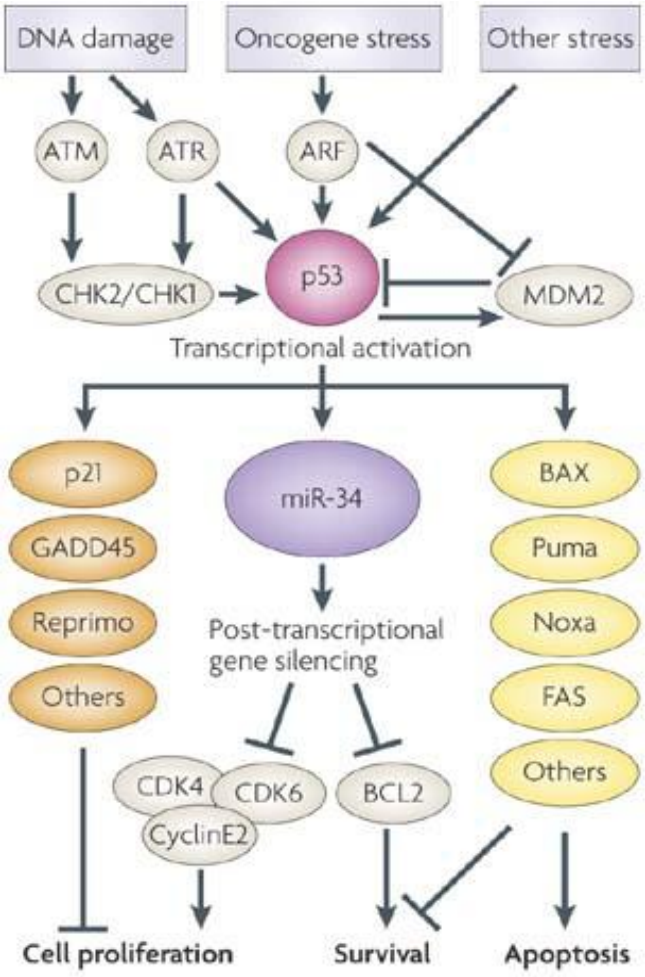


Fig. 1.8. *p53 activation and regulation of transcription (from (He et al 2007b)).*

p53 is regulated on multiple levels, including post-translational modifications, protein localisation, interaction with numerous cofactors and other mechanisms. Post-translational modifications of p53 including phosphorylation, acetylation, ubiquitination, methylation, glycosylation and ribosylation to name a few (Kruse & Gu 2008) together with the proteins that interact with p53 form a large network of p53 regulation.

Under normal conditions p53 is regulated through its interaction partner MDM2, an E3 ubiquitin ligase that together with p300 "transcriptional co-activator" mediates ubiquitination and proteasomal degradation of p53. MDM2 binding additionally blocks the interaction of p53 with transcriptional machinery and also promotes its translocation to the cytoplasm (Riley et al 2008). MDM2 is also a transcriptional target of p53, thus two proteins form an autoregulation loop (Fig. 1.8). This regulation loop is a common target for many stressors that induce p53. MDM2-related protein MDM4 has also been shown to bind to p53

and inhibit its transactivation activity by limiting the access to transcriptional coactivators. Unlike MDM2, MDM4 does not possess ubiquitin-ligase activity and its transcription is not regulated by p53 (Toledo & Wahl 2006). In response to oncogenes p14-ARF (alternative reading frame product of p16-INK4A) can activate p53 via binding and inhibiting MDM2 by antagonising its ubiquitination activity (Sherr 2006).

In response to DNA damage p53 stabilisation occurs via inhibition of its degradation by MDM2. This process is mediated by multi-site phosphorylation of both p53 and MDM2. DNA damage induces phosphorylation of Ser15 performed by two damage-sensitive kinases, ATM (ataxia telangiectasia mutated) and ATR (ataxia telangiectasia and Rad3 related) as well as by checkpoint kinases 1 and 2 (Chk1 and 2) (Cimprich & Cortez 2008, Lavin 2008). This primary phosphorylation event is believed to prime a series of other post-translational modifications (Saito et al 2003). Different posttranslational modifications of p53 are believed to be induced in response to different stressors and even to different levels of stress (Appella & Anderson 2001). ATM can also phosphorylate MDM2 blocking therefore its p53 nuclear export activity. p53 nuclear export is also inhibited by phosphorylation of p53 itself. p53 phosphorylation induces not only p53 stabilisation but also stimulates the recruitment of transcriptional factors p300, CBP (CREB binding protein) and PCAF(p300/CBP-associated factor), which all possess histone acetyltransferase activity. These factors stimulate transcription from p53-responsive promoters; they also acetylate a cluster of C-terminus lysines in p53 that normally target p53 for ubiquitination (Riley et al 2008).

Cell cycle progression is driven by activation and inactivation of cyclin dependent kinases (CDK) that trigger the transition to the next phase of the cycle. CDK is a class of small serine/threonine kinases that require interaction with a cyclin subunit for their activation. Cell cycle is tightly controlled through cyclin expression and destruction, phosphorylation and dephosphorylation of CDKs and expression and degradation of inhibitory proteins. Different cyclins (belonging to the A, B, D and E types), CDKs (interphase CDK 2, 4 and 6 and mitotic CDK1) and CDK inhibitors (belonging to two families: CIP/KIP family (p21, p27 and p57) and INK4A family (p15, p16, p18, p19)) are responsible for the regulation of different stages of the cell cycle (Malumbres & Barbacid 2009) (Fig. 1.9). Rb (retinoblastoma) protein plays a central role in cell cycle regulation by sequestering E2F transcriptional factors, thus preventing it from activation of proliferation-related genes. Upon Rb phosphorylation by the complex of CDK4 or 6 with cyclin D in the G1 phase and by CDK2/cyclin E in G1/S transition phase Rb becomes inactive, E2F are released and activate transcription of the genes necessary for the transition to S phase of cell

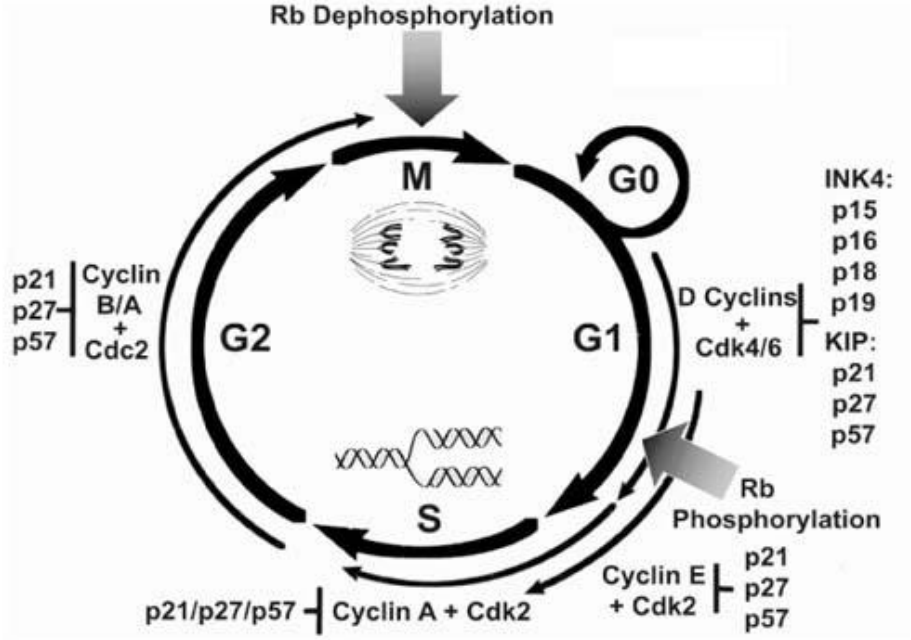


Fig. 1.8. *Cell cycle regulation (from(Donovan & Slingerland 2000)).*

cycle (Frolov & Dyson 2004, Polager & Ginsberg 2008, Senderowicz 2003). E2F also up-regulate the expression of cyclins and CDK inhibitors forming, therefore, several positive and negative feedback loops of cell cycle regulation.

p53 can induce cell cycle block by up-regulating among others CDK2 and 4 inhibitor p21, inducing therefore G1 arrest, and GADD45, which is responsible for G2/M block (Mak & Kultz 2004). p53 has also been shown to induce the specific down-regulation of CDK4 and Cyclin E2 (Spurgers et al 2006). Apart of genes coding the proteins involved in cell cycle arrest, p53 has recently been shown to induce the expression of the genes coding a family of miRNAs, miR-34a-c, that down-regulate a programme of genes promoting cell cycle progression (He et al 2007a).

The induction of apoptosis by p53 is mediated by up-regulation of apoptosis-related genes, such as Puma, Noxa, Bax, Fas and others. The decision whether cells undergo apoptosis or growth arrest is often cell type and DNA damage-specific (MacCallum et al 1996, Murray-Zmijewski et al 2008). It is believed that p53 can differentially transactivate promoters of the genes required for growth arrest or apoptosis. Few models have been proposed to explain this selectivity. The first model proposes that p53 can discriminate between high-affinity binding sites in promoters of growth arrest genes (p21, GADD45, MDM2) and low-affinity p53 binding sites in promoters of apoptosis genes (BAX) (Meek 2004, Weinberg et al 2005). Another model suggests that basal levels of p53 bind upstream of

promoter regions of p53-responsive genes and mediate the assembly of the RNA polymerase II initiation complex. Upon DNA damage the paused RNA polymerase II complex enters the elongation stage of transcription. The model assumes that the level of bound initiation complexes is higher in the genes required for growth arrest than in apoptosis genes, therefore allowing growth arrest upon small changes in p53 activity and requiring higher p53 activation for the induction of apoptosis (Espinosa et al 2003). The transactivation capacity of p53 can also be influenced by the structure of p53 response elements in gene promoters (Jegga et al 2008). p53 cofactors, such as ASPP (apoptosis stimulating proteins of p53) family have been shown to interact with p53 and enhance p53-dependent apoptosis by stimulating the binding of p53 to promoters of apoptotic genes (Samuels-Lev et al 2001).

### 1.3. HIF-1 pathway

HIF-1 is a family of transcription factors that are able to sense $O_2$ concentration and induce the expression of the genes required by the cell to cope with the lack of $O_2$. HIF-1 consists of two subunits, $O_2$-regulated HIF-1α and constitutively expressed HIF-1β. Two others isoforms of $O_2$–regulated subunit are known, HIF-2α and HIF-3α. HIF-1 activation includes HIF-1α stabilisation, nuclear translocation, heterodimerisation with HIF-1β, transcriptional activation and interaction with other proteins (Weidemann & Johnson 2008). A number of steps in this process are regulated by $O_2$ concentration.

Under conditions of normal oxygenation HIF-1α is very unstable due to the permanent targeting to proteasomal degradation. This process is mediated by ubiquitination in the oxygen-dependent degradation domain (ODDD) in HIF-1α by pVHL (von Hippel-Landau protein) that is a component of an ubiquitin E3 ligase complex that targets HIF-1α to proteolysis by the ubiquitin-proteasome pathway (Fig. 1.9). The complex also contains other proteins, such as elongin B, elongin C, Rbx1 and Cul2. It has been shown that two proline residues (Pro402 and Pro546) in the ODDD trigger pVHL binding to HIF-1α and, therefore, its degradation (Ivan et al 2001, Jaakkola et al 2001). A group of prolyl hydroxylase domain-containing proteins (PHD1-3) has been described to be responsible for hydroxylation of these proline residues (Epstein et al 2001). PHDs require iron, ascorbate, 2-oxoglutarate and, importantly, $O_2$ for their catalysis (Berra et al 2006). Different PHDs show different specificity and reaction rate of hydroxylation of above mentioned proline residues (Huang et al 2002). PHD activity is tightly regulated by $O_2$ concentration. Upon a drop in $O_2$ amount PHDs are inactivated, pVHL cannot bind to HIF-1α, which results in HIF-1α stabilisation.

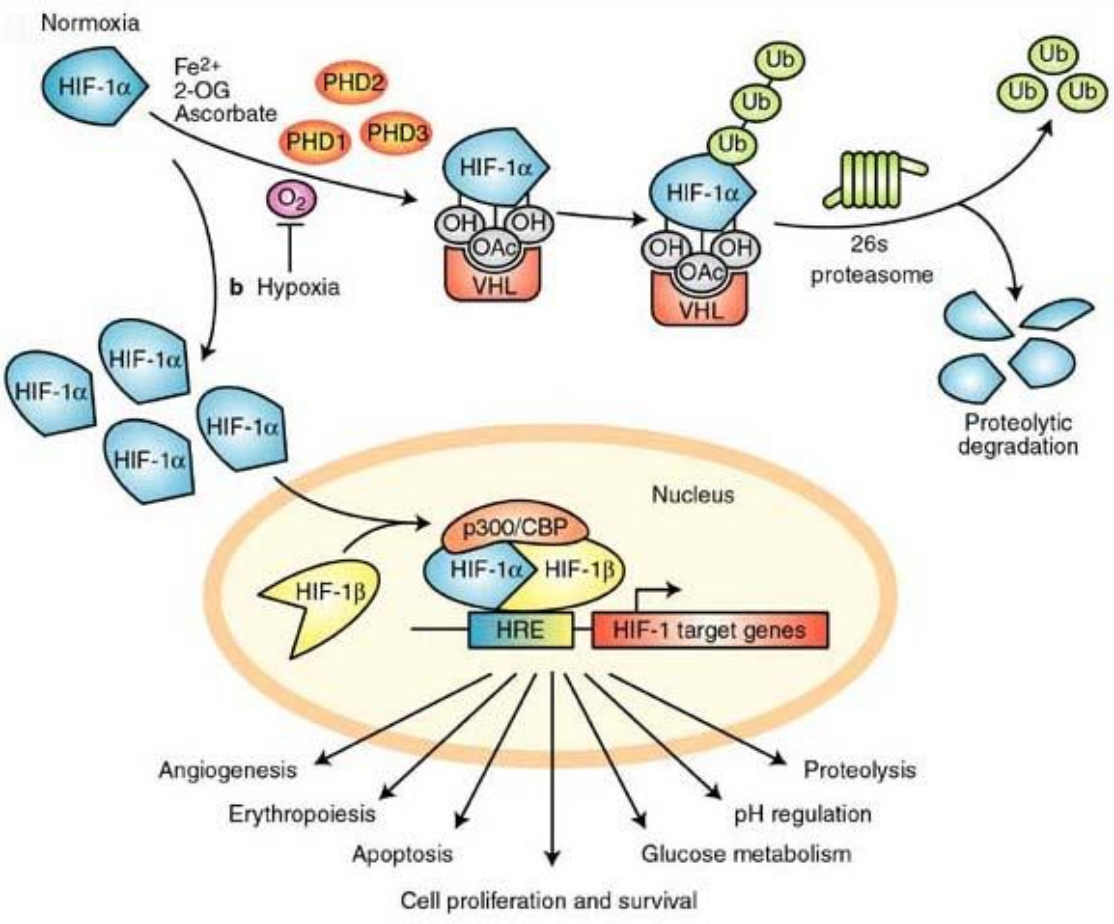


Fig. 1.9. *HIF-1α pathway (from(Carroll & Ashcroft 2005)).*

PHDs can also be degraded via ubiquitination performed by E3 ubiquitin ligases Siah 1 and 2, which are transcriptionally up-regulated by hypoxia, providing another way of oxygen-dependent HIF-1α stabilisation (Berra et al 2006). Interestingly, ROS are also believed to inhibit PHD activity via depletion of the $Fe^{2+}$ pool (Gerald et al 2004). Importantly, HIF-1 induces the expression of PHDs, thus forming an autoregulation mechanism. In addition to PHDs HIF-1α can be hydroxylated at Asn803 within the transactivation domain by factor inhibiting HIF (FIH), which is also oxygen-dependent dioxygenase. This hydroxylation inhibits HIF-1 binding to p300/CBP that are essential coactivators of HIF-induced transcription (Weidemann & Johnson 2008). FIH remains active at lower $O_2$ concentrations than PHD and might suppress the activity of HIF-1α protein that escaped degradation in mild hypoxia (Kaelin & Ratcliffe 2008).

HIF-1 up-regulates the expression of more than 70 genes, including genes involved in development and function of the vascular system, erythropoiesis, energy metabolism, pH regulation, cell proliferation and migration (Weidemann & Johnson 2008). Importantly, different HIF-α isoforms can have different transcriptional targets (Patel & Simon 2008).

Among the genes involved in cellular metabolism HIF-1α induces the expression of glucose transporters, the enzymes of glyconeogenesis, anaerobic glycolysis as well as mitochondrial respiration. HIF-1α is also able to induce the genes important for angiogenesis, such as VEGF, PDGF and matrix metabolism enzymes, such as urokinase-type plasminogen activator receptor (uPAR) (Weidemann & Johnson 2008). Cobalt ions have been shown to activate HIF-1α. As $Co^{2+}$ and other metal degradation products are known to influence angiogenesis HIF-1α-dependence of $Co^{2+}$ effects are of relevance for diverse biological reactions to metal implants.

## 1.4. Aim of the study

The involvement of endothelial cells in inflammation and angiogenesis makes them important for the integration of metal implants. Metal degradation products can, however, influence these processes, possibly leading to ineffective wound healing, prolonged inflammation and eventually aseptic loosening of implant. Different metal degradation processes have been shown to lead to ROS formation. Oxidative stress, therefore, can mediate the reactions of the human body to the implant. While the response of endothelial cells to oxidative stress has been well studied, the effects of ROS produced as the result of metal degradation have not been addressed as yet. Therefore, in this study the reactions of endothelial cells to the products of cathodic (on Ti6Al4V alloy) and anodic half-reaction ($Co^{2+}$) was investigated. The following aspects of such responses were examined:

- To simulate inflammation- and corrosion-induced oxidative stress $H_2O_2$ was applied to endothelial cells grown on Ti6Al4V alloy and on cell culture polystyrene (PS) as a control and the response of endothelial cells to oxidative and inflammatory stimuli (TNF-α and LPS) was compared on both materials.
- The effect of cathodic half-reaction of corrosion induced directly on Ti6Al4V alloy by electrochemical polarisation was investigated.
- The changes induced in endothelial cells by the growth on Co28Cr6Mo alloy were assessed and the effect of $TiO_2$-coating on biocompatibility of the alloy was investigated.
- $Co^{2+}$-induced oxidative stress and oxidative DNA damage were studied in endothelial cells and HIF-1α-dependent changes in gene expression induced by $Co^{2+}$ were compared to the response of endothelial cells to anoxia.

# 2. Materials and methods

## 2.1. Materials

### 2.1.1. Chemicals

| Name | Supplier |
|---|---|
| 1-Butanol | Merck, Darmstadt |
| 2-Propanol | Fluka, Basel |
| 40% Acrylamide/Bisacrylamide solution, 19:1 | Bio-Rad, Hercules |
| Acetone | Sigma-Aldrich, St. Luis |
| AlexaFluor 594 phalloidin | Invitrogen, Carlsbad |
| APS | Bio-Rad, Hercules |
| bFGF | Sigma-Aldrich, St. Luis |
| Blocking reagent | Roche, Freiburg |
| BSA | Sigma-Aldrich, St. Luis |
| $CaCl_2 \times 2H_2O$ | Merck, Darmstadt |
| Calcein AM | Invitrogen, Carlsbad |
| $CH_3COOH$ | Merck, Darmstadt |
| Citric acid | Sigma-Aldrich, St. Luis |
| $CoCl_2 \times 6H_2O$ | Sigma-Aldrich, St. Luis |
| Collagen type I | ICN Biomedicals, Eschwege |
| Coomasie Blue G250 | Sigma-Aldrich, St. Luis |
| Crystal violet | Merck, Darmstadt |
| DCDHF-DA | Alexis Biochemicals, Lörrach |
| Deoxycholic acid | Sigma-Aldrich, St. Luis |
| Dispase | Gibco, Carlsbad |
| DMSO | Sigma-Aldrich, St. Luis |
| DMTU | Sigma-Aldrich, St. Luis |
| DNA BER Pathway Inhibitor | Calbiochem, Darmstadt |
| dNTP Mix | Qiagen, Hilden |
| DTT | ICN Biomedicals, Eschwege |
| Dynabeads CD31 | Dynal, Hamburg |
| ECL Western Blotting Detection Reagents | Amersham Pharmacia Biotech, Freiburg |
| EDTA | Sigma-Aldrich, St. Luis |
| EDTA 0.5 M | Sigma-Aldrich, St. Luis |
| EGTA | Sigma-Aldrich, St. Luis |
| Endothelial Cell Basal Medium MV | PromoCell, Heidelberg |
| EtOH | AppliChem, Darmstadt |
| FBS | Perbio, Bonn |
| FBS | Sigma-Aldrich, St. Luis |
| Fibrinogen | Fluka, Basel |
| Fibronectin | Roche, Freiburg |
| Formalin | Sigma-Aldrich, St. Luis |

| | |
|---|---|
| Gelatine | Sigma-Aldrich, St. Luis |
| GenCarrier-1 Cell Transfection Reagent | Epoch Biolabs, Sugar Land |
| Glutaraldehyde | Serva, Heidelberg |
| Glycerol | Sigma-Aldrich, St. Luis |
| Glycine | Roth, Karlsruhe |
| GSH-MEE | Calbiochem, Darmstadt |
| GST | Sigma-Aldrich, St. Luis |
| $H_2O$ | Braun, Meslingen |
| $H_2O_2$ | Merck, Darmstadt |
| $H_2SO_4$ | Merck, Darmstadt |
| $H_3PO_4$ | Merck, Darmstadt |
| $H_3PO_4$ | Sigma-Aldrich, St. Luis |
| HCl | Merck, Darmstadt |
| HMDS | Merck, Darmstadt |
| Hoechst 33342 | Sigma-Aldrich, St. Luis |
| IMDM | Gibco, Carlsbad |
| Isopropanol | Fluka, Basel |
| KCl | Calbiochem, Darmstadt |
| KOH | Merck, Darmstadt |
| L-glutathione reduced | Sigma-Aldrich, St. Luis |
| LPS | Sigma-Aldrich, St. Luis |
| MetOH | VWR, Darmstadt |
| $MgCl_2 \times 6H_2O$ | Merck, Darmstadt |
| milk | AppliChem, Darmstadt |
| MMS | Acros Organics, Geel |
| Monochlorobimane | Fluka, Basel |
| MTS | Promega, Madison |
| $Na_2HPO_4$ | Roth, Karlsruhe |
| NaCl | Roth, Karlsruhe |
| NaOH | Roth, Karlsruhe |
| *n*-butanol | Fluka, Basel |
| Nonfat dried milk powder | AppliChem, Darmstadt |
| Normal goat serum | Vector, Burlingame |
| NP-40 | Sigma-Aldrich, St. Luis |
| o-Phenylenediamine dihydrochloride tablet | Sigma-Aldrich, St. Luis |
| Osmium tetroxyde | Sigma-Aldrich, St. Luis |
| PBS | Gibco, Carlsbad |
| PBS powder | AppliChem, Darmstadt |
| PBS tablets | Sigma-Aldrich, St. Luis |
| PEG | Sigma-Aldrich, St. Luis |
| Penicillin/streptomycin mix | Gibco, Carlsbad |
| PFA | Merck, Darmstadt |
| PIPES | Sigma-Aldrich, St. Luis |
| PMSF | Sigma-Aldrich, St. Luis |
| Ponceau S solution | Sigma-Aldrich, St. Luis |

| | |
|---|---|
| Power SYBR Green | Applied Biosystems, Foster City |
| Precision Plus Protein Standards Dual Colour | Bio-Rad, Hercules |
| Precision Plus Protein Standards Western C | Bio-Rad, Hercules |
| Precision StrepTactin-HRP Conjugate | Bio-Rad, Hercules |
| Protease Inhibitors Cocktail | Sigma-Aldrich, St. Luis |
| Proteinase K | Sigma-Aldrich, St. Luis |
| Random Primer, $d(N)_9$ | New England Biolabs, Frankfurt am Main |
| RNaseA | Roche, Freiburg |
| RNAse-Free Dnase | Qiagen, Hilden |
| RotiLoad-1 loading buffer | Roth, Karlsruhe |
| SDS | Serva, Heidelberg |
| Sodium cacodylate | Merck, Darmstadt |
| Sodium deoxycholate | Sigma-Aldrich, St. Luis |
| Sodium heparin | Sigma-Aldrich, St. Luis |
| Streptavidin HRP | R&D Systems, Wiesbaden |
| Streptavidin-biotinylated HRP complex | Amersham Pharmacia Biotech, Freiburg |
| Substrate Reagents | R&D Systems, Wiesbaden |
| Sucrose | Serva, Heidelberg |
| Supplement Mix | PromoCell, Heidelberg |
| TEMED | Bio-Rad, Hercules |
| Tetrabutoxytitanate | Fluka, Basel |
| Thrombin | Sigma-Aldrich, St. Luis |
| TNF-α | Sigma-Aldrich, St. Luis |
| Tris | Roth, Karlsruhe |
| Tris-HCl 1M | Sigma-Aldrich, St. Luis |
| Triton X-100 | Sigma-Aldrich, St. Luis |
| Trypsin | Gibco, Carlsbad |
| Trypsin-EDTA | Gibco, Carlsbad |
| Tween 20 | Serva, Heidelberg |
| VEGF | Biomol, Hamburg |
| Versene | Gibco, Carlsbad |
| β-Mercaptoethanol | Sigma-Aldrich, St. Luis |

### 2.1.2. Buffers

| | |
|---|---|
| **Cacodylate/HCl Buffer** | 150 mM NaCacodylate |
| | 1 mM $CaCl_2$ |
| | 0.5 mM $MgCl_2$ |
| | pH 7.2 |

| | |
|---|---|
| **CS Buffer** | 0.1 M PIPES |
| | 1 mM EGTA |
| | 4% PEG |
| | pH 7.2 |

| | |
|---|---|
| **TE Buffer** | 100 mM Tris/HCl pH 8.0 |
| | 10 mM EDTA pH 8.0 |

| | | |
|---|---|---|
| **SDS-Stacking gel** | $H_2O$ | 3.3 ml |
| | 1 M Tris-HCl pH 6.8 | 0.57 ml |
| | 20% SDS | 22.5 µl |
| | Acrylamide/Bisacrylamide | 0.57 ml |
| | TEMED | 4.5 µl |
| | 10% APS | 45 µl |

| | | | | |
|---|---|---|---|---|
| **SDS-Resolving gel** | | **12.5%** | **10%** | **7.50%** |
| | $H_2O$ | 5.1 ml | 5.7 ml | 6.5 ml |
| | 1.5 M Tris-HCl pH 8.8 | 3 ml | | |
| | 20% SDS | 60 µl | | |
| | Acrylamide/Bisacrylamide | 3.6 ml | 3 ml | 2.3 ml |
| | TEMED | 6 µl | | |
| | 10% APS | 60 µl | | |

| | |
|---|---|
| **Laemmli Stock for PAGE** | 30 g Tris |
| | 144 g Glycine |
| | adjust to 1 l with $H_2O$ |

| | |
|---|---|
| **PAGE Running buffer** | 200 ml Laemmli Stock |
| | 5 ml 20% SDS |
| | adjust to 1 l with $H_2O$ |

| | |
|---|---|
| **PAGE Transfer buffer** | 100 ml Laemmli Stock |
| | 250 ml MetOH |
| | adjust to 1 l with $H_2O$ |

| | |
|---|---|
| **10× NaCitrate Buffer pH 5.0** | 1 M Citric acid |
| | 2 M $Na_2HPO_4$ |

| | |
|---|---|
| **Bradford Reagent** | 50mg Coomasie Blue G250 |
| | 25 ml EtOH |
| | 50 ml $H_3PO_4$ |
| | adjust to 500ml with $H_2O$ |
| | filter |

| | |
|---|---|
| **RIPA buffer** | 50mM Tris-HCl pH 7.4 |

| | |
|---|---|
| | 150 mM NaCl |
| | 1 mM EDTA |
| | 1% Sodium deoxycholate |
| | 0.1% SDS |
| | 1% Triton X-100 |
| | 1mM PMSF |

| | |
|---|---|
| **Nuclear extraction buffer** | 10 mM Tris-HCl pH7.4 |
| | 10 mM NaCl |
| | 3 mM $MgCl_2$ |
| | 0.5 mM PMSF |
| | 2 mM DTT |

| | |
|---|---|
| **Sonication buffer** | 20 mM Tris-HCl pH 8.5 |
| | 1 mM EDTA |
| | 1 mM β-mercaptoethanol |
| | 5% glycerine |
| | 0.5 mM PMSF |
| | 1 mM DTT |

### 2.1.3. Instruments

| Instrument | Model | Supplier |
|---|---|---|
| Analytical balance | A120S | Sartorius, Goettingen |
| Balance | LC420 | Sartorius, Goettingen |
| Camera | DC 300 F | Leica, Wetzlar |
| CASY cell counter | TTC | Innovatis, Reutlingen |
| Centrifuge | Megafuge 1.0 | Kendro, Langenselbold |
| $CO_2$ incubator | $CO_2$-Auto-Zero | Heraeus, Hanau |
| $CO_2$/$O_2$ incubator | 3141 | Thermo Fisher Scientific, Bonn |
| Confocal microscope | DM RE | Leica, Wetzlar |
| Cooling centrifuge | 5403 | Eppendorf, Hamburg |
| Deep freezer | Hera freeze | Heraeus, Hanau |
| Electrophoresis and transfer apparatus | Mini-PROTEAN | Bio-Rad, Hercules |
| Fluorescent microplate reader | GENios Plus | TECAN, Crailsheim |
| Fluorescent microscope | DM RX | Leica, Wetzlar |
| Freezing container | Cryo 1°C | Nalgene, Rochester |
| Heating block | Dri-Block DB-20 | Techne, Burlington |
| Heating block | Thermomixer 5436 | Eppendorf, Hamburg |
| Inverted fluorescent microscope | DM IRBE | Leica, Wetzlar |

| | | |
|---|---|---|
| Inverted microscope | DM IRB | Leica, Wetzlar |
| Laminar Flow | HB2448 | Heraeus, Hanau |
| Liquid nitrogen tank | MVE Cryosystem 6000 | German-Cryo, Jüchen |
| Magnet | MPC-1 | Dynal, Hamburg |
| Magnetic stirrer | IKAMAG RET-GS | IKA-Werke, Staufen |
| Microcentrifuge | SD | Roth, Karlsruhe |
| Microcentrifuge | Biofuge Pico | Heraeus, Hanau |
| Microplate reader | Multiscan Plus MK II | Titerscan, Huntsville |
| Multichannel Potentiostat | VMP | Perkin Elmer, Waltham |
| NanoDrop | ND-1000 | NanoDrop, Wilmington |
| pH meter | InoLab 730 | WTW, Weilheim |
| Plate centrifuge | Biofuge Stratos | Heraeus, Hanau |
| Power supply | PowerPac HC | Bio-Rad, Hercules |
| Real Time PCR Cycler | 7300 | Applied Biosystems, Foster City |
| Roll-mixer | Assistent RM5 | Assistent, Sondheim |
| Scanning electron microscope | DSM 962 | Zeiss, Oberkochen |
| Shaker | Reax3 | Heidolph, Schwabach |
| Shaker with regulated temperature | Unimax 1010 with Incubator 1000 | Heidolph, Schwabach |
| Sonicator | Sonopuls | Bandelin, Berlin |
| Ultrasound water bath | Sonorex TK52 | Bandelin, Berlin |
| Vacuum pump | Vacusafe Comfort | Integra Biosciences, Fernwald |
| Vortex | | VWR International, Darmstadt |
| Water bath | SW-20C | Julabo, Seelbach |

### 2.1.4. Consumables

| **Consumable** | **Supplier** |
|---|---|
| 1,5 ml, 2 ml tubes | Eppendorf, Hamburg |
| 10 $cm^2$, 25 $cm^2$, 75 $cm^2$ cell culture flasks | TPP, Trasadingen |
| 12-well cell culture plates | Greiner bio-one, Kremsmünster |
| 15 ml, 50 ml tubes | BD Falcon, San Jose |
| 60 µ-Dish cell culture dishes | ibidi, Martinsried |
| 96, 24, 6-well cell culture plates | TPP, Trasadingen |
| 96-well cell culture plates | Nunc, Roskilde |
| Adhesive seal applicator | Applied Biosystems, Foster City |
| Anaerobic Indicator | Oxoid,Hampshire |
| AnaeroGen Anaerobic pouch system | Oxoid,Hampshire |
| CASYton dilution liquid | Innovatis, Reutlingen |
| Cell scraper | BD Falcon, San Jose |
| Cell Strainer 40 µm and 100 µm Nylon | BD Falcon, San Jose |
| Cover slips Ø15 mm, 18 mm | Roth, Karlsruhe |
| Cryovials | Nalgene, Rochester |
| Film development cassette | Appligene, Heidelberg |

| | |
|---|---|
| flexiPerm | Greiner bio-one, Kremsmünster |
| Gelmount mounting media | Biomedia |
| Hyperfilm, ECL | Amersham Pharmacia Biotech, Freiburg |
| Lab-Tek II CC2 Glass Chamber Slide | Nunc, Roskilde |
| Ø 3.5 cm, Ø6 cm, Ø10 cm cell culture dishes | Greiner bio-one, Kremsmünster |
| Object slides | Mentel, Braunschweig |
| Optical adhesive film | Applied Biosystems, Foster City |
| Protran Nitrocellulose Transfer Membrane | Schleicher & Schuell, Dassel |
| Real-time PCR optical 96-well reaction plates | Applied Biosystems, Foster City |
| Refinal film developer | Agfa, Mortsel |
| Scalpels | Braun, Tuttlingen |
| Syringe filters | Nalgene, Rochester |
| Tetenal Superfix Plus film fixer | Agfa, Mortsel |
| Whatman 3 mm filter paper | Schleicher & Schuell, Dassel |

### 2.1.5. Kits

| Kit | Supplier |
|---|---|
| The CytoTox 96® Non-Radioactive Cytotoxicity Assay | Promega, Madison |
| BCA Protein Assay Kit | Pierce, Rockford |
| BIOXYTECH $H_2O_2$-560 Quantitative Hydrogen Peroxide Assay | OXIS, Portland |
| Catalase Assay Kit | Calbiochem, Darmstadt |
| DNA Damage Quantification Kit | BioVision, Mountain View |
| DNeasy Blood & Tissue Kit | Qiagen, Hilden |
| Human Cyclooxygenase-II Enzyme Immunometric Assay kit | Assay Designs, Ann Arbor |
| Human HO-1 ELISA Kit | Assay Designs, Ann Arbor |
| Human IL-8 DuoSet ELISA | R&D Systems, Wiesbaden |
| NanoOrange Protein Quantification Kit | Molecular Probes, Carlsbad |
| RNeasy Mini Kit | Qiagen, Hilden |
| Superoxide Dismutase Assay Kit II | Calbiochem, Darmstadt |
| SuperScript II Reverse Transcriptase | Invitrogen, Carlsbad |

### 2.1.6. Antibodies

| Antibody | Source | Dilution | Supplier |
|---|---|---|---|
| AlexaFluor 488 anti-mouse IgG | goat | 1:400 | Molecular Probes, Carlsbad |
| Anti-8-oxoG | mouse | 1:250 | Trevigen, Gaithersburg |
| Anti-CD31 FITC conjugate | mouse | 1:40 | Chemicon, Billerica |
| Anti-ERK2 | rabbit | 1:3000 | Santa Cruz Biotechnology |
| Anti-E-selectin | mouse | 1:200 | Bender MedSystems, Vienna |
| Anti-HIF-1α | mouse | 1:250 | BD Biosciences, Franklin Lakes |
| Anti-ICAM-1 | rabbit | 1:1000 | Cell Signaling, Danvers |
| Anti-ICAM-1 | mouse | 1:400 | Bender MedSystems, Vienna |

| | | | |
|---|---|---|---|
| Anti-Ki67 | mouse | 1:40 | Dako, Glostrup |
| Anti-mouse IgG biotinylated | goat | 1:1000 | Amersham Pharmacia Biotech, Freiburg |
| Anti-mouse IgG HRP linked | sheep | 1:2000 | Amersham Pharmacia Biotech, Freiburg |
| Anti-mouse IgG HRP linked | rabbit | 1:400 | Dako, Glostrup |
| Anti-p21 | mouse | 1:2000 | Cell Signaling, Danvers |
| Anti-p53 | rabbit | 1:1000 | Cell Signaling, Danvers |
| Anti-p53 | mouse | 1:1000 | Calbiochem, Darmstadt |
| Anti-rabbit IgG HRP linked | donkey | 1:3000 | Amersham Pharmacia Biotech, Freiburg |
| Anti-rabbit IgG HRP linked | goat | 1:5000 | Jackson ImmunoResearch, Suffolk |
| Anti-β-actin | mouse | 1:2000 | Sigma-Aldrich, St. Luis |
| Isotype IgG 1 | mouse | 1:400 | Diatec, Oslo |
| Isotype IgG 2a | mouse | 1:200 | Dianova, Hamburg |

### 2.1.7. Oligonucleotides

#### *2.1.7.1. Primers*

| **Primer** | **Sequence** |
|---|---|
| 18s 3' | 5'-GGCATCGTTTATGGTCGGAA-3' |
| 18s 5' | 5'-AGCGAAAGCATTTGCCAAGA-3' |
| BNip3 3' | 5'-GGACAGAGTAGTTCCAGAGGCAGTTC-3' |
| BNip3 5' | 5'-GGTGTGCATTTCCACATCAAACAT-3' |
| E-selectin 3' | 5'-CCCGTGTTTGGCACTGTGT-3' |
| E-selectin 5' | 5'-GCCATTGAGCGTCCATCCT-3' |
| GAPDH 3' | 5'-ATGGGGAAGGTGAAGGTCG-3' |
| GAPDH 3' | 5'-TAAAAGCAGCCCTGGTGACC-3' |
| HIF-1α 3' | 5'-GCAAGCCCTGAAAGCG-3' |
| HIF-1α 5' | 5'- GGCTGTCCGACTTTGA-3' |
| ICAM-1 3' | 5'-CGGCTGACGTGTGCAGTAAT-3' |
| ICAM-1 5' | 5'-CACCTCGGTCCCTTCTGAGA-3' |
| IL-8 3' | 5'-TGGCAGCCTTCCTGATTTCT-3' |
| IL-8 5' | 5'-TTAGCACTCCTTGGCAAAACTG-3' |
| PHD2 3' | 5'-AGCAGCATGGACGACCTGAT-3' |
| PHD2 5' | 5'-TCGTCCGGCCATTGATTT-3' |
| SERPINE 3' | 5'-TGCTGGTGAATGCCCTCTACT-3' |
| SERPINE 5' | 5'-CGGTCATTCCCAGGTTCTCTA-3' |
| uPAR 3' | 5'-GCCCAATCCTGGAGCTTGA-3' |
| uPAR 5' | 5-'TCCCCTTGCAGCTGTAACACT-3' |
| VEGF 3' | 5'-CGAGGGCCTGGAGTGTGT-3' |
| VEGF 5' | 5'-CCGCATAATCTGCATGGTGAT-3' |

#### *2.1.7.2. siRNA*

| siRNA | Sequence (antisense) | Supplier |
|---|---|---|
| FAM-Labelled GAPDH siRNA | | Ambion, Austin |
| s6539 HIF-1α | 5'-UUUGAGUAUCUCUAUAUGGtg-3' | Ambion, Austin |
| s6541 HIF-1α | 5'-UCUUAUACCCACACUGAGGtt-3' | Ambion, Austin |
| *Silencer*®Negative Control #1 siRNA | | Ambion, Austin |

### 2.1.8. Biomaterials

#### *2.1.8.1. Ti6Al4V preparation*

Titanium alloy Ti6Al4V (ASTM 136) disks with a diameter of 16 mm and 2 mm thickness were used in this study. The titanium surfaces were prepared by grinding and polishing to roughness values below 25 nm ($R_{RMS}$) on a 100 µm length scale by Fa.Hegedüs. Before use ultrasonic cleaning was done in 1% Triton X-100, acetone, and ethanol for 20 min each. Titanium samples were sterilized with ethylene oxide.

#### *2.1.8.2. $CoCl_2$ solution*

$CoCl_2$ solution was used for treatment of the cells with $Co^{2+}$. $CoCl_2 \times 6H_2O$ was dissolved in sterile $H_2O$ at concentration of 1M. Solution was further sterilised with sterilisation filter (Ø 0.2 µm) and used as a stock solution.

#### *2.1.8.3. $TiO_2$-coating of Co28Cr6Mo alloy*

Co28Cr6Mo (ESKA IMPLANTS, Lübeck) disks with a diameter of 14.5 mm and 1.5 mm thickness were used as substrates. Disk surfaces were polished to the roughness values of $R_a$=0.014±0.009 µm. $TiO_2$-coating (140 nm thick) was produced by dip-coating via sol-gel process. The sol for dipping consisted of tetrabutoxytitanate and n-butanol with a molar ratio of 1:33. The exposure time in the sol was 20 s. The samples were pulled out at a speed of 1.7 mm $s^{-1}$. After exposing the disks to air for 1 h they were tempered at 500°C. Afterwards the samples were autoclaved in water and eventually air-dried under sterile conditions.

### 2.1.9. Software

| Software | Developer | Link |
|---|---|---|
| ImageJ | National Institute of Health | http://rsb.info.nih.gov/ij/download.html |
| ImageTool | University of Texas, Health Science Center, San Antonio | http://ddsdx.uthscsa.edu/dig/download.html |
| LinRegPCR | (Ramakers et al 2003) | |
| SDS Software | Applied Biosystems | |

## 2.2. Methods

### 2.2.1. Isolation and culture of endothelial cells

Human dermal microvascular endothelial cells (HDMEC) were isolated from juvenile foreskin (Kirkpatrick et al 2002). After washing in PBS and removing connective tissue foreskin was cut into small quadratic pieces and incubated in 2.36 U/ml dispase overnight at 4°C. Afterwards epidermis was removed from the dermis and the foreskin pieces were washed in PBS. Then the tissue was digested with 0.04% trypsin in 5ml of 0.48 mM versene in a sterile 50 ml tube for 2 h at 37°C in water bath under moderate shaking. Following digestion trypsin was inactivated by addition of 2 ml fetal bovine serum (FBS) and the tube was filled with PBS. Foreskin pieces were put into a glass Petri dish and squeezed with a flat side of a scalpel for 5 min. The resulting cell suspension was strained through a 100 µm filter into a fresh 50 ml tube and centrifuged at 1000 rpm for 5 min. The cell pellet was resuspended in 9 ml of PromoCell Endothelial Cell Basal Medium MV with 5% PromoCell Supplement Mix (Complete medium), seeded onto a 75cm$^2$ flask pre-coated with 0.2% gelatine and cultured in a humidified atmosphere at 37°C (5% $CO_2$). Next day the medium with unattached cells and remaining tissue parts was removed and 11 ml of fresh medium was added. Medium change was performed every 2-3 days.

After approximately 1 week HDMEC were separated from other cell types. For this purpose Dynabeads conjugated with antibody against CD31 were used. First, 15-20 µl of Dynabeads solution were washed with PBS in the tube fixed at a magnet. Subsequently Dynabeads were resuspended in 5 ml PBS-0.1% BSA and added to the reduced volume of cell culture medium in the cell culture flask. The beads were incubated with cells for 20 min at 37°C with the shaking of the flask after 10 min and microscopic control of the binding of the beads to endothelial cells. Afterwards the cells were detached with trypsin-EDTA solution and collected in PBS-10% FBS. The cell suspension was put into a 15 ml tube fixed in the

magnet; after approximately 1 min incubation cells labelled with CD31-Dynabeads were located at the side of the tube close to the magnet. The liquid was aspirated and the cells were resuspended in 3 ml PBS-0.1% BSA. The cells were mixed in the tube on a roll mixer for 10 min at 4°C and afterwards sieved through 40 µm filter. Subsequently, three washing steps 10 min each were performed with PBS-0.1% BSA at 4°C with magnetic separation in between. Following the last washing step HDMEC were resuspended in Complete medium and seeded on gelatine-coated cell culture flasks (passage 1). Cells were allowed to grow to confluence (4-5 days), then passaged 1:3 and 4 h later a second CD31 separation was performed (passage 2). When HDMEC reached confluence again cell culture medium was changed to PromoCell Endothelial Cell Basal Medium MV supplemented with 15% FBS, penicillin/streptomycin (40 units penicillin/ml, 40µg streptomycin sulphate/ml), sodium heparin (10 µg/ml) and bFGF (2.5 ng/ml) and the cells were passaged 1:3 the day after (passage 3). Alternatively, the cells were frozen in the cell culture medium containing 10% DMSO in a liquid nitrogen tank.

### 2.2.2. Cell seeding

For experiments HDMEC were used in passage 4. HDMEC were seeded at a density of 110 000 cells/cm$^2$ on cell culture plates or dishes pre-coated with 5 µg/ml fibronectin solution (96-well plates and LabTeks) or 0.2% gelatine (other vessels). Cell culture medium was changed 24 h after seeding.

For comparison of Ti6Al4V with an *in vitro* control HDMEC were seeded on polystyrene (PS) pre-coated with fibronectin (5 µg/ml solution) or on Ti6Al4V alloy disks. Glass cover slips coated with fibronectin were used for microscopy instead of PS. Two ways of seeding were used. In the first sterile flexiPerm silicon rings were placed on top of Ti6Al4V disks or on PS surface and 300 µl cell suspension was put into reservoirs formed by a flexiPerm ring. Alternatively, HDMEC were seeded on Ti6Al4V disks or fibronectin-coated glass as a 300 µl drop. After cell adhesion (4h) the drop was aspirated and fresh medium was added.

Co28Cr6Mo and $TiO_2$-coated Co28Cr6Mo were compared to fibronectin-coated glass. The seeding was performed similarly to Ti6Al4V.

### 2.2.3. Cell treatment with various compounds

HDMEC were generally allowed to grow for 48 h before treatment. For the experiments with Ti6Al4V PromoCell Basal Medium MV with lowered ascorbic acid content

(0.5 mg/l) and without phenol red was used to treat HDMEC with $H_2O_2$ or TNF-α and LPS. ROS scavengers were added to the cells 4 h after cell seeding and kept in the cell culture medium throughout the experiment, with the addition of fresh scavengers with each medium change. Experiments with $CoCl_2$ were performed in a humidified atmosphere containing 5% $CO_2$ and 10% $O_2$. All mentioned compounds were prepared shortly before treatment and added to the cells with fresh medium. Anoxia treatment was performed by sealing the cell culture plate in a plastic bag containing AnaeroGen anaerobic pouch.

### 2.2.4. Scanning electron microscopy (SEM)

For SEM cells were fixed in cacodylate/HCl buffer containing 10% glutaraldehyde for 30 min at RT. Afterwards the samples were washed 3 times with cacodylate/HCl buffer without glutaraldehyde, post-fixed in 2% osmium tetroxide for 2 h and dehydrated through grades of EtOH from 50 to 100% (15 min each step). After drying in hexamethyldisilizane (HMDS, 2 times 20 min) the samples were air-dried, mounted onto a holder and introduced into the chamber of a sputter coater, where they were coated with a thin layer of gold.

### 2.2.5. Immunofluorescent staining

At the end of an experiment cell culture medium was aspirated, cells were briefly washed with 3.7% paraformaldehyde (PFA) in cytoskeleton-buffer (SC-buffer) and then fixed in 3.7% PFA in CS-buffer for 15 min. Subsequently, the samples were washed 3 times with PBS and permeabilisation was performed with 0.1% Triton X-100 in PBS for 5 min followed by 4 times washing with PBS (5 min each washing step). Primary or isotype control-antibody (or phalloidin, dilution 1:40) was incubated with the cells in PBS-1% BSA for 1 h at RT. After 4 washing steps with PBS (5 min each) the cells were incubated with fluorescently labelled secondary antibody in PBS-1% BSA for 45 min in darkness. Afterwards the cells were washed twice with PBS and stained with 1 µg/ml Hoechst 33342 for 5 min. Finally the samples were washed and covered with mounting medium and glass cover slips. Before microscopical examination the samples were stored at 4°C until the mounting medium became solid.

### 2.2.6. Cytotoxicity assays

#### *2.2.6.1. LDH activity assay*

The CytoTox 96® Non-Radioactive Cytotoxicity Assay was performed following the manufacturer's protocol. This assay measures lactate dehydrogenase (LDH) activity in the cell culture supernatants. Briefly, 1 h before the end of the experiment lysis buffer was added to the untreated cells to obtain the maximum LDH release. Then 50 µl of supernatants from all samples were transferred to a new microplate and 50 µl of LDH Substrate mix was added to each well. Enzymatic reaction was carried out for 30 min in the darkness and after that terminated by the addition of 50 µl of stop solution. Optical density was then measured at 492 nm against a blank sample (medium without cells with LDH Substrate mix and stop solution). LDH release in each sample was calculated as the percentage of total LDH activity (maximum release sample).

#### *2.2.6.2. MTS conversion assay*

The metabolic cell activity (an indirect measure of cytotoxicity) was measured by the conversion of MTS (3-(4,5-dimethylthiazol-2-yl)-5-(3-carboxymethoxyphenyl)-2-(4-sulfophenyl)-2H-tetrazolium) to formazan, which can be photometrically detected. MTS was mixed with fresh medium at the ratio 1:5 and added to the cells for 1.5 h. The cells were placed in a $CO_2$ incubator at 37°C. After incubation time supernatants were transferred to a new microplate and optical density was measured photometrically at 492 nm against a blank sample (medium without cells with MTS).

#### *2.2.6.3. Crystal violet staining*

At the end of the experiment cell culture medium was aspirated, cells were washed once with PBS-0.05% Tween 20 and then fixed 15 min with 2-propanol. The samples were subsequently washed three times with PBS-0.05% Tween 20 and stained with 0.1% crystal violet solution for 20 min on a shaker. Afterwards the plates were washed in water to remove unbound stain. Crystal violet bound to the cells was extracted by incubation with 33% $CH_3COOH$ for 20 min on a shaker. Resulting solutions were transformed to a new microplate and optical density was measured at 600 nm against pure 33% $CH_3COOH$.

#### *2.2.6.4. Cell number quantification*

Relative cell number was determined by means of quantification of nuclei. The cells were fixed in 3.7% PFA in CS-buffer for 15 min (or with other fixatives when cell number quantification was performed after other assays) and washed with PBS. Nuclei were then stained with Hoechst 33342 solution (1 µg/ml) for 5 min and after washing with PBS the samples were covered with mounting medium and glass cover slips. Nine digital microscopic images were randomly taken for each sample. The number of nuclei on the images was quantified with ImageTool software.

### 2.2.7. Oxidative stress evaluation

#### *2.2.7.1. $H_2O_2$ quantification assay*

Hydrogen peroxide concentration was measured using the Bioxytech® $H_2O_2$-560 kit according to the manufacturer's instructions. $H_2O_2$ amount in cell culture medium was measured after different time points upon $H_2O_2$ addition. The concentration was calculated from a standard curve obtained by assaying a range of freshly prepared $H_2O_2$ solutions in cell culture medium. Briefly, 1 volume of sample or standard was mixed with 10 volumes of working reagent (1 volume of R1 and 100 volumes of R2 buffer) and incubated at RT for 30 min. The optical density was then measured at 560 nm against blank sample (1 volume of 2.5 M $H_2SO_4$ and 100 volumes R2 buffer).

#### *2.2.7.2. DCF assay*

Oxidative stress was assayed utilising the fluorescent probe 2´,7´-dichlorodihydro-fluoresceine-diacetate (DCDHF-DA). DCDHF-DA enters the cells where it is converted to 2´,7´-dichlorodihydrofluoresceine (DCDHF) by cellular esterase activity and is further oxidized by ROS with the formation of a fluorescent product (DCF). The cells were pre-incubated with DCDHF-DA solution (50 µM) in the cell culture medium for 30 min, then the cells were washed twice with medium and $H_2O_2$-containing medium was added. Fluorescence was measured after desired $H_2O_2$ treatment time using a 485 nm excitation filter and a 535 nm emission filter.

#### *2.2.7.3. Determination of GSH amount*

The amount of reduced glutathione (GSH) was determined using the fluorescent dye monochlorobimane. Briefly, cells were lysed with 20 mM Tris-HCl buffer pH 7.4 containing 150 mM NaCl, 1 mM EDTA, 1 mM EGTA 1% Triton X-100 and 1mM PMSF. Lysis was carried out for 10 min on ice with shaking. The lysates were collected and centrifuged at 14000 rpm at 4°C for 10min to eliminate cell debris. GSH in the supernatants was then stained with monochlorobimane solution (final concentration 0.1 mM) containing equine liver GST (1 U/ml) for 30 min at 37°C in the darkness. Finally fluorescence was measured using an excitation filter for 395 nm and emission filter for 480 nm. GSH amount was calculated from a standard curve and normalised to the protein concentration of the lysates.

#### *2.2.7.4. Catalase activity assay*

At the end of the experiment the cells were lysed with 10 mM Tris-HCl buffer pH 7.4 containing 150 mM NaCl, 0.1 mM EDTA, 0,5% Triton X-100 and 1mM PMSF for 10 min on ice and cell debris was removed by centrifugation at 14000 rpm at 4°C for 10min. The enzyme activity was measured using a catalase activity assay following the manufacturer's instructions. The assay utilises the reaction of the enzyme with methanol in the presence of $H_2O_2$. The formaldehyde produced is measured photometrically with purpald as the chromogen. Briefly, 100 µl Assay buffer was mixed with 30 µl MetOH and 20 µl of the samples or formaldehyde standards (for standard curve). The reaction was initiated by the addition of 20 µl $H_2O_2$ and proceeded for 20 min on a shaker. Afterwards the reaction was terminated by 30 µl KOH followed by the addition of 30 µl purpald to each well and further 10 min of incubation on the shaker. Finally 10 µl potassium periodate were added to the wells for 5 min and optical density was measured at 540 nm. Formaldehyde concentration was determined from the standard curve and catalase activity was calculated as nmol formaldehyde/min/ml. Enzyme activity was further normalised to the protein content of the sample.

#### *2.2.7.5. SOD activity assay*

The samples for SOD activity assay were prepared in the same way as for catalase activity assay. SOD activity assay utilises a tetrazolium salt for detection of superoxide radicals generated by xanthine oxidase and hypoxanthine and the inhibition of this reaction by the presence of SOD in the samples. This assay measures total SOD activity. In brief, 200 µl radical detector was mixed with 10 µ of samples or SOD standards (for standard curve generation). The reaction was then initiated by adding 20 µl of xanthine oxidase solution to each well. The plate was then incubated on a shaker for 20 min at RT and absorbance was measured at 450 nm. The absorbance value of the zero standard (no SOD addition) was divided by itself and by all other absorbance values to yield the linearised rate. The latter value of the standards was then plotted as a function of SOD activity (U/ml). The resulting standard curve was used to determine SOD activity of the samples. Enzyme activity was further normalised to the protein concentration of the sample.

#### *2.2.7.6. Cathodic corrosion model*

Cathodic polarization was performed with a multichannel potentiostat, which was equipped with 8 channels. The electrochemical cell was built from a 12-well tissue culture plate and a self-made contact plate, which together with the electrical connection to the multi-potentiostat were specially designed for use in a $CO_2$ incubator (Kalbacova et al 2007). The contact plate was made from Teflon and contained the connections for the working, reference and counting electrodes. The electrical connection to the Ti6Al4V samples (working electrode) was achieved through the back via gold contact pins on the contact plate, for which holes were drilled in 4 wells in the upper and 4 wells in the lower row of the plate. Ti6Al4V-samples were glued over these holes using a combination of silicone (Silastic) and toluene. The well plate with the Ti6Al4V-samples was sterilized by gamma-irradiation or rinsing with 70 % ethanol.

Figure 2.1 shows the assembly of electrodes within the tissue culture plate. Two small cups with KCl solution were placed in the middle row of the well plate. The well plate was then covered with the lid containing holes for the electrodes. The reference electrode was placed in the cup and connected to the electrolyte/cell medium via a salt bridge. The latter was made from a tube filled with 2 % agarose dissolved in sterile PBS. Conductivity of the samples was measured with an ohmmeter before each experiment. A platinum wire served as counter electrode and was placed in a ceramic frit containing 1 ml of electrolyte (e.g. cell

culture medium) directly above the working electrode. The frit was used in order to avoid any influence of by-products formed at the counter electrode on cells.

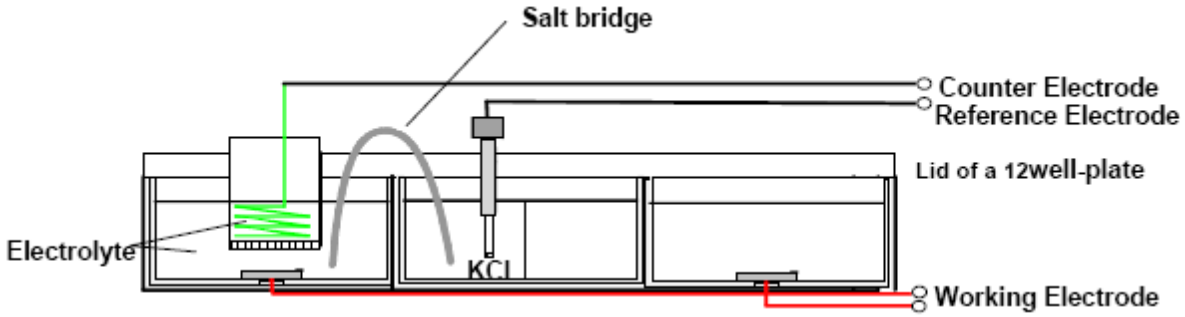


*Fig. 2.1. Scheme of the electrochemical cell. The figure shows the cross section of a 12-well plate, which was adapted for 8 single electrochemical cells.*

HDMEC were seeded on Ti6Al4V disks placed in the plates for cathodic polarisation. The control samples of HDMEC seeded on PS and Ti6Al4V in normal cell culture plates were always prepared in parallel. Medium was changed at 24 h and cathodic polarisation was induced 48 h after cell seeding. The cell culture plate was adjusted on the contact plate in sterile conditions as quickly as possible. The contact plate with the samples was then placed into a $CO_2$ incubator and connected to the potentiostat. Cathodic polarisation was carried out in a galvanostatic mode at different current densities for different time periods. Afterwards the system was disassembled and the samples were immediately used for various assays.

### 2.2.8. DNA damage assessment

#### *2.2.8.1. 8-oxoG staining*

8-oxoG in DNA was assessed via immunofluorescent staining. For this HDMEC were grown on LabTek glass slides and treated with $H_2O_2$ or $CoCl_2$. At the end of the incubation time the cells were fixed first in MetOH and then in acetone at -20°C for 15 min. The samples were then air-dried and treated with 0.05 N HCl for 5 min on ice. After 3 washing steps with PBS (5 min each) the cells were incubated with 100 µg/ml RNase in 150 mM NaCl, 15 mM NaCitrate for 1 h at 37°C.Then the cells were sequentially washed in PBS, 35%, 50% and 75% EtOH for 3 min each and DNA was denatured with 0.15 N NaOH in 70%

EtOH for 4 min. After brief washing in PBS the samples were sequentially washed in 70% EtOH containing 4% v/v formaldehyde, 50% EtOH, 35% EtOH and PBS for 2 min each. Proteins were subsequently digested with 100 µg/ml proteinase K in 20 mM Tris-HCl pH 7.5 with 2 mM $CaCl_2$ for 10 min at 37°C. After 3 washes with PBS unspecific binding was blocked with 5% normal goat serum in PBS for 1 h to block. The cells were then incubated with anti-8-oxoG antibody (dilution 1:250) in PBS-1% BSA-0.01% Tween 20 overnight at 4°C. Following 3 washing steps with PBS-1% BSA-0.01% Tween 20 the samples were incubated with secondary goat anti-mouse AlexaFluor 488 antibody (dilution 1:1000), newly washed and covered with mounting medium and glass cover slips.

#### *2.2.8.2. DNA isolation*

Genomic DNA was isolated with DNeasy Blood and Tissue Kit. Cell pellets obtained after trypsinisation were resuspended in 200 µl PBS and RNA was digested by the addition of 20 µl RNase A (10 mg/ml) for 2 min. Subsequently 20 µl of proteinase K and 200 µl Buffer AL were added and the samples were incubated at 70°C for 10 min. DNA was then precipitated by 200 µl 100% EtOH, the mixture was applied onto the DNeasy Mini spin column and centrifuged at 8000 rpm for 1min. DNA bound to the membrane in the column was washed first with 500 µl Buffer AW1 and centrifuging for 1 min at 8000 rpm and then with 500 µl Buffer AW2 followed by centrifuging for 3 min at 14000 rpm. Finally DNA was eluted from the column with 50 µl TE Buffer (1 min at 8000 rpm). DNA concentration was measured with a NanoDrop spectrophotometer.

#### *2.2.8.3. AP sites quantification*

AP sites were detected in genomic DNA with a DNA Damage Quantification Kit. The kit utilises the ARP (Aldehyde Reactive Probe) reagent that reacts specifically with an aldehyde group, which is the open ring form of the AP sites. Afterwards AP sites are tagged with biotin residues, which are then detected colorimetrically using HRP-linked streptavidin. Briefly, the DNA concentration of the samples was adjusted in TE buffer to 0.1 µg/µl. AP sites were then tagged by mixing 5 µl of this DNA solution with 5 µl of ARP solution and incubating the mixture at 37°C for 1 h. 88 µl TE buffer and 2 µl glycogen were then added to the reaction solution and DNA was precipitated by 0.3 ml 100% EtOH at -20°C for 20 min. Afterwards the mixture was centrifuged at 15000 rpm at 4°C for 10 min and the DNA pellet

was washed three times with 0.5 ml 70% EtOH. This biotin-tagged DNA was then air dried and dissolved with 1ml of TE buffer. 60 µl of resulting solution was put into each well of a microplate. 100 µl of the DNA Binding Solution was added to each well and the plate was incubated at RT overnight to bind DNA to the plate surface. The wells were then washed 5 times with washing buffer followed by incubation with 100 µl of HRP-Streptavidin solution on the shaker for 1 h. After 5 further washing steps 100 µl of HRP Developer was added to each well and the plate was incubated at 37°C for 1 h. Finally, the reaction was stopped with 100 µl of 6 M HCl and optical density was measured at 450 nm. The amount of AP sites was determined from a standard curve run with ARP-DNA Standard in parallel.

### 2.2.9. siRNA technique

Synthetic siRNAs from Ambion were used to decrease the amount of mRNA and proteins in HDMEC. The cells were transiently transfected with siRNA by means of liposomal transfection (GenCarrier-1 transfection reagent). 1-100 nM siRNA and 24-72 h time points were used to determine the optimal conditions for down-regulation. 70% decrease of mRNA was considered a significant down-regulation.

200000 cells were seeded in each well of a 6-well plate and transfected 24 h after seeding. siRNA (end concentration 50 nM) was diluted in 100 µl of serum-free medium and mixed with 100 µl of diluted GenCarrier-1 (4 µl GenCarrier-1 in 100 µl serum-free medium). The mixture was incubated at RT for 30 min. In the meantime the cells were washed twice with serum-free medium and 800 µl of low-serum medium (Endothelial Cell Basal Medium MV with 1% FBS and 0.17 ng/ml bFGF) was added to each well. After 30 min of incubation 200 µl of the mixture of siRNA and GenCarrier-1 was added in a drop-wise fashion and the plates were swirled to ensure equal mixing. After 7 h incubation 1 ml of high-serum medium (Endothelial Cell Basal Medium MV with 30% FBS, 5 ng/ml bFGF and 20 µg/ml sodium heparin) was added to each well and the plates were incubated for further 17 h. Afterwards (24 h after transfection start) the medium was changed to the one with the usual amount of serum and supplements. HDMEC transfected with specific siRNA were compared to the cells transfected with Silencer Negative Control siRNA #1 and to untransfected cells. FAM-labelled GAPDH siRNA was used as a positive control for effective mRNA down-regulation.

### 2.2.10. Analysis of gene expression

#### *2.2.10.1. RNA Isolation*

RNA isolation was performed with RNeasy Mini Kit. HDMEC were lysed with RLT Buffer containing β-mercaptoethanol (10 µl per 1 ml buffer) directly on the growth surface and collected with a cell scraper. If not processed immediately cell lysates were stored at -80°C. RNA was precipitated with 1 volume of 70% EtOH, the mixture was pipetted to an RNeasy spin column and afterwards centrifuged for 15 s at 10000 rpm. 350 µl of Buffer RW1 were added to the column and then centrifuged for 15 s at 10000 rpm. DNA bound to the membrane in the column was digested for 15 min with DNase I and then the previous step with RW1 buffer was repeated. The membrane was subsequently washed twice with RPE Buffer (centrifugation at 8000 rpm for 15s and 2 min) and dried by centrifugation at 15000 rpm for 1 min. RNA was then eluted in 30 µl of $H_2O$ by centrifugation at 8000 rpm for 1 min. To increase the concentration of RNA the elution step was repeated with the RNA solution eluted in the first step. RNA concentration was measured with a NanoDrop spectrophotometer.

#### *2.2.10.2. Reverse transcription*

From 10 to 1000 ng RNA was reverse transcribed into cDNA depending on the sample RNA concentration. The same amount of RNA was taken from different samples. The volume was adjusted to 10 µl and 2 µl of random primers (0.1 µg/µl) were added to RNA. The mixture was heated for 10 min at 65°C and then cooled on ice. Afterwards 8 µl of mastermix (containing 4 µl 5× First-Strand Buffer, 2 µl 0.1 M DTT, 1 µl dNTP Mix (10 mM each) and 1 µl SuperScript II) were added to each sample and the reaction was carried out at 42°C for 50 min. At the end the reaction was inactivated by heating at 70°C for 15 min.

#### *2.2.10.3. Quantitative RT-PCR*

Quantitative real-time PCR was performed using SYBR Green DNA binding fluorescent dye. 3.75 ng cDNA was used per reaction. 12.5 pmol of each 3´ and 5´ primers were mixed with cDNA. The volume was adjusted to 12.5 µl with $H_2O$ and 12.5 µl Power SYBR Green Mix was added resulting in a total volume of 25 µl. PCR amplification was carried out in Applied Biosystems 7300 Real-Time PCR System. Reaction conditions were 10 min at 95°C followed by 40 amplification cycles (15 s at 95°C and 1 min at 60°C). At the end DNA dissociation was performed by slowly elevating the temperature from 60°C to 95°C.

The data were analysed with SDS Software to obtain Ct (cycle threshold) values. Relative gene expression was then determined with the ΔΔCt method using 18s RNA as an endogenous control. Briefly Ct of endogenous control was subtracted from the Ct of the gene studied to obtain the ΔCt value. Afterwards ΔCt of the control sample was subtracted from ΔCt of the experimental sample to obtain the ΔΔCt value. Relative expression was then calculated with the formula $2^{-\Delta\Delta Ct}$. Data are presented as means of relative expression, error bars indicate 95% confidence interval. For statistical analysis the one-way ANOVA test for independent samples was performed on ΔΔCt values (Yuan et al 2006). To take into account possible differences in PCR efficiencies the data were additionally analysed with the REST method (Pfaffl et al 2002) using LinRegPCR Software (Ramakers et al 2003) to determine efficiencies of single PCR reactions.

#### *2.2.10.4. Microarrays*

RNA for microarrays was isolated from HDMEC derived from 3 different donors. RNA concentration and quality were controlled and corresponding RNA samples from different donors were pooled together. Microarray analysis was performed by Myltenyi Biotec Genomics Service. Briefly, for the linear T7-based amplification step, 0.5 µg of each total RNA sample was used. To produce Cy3-labeled cRNA, the RNA samples were amplified and labelled using the Agilent Low RNA Input Linear Amp Kit (Agilent Technologies) following the manufacturer's protocol. Yields of cRNA and the dye-incorporation rate were measured with the ND-1000 Spectrophotometer (NanoDrop Technologies). The hybridization procedure was performed according to the Agilent 60-mer oligo microarray processing protocol using the Agilent Gene Expression Hybridization Kit (Agilent Technologies). Briefly, 1.65 µg Cy3-labeled fragmented cRNA in hybridization buffer was hybridized overnight (17 hours, 65 °C) to Agilent Whole Human Genome Oligo Microarrays 4x44K using Agilent's recommended hybridization chamber and oven. Finally, the microarrays were washed once with 6x SSPE buffer containing 0.005% N-lauroylsarcosine for 1 min at RT followed by a second wash with preheated 0.06x SSPE buffer (37 °C) containing 0.005% N-lauroylsarcosine for 1 min. The last washing step was performed with acetonitrile for 30 sec. Fluorescence signals of the hybridized Agilent Microarrays were detected using Agilent's Microarray Scanner System (Agilent Technologies). The Agilent Feature Extraction Software (FES) was used to read out and process the microarray image files. The software determines feature intensities (including

background subtraction), rejects outliers and calculates statistical confidences. For determination of differential gene expression FES-derived output data files were further analyzed using the Rosetta Resolver gene expression data analysis system (Rosetta Biosoftware). This software offers the possibility to compare two single intensity profiles in a ratio experiment. The ratios were calculated by dividing sample signal intensity through control signal intensity.

Alternatively, PIQOR Skin Microarray Human Antisense was used. In this case experimental and control RNA were labelled with Cy5 and Cy3, respectively, and hybridized to the same array. Fluorescence intensities were then compared to obtain relative gene expression. 1.7-fold induction and 0.58-fold gene down-regulation were considered significant.

### 2.2.11. Analysis of protein expression

#### *2.2.11.1. ELISA*

For detection of IL-8 released by HDMEC in cell culture medium the DuoSet IL-8 ELISA kit was used. Briefly, microplate wells were coated with 100 µl capture antibody (4 µg/ml) overnight and washed subsequently with PBS-0.05% Tween 20. Unspecific binding sites were saturated with blocking buffer (1% BSA, 5% sucrose in PBS, 1 h incubation) followed by further washing. 100 µl standards or samples were added to the wells and binding to the antibody was allowed to take place during 2 h followed by the addition of 100 µl of biotinylated detection antibody (20 ng/ml) for 2 h with washing before and after incubation. For the detection of antibody-antigen complexes 100 µl of working dilution of streptavidin-HRP were then added to the wells, incubated for 1 h and after washing 100 µl of substrate solution (mixture of $H_2O_2$ and tetramethylbenzidine) were applied for 20min. The reaction was terminated by 50 µl of 2 N $H_2SO_4$ and optical density measured at 450 nm with the wavelength correction at 540 nm. IL-8 amount was determined from the standard curve.

Heme oxygenase-1 (HO-1) and cyclooxygenase II (COX II) were assayed in cell lysates with corresponding ELISA kits. In brief, lysis buffer was added directly to the cells and lysis was carried out on ice for 30 min on a shaker. Lysates were then centrifuged for 10 min at 15000 rpm at 4°C. Supernatants were transferred to the microplate coated with the corresponding antibody followed by addition of detection antibody and HRP-linked secondary antibody according to manufacturer's protocol. HO-1 And COX II amount was

determined from the standard curve run in parallel with recombinant HO-1 and COX II standards and normalised to the protein concentration of the cell lysates.

#### *2.2.11.2. Detection of protein expression in fixed cells*

Detection of ICAM-1, E-selectin and Ki67 expression was detected in the fixed HDMEC by enzyme immunoassay (EIA). HDMEC were washed briefly with PBS and fixed with MetOH/EtOH mixture (2:1) for 15 min at RT. Following washing with PBS unspecific binding sites were saturated with 10-times diluted blocking reagent (Roche) with 1% $H_2O_2$ to deplete the activity of endogenous peroxidases (30 min at 37°C). The samples were then incubated with primary antibody diluted in blocking reagent for 45 min at 37°C with shaking and subsequently washed 3 times with PBS-0.025% Tween 20. Biotinylated secondary antibody was then added to the samples and incubated for 45 min at 37°C with shaking. Following 3 washing steps the samples were incubated with biotinylated streptavidin-HRP for 60min at 37°C with shaking and again washed 6 times. Colorimetric reaction was initiated by the addition of substrate solution (prepared from 5 ml 10× Na Citrate buffer, 45 ml $H_2O$, 1 tablet o-PD (20 mg) and 20 µl 30% $H_2O_2$) for 20 min at 37°C and terminated by 3 M HCl. The solution was then transformed to a new microplate and optical density was measured at 492 nm against a blank sample (containing the mixture of substrate and stop solution that was not in contact to the cells). For detection of nuclear antigen Ki-67 an additional permeabilisation step with 0.1% Triton X-100 in PBS for 5 min at RT was carried out after cell fixation. Moreover, the secondary antibody used for Ki-67 assay was HRP-linked.

#### *2.2.11.3. Whole cell protein extraction*

For whole cell protein extraction HDMEC were lysed with RIPA buffer (with fresh PMSF and protease inhibitors cocktail). Cells were either trypsinised for the lysis or lysed directly on the growth substrate after PBS washing. The lysis was carried out for 10 min on ice and the lysates were centrifuged at 14000 rpm at 4°C for 5 min. Supernatants were transferred to new tubes and stored at -20°C.

Alternatively, the cells were lysed directly with RotiLoad-1 loading buffer diluted 1:3 with $H_2O$. To decrease the viscosity of the lysates DNA in the solution was destroyed using 10 impulses of sonication.

#### *2.2.11.4. Nuclear protein extraction*

For isolation of nuclear proteins cells were trypsinised and washed in PBS. Obtained cell pellets were resuspended in 1 ml Nuclear extraction buffer (with freshly added PMSF, DTT and protease inhibitors cocktail) and incubated on ice for 10min. Afterwards 50 µl of 10% NP-40 (v/v) was added to a final concentration of 0.5% and the suspension was vortexed and incubated on ice for further 5 min. Under these conditions only cell membranes are lysed, leaving nuclei intact. The nuclei were then pelleted by centrifugation at 400 g at 4°C for 5 min and the pellet was washed in 1 ml of Nuclear extraction buffer followed by another centrifugation step. Nuclei pellets were eventually suspended in 2 volumes of sonication buffer (with freshly added PMSF, DTT and protease inhibitors cocktail) and sonicated twice with 10 impulses. The lysates were centrifuged at 14000 rpm at 4°C for 5 min to remove cell debris, transferred to new tubes and stored at -20°C.

#### *2.2.11.5. Protein quantification assays*

Different assays for measurement of protein concentration were used depending on the assay compatibility with the components of the buffer used in the upstream method.

##### 2.2.11.5.1. BCA assay

BCA assay uses the reduction of $Cu^{2+}$ to $Cu^{+}$ by proteins in alkaline medium and detection of $Cu^{+}$ by a reagent containing bicinchoninic acid (BCA). Briefly 25 µl of samples and BSA standard solutions were transferred to a microplate and 200 µl of Working reagent were added to each well. The plate was incubated at 37°C in darkness for 30 min and optical density was measured at 550 nm. Protein concentration was calculated from a standard curve, derived from the assaying a range of known BSA concentrations.

##### 2.2.11.5.2. Bradford assay

Bradford assay (Bradford 1976) uses Coomassie Blue G250 that in acidic pH binds to hydrophobic amino acids in proteins. In brief, 10 µl of diluted samples and BSA standards were transformed to microplates and 200 µl Bradford reagent was added to each well. After 20 min of incubation optical density was measured at 600 nm and protein concentration was calculated from the standard curve.

2.2.11.5.3. NanoOrange assay

NanoOrange assay uses NanoOrange dye that becomes fluorescent upon binding to proteins. The assay allows measurement of highly diluted samples, thus avoiding disturbances by lysis buffer components. Briefly, the samples were diluted in the Working solution containing NanoOrange reagent. Different concentrations of BSA were prepared in the same solution for the standard curve. Both the samples and the standards were then heated for 10 min at 95°C, allowed to cool down for minimum 20 min and transferred to a microplate. Fluorescence was measured using 485 nm excitation and 590 nm emission filters.

### *2.2.11.6. SDS-polyacrylamide gel electrophoresis (SDS-PAGE)*

Protein extracts were separated according to molecular weight in denaturing polyacrylamide gel (Laemmli 1970). The gels consisted of 7.5, 10 or 12.5 % Resolving and 5% Stacking gel. The resolving gel solution (7.5 – 12.5 % PAA, 375 mM Tris-HCl, pH 8.8, 0.1% SDS, 0.05% APS, 0.005% TEMED) was cast between two glass plates and n-butanol was put on top of the resolving gel solution layer. After gel polymerisation n-butanol was removed, stacking gel solution (5 % PAA, 125 mM Tris-HCl, pH 6.8, 0.1% SDS, 0.05% APS, 0.005% TEMED) was cast on top of resolving gel and a comb was inserted between the glasses in order to get 10 wells after gel polymerisation. From 5 to 30 µg protein was mixed with 1/4 volume of RotiLoad-1 loading buffer and the samples were denatured at 95°C for 5 min and loaded into the wells of the stacking gel. Electrophoretic separation of proteins was carried out in SDS-Running Buffer (25 mM Tris, 192 mM Glycine, 0,1% SDS) at 25 mA per gel.

### *2.2.11.8. Western blot*

After separation with SDS-PAGE proteins were transferred to a nitrocellulose membrane. The membrane and the gel were equilibrated in SDS-transfer buffer (25 mM Tris-HCl, pH 8.0, 100 mM Glycine, 25% MetOH), the gel was put on top of the membrane and covered with 3 sheets of wet filter paper from both sides. Finally, the gel was covered with wet sponges and put vertically into a holder of PROTEAN Mini transfer chamber so that the membrane is orientated to the anode side. An ice container was inserted into the chamber and the chamber was filled with SDS-transfer buffer. The transfer of proteins from the gel to the membrane was carried out for 1 h at 350 mA. Afterwards protein transfer was controlled by

Ponseau S staining, which was then washed out with PBS. For saturation of the unspecific binding sites the membrane was incubated 1 h at RT in blocking solution (5% Milk powder in PBS-0.2% (v/v) Tween 20). Afterwards the membrane was incubated with primary antibody diluted in blocking solution for 2 h at RT or overnight at 4°C and subsequently washed twice with PBS-0.2 % Tween 20 for 5min each to remove unbound antibody. At the end the membrane was incubated with correspondent HRP-linked secondary antibody and washed again (3 times for 5 min in PBS-0.2% Tween-20). The antibody bound to the protein of interest was detected with ECL detection reagents and high performance chemiluminescent film. To probe the same membrane with another antibody membrane stripping was performed in stripping buffer (100 mM Glycine-HCl pH 2.8, 2 times 20 min) to remove previously bounded antibodies. To correct for the possible unequal protein loading each membrane was incubated with antibody against ERK2.

### 2.2.12. Angiogenesis assay

To assess the angiogenic potential of endothelial cells HDMEC were embedded into gel consisting of collagen type I and fibrin and stimulated by addition of VEGF and bFGF (Peters et al 2002). 1.5 mln cells were used per 1 ml of gel. Gel was polymerised in flexiPerm silicon rings placed on top of PS or Ti6Al4V. 1 ml of gel was prepared on ice from 255 µl double-concentrated IMDM, 100 µl fibrinogen (end concentration 1 mg/ml), 300 ml PromoCell medium without supplements, 80 µl cell suspension, 255 µl collagen type I (end concentration 0.77 mg/ml) and polymerised by addition of 10 µl of thrombin (0.5 U/ml) for 45 min at 37°C. Afterwards PromoCell medium containing 15% FBS (not heat inactivated), 1% Pen/Strep, 5 ng/ml bFGF and 50 ng/ml VEGF was carefully applied to the gel surface. The medium was changed every 2 days and HDMEC were left in the gel for 6 days. Eventually tube-like structures were visualised via vital cell staining with 10 mM calcein-AM solution.

### 2.2.13. Statistical analysis

All experiments were repeated at least three times and the results are presented as means ± standard deviations (SDs). Statistical analysis was carried out with Microsoft Excel one-way ANOVA test for independent samples. Normal distribution was tested by the Shapiro-Wilk test.

# 3. Results

## 3.1. Oxidative stress in endothelial cells on Ti6Al4V alloy

### 3.1.1. Response of endothelial cells to $H_2O_2$

Corrosion of the metal implant surfaces can lead to the formation of ROS and $H_2O_2$ as intermediate products of the cathodic partial reaction. $H_2O_2$ interacts with $TiO_2$, that normally covers the surface of titanium-containing materials, resulting in the production of further ROS. Moreover, excessive $H_2O_2$ amounts induce intercellular oxidative stress. Therefore, $H_2O_2$ was used in this study to mimic/elevate the corrosion of Ti6Al4V alloy and induce oxidative stress in endothelial cells in contact with the metal surface.

To choose the optimal experimental conditions cytotoxicity and viability were assessed in endothelial cells treated with different $H_2O_2$ concentrations on cell culture plastic. $H_2O_2$ treatment induced LDH release, which is a sign of the cell membrane damage. While the lower concentrations (up to 0.25 mM) caused no cytotoxic effects, concentrations higher than 0.5 mM provoked LDH release, thus indicating cell death (Fig. 3.1.A).

Evaluation of cellular metabolic activity with MTS assay, that is an indirect measure for viability, showed a similar tendency: $H_2O_2$ provoked dose-dependent decrease in cell viability starting from 0.5 mM (Fig. 3.1.B). Interestingly, lower $H_2O_2$ concentrations slightly increased MTS conversion, thus indicating an elevated viability of endothelial cells. Quantification of cell number by DNA staining with crystal violet showed that $H_2O_2$ treatment also led to a reduction of cell number (Fig. 3.1.C): lower $H_2O_2$ concentrations caused a slight decrease in cell number, while concentrations higher than 0.5 mM led to a more pronounced reduction.

It is known that ROS and $H_2O_2$ are very unstable. To evaluate the rate of $H_2O_2$ decomposition the $H_2O_2$ concentration was measured in the cell culture medium 0.5 and 1 h after its addition (Fig. 3.1.D). After 30 min the $H_2O_2$ concentration in the cell culture medium was approximately 10- and 5-fold lower (0.03 and 0.11 mM) compared to the applied concentrations (0.25 and 0.5 mM $H_2O_2$, respectively). Only trace amounts of $H_2O_2$ were left in the cell culture medium 1 h after addition of 0.25 mM $H_2O_2$ and an almost 10-fold reduced amount (0.06 mM) was detected 1 h after addition of 0.5 mM $H_2O_2$. Such fast $H_2O_2$ decay in the cell culture medium reflects two processes: natural $H_2O_2$ instability and active $H_2O_2$ decomposition by components of the medium. Most probably, catalase and other antioxidants

present in the serum used for medium preparation are responsible for this effect. The $H_2O_2$ decomposition rate was slower in other cell culture media, thus indicating that the medium used for endothelial cell culture was particularly rich in antioxidants. To reduce this effect medium with a decreased amount of ascorbic acid and without phenol red was used for the experiments. Interestingly, the rate of $H_2O_2$ decay was even faster in the presence of endothelial cells. A 10-fold reduction of $H_2O_2$ concentration upon addition of 0.5 mM $H_2O_2$ was observed already after 0.5 h, while only 0.01 mM $H_2O_2$ (50-fold decrease) remained in the medium after 1 h. This indicates that endothelial cells participate actively in $H_2O_2$ decomposition either by releasing antioxidants into the medium or eradicating $H_2O_2$ inside the cells.

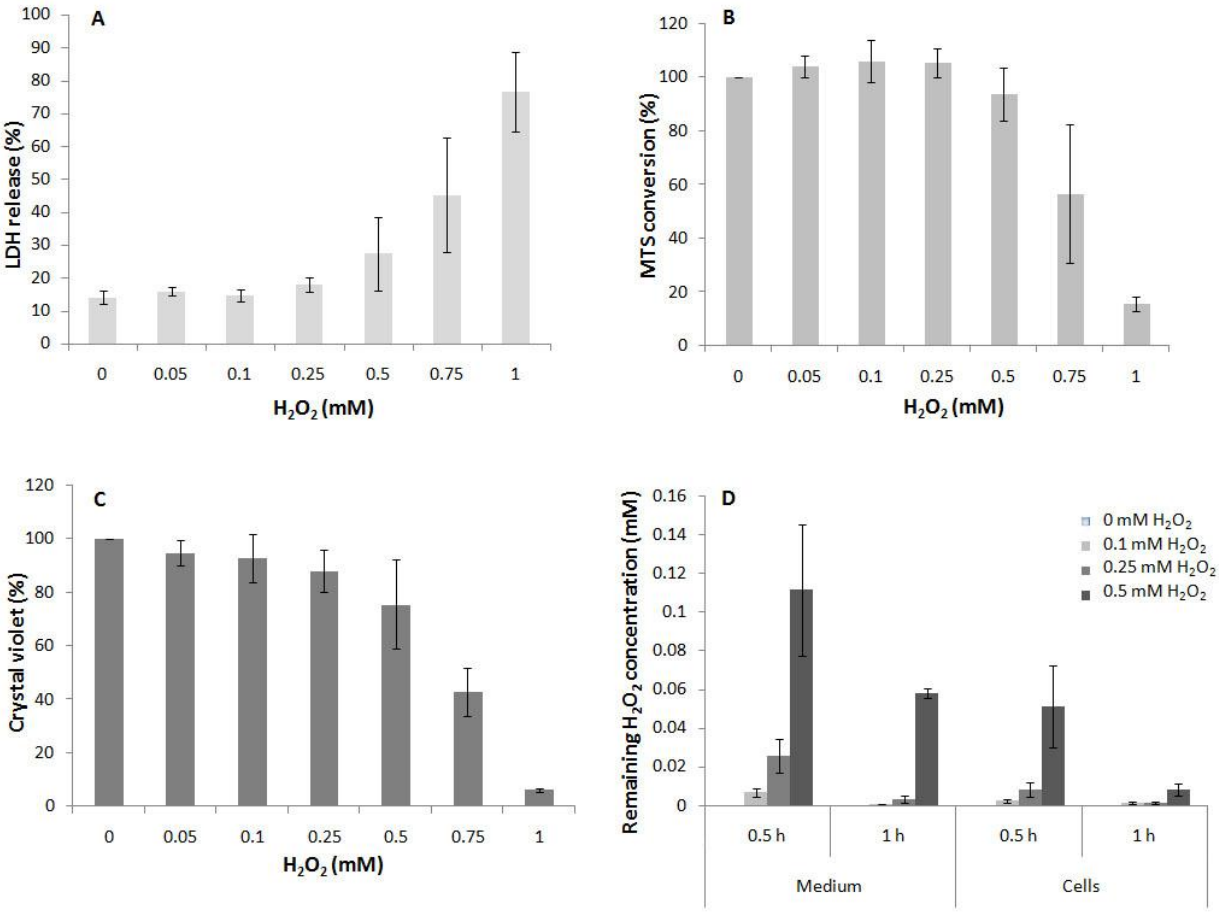


**Fig. 3.1.** *Cytotoxicity of $H_2O_2$ in HDMEC. LDH release (**A**), MTS conversion assay (**B**) and relative cell number quantification by crystal violet staining (**C**)were performed 24 h after $H_2O_2$ treatment (untreated control was set as 100%). **D.** $H_2O_2$ decomposition in HDMEC cell culture medium in the absence and presence of cells (means±SDs).*

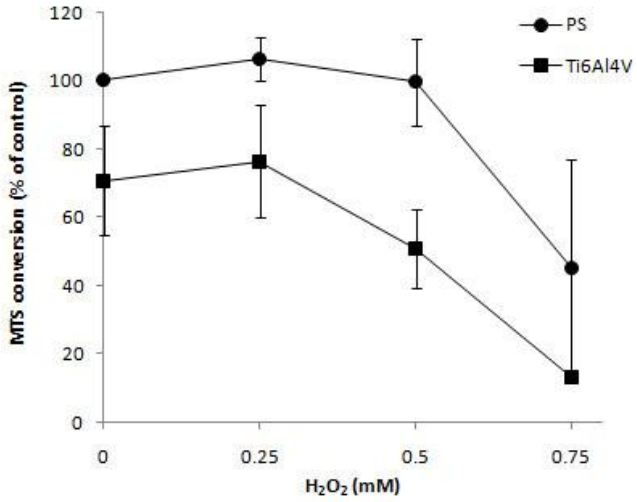


**Fig. 3.2.** *Dose response of HDMEC grown on PS and Ti6Al4V to $H_2O_2$ treatment. MTS conversion was measured 24 h after $H_2O_2$ addition (means ± SDs; untreated control on PS set as 100%).*

HDMEC grown on cell culture plastic (tissue culture polystyrene (PS)) were chosen as an *in vitro* control in this study and the response of endothelial cells to Ti6Al4V alloy and to the $H_2O_2$ treatment was compared to the control cells on PS in all experiments. To further optimise the experimental conditions HDMEC grown on Ti6Al4V alloy were treated with different $H_2O_2$ concentrations chosen from the testing on PS. $H_2O_2$ was generally more toxic to HDMEC grown on Ti6AlV alloy compared to cells on PS, leading to the dose-dependent decline in metabolic activity of cells with the highest concentration tested (0.75 mM) and causing more than 85% reduction in MTS conversion (Fig. 3.2). Since such high $H_2O_2$ doses often led to detachment of the cell monolayer, most experiments were performed using lower $H_2O_2$ concentrations, i.e. 0.25 and 0.5 mM.

### 3.1.2. Phenotype of endothelial cells growing on Ti6Al4V alloy

The phenotype of endothelial cells on Ti6Al4V alloy was visualised with SEM 72 h after seeding the cells on the material and compared to the phenotype of endothelial cells grown on PS (Fig. 3.3). While optically the amount of cells seemed to be comparable on both materials, higher magnification images (200× and 500×) indicated the differences in the shape and distribution of HDMEC on PS and Ti6Al4V. HDMEC grown on PS had an almost uniform spindle-like form lying roughly parallel and forming an almost confluent cell layer. HDMEC on Ti6Al4V alloy, in contrast, had diverse cell shapes with some cells being more

rounded and some more elongated than the cells on PS. Cell monolayers on Ti6Al4V alloy had gaps between the cells and lacked the ordered alignment of HDMEC on PS with the cells growing in different directions.

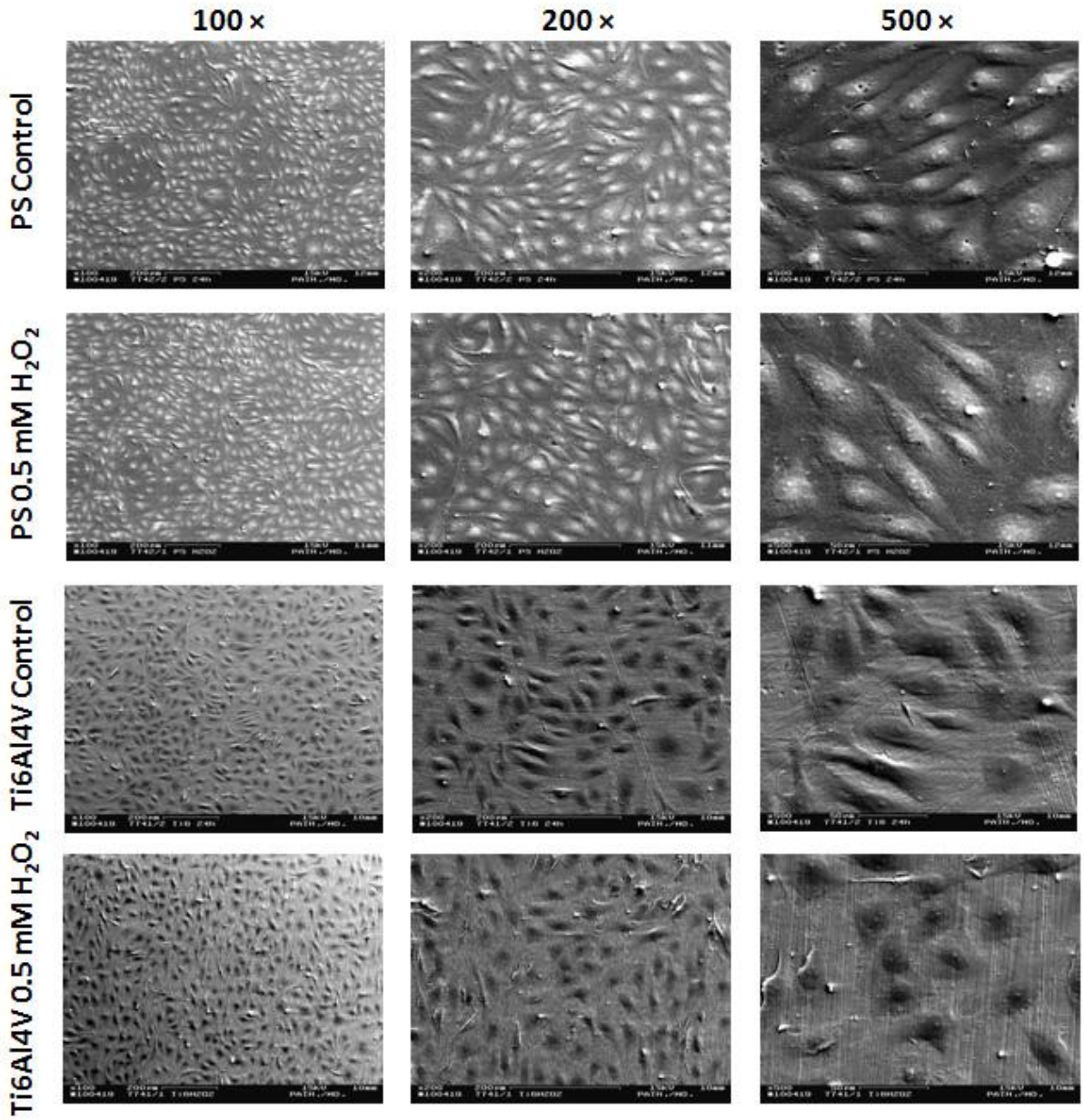


**Fig. 3.3.** *The phenotype of HDMEC grown on PS and Ti6Al4V alloy. HDMEC were cultured on PS and Ti6Al4V alloy for 72 h, untreated or treated with 0.5 mM $H_2O_2$ for 24h ($H_2O_2$ was added 48 h after seeding of the cells on the materials). Eventually the cells were fixed and scanning electron microscopy images were taken.*

To examine the effects of $H_2O_2$ on the phenotype of endothelial cells $H_2O_2$ was added for 24 h to HDMEC growing on PS and Ti6Al4V alloy. 0.5 mM $H_2O_2$ did not induce drastic changes in the phenotype of HDMEC on PS (Fig. 3.3). The cells retained their spindle-like shape, organised alignment and the degree of confluence. HDMEC grown on Ti6Al4V alloy appeared to be more influenced by $H_2O_2$. The alignment of the cells became more disordered, most of the cells lost the spindle-like shape and appeared rounded, and the amount and the size of the gaps in the cell monolayer increased. In general this points to the higher toxicity of $H_2O_2$ to HDMEC grown on Ti6Al4V alloy, compared to HDMEC on PS.

### 3.1.3. Evaluation of cytotoxicity of $H_2O_2$ on endothelial cells grown on Ti6Al4V

To study cytotoxic effects the response to $H_2O_2$ elicited in HDMEC grown on Ti6Al4V was compared with the reaction of HDMEC grown on PS. Therefore, cell proliferation, cell integrity and metabolic activity were evaluated.

The cell numbers between both growth substrates tested did not differ significantly in the untreated state (Fig. 3.4.A). On both surfaces $H_2O_2$ treatment led to the reduction of cell

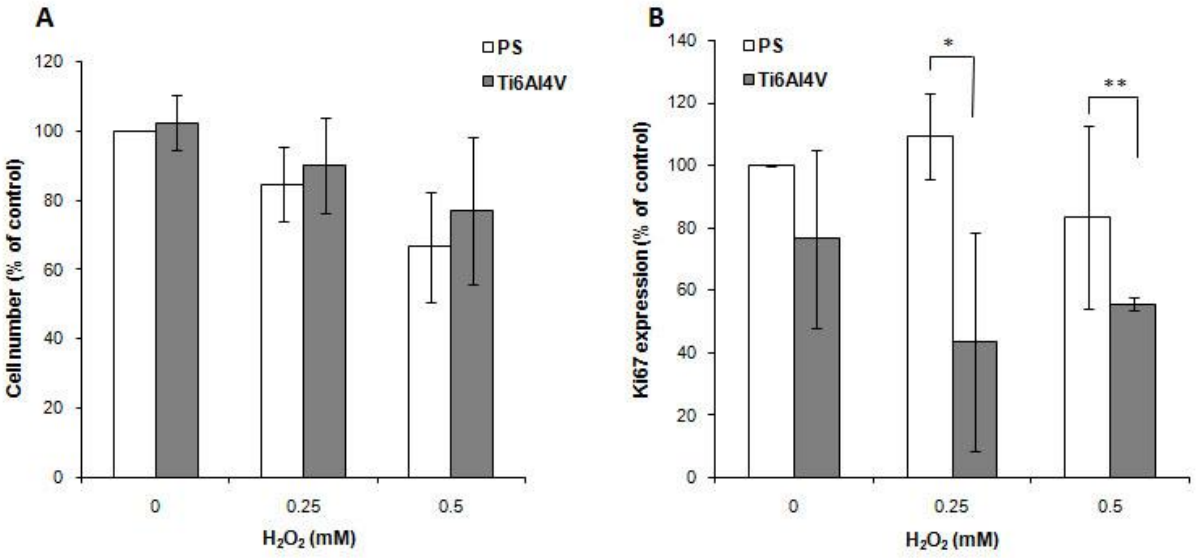


**Fig. 3.4.** *Quantification of the cell number and proliferation status of HDMEC grown on PS and Ti6Al4V 24 h after treatment with $H_2O_2$.* ***A.*** *Cell number of HDMEC was determined via quantification of the images of the nuclei staining with Hoechst 33234.****B.*** *Proliferation status was assessed by measuring Ki67 expression in HDMEC on PS and Ti6Al4V with EIA. Ki67 expression was related to the cell number (means ± SDs; untreated control on PS set as 100%, significant difference:* $p<0.05$, ** $p<0.01$).*

number after 24 h without significant differences (0.25 mM $H_2O_2$ led to a reduction of 15% on PS and to 10% reduction on Ti6Al4V, 0.5 mM $H_2O_2$ induced a reduction of >30% on PS and >20% on Ti6Al4V). Another parameter related to the cell proliferation is the expression of Ki67 protein, which is exclusively present in the nuclei of proliferating cells. The expression of Ki67 in HDMEC on Ti6Al4V alloy was lower than that on PS, although the difference was not significant (Fig. 3.4.B). 0.5 mM $H_2O_2$ caused around 20% reduction of the number of proliferating cells on PS, while 0.25 mM $H_2O_2$ slightly increased this value. In contrast, both concentrations induced a decrease in Ki67 expression in HDMEC on Ti6Al4V (around 60% reduction in the case of 0.25mM and around 50% in the case of 0.5 mM $H_2O_2$). Interestingly, there was a significant difference between Ki67 expression in HDMEC grown on Ti6Al4V 24 h after $H_2O_2$ addition compared to the $H_2O_2$-treated cells on PS. Such an effect indicates that $H_2O_2$ inhibited HDMEC proliferation on Ti6Al4V alloy to a greater extent than on PS, although probably due to a slow proliferation rate of endothelial cells it did not lead to notable differences in total cell number at the time point of the measurement.

The reduction of the number of HDMEC points to the cytotoxicity of $H_2O_2$ at the concentrations used in this study (0.25 and 0.5 mM). To determine the cytotoxicity of $H_2O_2$ on HDMEC grown on titanium alloy and PS LDH-activity in the cell culture supernatant was measured 24 h after the addition of $H_2O_2$. An increased release of LDH from HDMEC was

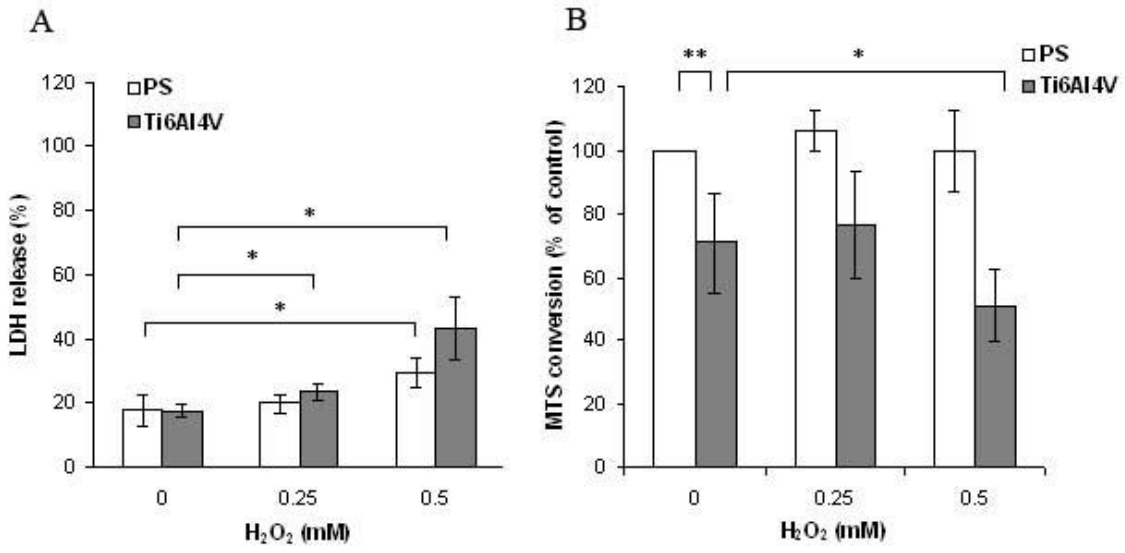


**Fig. 3.5.** *Evaluation of $H_2O_2$ cytotoxicity in HDMEC.* ***A.*** *Membrane damage manifested by LDH release from HDMEC grown on PS and Ti6Al4V measured 24 h after treatment with $H_2O_2$.* ***B.*** *Metabolic activity of HDMEC grown on PS and Ti6Al4V determined with MTS conversion assay 24 h after $H_2O_2$ application (untreated control on PS set as 100%; means ± SDs; significant difference: *p<0.05, **p<0.01).*

observed after $H_2O_2$ treatment, with the higher $H_2O_2$-induced LDH release being observed in cells grown on Ti6Al4V alloy (Fig 3.5.A, increase in LDH-release of ca. 10% on PS and 20% on Ti6Al4V by 0.5 mM $H_2O_2$ in comparison to the untreated control). The increased release of LDH indicates elevated damage of cell membranes upon $H_2O_2$ treatment, a characteristic sign of necrotic cell death.

The measurement of cellular metabolic activity by the MTS conversion assay revealed that untreated HDMEC grown on Ti6Al4V alloy surfaces displayed a significantly ($p$<0.01) lower MTS conversion rate than HDMEC on PS, thus indicating reduced metabolic activity of cells grown on Ti6Al4V. Impaired cellular metabolic activity in HDMEC on Ti6Al4V alloy could not be explained by the differences in the number of cells, which was equal on PS and Ti6Al4V at the time of MTS measurement (see Fig. 3.4.A). Furthermore, the $H_2O_2$ treatment of HDMEC grown on PS did not significantly change metabolic activity of the cells, whereas 0.5 mM $H_2O_2$ led to a reduction of about 20% of the MTS conversion in comparison to the untreated cells on Ti6Al4V (Fig 3.5.B). Thus, the basic metabolic activity of cells grown on Ti6Al4V was reduced and the highest tested $H_2O_2$-concentration (0.5 mM) exerted a significant cytotoxic effect (shown by LDH release and MTS conversion) only in cells in contact with Ti6Al4V.

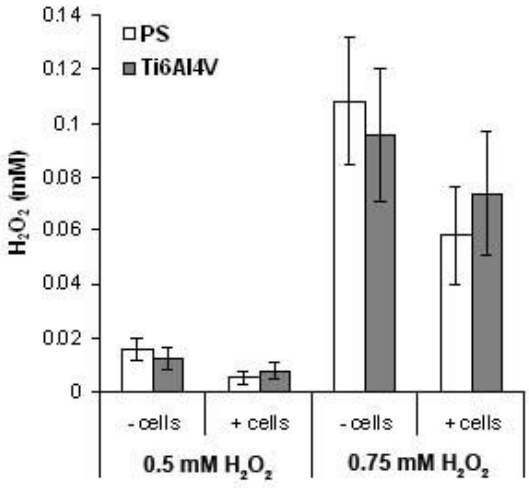


**Fig. 3.6.** A*ssessment of $H_2O_2$ decay in cell culture medium in contact with PS and Ti6Al4V with and without HDMEC. Freshly prepared $H_2O_2$ solutions in cell culture medium were added to PS and Ti6Al4V in the presence or absence of growing HDMEC and after 1 h remaining $H_2O_2$ amount was measured with a colorimetric assay (means ± SDs).*

$H_2O_2$ is unstable and may rapidly decompose in the cell culture medium by e.g. catalase present in the serum or released by cells. To determine whether the differences in the

sensitivity of HDMEC grown on titanium alloy and PS might be induced by differences in $H_2O_2$ decay rates in cell culture medium depending on the adhesion substrates the $H_2O_2$ concentration in the medium was analysed (Fig. 3.6). One hour after the addition of 0.5 mM to the medium $H_2O_2$ was nearly completely decomposed (i.e. ca. 0.02 mM $H_2O_2$ for PS and 0.015 mM for Ti6Al4V was detected). This indicated that only about 3% of the added amount of $H_2O_2$ remained in contact with PS and Ti6Al4V. When a 50% higher $H_2O_2$ concentration (0.75 mM) was added the decomposition was not as pronounced. After 1 h a $H_2O_2$ concentration of approximately 0.1 mM was detectable, which was approximately 14% of the initial amount of $H_2O_2$ added. In the presence of HDMEC the $H_2O_2$ decomposition occurred even more rapidly. There were no statistically significant differences in $H_2O_2$ decomposition between Ti6Al4V and PS indicating that the growth substrates did not influence the amount of $H_2O_2$ to which the cells were exposed.

Altogether these assays showed no differences in the cell number of HDMEC on PS and Ti6Al4V alloy but a clear response of HDMEC on Ti6Al4V to $H_2O_2$ with an increased LDH release and decreased proliferation and metabolic activity. Importantly, metabolic activity was impaired even in untreated cells on Ti6Al4V. Corrosion of the titanium alloy, with ROS as the intermediate corrosion products, could possibly be the cause of impairment of cell viability of HDMEC on Ti6Al4V. Therefore, the signs for oxidative stress were further analysed.

### 3.1.4. Oxidative stress in endothelial cells exposed to Ti6Al4V surface

$H_2O_2$ is known to induce the formation of other radicals in the cell. It is also known that $H_2O_2$ can react with $TiO_2$, which normally covers the surface of titanium alloys. Therefore the induction of ROS by $H_2O_2$ was measured in HDMEC growing on PS and Ti6Al4V. To study intracellular radical formation after $H_2O_2$ treatment the DCF-assay was utilised. The assay demonstrated that $H_2O_2$ induced a dose-dependent formation of ROS in HDMEC as early as 1 h after treatment (Fig. 3.7.A). One hour after applying 0.5 mM $H_2O_2$, DCF fluorescence in the cells grown on Ti6Al4V alloy was significantly higher ($p<0.05$) then the corresponding values in cells grown on PS (i.e. >5-fold higher on Ti6Al4V vs. >3-fold higher on PS compared to the untreated control). The data suggest that $H_2O_2$ provokes a stronger oxidative stress response in HDMEC in contact with Ti6Al4V alloy compared to HDMEC grown on PS.

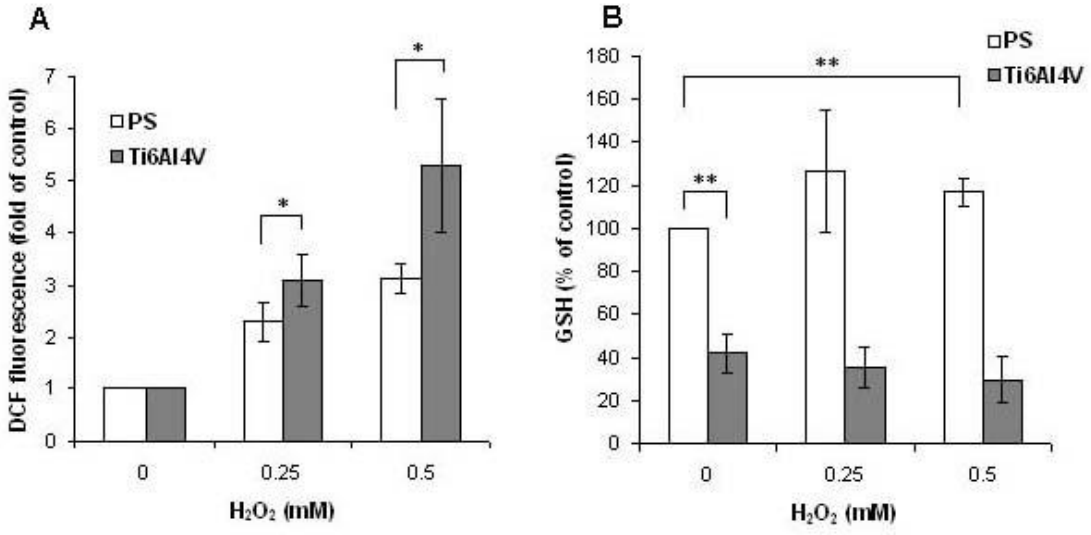


**Fig. 3.7.** *Evaluation of oxidative stress in HDMEC grown on PS and Ti6Al4V.* ***A.*** *ROS formation in HDMEC grown on PS and Ti6Al4V measured with DCF assay 1 h after addition of $H_2O_2$ (DCF fluorescence in untreated cells on each surface set as 1).* ***B.*** *GSH amount in HDMEC grown on PS and Ti6Al4V determined 24 h after $H_2O_2$ treatment with the specific fluorescent probe monochlorobimane and normalized to the protein amount (untreated control on PS set as 100%; means ± SDs; significant difference: *p<0.05, **p<0.01).*

GSH is a component of the cellular antioxidant defence system and is oxidised during detoxification of hydrogen peroxide and $H_2O_2$-induced organic peroxides. Therefore, to estimate the intracellular oxidation status induced by exposure to $H_2O_2$ the amount of GSH in HDMEC cultured on Ti6Al4V and PS was analysed 24 h after treatment. Interestingly, the level of GSH in the cells exposed to the Ti6Al4V alloy surface without the addition of $H_2O_2$ was significantly lower ($p$<0.01) and exhibited only 40% of the GSH amount in the cells grown on PS (Fig. 3.7.B). Furthermore, while the concentration of GSH increased in the cells cultured on PS following $H_2O_2$ treatment (around 20% increase for treatment with 0.5 mM $H_2O_2$, $p$<0.01), the GSH-concentration was slightly reduced in the cells grown on titanium alloy after 24 h. These observations correlate with reduced metabolic activity on Ti6Al4V alloy and point to a permanent oxidative stress state of HDMEC in contact with Ti6Al4V surfaces.

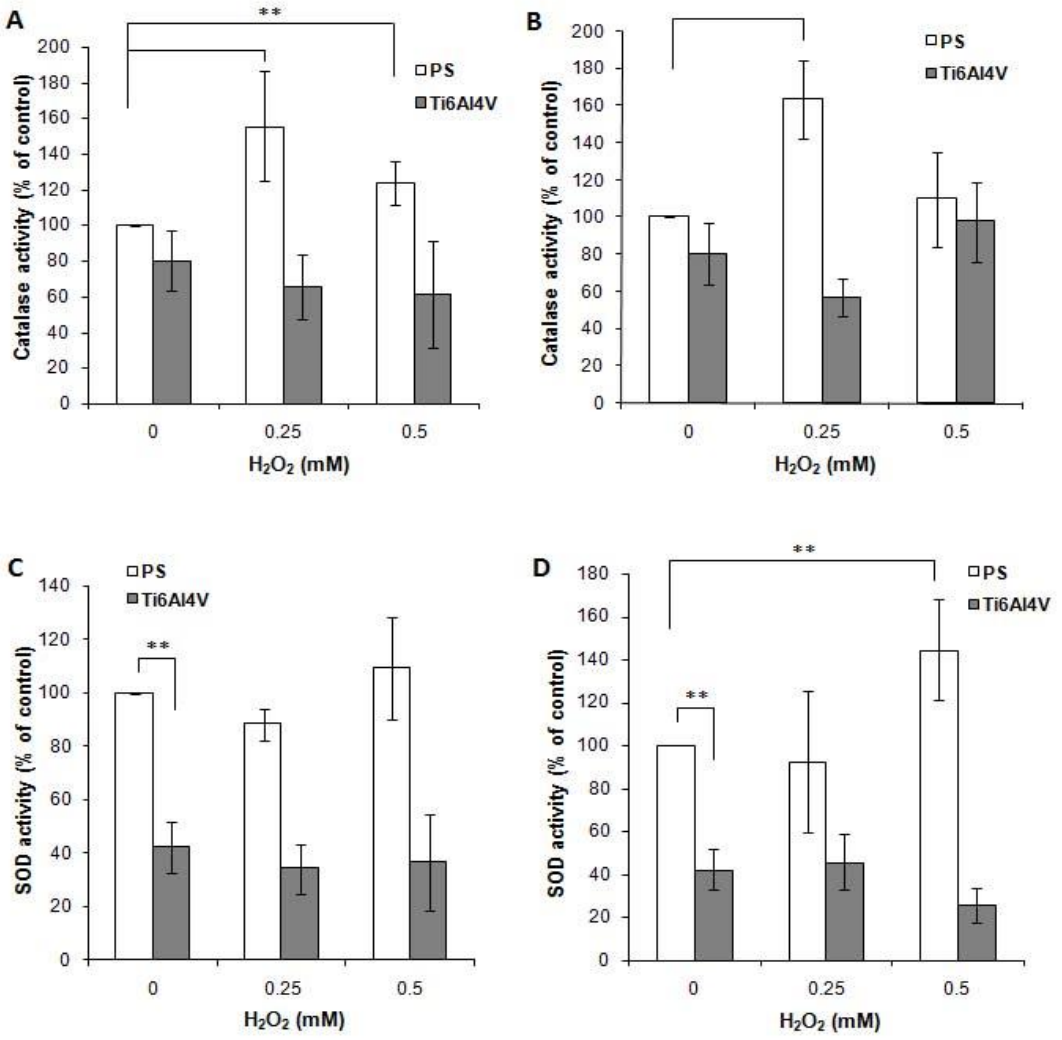


**Fig. 3.8.** *Measurement of antioxidant enzymes activity in HDMEC grown on PS and Ti6Al4V. Catalase (**A, B**) and SOD (**C, D**) activities were measured in HDMEC 4 (**A, C**) or 24 h (**B, D**) after $H_2O_2$ treatment with corresponding activity assay and related to protein concentration of the samples. The data are presented as % of control (untreated HDMEC on PS; means ± SDs; significant difference: **p<0.01).*

To further investigate the reactions of HDMEC on Ti6Al4V and PS to $H_2O_2$ the activity of two antioxidant enzymes, catalase and SOD, was studied 4 and 24 h after treatment. Catalase activity in untreated HDMEC grown on Ti6Al4V was slightly lower than in cells grown on PS at both time points, although the differences were not statistically significant (Fig. 3.8.A, B). However, the changes in catalase activity of HDMEC in response to $H_2O_2$ were divergent on the different adhesion substrates. On PS, catalase activity was increased 4 h after treatment with both $H_2O_2$ concentrations with 0.25 mM inducing a stronger effect (Fig.3.8.A). 24 h after exposure to 0.25 mM $H_2O_2$ catalase activity in HDMEC on PS significantly increased (around 60% increase) but was at the control level after exposure to

0.5 mM (Fig. 3.8.B). In contrast, catalase activity decreased in HDMEC grown on Ti6Al4V exposed to $H_2O_2$ for 4 h (approximately 30% reduction for both concentrations). After 24h the decrease in catalase activity was only observed upon addition of 0.25 mM $H_2O_2$ but was around the control levels after exposure to 0.5 mM $H_2O_2$. Overall the data point to the diverse regulation of catalase activity in HDMEC on PS and Ti6Al4V. While on PS $H_2O_2$ seemed to induce adaptive increase in catalase activity, more prominent with the lower concentration, on Ti6Al4V catalase activity was reduced after $H_2O_2$ exposure with probable adaptive increase appearing later and at higher $H_2O_2$ concentration (24 h after addition of 0.5 mM $H_2O_2$).

The activity of SOD was significantly lower in untreated HDMEC grown on Ti6Al4V than in cells grown on PS at both time points (Fig. 3.8.C, D, ca. 60% less SOD-activity on Ti6Al4V than on PS). The $H_2O_2$ treatment resulted in more pronounced differences in the overall SOD activity on the two materials. Although low $H_2O_2$-concentrations (0.25 mM) did not induce significant changes compared to the respective untreated control, higher $H_2O_2$-amounts (0.5 mM) increased SOD activity in HDMEC grown on PS with the difference becoming significant after 24 h (around 50% increase after treatment with 0.5 mM $H_2O_2$, $p<0.01$). 0.5 mM $H_2O_2$ also led to the reduction in SOD-activity in HDMEC on Ti6Al4V 24 h upon $H_2O_2$ treatment (around 40% reduction). Altogether, the data support the occurrence of permanent oxidative stress in HDMEC on Ti6Al4V compared to HDMEC on PS, which increases further following exposure to $H_2O_2$.

To support further the observations on permanent oxidative stress on Ti6Al4V alloy HDMEC were grown on PS and Ti6Al4V alloy in the presence of ROS scavengers. Dimethylthiourea (DMTU) and glutathione monoethyl ester (GSH-MEE) were added to cell culture medium 4 h after seeding HDMEC on growth substrate and were present during the entire experiment (4 days) with addition of fresh scavengers with each medium change (every 24 h). DMTU addition did not have any significant effect on metabolic activity of HDMEC, either on PS or on Ti6Al4V alloy (Fig. 3.9.A). In contrast, exposure to GSH-MEE led to a significant increase in metabolic activity of HDMEC on both materials (Fig. 3.9.B). Taking into account diminished metabolic activity in untreated HDMEC grown on Ti6Al4V a higher elevation of MTS conversion by GSH-MEE was observed on Ti6Al4V (1.74 fold against 1.62 on PS). Elevated MTS conversion in HDMEC grown on PS could be explained by the protective effect of GSH-MEE against a spontaneous oxidative stress occurring in all cells under culture conditions. While part of the increase in metabolic activity of HDMEC on Ti6Al4V can also be explained by a shielding effect of GSH-MEE on spontaneous oxidative

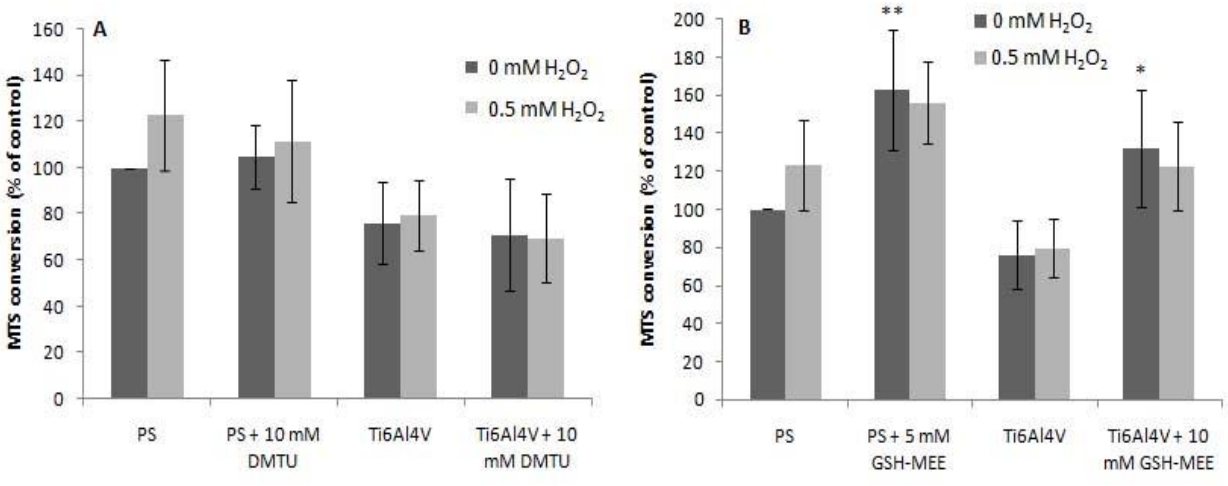


**Fig. 3.9.** *Effect of ROS scavengers on metabolic activity of HDMEC grown on PS and Ti6Al4V. DMTU (**A**) and GSH-MEE (**B**) were added to the cells 4 h after seeding and were present during the whole experiment. $H_2O_2$ treatment was performed for 24 h. MTS conversion assay and cell number quantification with Hoechst 33342 staining were performed and MTS conversion was related to the cell number in each sample (untreated HDMEC on PS are set as 100%; means ± SDs; significant difference: **p<0.1, *p<0.05).*

stress, at least part of it is likely to result from protection against oxidative stress induced on the surface of Ti6Al4V.

### 3.1.5. Effects of cathodic partial reaction of Ti6Al4V corrosion on HDMEC

Although Ti6Al4V is normally coated with an inactive $TiO_2$ layer corrosion is still taking place on Ti6Al4V in solution. ROS formation as a result of cathodic partial reaction of corrosion might be one of the reasons for the observed oxidative stress state of HDMEC grown on Ti6Al4V alloy. Therefore, HDMEC were grown on Ti6Al4V placed in an electrochemical setup, which allows spatial separation of cathodic and anodic partial reactions, and Ti6Al4V was polarised to induce specifically a cathodic partial reaction of corrosion.

Electrochemical polarisation of Ti6Al4V for 1 h did not lead to the reduction of metabolic activity of HDMEC. In fact, polarisation with current densities of -2.5 µA/cm$^2$ and -5 µA/cm$^2$ slightly increased MTS conversion, but the increase was not significant (Fig. 3.10.A). In contrast, Ti6Al4V polarisation for 24 h led to current density-dependent decrease

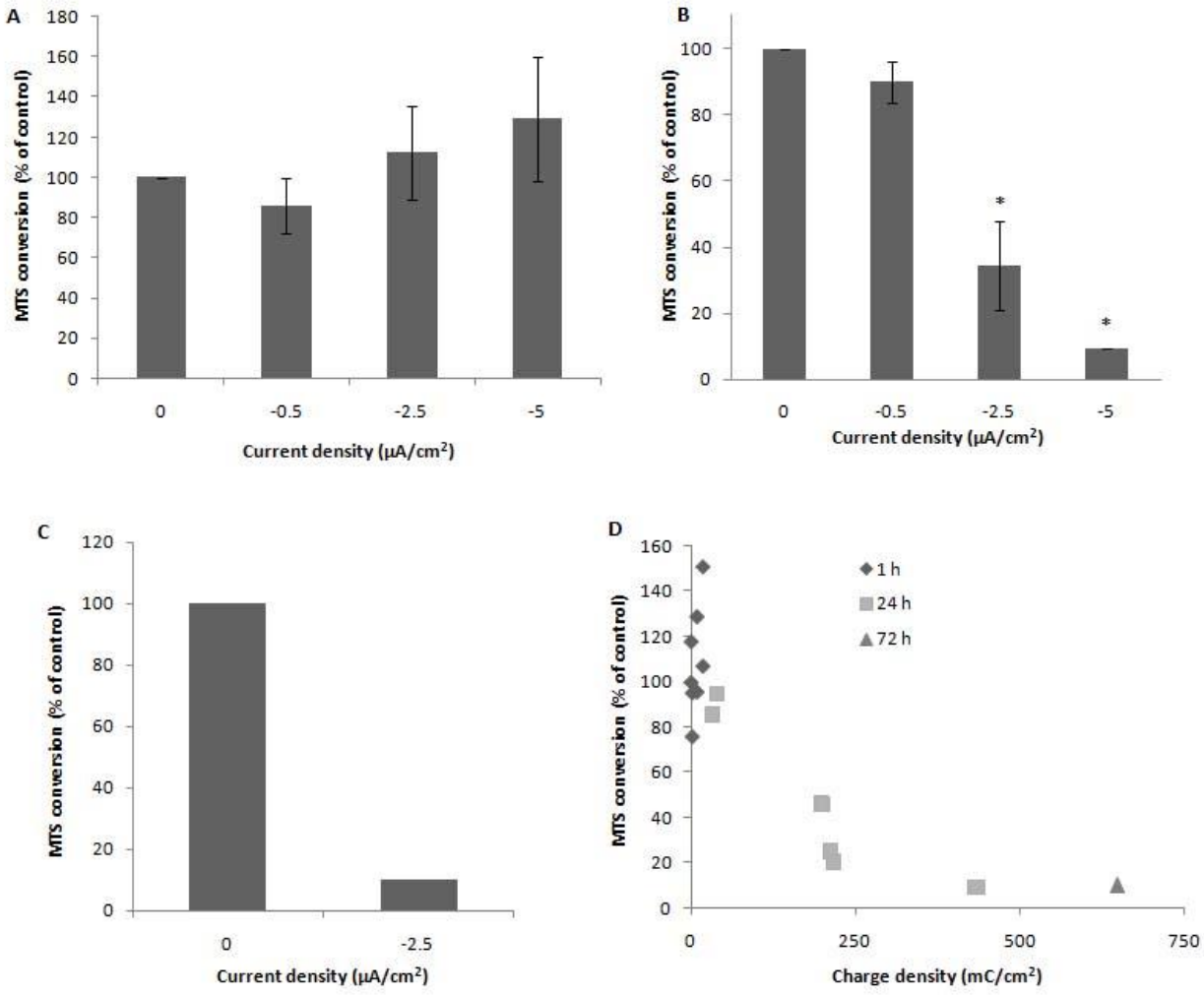


**Fig. 3.10.** *The effect of cathodical partial reaction of corrosion on viability of HDMEC. Metabolic activity of HDMEC on Ti6Al4V was measured with MTS conversion assay after Ti6Al4V cathodical polarisation for 1 h (**A**), 24 h (**B**) or 72 h (**C**). **D**. Dependency of MTS conversion in HDMEC on charge density applied to Ti6Al4V (untreated HDMEC are set as 100%; means ± SDs; significant difference:*p<0.001).*

in HDMEC metabolic activity (around 65% reduction in case of -2.5 µA/cm$^2$ and more than 90% decrease after polarisation with -5 µA/cm$^2$, p<0.001, Fig. 3.10.B). Electrochemical treatment with -2.5 µA/cm$^2$ for 72 h led to almost complete loss of viability (around 90% reduction of cellular metabolic activity, Fig. 3.10.C). Fig. 3.10.D. shows the dependency of HDMEC cell viability on charge density, which represents the amount of radicals formed on the interface of Ti6Al4V alloy during the whole duration of treatment. The data show the charge density-dependent reduction in metabolic activity of HDMEC. At the low charge density cell viability did not change significantly with 1 h and 24 h treatments, which gave

similar viability values. Electrochemical polarisation of Ti6Al4V alloy with charge densities around 200 mC/cm$^2$ (that results in the production of around 1 µmol/cm$^2$ $H_2O_2$ according to

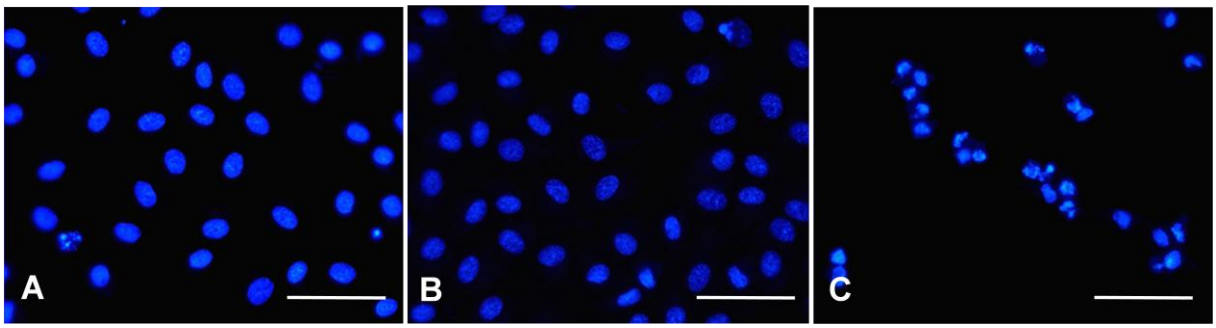


**Fig. 3.11.** *Nuclear phenotype in untreated HDMEC (**A**) on Ti6Al4V alloy and after cathodic polarisation for 24 h with -0,5 µA/cm$^2$ (**B**) and -2,5 µA/cm$^2$ (**C**, fluorescent microscopy of nuclei stained with Hoechst 33342, scale bar: 50 µm ).*

theoretical calculations using Faraday's law) led to around 70% decrease in cellular metabolic activity with higher charge densities causing even higher (approximately 90%) decline in cell viability.

HDMEC on cathodiacally polarised Ti6Al4V alloy also showed altered cell nuclear shape, pointing to cell death. While the nuclear phenotype of HDMEC exposed to -0.5 µA/cm$^2$ was similar to that of untreated cells, current density of -2.5 µA/cm$^2$ induced the condensation of cell nuclei (Fig. 3.11). The appearance of the nuclei did not, however, give any indication of the type of cell death.

To study the effect of electrochemical treatment on HDMEC phenotype the distribution of F-actin and CD31 was visualised with fluorescent staining (Fig. 3.12). Untreated HDMEC grown on Ti6Al4V showed the phenotype characteristic of endothelial cells. Most F-actin fibres were lying close to the cell membrane and formed so called peripheral actin rings. Some actin stress fibres were also seen in the cytoplasm. CD31 located at the cell surface in the area of cell contacts. HDMEC formed a confluent monolayer with no visible gaps between the cells. The phenotype of HDMEC grown on Ti6Al4V electrochemically polarised with -0.5 µA/cm$^2$ for 24 h did not differ significantly from the phenotype of untreated cells. On the contrary, cathodic polarisation with -5 µA/cm$^2$ for 24 h induced severe changes in cell shape and distribution of F-actin and CD31. Endothelial cell-typical F-actin distribution was completely lost, with actin staining disseminated through the cytoplasm and no distinct actin fibres visible. CD31 staining also indicated altered cell shape, with HDMEC loosening intercellular contacts.

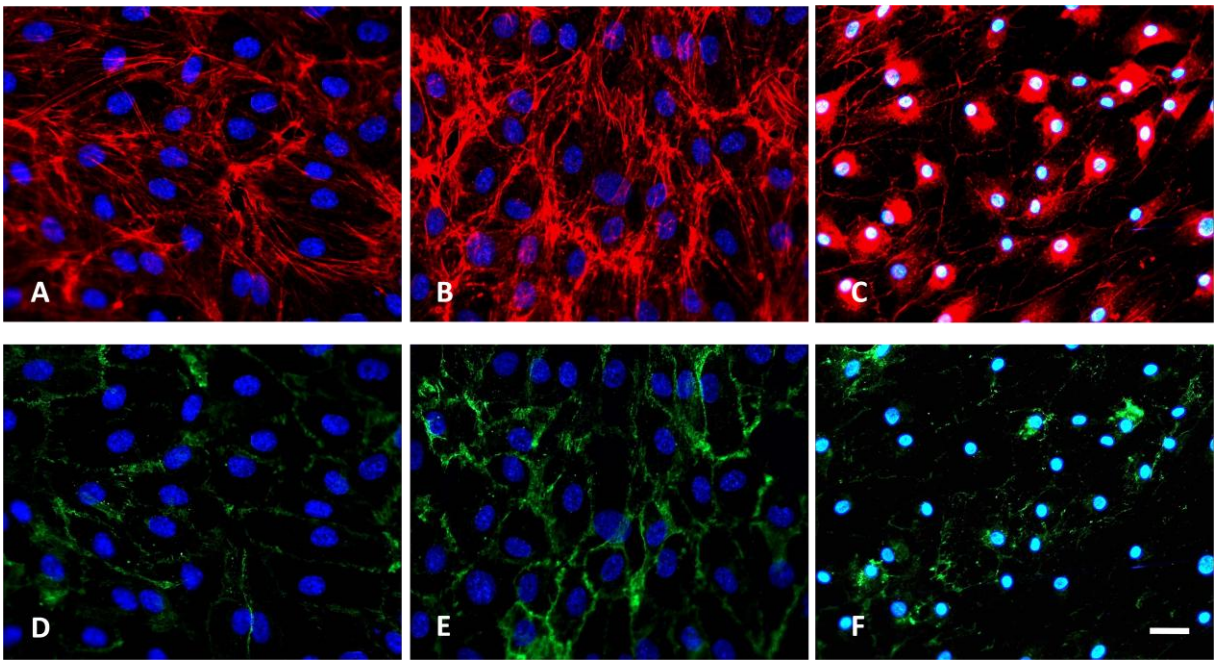


**Fig. 3.12.** *F-actin (**A-C**, red) and CD31 (**D-F**, green) staining of untreated HDMEC (**A, D**) on Ti6Al4V and after cathodic polarisation of Ti6Al4V alloy for 24 h with -0,5 µA/cm$^2$ (**B, E**) and -5 µA/cm$^2$ (**C, F,** fluorescent microscopy, nuclei were stained blue with Hoechst 33342, scale bar: 50 µm).*

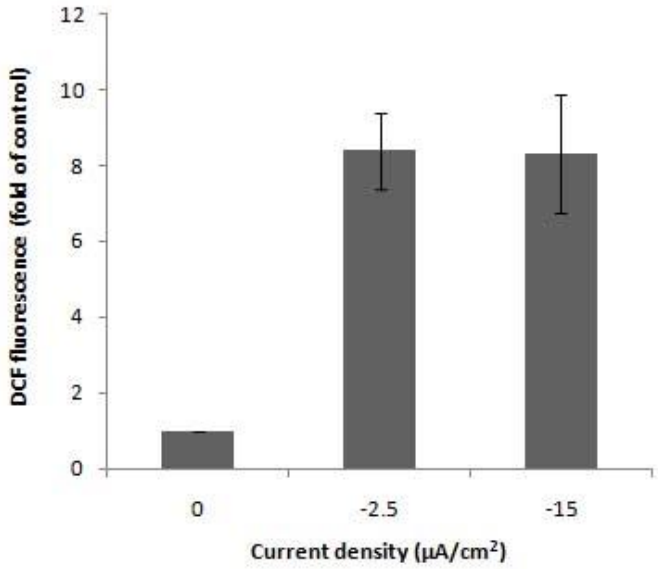


**Fig. 3.13. *A.*** *Evaluation of ROS formation in HDMEC grown on Ti6Al4V polarized for 24 h. ROS production was assessed with DCF assay (DCF fluorescence in untreated cells was set as 1).*

Altogether, the data point to the reduced viability of HDMEC exposed to cathodic partial reaction of Ti6Al4V corrosion. Since the production of radicals as intermediates of

cathodic partial reaction is one of the main processes which could be responsible for increased cytotoxicity on polarised Ti6Al4V, intercellular ROS production in HDMEC was measured. Electrochemical polarisation of Ti6Al4V alloy with -2.5 µA/cm$^2$ and -15 µA/cm$^2$ induced 8-fold induction in DCF fluorescence compared to the cells on unpolarised Ti6Al4V (Fig. 3.13). This observation indicates the elevated ROS production in HDMEC that can be explained as an amplified reaction of endothelial cells to the ROS formed during cathodic partial reaction of corrosion.

### 3.1.6. Effects of oxidative stress on Ti6Al4V alloy on pro-inflammatory activity of HDMEC

Since F-actin and CD31 are not only useful for endothelial cell visualisation but also provide information about their pro-inflammatory activation, actin and CD31 distribution was assessed in HDMEC grown on PS and Ti6Al4V in combination with $H_2O_2$ treatment.

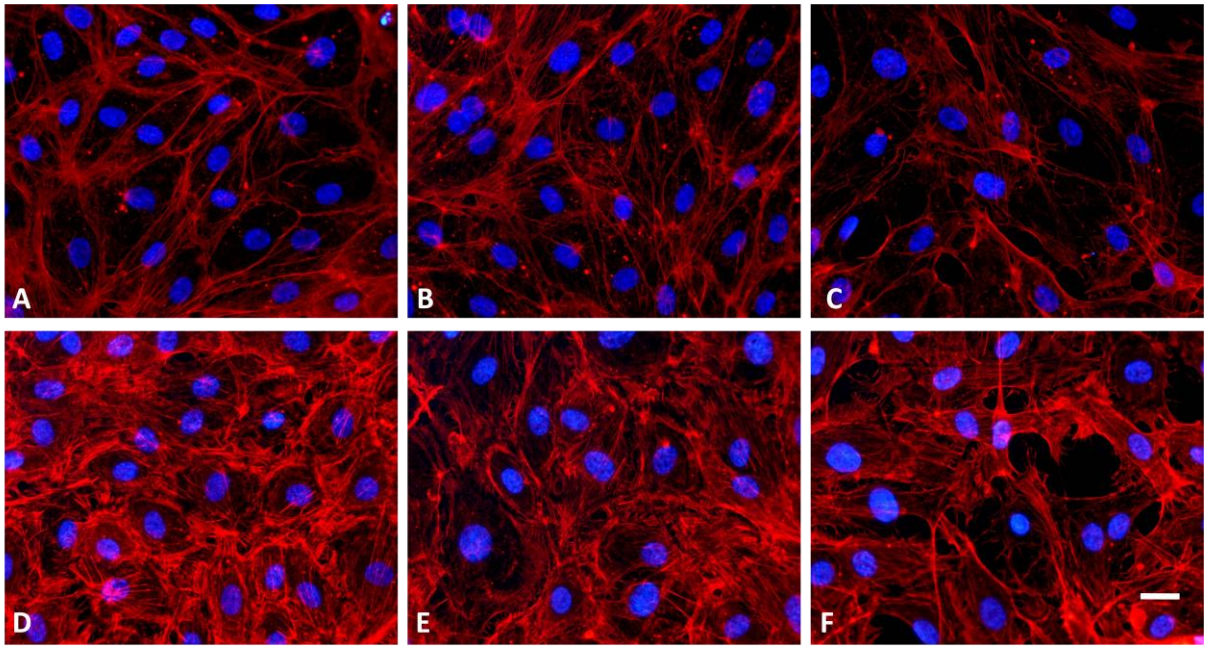


**Fig. 3.14.** *F-actin staining of HDMEC grown on PS (**A-C**) and Ti6Al4V (**D-F**). Cells were untreated (**A, D**) or treated with 0.25 mM (**B, E**) or 0.5 mM $H_2O_2$ (**C, F**) for 24 h (fluorescent miscroscopy, nuclei were stained blue with Hoechst 33342, scale bar: 50 µm).*

HDMEC grown on PS showed actin distribution typical for endothelial cells, i.e. a peripheral actin ring with almost no stress fibres in the cytoplasm (Fig. 3.14). $H_2O_2$ treatment (0.25 mM) induced the formation of stress fibres, although the cell shape and acting ring were

largely preserved. Higher $H_2O_2$ concentration caused more marked changes in actin distribution, with many stress fibres and no actin ring detectable. In contrast to untreated cells on PS, HDMEC grown on Ti6Al4V alloy showed actin distribution resembling pro-inflammatory activation. The cells exhibited a high number of actin stress fibres in the cytoplasm and the actin ring had almost disappeared. $H_2O_2$ treatment also caused changes in actin staining appearance, with 0.5 mM $H_2O_2$ inducing more severe changes.

CD31 in HDMEC on PS also had endothelial cell-specific distribution locating at intercellular contacts (Fig. 3.15). 0.25 mM $H_2O_2$ did not cause detectable changes in CD31 staining on PS, while 0.5 mM $H_2O_2$ abolished normal CD31 distribution, thus indicating loosening of cell contacts. HDMEC grown on Ti6Al4V showed less ordered CD31 distribution than the cells on PS. $H_2O_2$ addition induced more pronounced changes on Ti6Al4V alloy; sparser distribution of intercellular contacts was seen in HDMEC on Ti6Al4V treated with 0.5 mM $H_2O_2$ compared to $H_2O_2$-treated cells grown on PS.

The altered phenotype of HDMEC on Ti6Al4V alloy pointed to the stress state of the cells, which was in agreement with the observation of oxidative stress of endothelial cells on titanium alloy. It could also indicate the induction of an inflammatory response in endothelial cells by contact with the Ti6Al4V alloy. Therefore, expression of the pro-inflammatory adhesion molecules E-selectin and ICAM-1, as well as release of the cytokine

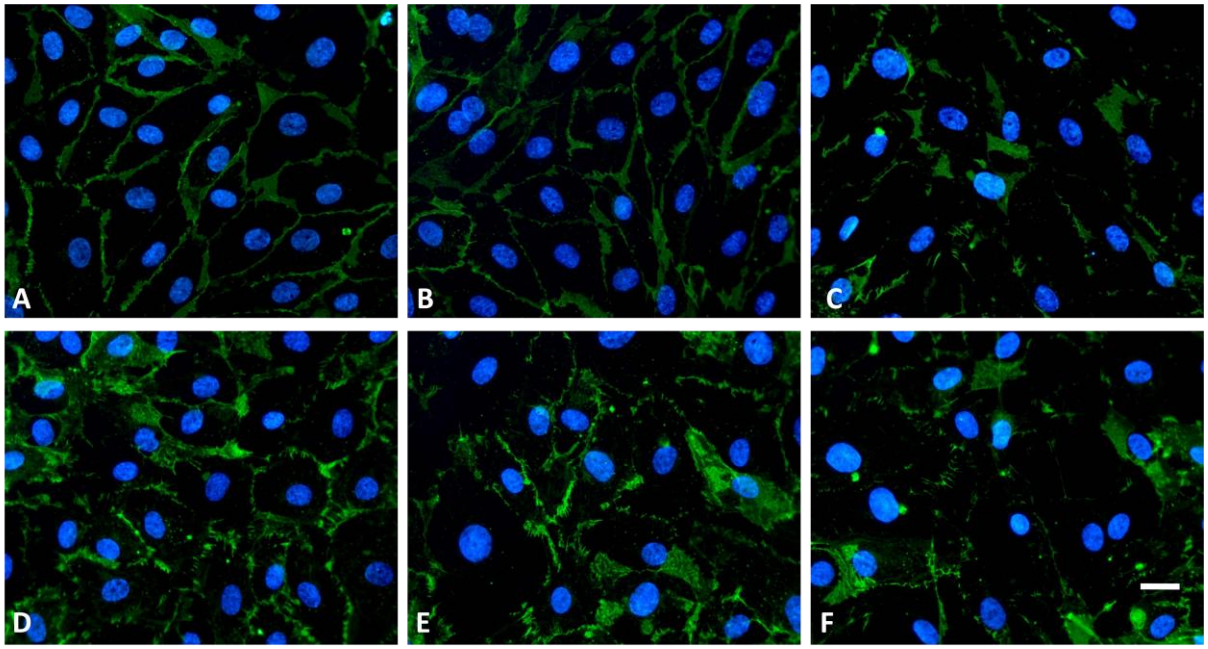


**Fig. 3.15.** *CD31 staining of HDMEC grown on PS (**A-C**) and Ti6Al4V (**D-F**). Cells were untreated (**A, D**) or treated with 0.25 mM (**B, E**) or 0.5 mM $H_2O_2$ (**C, F**) for 24 h (fluorescent miscroscopy, , nuclei were stained blue with Hoechst 33342, scale bar: 50 µm).*

IL-8 were compared in HDMEC grown on PS and Ti6Al4V (Fig. 3.16). The expression of E-selectin and ICAM-1 on the cell surface and the release of IL-8 into the cell culture medium was lower in HDMEC grown on Ti6Al4V. $H_2O_2$ treatment further decreased the amount of pro-inflammatory molecules on Ti6Al4V. In contrast, on PS the response of HDMEC to $H_2O_2$ was less homogenous: while E-selectin expression declined, $H_2O_2$ induced a modest increase in ICAM-1 expression and IL-8 release remained largely unaffected. However, the relevance of these changes is uncertain, since the expression of E-selectin, ICAM-1 and IL-8 release in untreated cells was at least 10-fold lower than in HDMEC stimulated with 75 U/ml TNF-α, a known pro-inflammatory factor. This indicated that the contact to Ti6Al4V alloy did not induce a pro-inflammatory activation in endothelial cells.

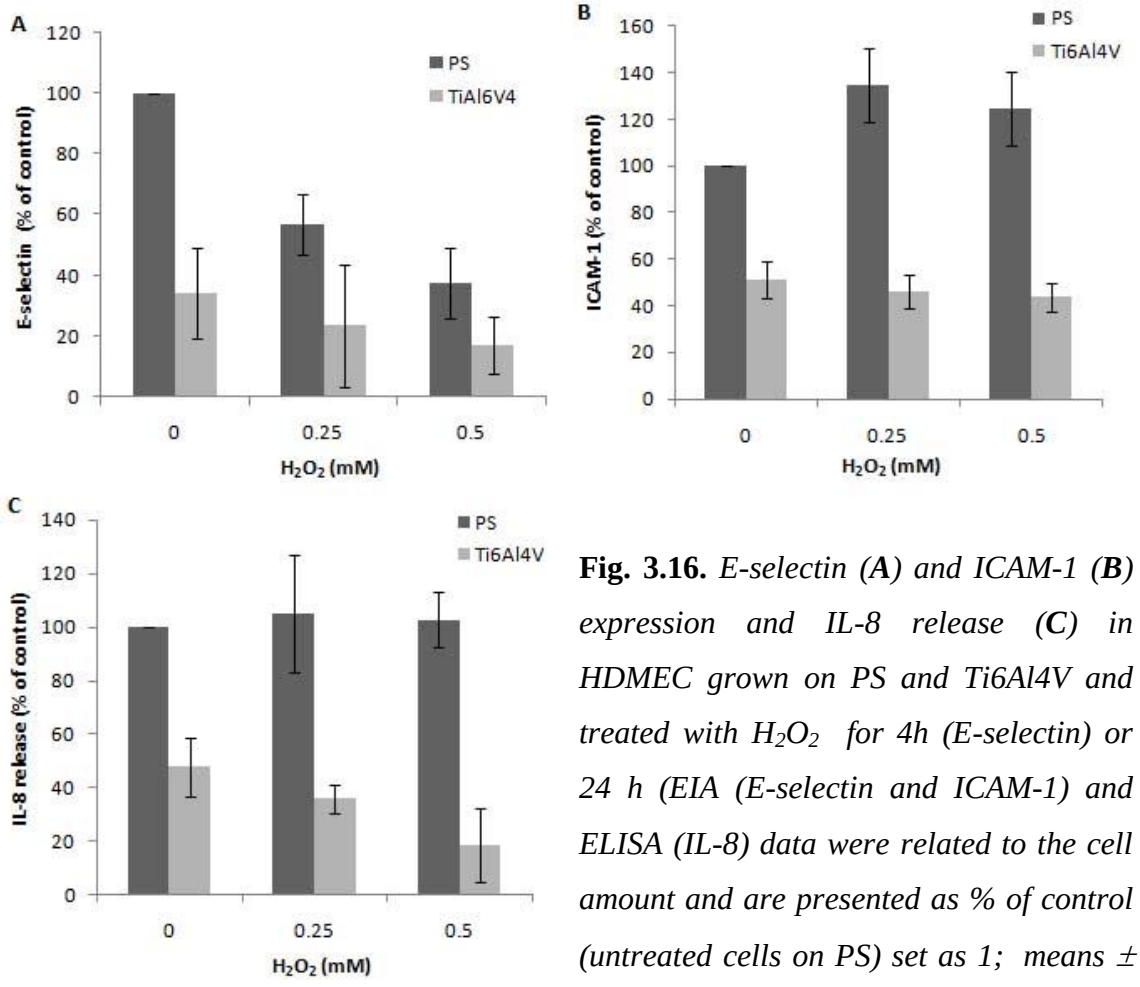


**Fig. 3.16.** *E-selectin (**A**) and ICAM-1 (**B**) expression and IL-8 release (**C**) in HDMEC grown on PS and Ti6Al4V and treated with $H_2O_2$ for 4h (E-selectin) or 24 h (EIA (E-selectin and ICAM-1) and ELISA (IL-8) data were related to the cell amount and are presented as % of control (untreated cells on PS) set as 1; means ± SDs).*

To study the differences in reactions of HDMEC on different growth substrates to inflammatory stimuli the cells were treated with pro-inflammatory molecules, TNF-α and LPS. The induction of E-selectin and ICAM-1 expression and IL-8 release by TNF-α and LPS was generally lower in HDMEC grown on Ti6Al4V compared to the cells on PS. The

induction of E-selectin expression on the surface of HDMEC grown on titanium alloy was around 45% lower for both TNF-α and LPS-treated cells (Fig. 3.17. A, B). $H_2O_2$ treatment additionally lowered E-selectin induction in HDMEC on Ti6Al4V. $H_2O_2$ also reduced TNF-α and LPS-induced up-regulation of E-selectin expression in the cells on PS but the effect was not as pronounced as on Ti6Al4V. The induction of ICAM-1 expression in HDMEC on Ti6Al4V was only 67 and 52% of the ICAM-1 up-regulation on PS by TNF-α and LPS, respectively (Fig. 3.17. C, D). Interestingly, $H_2O_2$ provoked a modest but significant increase in TNF-α-induced ICAM-1 up-regulation in HDMEC on PS. In contrast, there was no significant change in TNF-α-induced ICAM-1 expression in HDMEC on Ti6Al4V in case of $H_2O_2$ treatment. $H_2O_2$ did not influence LPS-induced ICAM-1 expression on either of the materials. IL-8 release after pro-inflammatory stimulation showed a pattern similar to ICAM-1 expression. TNF-α-induced IL-8 release was around 19% lower in cells grown on Ti6Al4V compared to PS, although the difference was not significant (Fig. 3.17. E). $H_2O_2$ treatment further increased TNF-α-induced IL-8 release by HDMEC on PS, while it did not induce any significant changes in HDMEC on Ti6Al4V. In case of LPS, up-regulation of IL-8 release by HDMEC grown on Ti6Al4V alloy was significantly lower (around 50%) than by cells grown on PS (Fig. 3.17. F). $H_2O_2$ treatment did not affect LPS-induced IL-8 release by HDMEC either on PS or on Ti6Al4V. Altogether, these data indicate a reduced pro-inflammatory response of HDMEC grown on Ti6Al4V alloy to pro-inflammatory stimuli. A synergistic effect of TNF-α and $H_2O_2$ on ICAM-1 expression and IL-8 release observed in HDMEC grown on PS could not be seen in the cells grown on Ti6Al4V, further pointing to the reduced ability of endothelial cells in contact to Ti6Al4V to respond to inflammatory stimulation.

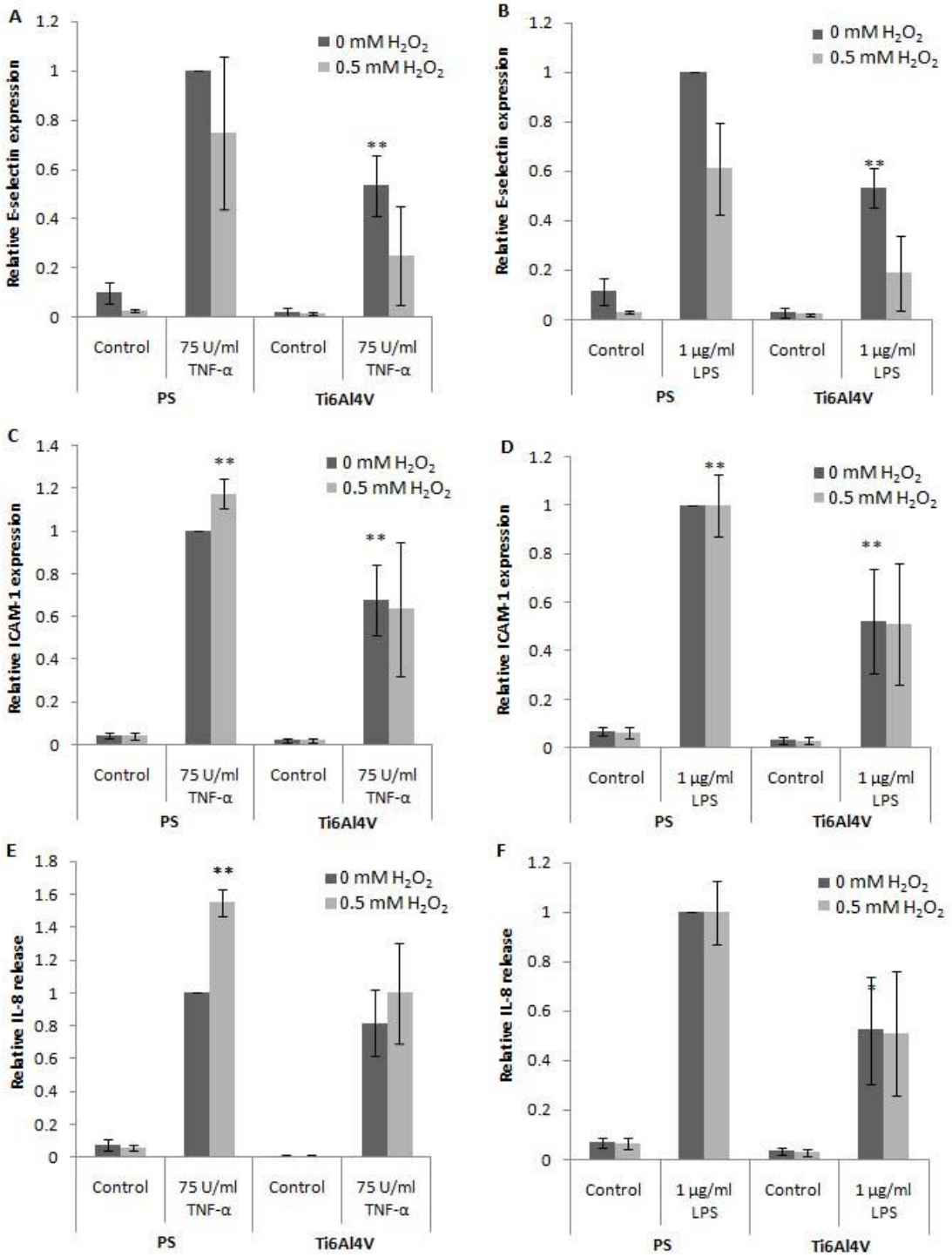


**Fig. 3.17.** *E-selectin (**A, B**) and ICAM-1 (**C, D**) expression and IL-8 release (**E, F**) in HDMEC grown on PS and Ti6Al4V and stimulated with 75 U/ml TNF-α (**A, C, E**) or 1µg/ml LPS (**B, D, F**) and treated with 0.5 mM $H_2O_2$ for 4h (E-selectin) or 24 h (ICAM-1 and IL-8). E-selectin and ICAM-1 expression and IL-8 release were related to cell number. EIA (E-selectin and ICAM-1) and ELISA (IL-8) data are presented as fold of control (TNF-α or LPS treated cells on PS) set as 1. Cell number was determined with quantification of nuclear staining with Hoechst 33342 (means ± SDs, significant difference: *p<0.05, **p<0.01).*

To study if this reduced response to pro-inflammatory stimuli could be explained

simply by lower viability of TNF-α and LPS-treated HDMEC, metabolic activity and cell number were quantified under the same experimental conditions. As expected MTS conversion was lower in HDMEC grown on Ti6Al4V compared to the cells grown on PS and $H_2O_2$ treatment further substantiated this difference (Fig. 3.18.A). Importantly, TNF-α and LPS did not change metabolic activity of HDMEC on either of the growth substrates. In contrast, stimulation with TNF-α induced a slight decrease in cell number compared to untreated cells, however, there were no significant differences in the number of cells on PS and Ti6Al4V in any of treatment combinations (Fig. 3.18.B). Therefore, the disparities in the responses of HDMEC to pro-inflammatory stimuli on PS and Ti6Al4V could not be caused by diverse cell numbers on different materials, but could be related to the reduced metabolic activity of the cells on Ti6Al4V.

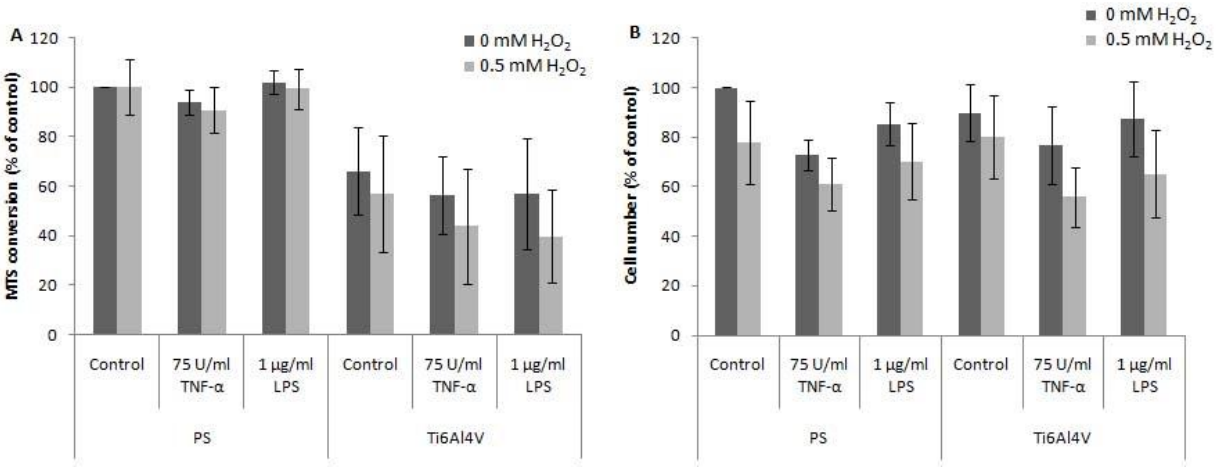


**Fig. 3.18.** *The effect of pro-inflammatory stimuli on metabolic activity (**A**) and cell number (**B**). HDMEC grown on PS and Ti6Al4V were stimulated with 75 U/ml TNF-α or 1µg/ml LPS and treated with 0.5 mM $H_2O_2$ for 24 h. Metabolic activity was measured with MTS conversion assay and cell number was assessed via quantification of nuclear staining with Hoechst 33342. The data are presented as % of control (untreated cells on PS) set as 1; means ± SDs).*

The induction of adhesion molecule expression and cytokine release by pro-inflammatory stimuli are known to be regulated at transcriptional level. Therefore, mRNA expression of E-selectin, ICAM-1 and IL-8 was estimated in TNF-α–stimulated HDMEC grown on PS and Ti6Al4V alloy. Surprisingly, the induction of mRNA expression of the studied inflammatory markers in HDMEC grown on Ti6Al4V was generally higher than in cells on PS. This observation was in contrast to the results at protein level, where HDMEC on

Ti6Al4V showed a slightly reduced reaction to TNF-α stimulation. TNF-α-induced E-selectin mRNA up-regulation was around twice as high in HDMEC on Ti6Al4V as in HDMEC grown on PS. On both materials $H_2O_2$ treatment further increased TNF-α-induced expression of E-selectin mRNA (Fig. 3.19.A). The same induction pattern was detected for ICAM-1 mRNA: TNF-α induced slightly higher up-regulation in cells on Ti6Al4V, with $H_2O_2$ inducing a further increase in ICAM-1 mRNA expression which was more pronounced on Ti6Al4V (Fig. 3.19.B). IL-8 mRNA was also induced by TNF-α in HDMEC on Ti6Al4V alloy to a higher extent (around 2-fold) then in the cells grown on PS. $H_2O_2$-treatment caused additional elevation of IL-8 mRNA levels that was slightly higher in HDMEC on PS. Generally, mRNA up-regulation patterns were similar in cells growing on different substrates. Conversely, the pattern of mRNA expression in HDMEC on PS upon TNF-α stimulation correlated to the protein expression in HDMEC under the same conditions (except for E-selectin). In contrast, on Ti6Al4V TNF-α-induced up-regulation of pro-inflammatory markers was reduced at the protein level compared to PS, while mRNA for the corresponding proteins was up-regulated even more efficiently in HDMEC on Ti6Al4V alloy than on PS. This pointed to a possibility

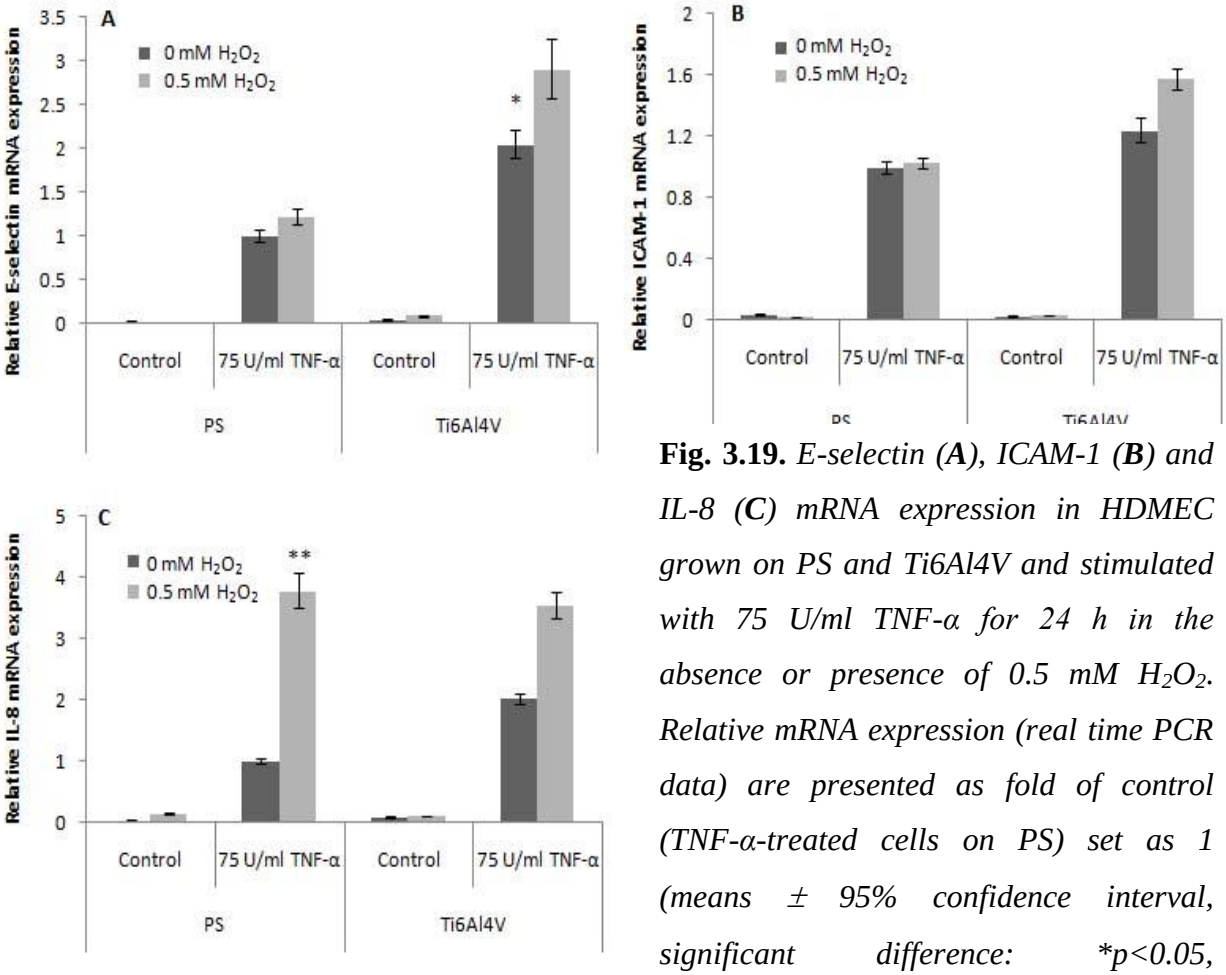


**Fig. 3.19.** *E-selectin (**A**), ICAM-1 (**B**) and IL-8 (**C**) mRNA expression in HDMEC grown on PS and Ti6Al4V and stimulated with 75 U/ml TNF-α for 24 h in the absence or presence of 0.5 mM $H_2O_2$. Relative mRNA expression (real time PCR data) are presented as fold of control (TNF-α-treated cells on PS) set as 1 (means ± 95% confidence interval, significant difference: *p<0.05, **p<0.01).*

of deregulation of mRNA to protein transition in the cells in contact with titanium alloy.

To test if oxidative stress occurring on Ti6Al4V alloy could be responsible for the reduced response of endothelial cells to inflammatory stimuli HDMEC grown on PS and Ti6Al4V were stimulated with TNF-α in the presence of the ROS scavengers DMTU and GSH-MEE. Treatment of HDMEC with DMTU increased TNF-α-induced expression of E-selecin, ICAM-1 and IL-8 mRNA on both materials (Fig. 3.20). Interestingly, however, the induction was more prominent in HDMEC grown on Ti6Al4V: around 3-fold higher for E-selectin ($p<0.05$), approximately 1.5-fold higher in the case of ICAM-1 and around 3-fold higher for IL-8 mRNA (for both $p<0.01$) compared to the cells treated with TNF-α and DMTU on PS. This was in agreement with the increased signs of oxidative stress in the cells growing on Ti6Al4V. In contrast, GSH-MEE did not induce any significant changes in the expression of mRNA under examination. Such disparity in the effects of different ROS scavengers (e.g. with different activity towards different ROS) on TNF-α-induced reactions together with the fact that $H_2O_2$ also elevated TNF-α-induced expression of E-selectin,

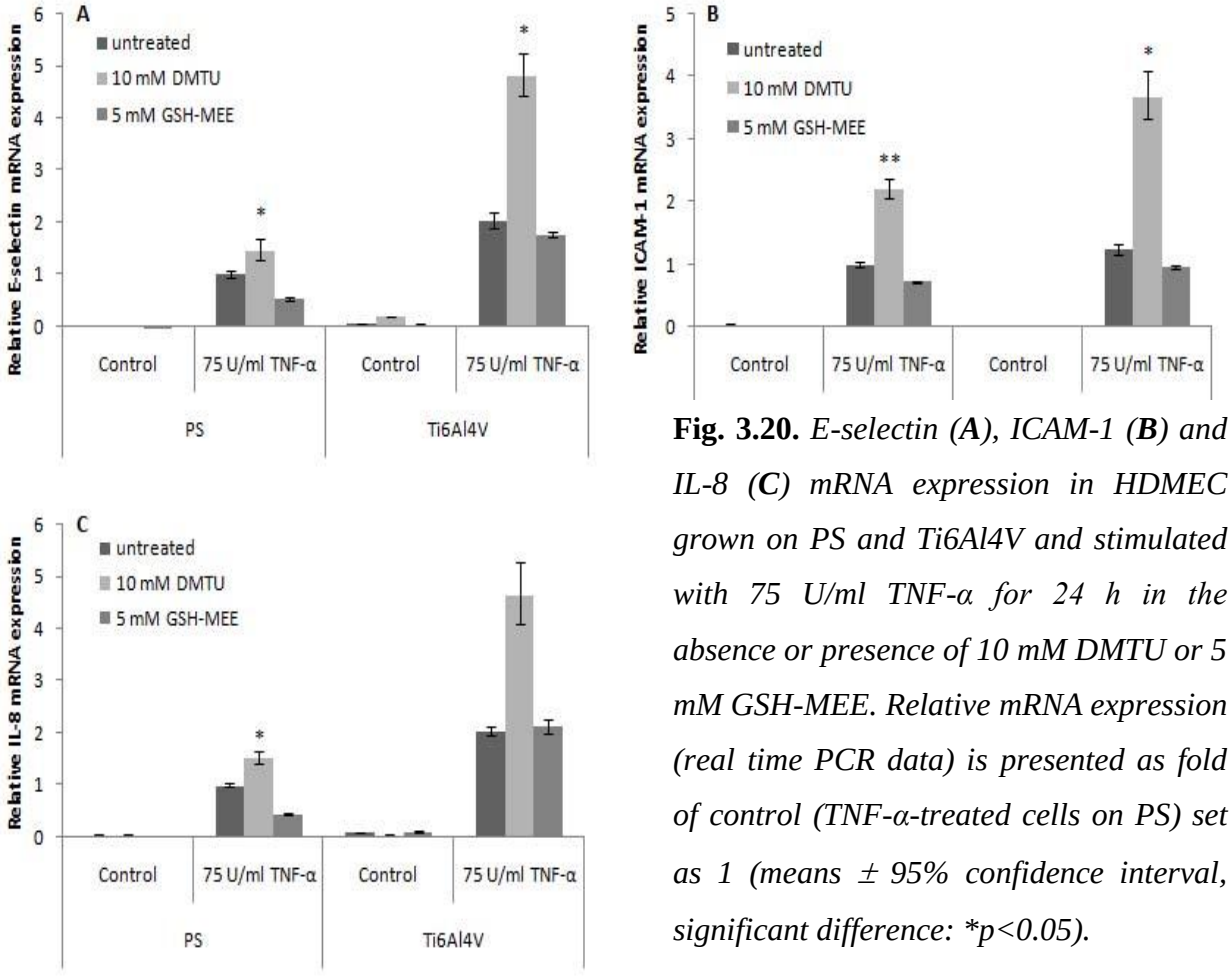


**Fig. 3.20.** *E-selectin (**A**), ICAM-1 (**B**) and IL-8 (**C**) mRNA expression in HDMEC grown on PS and Ti6Al4V and stimulated with 75 U/ml TNF-α for 24 h in the absence or presence of 10 mM DMTU or 5 mM GSH-MEE. Relative mRNA expression (real time PCR data) is presented as fold of control (TNF-α-treated cells on PS) set as 1 (means ± 95% confidence interval, significant difference: *p<0.05).*

ICAM-1 and IL-8 mRNA could suggest that different ROS might influence TNF-α signalling differently. DMTU and GSH-MEE also displayed different patterns regarding the influence on TNF-α-induced signalling and cellular metabolic activity: in the latter case GSH-MEE was able to restore metabolic activity of HDMEC on Ti6Al4V, while DMTU exerted no positive effect (Fig. 3.9).

To examine if the used ROS scavengers had the same effects on TNF-α-induced responses on the protein level IL-8 release and the expression of ICAM-1 on the surface of HDMEC grown on PS and Ti6Al4V alloy were studied. Similar to the effect on ICAM-1

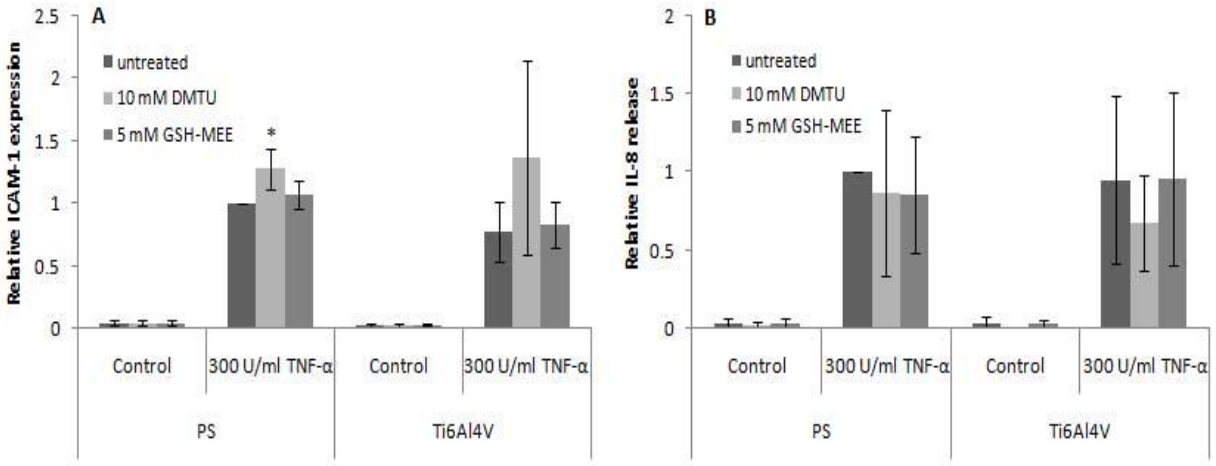


**Fig. 3.21.** *ICAM-1 (**A**) expression and IL-8 release (**B**) in HDMEC grown on PS and Ti6Al4V and stimulated with 75 U/ml TNF-α for 24 h in the absence or presence of 10 mM DMTU or 5 mM GSH-MEE. ICAM-1 expression on cell surface was measured with EIA and IL-8 with ELISA. The data were normalised to the cell number and are presented as fold of control (TNF-α-treated cells on PS) set as 1 (means ± SDs, significant difference: *p<0.05).*

mRNA DMTU treatment induced a significant increase in TNF-α-induced expression of ICAM-1 on the surface of HDMEC grown on PS. DMTU also elevated ICAM-1 induction by TNF-α in HDMEC on Ti6Al4V, although not significantly and to a much lesser extent than the increase of ICAM-1 mRNA under the same conditions (Fig. 3.21.A). In contrast, the effect of DMTU was not detectable for IL-8 (Fig. 3.21.B). Like on the mRNA level GSH-MEE did not have any significant influence on the release of IL-8 and the expression of ICAM-1 on the surface of HDMEC on PS and Ti6Al4V. Such disparity in the effects of ROS scavengers on different growth surfaces could possibly indicate the inhibition of mRNA translation in endothelial cells grown on Ti6Al4V. Alternatively, the transport of already synthesised adhesion molecules to the cell surface or cytokine release could be less efficient in the cells exposed to Ti6Al4V. Therefore, to investigate if the expression of ICAM-1 on the

surface reflected the amount of the whole ICAM-1 protein produced by the cells, ICAM-1 expression was detected in whole cell extracts of HDMEC grown on PS and Ti6Al4V and

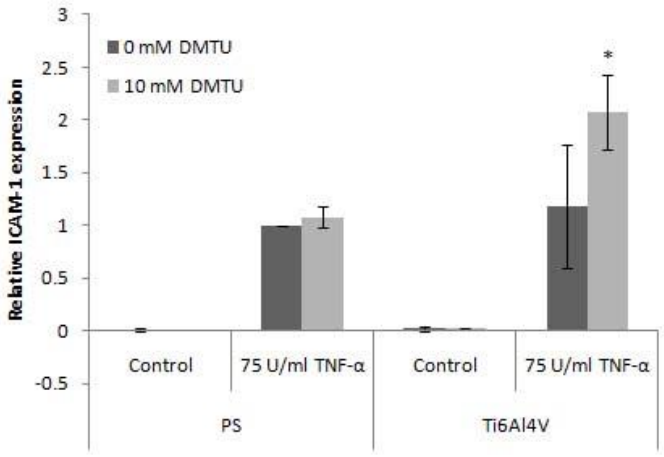


**Fig. 3.22.** *ICAM-1 expression in whole cell extracts of HDMEC grown on PS and Ti6Al4V and stimulated with 75 U/ml TNF-α for 24 h in the absence or presence of 10 mM DMTU. ICAM-1 expression was determined with western blot, related to the expression of ERK2 and presented as fold of control (TNF-α-treated cells on PS) set as 1 (means ± SDs, significant difference: *p<0.05).*

treated with DMTU. Indeed, ICAM-1 induction pattern in whole cell extracts after stimulation with TNF-α resembled the induction of ICAM-1 mRNA (Fig. 3.22). ICAM-1 induction by TNF-α was slightly higher in HDMEC on Ti6Al4V compared to the cells on PS and DMTU treatment significantly elevated ICAM-1 up-regulation in the cells on Ti6Al4V further pointing to the possible involvement of oxidative stress on Ti6Al4V alloy. The observation also favoured the hypothesis of ineffective transport of synthesised proteins to the cell membrane possibly in combination with inhibition of mRNA translation. Altogether, the data revealed deregulation of the inflammatory response of HDMEC in contact to Ti6Al4V alloy.

### 3.1.7. Angiogenic potential of HDMEC on Ti6Al4V

One of the main functions of endothelial cells is the formation of new blood vessels, a process important in wound healing. To study if contact with Ti6Al4V affected this specific function of endothelial cells HDMEC were embedded in a gel of fibrin and collagen type I. This gel was placed on PS or Ti6Al4V and formation of tube-like structures (named *in vitro*-capillaries) was induced by the addition of VEGF and bFGF. There was no difference in *in*

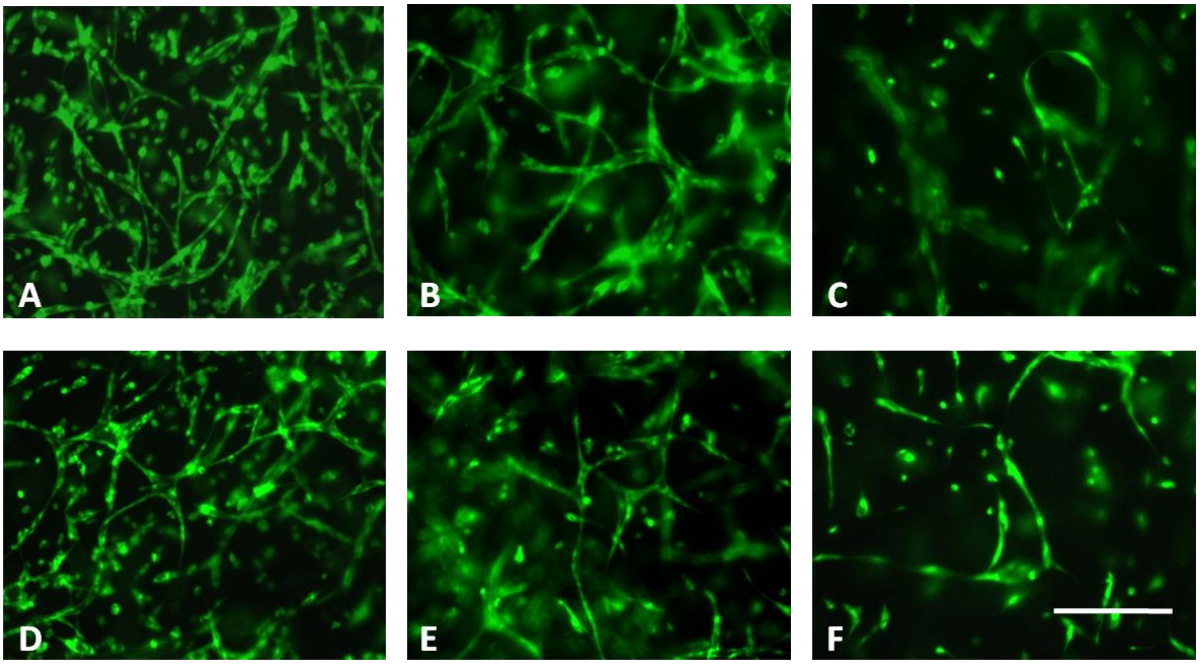


**Fig. 3.23.** *Formation of in vitro capillaries by HDMEC embedded in fibrin/collagen type I gel polymerised on top of PS (**A-C**) or Ti6Al4V alloy(**D-F**) untreated (**A, D**) or treated with 0.25 (**B, E**) or 0.5 mM $H_2O_2$ (**C, F**) 4 h after gel polymerisation. The cells were stained with calcein AM for fluorescent microscopy (scale bar: 300 µm).*

*vitro*-capillary formation by HDMEC 6 days after embedding them in the gels on top of PS or Ti6Al4V alloy (Fig. 3.23.A, D). To study if $H_2O_2$ induced different effects on *in vitro*-capillary formation potential on different surfaces, HDMEC were treated with $H_2O_2$ shortly after gel polymerisation, when there was still no *in vitro*-capillary formation. $H_2O_2$ had a negative effect on *in vitro*-capillary formation on both materials. While 0.25 mM induced rather moderate changes (Fig. 3.23.B, E), 0.5 mM $H_2O_2$ markedly inhibited *in vitro*-capillary formation by HDMEC in the gels on PS and Ti6Al4V (Fig. 3.23. C, F). There was no difference observed in $H_2O_2$ effects on *in vitro*-capillary formation on the two materials. Importantly, in this model system most of the endothelial cells were not in direct contact with the surface of the Ti6Al4V alloy, therefore further analysis of *in vitro*-capillary formation directly on Ti6Al4V surface or in gels on electrochemically polarised Ti6Al4V would be necessary to prove or rule out a possible influence of Ti6Al4V alloy and its corrosion products on blood vessel formation potential of endothelial cells.

## 3.2. The effect of $TiO_2$-coating of Co28Cr6Mo alloy on endothelial cells

Despite a broad use of CoCrMo alloys diverse detrimental effects of its corrosion products were shown. In vitro as well as in vivo studies have shown that CoCrMo alloys affect the functionality of endothelial cells (Kraft et al 2005, Peters et al 2008). Since titanium based alloys are believed to be more biocompatible due to the presence of an inactive $TiO_2$-layer on the metal surface, modification of Co28Cr6Mo alloy via $TiO_2$-coating was performed in order to shield the CoCrMo alloy.

HDMEC grown on Co28Cr6Mo alloy displayed an altered appearance of the actin cytoskeleton. While on fibronectin-coated glass actin was concentrated in actin rings typical for endothelial cells, a high number of actin stress fibres was observed in the cytoplasm of HDMEC in contact with Co28Cr6Mo alloy. The CD31 pattern within the intercellular contacts was also altered in HDMEC on Co28Cr6Mo compared to HDMEC on glass (Fig. 3.24). $TiO_2$-coating of Co28Cr6Mo on the other hand induced a normal HDMEC appearance: actin and CD31 distribution resembled the pattern displayed by control endothelial cells on glass. Altogether, changes in actin and CD31 distribution in HDMEC on Co28Cr6Mo pointed to an activated state of endothelial cells; $TiO_2$-coating, in turn, had a protective effect leading

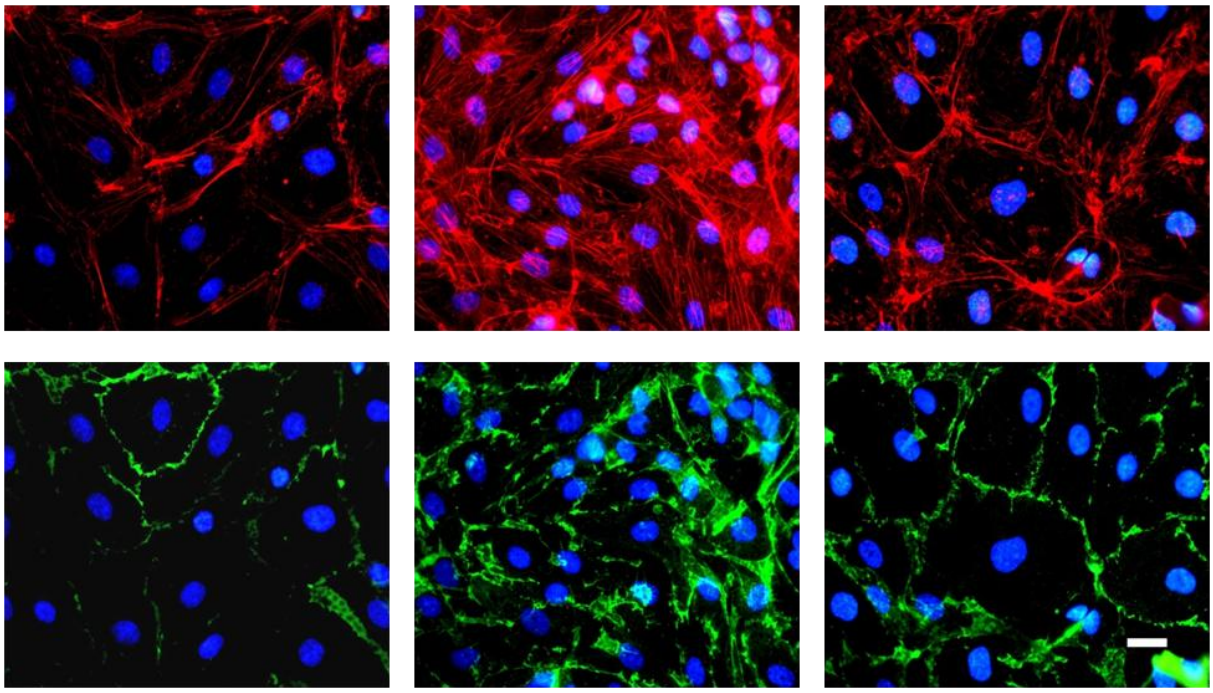

**Fig. 3.24.** *Actin (**A**-**C**) and CD31 (**D**-**F**) staining of HDMEC grown on glass (**A, D**), Co28Cr6Mo (**B, E**) or $TiO_2$-coated Co28Cr6Mo (C, F) for 40 h. The nuclei were stained blue with Hoechst 33324 (fluorescent microscopy, scale bar: 50 µm)*

to an almost unaltered cell phenotype similar to the control cells.

To study responses of HDMEC to Co28Cr6Mo and the effects of $TiO_2$-coating on mRNA expression level microarray analyses were performed 30 h after seeding of cells on the chosen materials. Growth on Co28Cr6Mo alloy induced considerable changes in the gene expression pattern in HDMEC compared to the cells grown on glass. Out of 1308 genes studied 247 were differentially expressed (125 genes were up- and 122 genes down-regulated). $TiO_2$-coating of Co28Cr6Mo, in contrast, markedly reduced the number of regulated genes. In this case only 34 genes were differentially expressed (13 were up- and 21 down-regulated) as compared to HDMEC grown on glass (Fig. 3.25). Notably, differential expression patterns in HDMEC on uncoated and $TiO_2$-coated Co28Cr6Mo alloy overlapped almost completely: out of 13 genes up-regulated on $TiO_2$-coated Co28Cr6Mo alloy 12 were up-regulated on uncoated Co28Cr6Mo and out of 21 down-regulated genes 20 overlapped with down-regulated genes in HDMEC on Co28Cr6Mo.

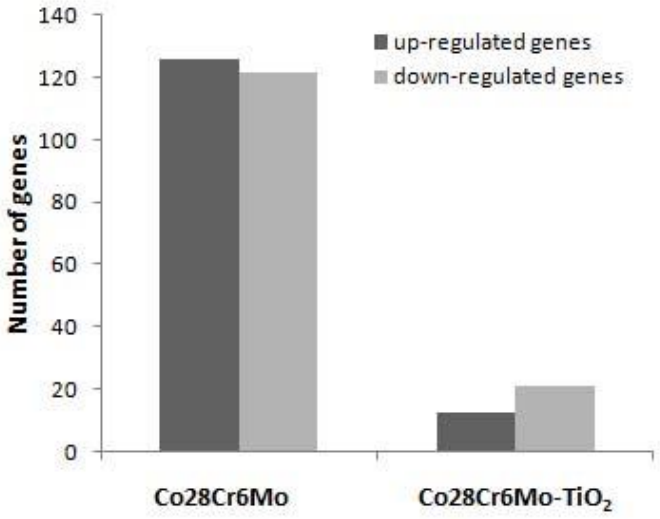


**Fig. 3.25.** *Number of differentially expressed genes in HDMEC grown on uncoated and $TiO_2$-coated Co28Cr6Mo alloy compared to the cells on glass 30 h after cell seeding (out of 1308 genes studied with cDNA microarrays).*

Among the genes differentially expressed in HDMEC on CoCr286Mo compared to control cells few functional groups could be separated. Within these, a number of mRNA of cell cycle-related genes was regulated in HDMEC on Co28Cr6Mo alloy compared to the cells on glass (Table 3.1). Here, proliferation markers (Ki67, PCNA, RCF (replication factor C), RPA (replication protein A)), a number of cyclins (A2, B2, D1, E1), cyclin-dependent kinases 1 and 2 (CDK1 and CDK2) were down-regulated in HDMEC on Co28Cr6Mo. These mRNAs were in general also down-regulated in the cells on $TiO_2$-coated Co28Cr6Mo, but to a lesser extent than on uncoated material. A few CDK inhibitors (p21CIP1, p57KIP2 and p16-INK4A) were up-regulated in the cells in contact with Co28Cr6Mo and were not regulated on $TiO_2$-coated alloy. Some of the cyclins and CDK inhibitors (cyclin G2, p27KIP1 and p18-

**Table 3.1.** *Expression of cell cycle-related genes in HDMEC grown on uncoated and $TiO_2$-coated Co28Cr6Mo alloy 30 h after seeding (cDNA microarray data are presented as fold of glass control set as 1; light grey indicates down-regulation <0.58, dark grey marks up-regulation >1.7-fold; fold change/CV).*

| | Co28Cr6Mo | Co28Cr6Mo-$TiO_2$ |
|---|---|---|
| Ki-67 | 0.09 / 64 % | 0.33 / 19 % |
| PCNA | 0.12 / 12 % | 0.47 / 2 % |
| RFC | 0.25 / 23 % | 0.64 / 13 % |
| RPA | 0.40 / 14 % | 0.84 / 7 % |
| CYCLIN A2 | 0.58 / 13 % | 0.53 / 19 % |
| CYCLIN B2 | 0.15 / 32 % | 0.52 / 9 % |
| CYCLIN D1 | 0.49 / 21 % | 0.55 / 6 % |
| CYCLIN E1 | 0.41 / 18 % | 0.49 / 33 % |
| CYCLIN G2 | 1.72 / 11 % | 1.27 / 16 % |
| CDK1 | 0.25 / 21 % | 0.57 / 13 % |
| CDK2 | 0.32 / 29 % | 0.52 / 18 % |
| p21CIP1 | 3.94 / 19 % | 1.50 / 17 % |
| p27KIP1 | 0.80 / 27 % | 0.91 / 51 % |
| p57KIP2 | 4.48 / 25 % | 0.95 / 11 % |
| p16-INK4A | 1.89 / 13 % | 1.38 / 5 % |
| p18-INK6 | 0.35 / 32 % | 0.53 / 12 % |

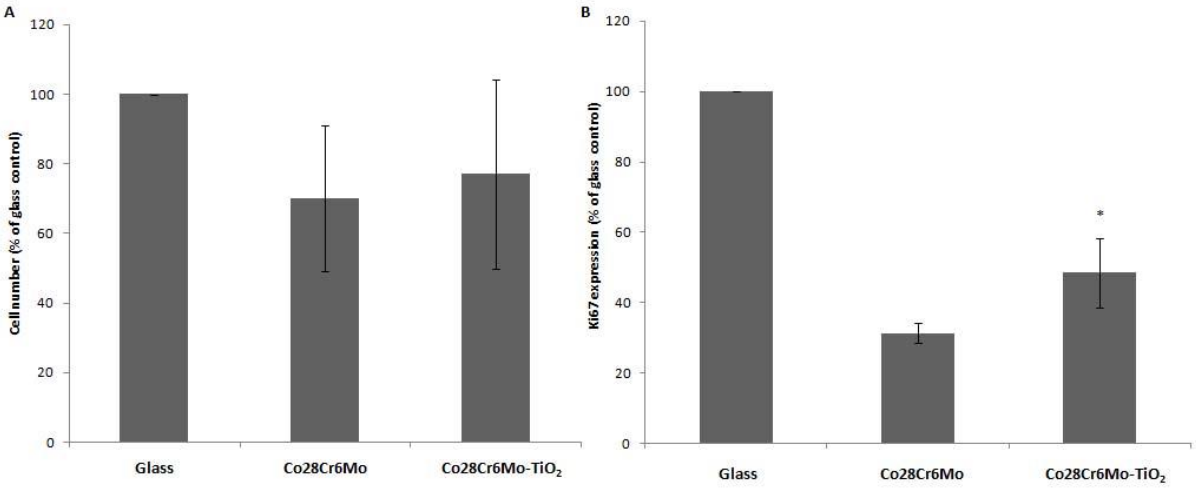


**Fig. 3.26.** *Cell number (**A**) and Ki67 expression (**B**) in HDMEC grown on glass Co28Cr6Mo and Co28Cr6Mo coated with $TiO_2$-layer 40 h after cell seeding. Cell number was estimated via quantification of nuclear staining with Hoechst 33342. Ki67 expression was measured with EIA and related to the cell number. The data are presented as % of control (cells on glass; means±SDs; statistical difference *p<0.05).*

INK4) did not match the regulation pattern observed for the majority of the genes. In general microarray data indicated reduced proliferation and cell cycle block in HDMEC grown on

Co28Cr6Mo. To confirm this effect cell number and Ki67 protein expression was compared in HDMEC. Lower cell numbers were detected on both Co28Cr6Mo and Co28Cr6Mo-$TiO_2$ compared to glass (Fig. 3.26.A). There was, however, no significant difference in the cell number between metal surfaces. Ki67 protein was expressed significantly lower in HDMEC on both alloys compared to the cells on glass (Fig. 3.26.B). Ki67 expression in HDMEC on $TiO_2$-coated Co28Cr6Mo was significantly higher than on uncoated Co28Cr6Mo, which correlated with the microarray data.

HDMEC grown on Co28Cr6Mo also showed regulation in oxidative stress response genes (Table 3.2). Various genes for antioxidant enzymes (SOD1, SOD2, GPX3, GST12) were up-regulated, while some genes (GPX1 and GSTT2) were down-regulated in HDMEC on Co28Cr6Mo compared to the cells on glass. Importantly, the expression of these genes did not differ in HDMEC on $TiO_2$-coated Co28Cr6Mo compared to the glass control. Regulation of antioxidant enzymes indicated the oxidative stress in HDMEC on Co28Cr6Mo. To study if the signs of oxidative stress could be detected biochemically, GSH amount and SOD activity were quantified in HDMEC on different growth substrates. GSH amount in HDMEC on both metallic materials was lower than in the cells on glass but was around 20% higher on $TiO_2$-coated Co28Cr6Mo than on uncoated Co28Cr6Mo (Fig. 3.27.A). This could point to the exhaustion of the GSH pool in the cells on Co28Cr6Mo and a protective effect of the $TiO_2$ layer. SOD activity was 55% lower in HDMEC grown on Co28Cr6Mo compared to the cells on glass, in contrast, SOD activity in HDMEC on $TiO_2$-coated Co28Cr6Mo was significantly higher than on uncoated material and was even slightly higher than on glass (Fig. 3.27.B).

**Table 3.2.** *Expression of oxidative stress response genes in HDMEC grown on uncoated and $TiO_2$-coated Co28Cr6Mo alloy 30 h after seeding (cDNA microarray data are presented as fold of glass control; light grey indicates down-regulation <0.58, dark grey marks up-regulation >1.7-fold; fold change/CV).*

| | Co28Cr6Mo | Co28Cr6Mo-$TiO_2$ |
|---|---|---|
| SOD1 | 1.95 / 3 % | 0.95 / 3 % |
| SOD2 | 3.49 / 17 % | 0.69 / - % |
| GPX1 | 0.46 / 5 % | 0.90 / 2 % |
| GPX3 | 2.15 / 10 % | 1.25 / 7 % |
| GSTT2 | 0.44 / 18 % | 1.06 / 16 % |
| GST12 | 1.97 / 7 % | 1.42 / 5 % |

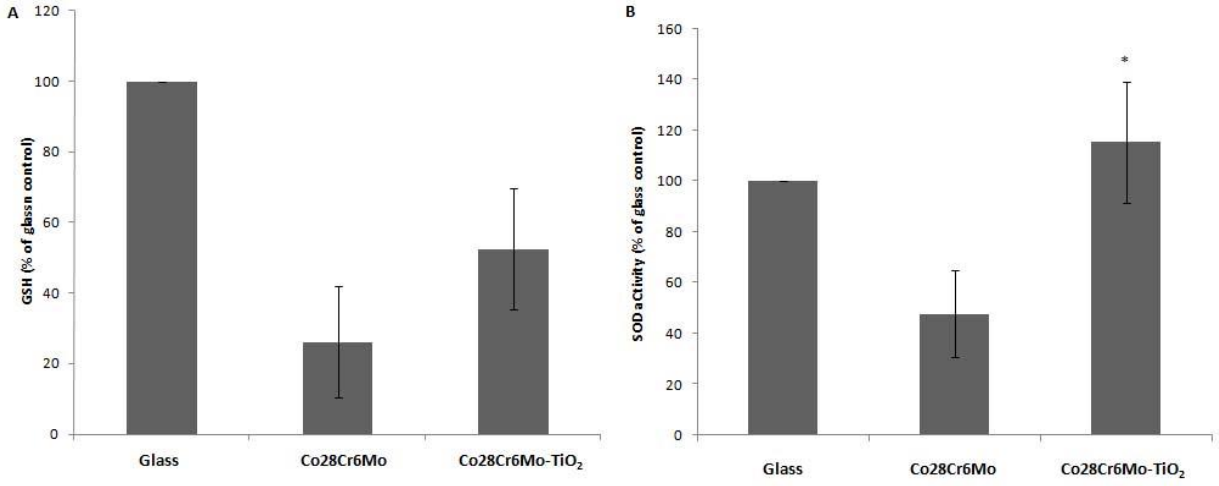


**Fig. 3.27.** *GSH amount (**A**) and SOD activity (**B**) in HDMEC grown on glass Co28Cr6Mo and $TiO_2$-coated Co28Cr6Mo for 40 h. GSH amount was measured using fluorescent probe monochlorobimane and SOD activity with a biochemical assay. Both parameters were normalised to protein concentration. The data are presented as % of control (cells on glass; means±SDs; statistical difference *p<0.05).*

Another group of genes up-regulated in HDMEC on Co28Cr6Mo were genes for heat shock proteins. A number of mRNAs for heat shock proteins and their accessory proteins were highly up-regulated in HDMEC on Co28Cr6Mo alloy (Table 3.3). Importantly, most of these genes were not regulated, when Co28Cr6Mo was coated with a $TiO_2$ layer. Heat shock proteins are chaperones involved in the folding of unfolded and misfolded proteins. Their induction could indicate that HDMEC on Co28Cr6Mo experience stress conditions, which lead to unfolding of proteins. In line with this XBP1, a transcription factor, involved in UPR,

**Table 3.3.** *Expression of heat shock protein genes in HDMEC grown on uncoated and $TiO_2$-coated Co28Cr6Mo alloy 30 h after seeding (cDNA microarray data are presented as fold of glass control; light grey indicates down-regulation <0.58, dark grey marks up-regulation >1.7-fold; fold change/CV).*

| | Co28Cr6Mo | Co28Cr6Mo-$TiO_2$ |
|---|---|---|
| HSP70B' | 131.85 / 30 % | 0.30 / 26 % |
| HSPA9 | 1.94 / 11 % | 0.69 / 3 % |
| HSP70.1 | 23.63 / 9 % | 0.69 / 5 % |
| HSP86 | 2.90 / 5 % | 0.70 / 2 % |
| HSP105 | 5.64 / 11 % | 0.64 / 5 % |
| HSP73 | 1.87 / 17 % | 0.70 / 3 % |
| DNAJA1 | 2.32 / 14 % | 0.66 / 5 % |
| DNAJB6 | 1.85 / 7 % | 0.86 / 2 % |
| XBP1 | 2.60 / 5 % | 1.29 / 6 % |
| GRP78 | 0.78 / 5 % | 0.65 / 6 % |

was also up-regulated in HDMEC on Co28Cr6Mo and not differentially expressed in HDMEC on $TiO_2$-coated Co28Cr6Mo.

The mRNA expression of inflammation and stress-related IL-8, heme oxygenase-1 (HO-1) and cyclooxygenase II (COX II) were also differentially expressed on Co28Cr6Mo alloy compared to controls. Among them, IL-8 mRNA was strongly increased on Co28Cr6Mo (almost 20-fold) and was close to the control level in HDMEC on $TiO_2$-coated Co28Cr6Mo. Expression of both mRNA and protein for HO-1 and COX II was also markedly elevated in HDMEC on Co28Cr6Mo compared to the cells grown on glass, and $TiO_2$-coating decreased the expression of these genes. HO-1 mRNA was up-regulated 15-fold in HDMEC on Co28Cr6Mo, whereas the induction was only around 2-fold on $TiO_2$-coated alloy. COX II mRNA expression was also 7-fold higher in HDMEC on Co28Cr6Mo compared to the cells on glass and only 3-fold higher in cells on Co28Cr6Mo-$TiO_2$ (Table 3.4.). The results at

**Table 3.4.** *Expression of IL-8, HO-1 and COX II in HDMEC grown on uncoated and $TiO_2$-coated Co28Cr6Mo alloy 30 h after seeding (cDNA microarray data are presented as % of glass control; dark grey marks up-regulation>1.7-fold; fold change/CV).*

| | Co28Cr6Mo | Co28Cr6Mo-$TiO_2$ |
|---|---|---|
| IL-8 | 19.68 / 28 % | 1.59 / 11 % |
| HO-1 | 15.55 / 18 % | 2.79 / 9 % |
| COX II | 7.19 / 24 % | 1.89 / 5 % |

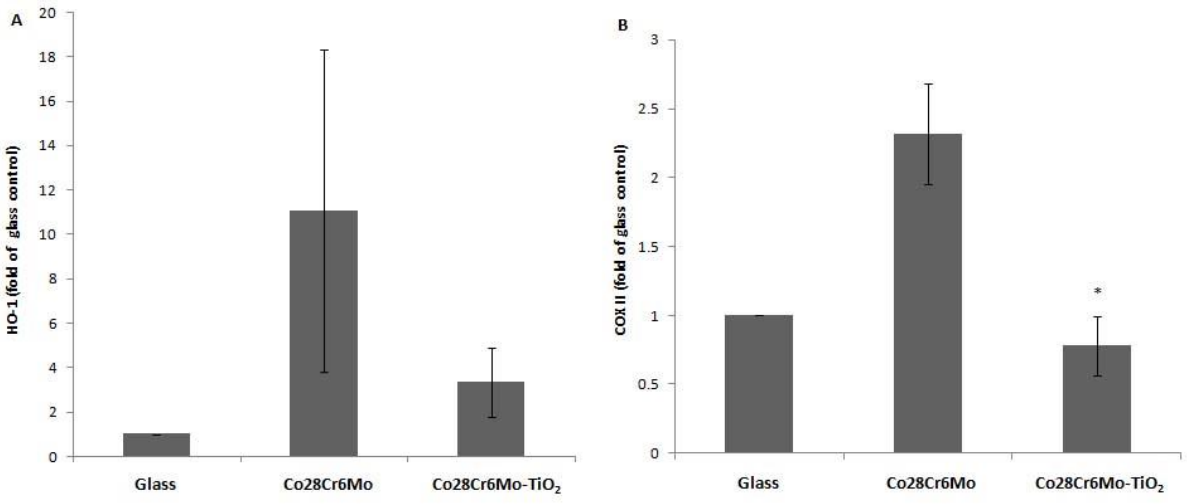


**Fig. 3.28.** *HO-1(**A**) and COX II (**B**) expression in HDMEC grown on glass, Co28Cr6Mo and $TiO_2$-coated Co28Cr6Mo for 40 h. HO-1 and COX II expression was determined with ELISA and normalised to protein concentration. The data are presented as fold of control (cells on glass set as 1; means±SDs; statistical difference *p<0.05).*

mRNA level correlated with protein expression. Both HO-1 and COX-II expression were higher in HDMEC on Co28Cr6Mo, and $TiO_2$-coating strongly decreased protein expression level, with the difference for COX II being statistically significant (Fig. 3.28). Altogether, the data pointed to the induction of a stress response in endothelial cells in contact with Co28Cr6Mo alloy, this being attenuated by $TiO_2$-coating.

## 3.3. Response of endothelial cells to $CoCl_2$

### 3.3.1. $CoCl_2$ induces cytotoxicity and oxidative stress in HDMEC

Metal ions are known to be formed during metal corrosion and are detected in high quantities in blood and peri-implant tissues after implantation of metal devices. Since endothelial cells are exposed to metal ions in blood throughout the body as well as in peri-implant tissues, response of HDMEC to $Co^{2+}$ (applied as $CoCl_2$) was studied. Because $CoCl_2$ is often used as an oxygen deficiency mimicking agent the influence of $CoCl_2$ on endothelial cells was compared in some cases with the response to anoxia (complete lack of oxygen).

$CoCl_2$ induced a dose-dependent reduction in the metabolic activity of HDMEC 24 h after treatment (Fig. 3.29.A). This correlated with a dose-dependent decrease in HDMEC cell number 24 h after $CoCl_2$ addition (Fig. 3.29.B). Interestingly, $CoCl_2$ cytotoxicity was rather low when HDMEC were treated with $CoCl_2$ for only 1 h (maximum 15% reduction of

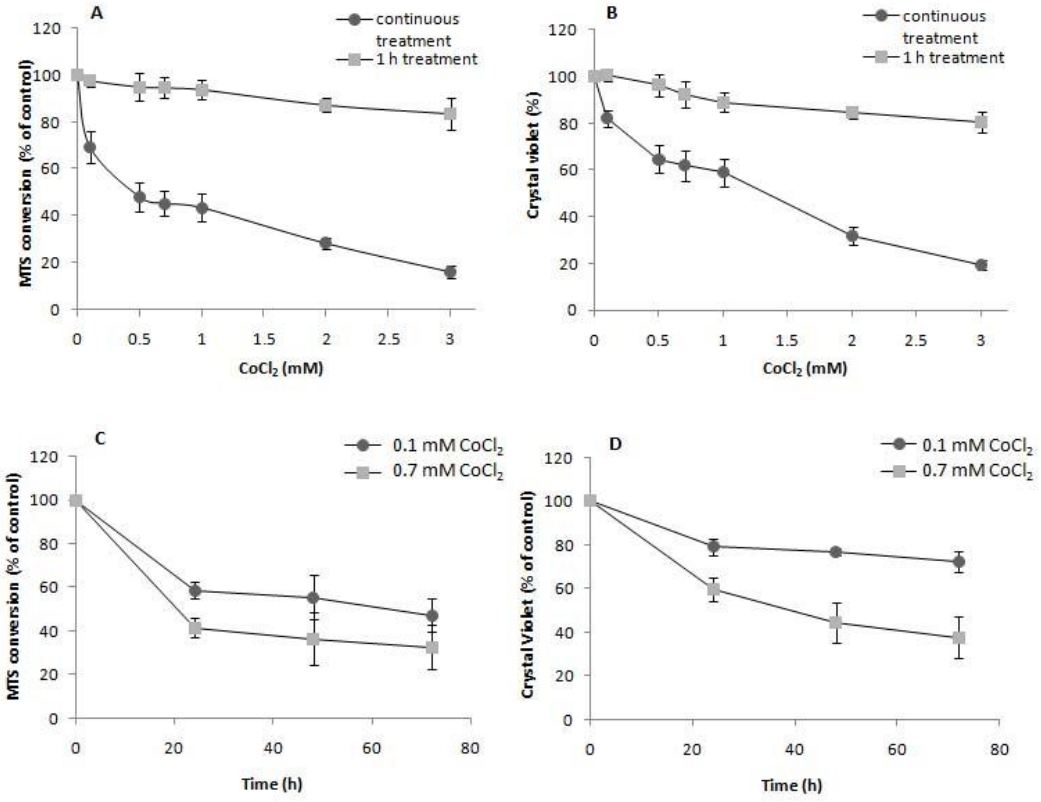


**Fig. 3.29.** *The effect of $CoCl_2$ on MTS conversion (**A, C**) and cell number (**B, D**) of HDMEC. **A, B**. Different $CoCl_2$ concentrations were added to HDMEC for 1 h or continuously and MTS or crystal violet assays were performed after 24 h. **C, D**. HDMEC were treated with 0.1 or 0.7 mM $CoCl_2$ for 24, 48 or 72 h (means±SDs).*

metabolic activity and cell number was observed after treatment with 3 mM $CoCl_2$, Fig. 3.29. A, B). This observation suggested that the reactions induced by $CoCl_2$ in HDMEC could be reversed after $CoCl_2$ was removed. However, since permanent exposure to $CoCl_2$ more closely reflects the situation in peri-implant tissue, continuous $CoCl_2$ treatment was used for further experiments. Time course experiments were performed with two $CoCl_2$ concentrations (0.1 and 0.7 mM $CoCl_2$) that are in the range of peri-prosthetic and blood $CoCl_2$ concentration in patients with failed Co-based implants. 0.1 mM $CoCl_2$ induced reduction of HDMEC metabolic activity by 40% and cell number by around 20% 24 h after treatment begin. The effects of 0.7 mM $CoCl_2$ were higher: it caused approximately 60% decrease in metabolic activity of HDMEC and 40% in cell number 24 h after $CoCl_2$ addition (Fig. 3.29.C, D). HDMEC incubation with $CoCl_2$ for longer times induced further reduction of cell viability, although the changes were rather small compared to the 24 h time point (only 0.7 mM $CoCl_2$ led to further 20% decline in HDMEC cell number).

The toxicity of $CoCl_2$ could be explained at least in part by the formation of ROS, as was shown by the increased DCF fluorescence in HDMEC 4 h after treatment with $CoCl_2$ (Fig. 3.30.A). $CoCl_2$ induced an approximately 7-fold increase in ROS production, this value being significant and similar to the ROS formation caused by $H_2O_2$ treatment. The induction of oxidative stress by $Co^{2+}$ was confirmed by the determination of the GSH level. While $H_2O_2$ induced the increase in GSH level, exposure to both 0.5 and 1 mM $CoCl_2$ for 24 h led to approximately 35% reduction in the level of GSH compared to untreated controls (statistically significant for both concentrations, Fig. 3.30.B). This observation pointed to a possibility of the exhaustion of the GSH pool that is involved in the elimination of radicals. Measurement of the activity of the antioxidant enzymes catalase and SOD did not reveal any significant changes in HDMEC treated with 0.7 mM $CoCl_2$ for 24 or 48 h (Fig. 3.30.C, D).

Interestingly, however, the ROS scavengers DMTU and GSH-MEE could not efficiently protect HDMEC from cytotoxic effects of $CoCl_2$. Both DMTU and GSH-MEE were able to restore metabolic activity of HDMEC treated with $H_2O_2$ to the levels even higher than in untreated control samples (Fig. 3.31). In contrast, only addition of cell permeable GSH could elevate metabolic activity of HDMEC after $CoCl_2$ treatment. However, the increase was rather small and similar to the stimulating effect of GSH-MEE in untreated cells that could be attributed to the protection against spontaneous ROS production taking place in all cells. Importantly, $H_2O_2$ is unstable in the medium used and decomposes rapidly after addition. Therefore, such short-term treatment is in contrast to $CoCl_2$ treatment, where $Co^{2+}$ potentially serves as a permanent source of ROS.

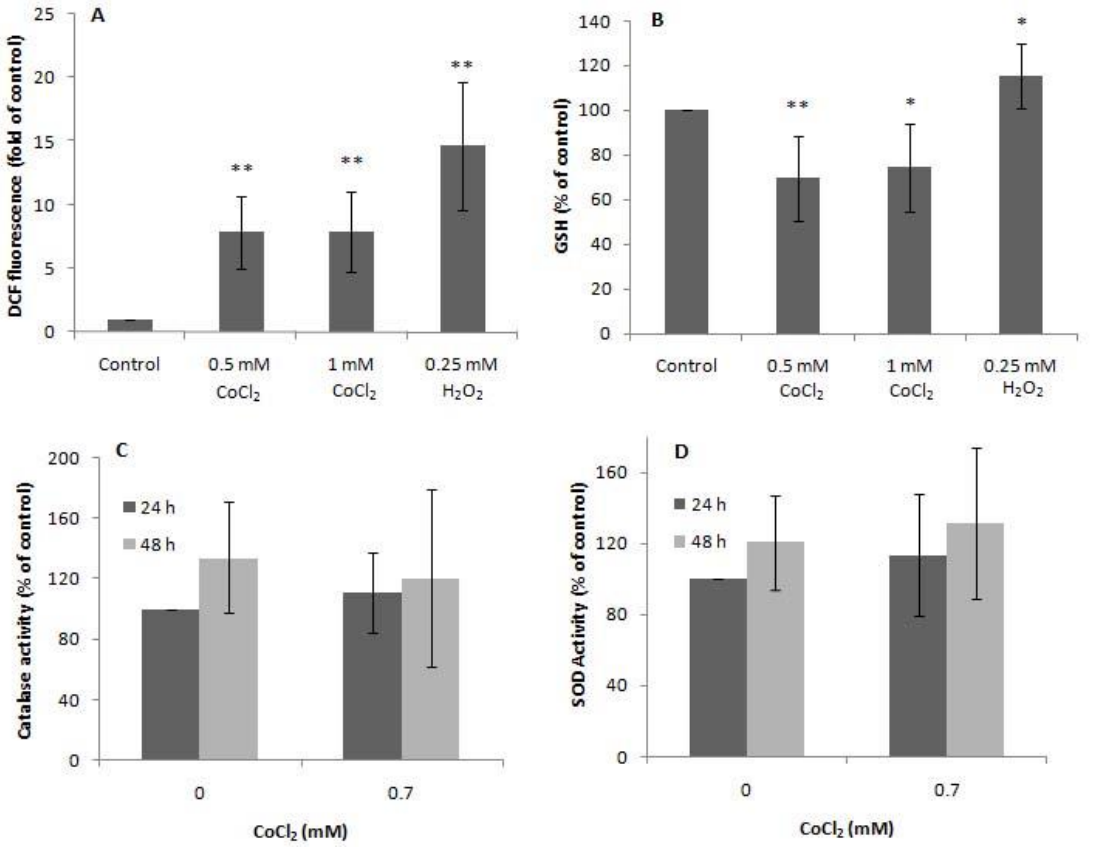


**Fig. 3.30.** Examination of *$CoCl_2$-induced oxidative stress in HDMEC.* ***A.*** *Induction of ROS formation 4 h after $CoCl_2$ or $H_2O_2$ treatment.* ***B.*** *GSH amount in HDMEC 24 h after addition of $CoCl_2$ or $H_2O_2$. Catalase (**C**) and SOD (**D**) activity in HDMEC treated with 0.7 mM $CoCl_2$ for 24 or 48 h. ROS production was determined with DCF assay and the data are presented as fold of untreated control. GSH amount was measured with fluorescent probe monochlorobimane. Catalase and SOD activities were assessed with corresponding activity assays. GSH, catalase and SOD data were normalised to protein concentration and are presented as % of untreated control (means±SDs; significant difference: *p<0.05, **p<0.01).*

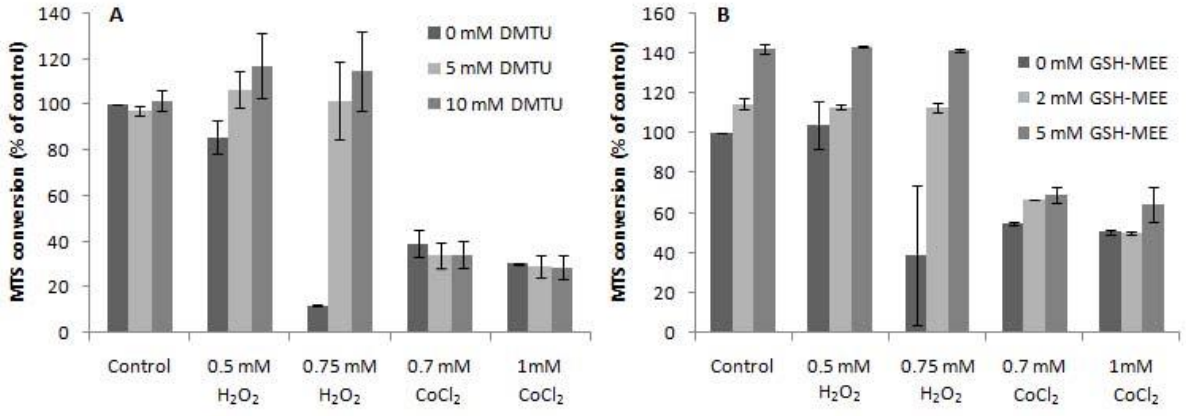


**Fig. 3.31.** *The effect of DMTU (**A**) and GSH-MEE (**B**) on metabolic activity of HDMEC 24 h after $H_2O_2$ or $CoCl_2$ treatment. MTS conversion is presented as % of control (untreated cells; means±SDs)*

### 3.3.2. $CoCl_2$ causes DNA damage and p53 up-regulation in HDMEC

ROS are known to cause damage to DNA with the most common DNA adduct being 8-oxoguanine (8-oxoG). Therefore, 8-oxoG was detected in DNA of HDMEC after $CoCl_2$ treatment with immunofluorescent staining using an antibody specific to 8-oxoG. $CoCl_2$ induced an increase in nuclear fluorescence after short-term treatment (20 min with 3 mM $CoCl_2$, Fig. 3.32. D and 1 h with 1 mM $CoCl_2$, Fig. 3.32. E) as well as after 24 h treatment with 1 mM $CoCl_2$ (Fig. 3.32.F). Nuclear fluorescence in HDMEC after $CoCl_2$ treatment was similar to that induced by $H_2O_2$ treatment (Fig. 3.32. B, C).

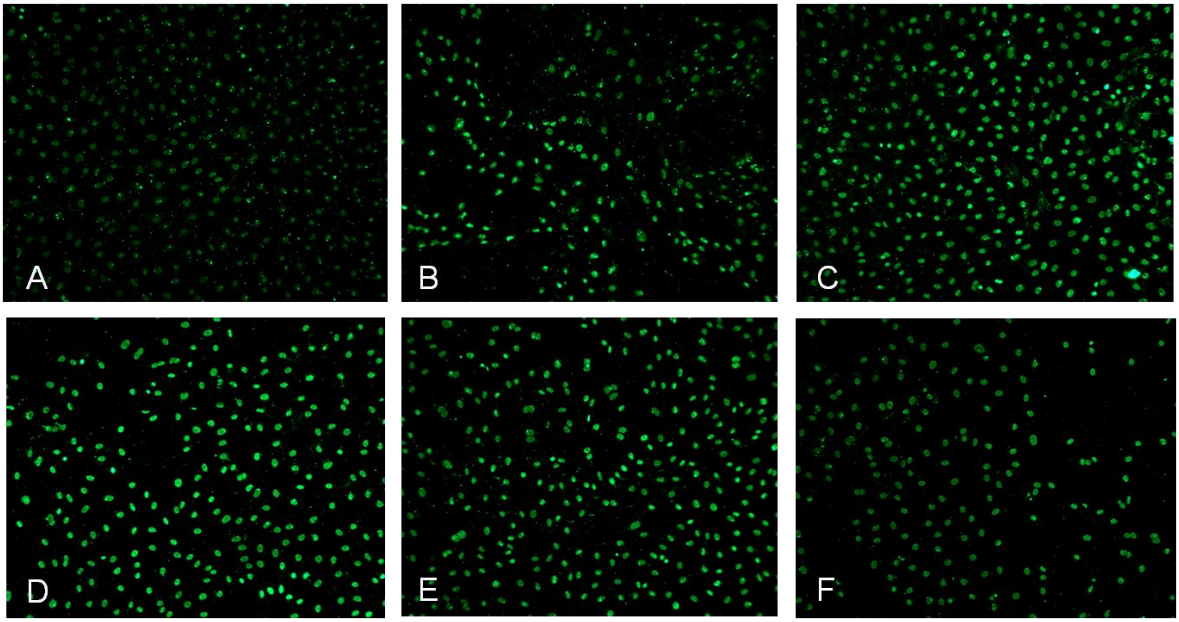


**Fig. 3.32.** *8-oxoG staining in the nuclei of untreated HDMEC (**A**), in HDMEC treated with 1 mM $H_2O_2$ for 20 min (**B**) or 0.5 mM $H_2O_2$ for 24 h (**C**). Alternatively, 3 mM $CoCl_2$ was added to HDMEC for 20min (**D**) or 1 mM $CoCl_2$ was added for 1 h (**E**) or 24 h (**F**). Fluorescent microscopy of immunostaining with a specific anti-8-oxoG antibody.*

Another type of oxidative DNA lesion is apurinic/apyrimidinic (AP) sites. They are formed spontaneously or in the course of repair of oxidative adducts of DNA aminobases, such as 8-oxoG. Thus, AP sites were quantified in the DNA of HDMEC exposed to $CoCl_2$. A significant increase in the amount of AP sites was observed in the DNA of HDMEC 4 h after treatment with 0.7 mM $CoCl_2$ (Fig. 3.33). It was similar to the level of AP sites in the DNA of the cells exposed to anoxia or 0.25 mM $H_2O_2$. Even higher induction of AP sites formation was detected in HDMEC 18 h after treatment with $CoCl_2$, pointing to a constant DNA damaging caused by $Co^{2+}$presence.

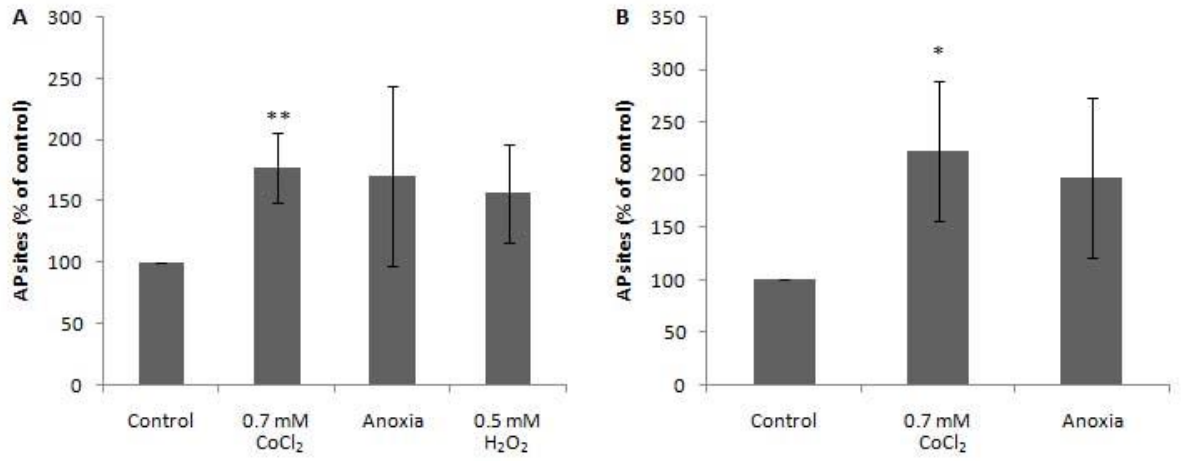


**Fig. 3.33.** *Examination of AP sites in the DNA of HDMEC exposed to 0.7 mM $CoCl_2$, anoxia or 0.5 mM $H_2O_2$ for 4 h (**A**) or 18 h (**B**). AP sites formation was measured with ELISA and the data are presented as % of control (untreated cells; means±SDs; significant difference: *p<0.05, **p<0.01).*

Many types of DNA damage have been shown to up-regulate p53 protein expression level. Since $CoCl_2$ induces the formation of oxidative DNA lesions p53 expression was studied in HDMEC exposed to $CoCl_2$. The addition of 0.7 mM $CoCl_2$ induced a rapid increase

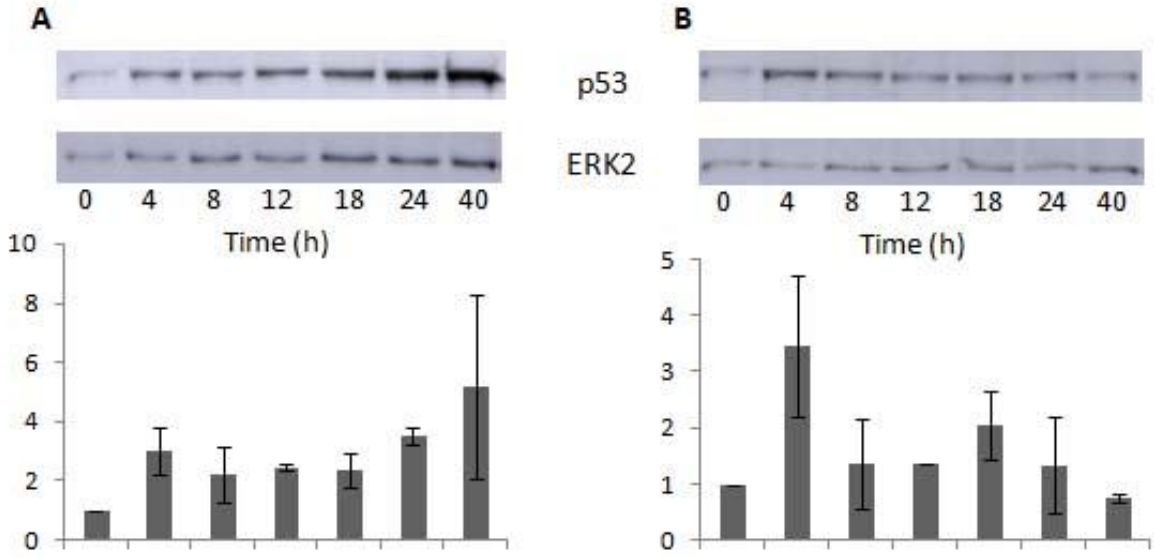


**Fig. 3.34.** *p53 expression in HDMEC treated with 0.7 mM $CoCl_2$ (**A**) or anoxia (**B**). p53 expression in nuclear extracts was determined with western blot. Representative blots are presented. ERK2 expression was used to control protein loading. The graphs depict the quantification of p53 expression normalised to ERK2 level, n=2-3, means±SDs).*

in the amount of p53 in the nuclear extracts of HDMEC. As early as 4 h after $CoCl_2$ treatment p53 expression was increased 3-fold compared to untreated cells. Further increase in p53

protein level was observed at later time points studied (24 and 40 h, Fig. 3.34.A). In contrast, anoxia induced a less uniform reaction. p53 was up-regulated after 4 h but returned to the levels close to untreated controls at later time points (Fig. 3.34.B).

One of the direct transcriptional targets of p53 is the CDK inhibitor p21 involved in cell-cycle arrest. A strong elevation of p21 in whole cell extracts of HDMEC was observed

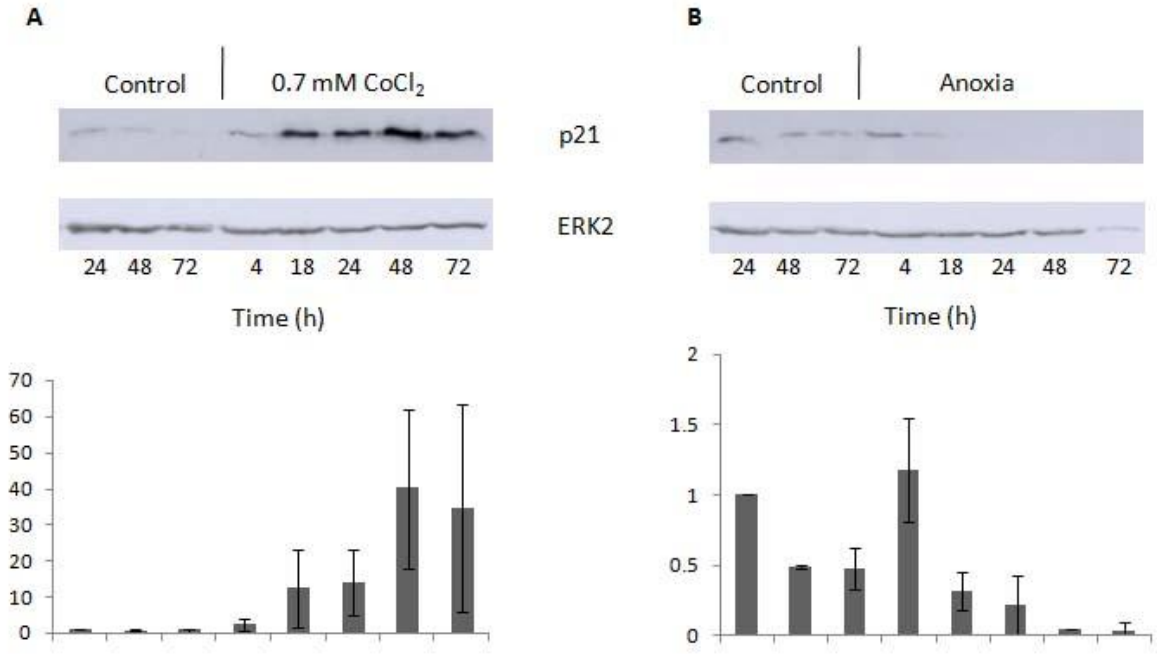


**Fig. 3.35.** *p21 expression in HDMEC treated with 0.7 mM $CoCl_2$ (**A**) or anoxia (**B**). p21 expression was analysed with western blot. ERK2 expression was used as loading control Rrepresentative blots and quantification of p21 expression normalised to ERK2 amount are presented, n=2-3, means±SDs).*

already 18 h after treatment with 0.7 mM $CoCl_2$. p21 expression increased further reaching its maximum after 48 h (Fig. 3.35.A). In contrast, p21 level declined constantly during the course of experiments placing HDMEC in an anoxic atmosphere (Fig. 3.35.B).

Oxidative DNA damage is eliminated in the cell mainly by base excision repair (BER). To connect $CoCl_2$-induced DNA damage with p21 up-regulation a general BER inhibitor was used. Addition of BER inhibitor potentiated $CoCl_2$-induced reduction of HDMEC metabolic activity, especially after 48 and 72 h (Fig. 3.36.A). Importantly, however, HDMEC treated with only BER inhibitor also had slightly decreased metabolic activity. This can be attributed to the inhibition of the repair of oxidative DNA lesions forming in the cells during normal metabolism. The same potentiating effect of a BER inhibitor on the reduction of metabolic activity of HDMEC was observed after treatment with $H_2O_2$, a known inducer of oxidative DNA damage (Fig. 3.36. B). Although the effect of BER inhibitor on cytotoxicity of

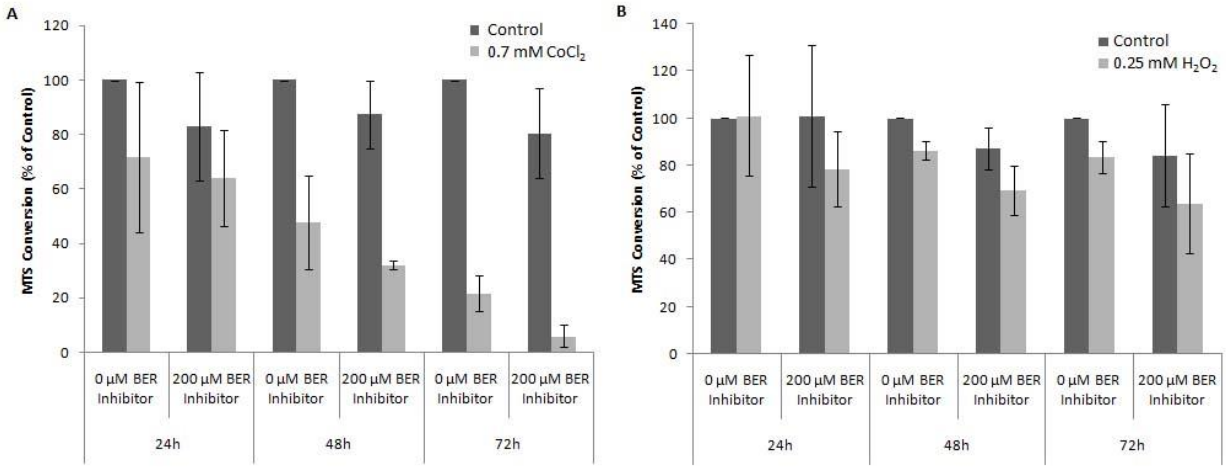


**Fig. 3.36.** *Metabolic activity of HDMEC treated with 0.7 mM $CoCl_2$ (**A**) or 0.25 mM $H_2O_2$ (**B**) for 24, 48 or 72 h in the absence or presence of 200 µM BER inhibitor. BER inhibitor was added 1 h before $CoCl_2$ or $H_2O_2$ treatment. MTS conversion assay data are presented as % of control (untreated cells at each time point, means±SDs).*

$CoCl_2$ was rather small, inhibition of BER had an effect on p21 induction. The induction of p21 expression 18 h after treatment with 0.7 mM $CoCl_2$ was twice as high in the presence of BER inhibitor as with $CoCl_2$ alone (Fig. 3.37). This pointed to a possible connection between DNA damage induced by $CoCl_2$ and p21 up-regulation (presumably p53-dependent). However, more detailed functional studies would be necessary to draw such a conclusion.

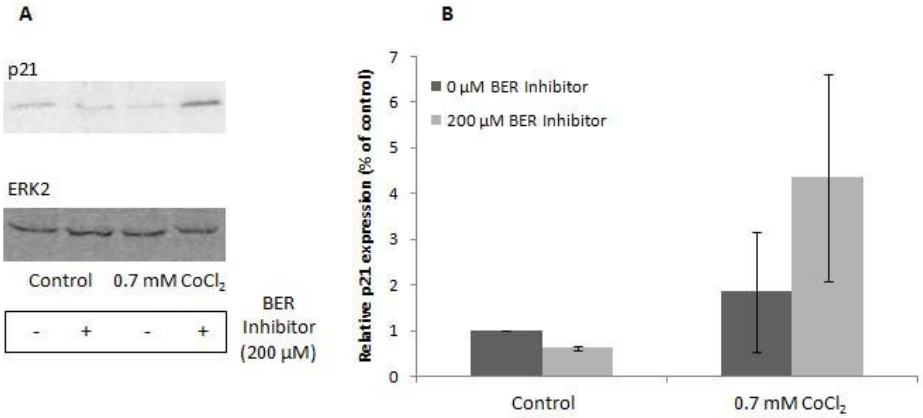


**Fig. 3.37.** *p21 expression in HDMEC treated with 0.7 mM $CoCl_2$ for 18 h in the absence or presence of 200 µM BER inhibitor. BER inhibitor was added 1 h before $CoCl_2$ treatment. Representative blots (**A**) of p21 and ERK2 (loading control) expression are presented. **B.** Quantification of p21 expression normalised to ERK2 level (untreated cells were set as 100%, n=3, means±SDs).*

### 3.3.3. HIF-1α dependency of $CoCl_2$-induced response in HDMEC

$CoCl_2$ is widely used as an hypoxia-mimicking agent. This is due to its ability to activate HIF-1 transcriptional factor by stabilising HIF-1α protein, that is also one of the main events in the cell response upon reduction of oxygen concentration. Both $CoCl_2$ and anoxia

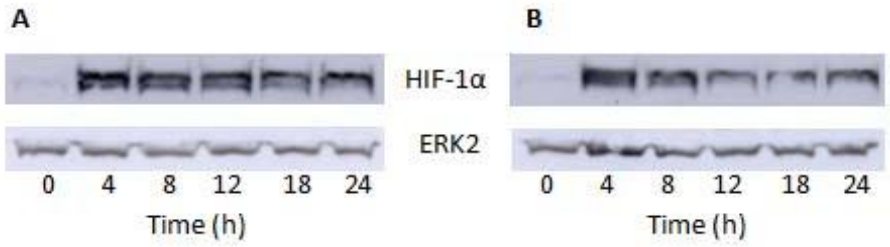


**Fig. 3.38.** *HIF-1α stabilisation in HDMEC treated with 0.7 mM $CoCl_2$ (**A**) or anoxia (**B**) after different time points. HIF-1α expression was assessed with western blot. ERK2 blots are presented for controlling of protein loading.*

induced a substantial increase in HIF-1α protein in HDMEC. The extent and kinetics of up-regulation were largely similar in HDMEC treated with 0.7 mM $CoCl_2$ and anoxia (Fig. 3.38). It was shown, however, that $CoCl_2$ and hypoxia may exert diverse reactions on endothelial cells (Peters et al 2005). Therefore, to separate HIF-1α-dependent and HIF-1α-independent reactions to $CoCl_2$ in endothelial cells, HIF-1α mRNA was knocked down with siRNA and cDNA microarray analysis was performed to compare $CoCl_2$ and anoxia-induced changes in mRNA expression.

Both siRNAs used could effectively down-regulate HIF-1α mRNA 48 h after transfection (more than 90% for s6539 and around 85% for s6541, Fig. 3.39.A). HIF-1α mRNA amount was still reduced 72 h after siRNA transfection (the latest time point measured). Since the effects of $CoCl_2$ and anoxia on HDMEC were to be compared, HIF-1α mRNA was quantified in siRNA-transfected cells after $CoCl_2$ or anoxia treatment. HIF-1α mRNA amount increased in siRNA-transfected cells after $CoCl_2$ and anoxia treatment, but was still lower than in HDMEC transfected with negative control siRNA (Neg siRNA) or in untransfected cells. While s6539 was more efficient in untreated cells, down-regulation of HIF-1α mRNA induced by s6541 was still above 70%, which was considered to be a lowest significant down-regulation level (Fig. 3.39.B). Notably, HIF-1α mRNA in siRNA-transfected cells was reduced to a lesser extent in case of anoxia treatment compared to exposure to $CoCl_2$.

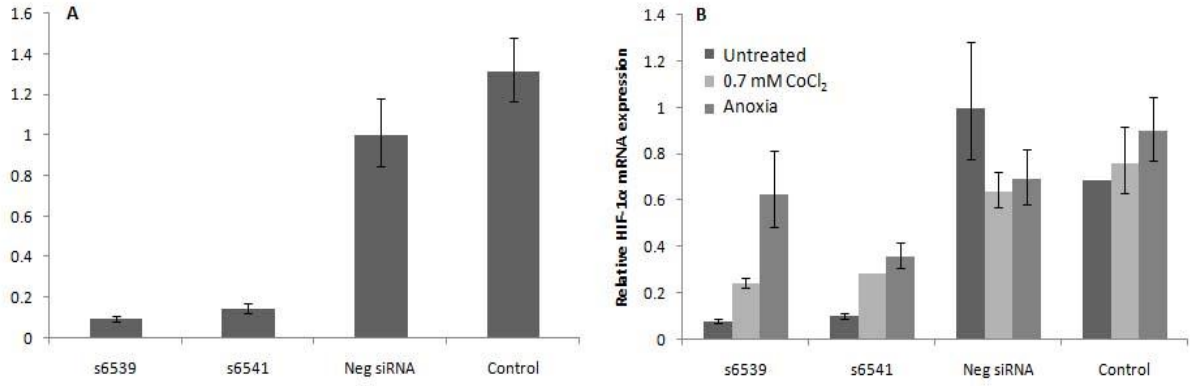


**Fig. 3.39.** *HIF-1α mRNA down-regulation in HDMEC 48 h after transfection with siRNA (**A**). **B**. HIF-1α mRNA expression in HDMEC transfected with siRNA for HIF-1α and treated with 0.7 mM $CoCl_2$ or anoxia for 18 h. mRNA expression was determined with real time PCR. The data are presented as fold of control (the sample transfected with negative control siRNA) set as 1, (means ± 95% confidence interval).*

To find out if decrease in mRNA amount correlated with the protein down-regulation, HIF-1α was detected with western blotting. Because HIF-1α protein is extremely unstable, it was almost non-detectable in untreated cells. Therefore, HIF-1α down-regulation was studied in $CoCl_2$- and anoxia-treated cells. Both siRNAs induced a potent knock-down of HIF-1α protein (more than 90% down-regulation) as compared to HDMEC treated with $CoCl_2$ and anoxia for 18 h (48 h after transfection, Fig. 3.40).

To exclude possible cytotoxicity of siRNA transfection and to reveal any potential protective or synergetic effects of HIF-1α down-regulation towards $CoCl_2$-induced loss of cell

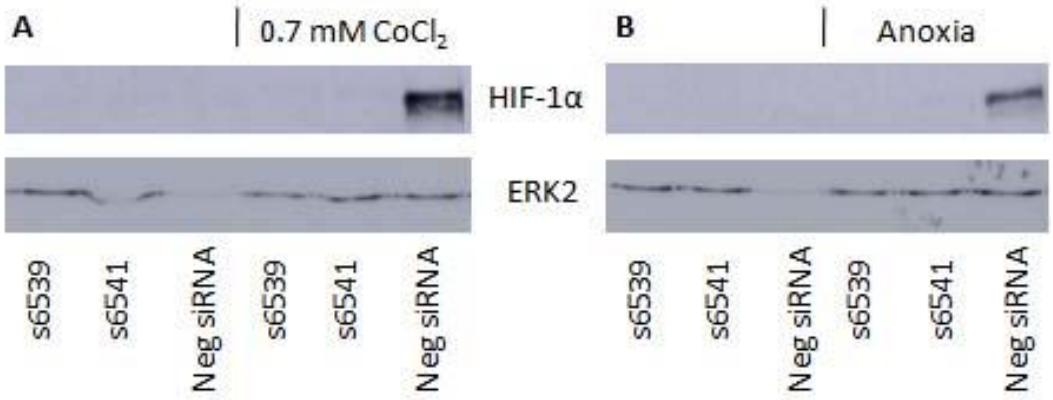


**Fig. 3.40.** *HIF-1α protein down-regulation in HDMEC 48 h after transfection with siRNA and 18h after treatment with 0.7 mM $CoCl_2$ (**A**) or anoxia (**B**). HIF-1α expression was visualised with western blot. ERK2 expression is presented as loading control.*

viability MTS assay and crystal violet staining were performed. The results did not show any reduction in cellular metabolic activity or cell number after transfecting HDMEC with siRNA. Furthermore, there were no significant effects of HIF-1α down-regulation on cytotoxicity induced by $CoCl_2$ and $H_2O_2$ (Fig. 3.41).

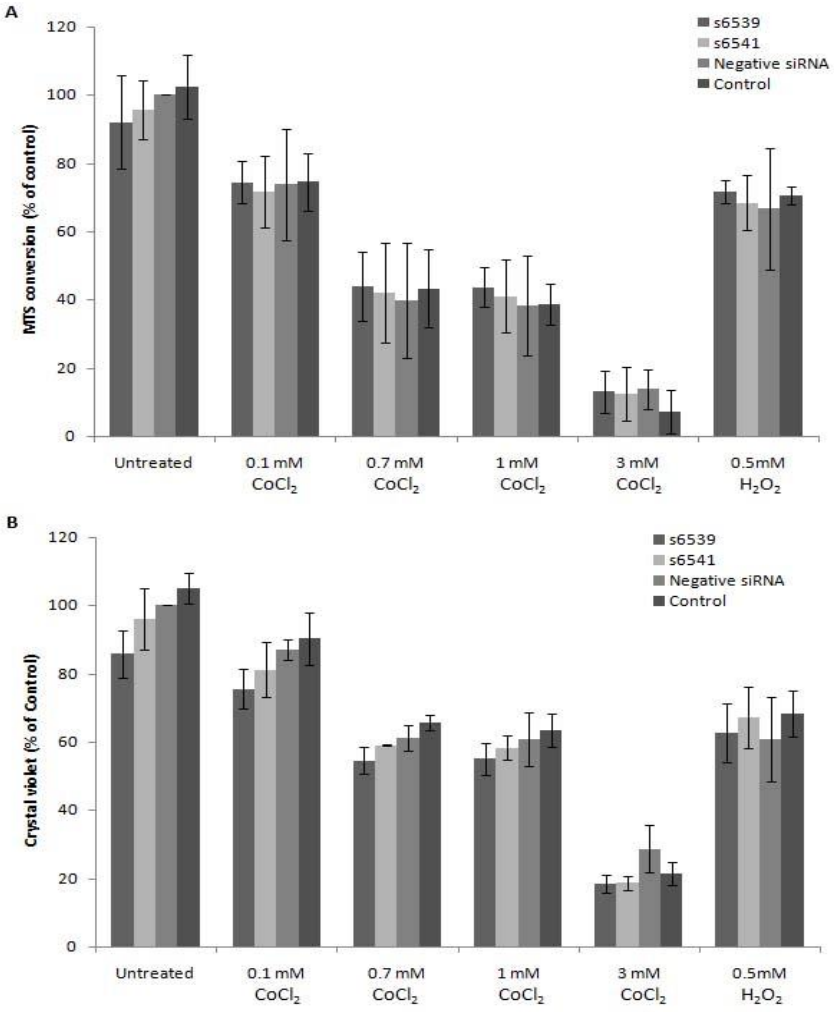


**Fig. 3.41.** *Metabolic activity (**A**) and cell number (**B**) of HDMEC transfected with siRNA for HIF-1α and treated with $CoCl_2$ or $H_2O_2$ for 18 h. Metabolic activity was assessed with MTS conversion assay and cell number with crystal violet assay.The data are presented as % of control (untreated sample transfected with negative siRNA; means±SDs).*

To see if the knockdown of HIF-1α had an effect on the expression of other genes, mRNA for two known transcriptional targets of HIF-1α, BNip3 (Bcl-2/E1B 19 kDa interacting protein 3) and PHD2 was quantified in siRNA-transfected HDMEC after treatment with $CoCl_2$ and anoxia. BNip3 mRNA was elevated in HDMEC after both $CoCl_2$ (around 5-fold) and anoxia (8-fold increase) treatment (Fig.3.42.A). As expected, BNip3 up-regulation

was lower in HDMEC transfected with siRNAs to HIF-1α (only 2-fold increase was induced by $CoCl_2$ and anoxia). PHD2 expression showed a comparable pattern. $CoCl_2$ and anoxia induced the increase in PHD2 mRNA amount (2.5- and 5-fold, correspondingly). HIF-1α down-regulation blocked PHD2 induction by $CoCl_2$ almost completely and reduced the induction level after anoxia treatment (Fig. 3.42.B).

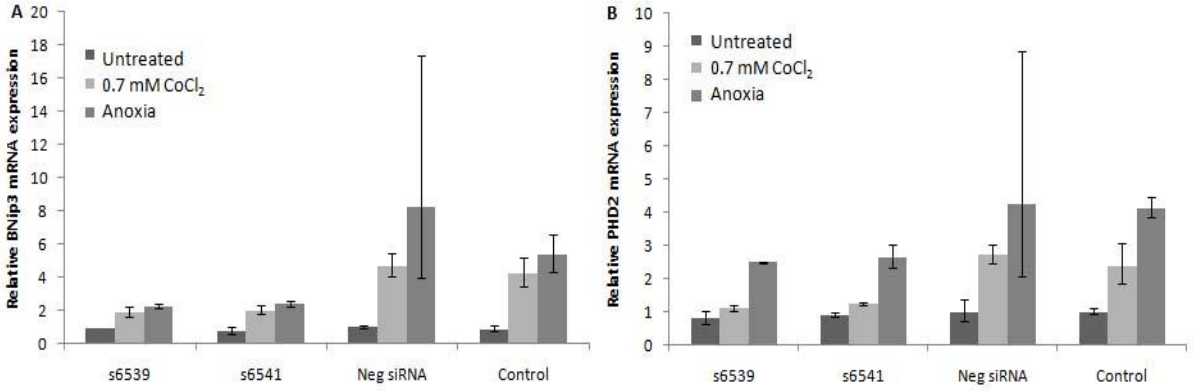


**Fig. 3.42.** *BNip3(**A**) and PHD2 (**B**) mRNA expression in HDMEC transfected with siRNA for HIF-1α and treated with 0.7mM $CoCl_2$ or anoxia for 18 h. mRNA expression was measured with real-time PCR and the data are presented as fold of control (untreated sample transfected with negative siRNA; means ± 95% confidence intervals*

Microarray analysis was performed with HDMEC transfected with s6541 siRNA and treated with 0.7 mM $CoCl_2$ and anoxia for 18 h. Since transfection of siRNAs itself may induce changes in gene expression, HDMEC transfected with negative control siRNA were chosen as a control for the experiment, although an additional control with untransfected and untreated cells was also used to control for unspecific effects of siRNA transfection (Control).

While approximately the same number of genes were regulated by $CoCl_2$ and anoxia only a small amount of these genes were common for both. Manual analysis of microarray data revealed few functional groups of genes induced by $CoCl_2$ treatment, whose regulation was HIF-1α-dependent (Table 3.5). Importantly, however, HIF-1α-independent regulation of the genes in the same functional groups by $CoCl_2$ was observed, thus pointing to the requirement of more rigorous analysis of microarray data based on cluster analysis and grouping of the genes according to gene ontology information.

A group of transcription factors was strongly induced in HDMEC 18 h after $CoCl_2$ treatment. It included ATF2, STAT3 (signal transducer and activator of transcription 3), NF-κB subunit RELA and VEZF1 (vascular endothelial zinc finger 1). Induction of these

**Table 3.5.** *mRNA expression in HDMEC transfected with siRNA against HIF-1α (s6541) and negative control siRNA (Neg siRNA) and exposed to 0.7 mM $CoCl_2$ or anoxia for 18 h. The expression in untreated HDMEC, transfected with Neg siRNA was set as 1; Control – untransfected and untreated cells (cDNA microarray data).*

| | Untreated | | 0.7 mM $CoCl_2$ | | Anoxia | | Control |
|---|---|---|---|---|---|---|---|
| Gene | s6541 | Neg siRNA | s6541 | Neg siRNA | s6541 | Neg siRNA | |
| | | | | | | | |
| **ATF2** | 1.14 | 1 | 1.20 | 4.77 | 0.93 | 0.96 | 1.55 |
| **STAT3** | 1.36 | 1 | 1.37 | 8.31 | 0.59 | 0.51 | 1.22 |
| **RELA** | 0.88 | 1 | 0.98 | 7.82 | 1.98 | 0.53 | 1.03 |
| **VEZF1** | 0.95 | 1 | 1.01 | 7.82 | 1.15 | 1.02 | 1.12 |
| | | | | | | | |
| **TGFβ1** | 1.01 | 1 | 1.05 | 3.00 | 0.88 | 4.09 | 1.65 |
| **FGFRL1** | 0.80 | 1 | 0.66 | 4.41 | 1.88 | 23.12 | 1.52 |
| **Ang1** | 0.97 | 1 | 2.74 | 2.75 | 0.51 | 1.09 | 0.98 |
| **FGF5** | 0.97 | 1 | 1.13 | 0.66 | 1.14 | 4.05 | 1.32 |
| **FGF2** | 0.87 | 1 | 2.07 | 1.21 | 2.60 | 0.73 | 1.38 |
| | | | | | | | |
| **OGG1** | 0.70 | 1 | 1.33 | 11.18 | 1.69 | 0.82 | 0.95 |
| **MDM2** | 1.01 | 1 | 1.36 | 2.59 | 0.44 | 0.48 | 0.93 |
| **p53** | 0.99 | 1 | 0.93 | 1.10 | 0.95 | 1.04 | 1.22 |
| **p21CIP1** | 0.21 | 1 | 0.82 | 3.75 | 0.82 | 1.56 | 1.06 |
| **GADD45B** | 0.96 | 1 | 0.93 | 3.44 | 1.29 | 0.84 | 0.94 |
| **GADD45A** | 1.17 | 1 | 0.72 | 2.31 | 0.89 | 0.37 | 1.22 |
| **β-catenin** | 0.81 | 1 | 0.72 | 2.85 | 2.00 | 0.94 | 1.19 |
| **Cyclin D3** | 0.98 | 1 | 0.85 | 1.03 | 1.05 | 13.34 | 0.89 |
| **Cyclin E1** | 0.88 | 1 | 0.91 | 0.45 | 0.62 | 13.74 | 0.83 |
| | | | | | | | |
| **GSTM4** | 0.71 | 1 | 0.45 | 2.38 | 1.30 | 0.72 | 1.78 |
| **GSTO1** | 1.17 | 1 | 0.80 | 4.94 | 0.24 | 0.61 | 0.82 |
| **GSTT2** | 0.80 | 1 | 0.62 | 4.75 | 1.12 | 2.27 | 1.03 |
| **TXNDC6** | 0.96 | 1 | 1.01 | 12.28 | 1.28 | 0.69 | 0.99 |
| **TXNDC10** | 1.01 | 1 | 0.95 | 5.69 | 0.43 | 1.38 | 0.83 |
| | | | | | | | |
| **HSPA1A** | 1.14 | 1 | 0.98 | 2.30 | 1.84 | 0.99 | 0.86 |
| **HSPA8** | 1.01 | 1 | 0.99 | 3.17 | 2.43 | 0.94 | 0.86 |
| **HSPA14** | 0.99 | 1 | 0.90 | 14.82 | 1.09 | 1.10 | 1.03 |
| **HSPA4** | 0.90 | 1 | 1.10 | 1.25 | 0.51 | 60.63 | 0.98 |
| **DNAJA3** | 1.02 | 1 | 0.54 | 1.22 | 1.67 | 6.01 | 0.96 |

transcription factors could explain a broad range of $CoCl_2$-induced reactions. Interestingly, $CoCl_2$-induced up-regulation of all mentioned transcription factors was abrogated by transfection of cells with siRNA against HIF-1α suggesting that these genes are either direct HIF-1α targets or that their transcription is induced by other factors, which are HIF-1α-dependent. As for the most of the genes described below, HIF-1α siRNA did not induce any striking changes in gene expression of transcription factors in HDMEC that were treated with $CoCl_2$ or subjected to anoxia. Importantly, the gene expression pattern in untreated cells that were also not transfected with any siRNA did not differ drastically from gene expression in the cells transfected with negative control siRNA. Therefore, siRNA transfection itself did not seem to induce changes in gene expression, making the system plausible to study specific effects of HIF-1α.

A number of growth factors and growth factor receptors was also differentially expressed in HDMEC 18 h after treatment with 0.7 mM $CoCl_2$. Thus, TGFβ1 and FGFRL1 (fibroblast growth factor receptor like 1) were induced 3- and 4.4-times, respectively, in $CoCl_2$-treated cells. Importantly, their expression was reduced to the control level in $CoCl_2$-treated cells, in which HIF-1α was down-regulated with siRNA. These genes were also induced in anoxia-treated HDMEC (TGFβ1 was elevated 4-fold and FGFRL1 – 23-fold) and the regulation was also HIF-1α-dependent. Ang1 (angiopoietin 1) expression was also induced by $Co^{2+}$ (2.7-fold) but the induction could not be abrogated by HIF-1α siRNA. In contrast, FGF5 mRNA expression was elevated only in HDMEC in an anoxic atmosphere (4-fold induction) and the expression was HIF-1α-dependent. A remarkable mode of regulation was observed for FGF2. mRNA coding for FGF2 was not affected either by $CoCl_2$ treatment or by anoxia. However, HIF-1α knock-down led to the induction of FGF2 mRNA (more than 2-fold) by both stimuli, pointing to a possible negative role of HIF-1α in FGF2 regulation.

A group of genes, involved in DNA damage response and cell cycle regulation was also differentially expressed in HDMEC after $CoCl_2$ or anoxia treatment. Since $CoCl_2$ has been shown to cause 8-oxoG formation in DNA, induction of mRNA coding for OGG1 (11-fold), an enzyme involved in the repair of this DNA lesion, by $CoCl_2$ was of high interest. Importantly, OGG1 induction was HIF-1α-dependent, since no difference to control in OGG1 mRNA level were observed in HDMEC transfected with HIF-1α siRNA. No induction was seen upon anoxia application. Additionally, mRNA for MDM2, a protein regulating p53 stability, was up-regulated in HDMEC after $CoCl_2$ treatment (2.6-fold induction). It is known that MDM2 is also a transcriptional target of p53 in an autoregulation loop, therefore, MDM2

mRNA elevation could indicate the activation of the p53 pathway. p53 mRNA was, however, not regulated by $Co^{2+}$, which could be explained by the fact that p53 is mostly regulated on the protein level. Importantly, known p53 targets, p21CIP1, GADD45A and GADD45B involved in cell cycle arrest, were up-regulated by $CoCl_2$ at the mRNA level (3.7-, 3.4- and 2.3-fold induction, respectively). However, the expression of MDM2, p21CIP1, GADD45A and GADD45B induced by $CoCl_2$ could be reduced to a control level by transfecting the cells with siRNA against HIF-1α. Interestingly, p21 mRNA expression was markedly reduced (5-fold) even in untreated HDMEC with down-regulated HIF-1α. The data, therefore, pointed to a possible role of HIF-1α in regulation of these genes. It might be possible, however, that an upstream event (e.g. stabilisation of p53) is HIF-1α-dependent. Furthermore, mRNA for β-catenin, which was also shown to induce p21 expression, was up-regulated in $CoCl_2$-treated HDMEC and the regulation was HIF-1α-dependent. In contrast to $CoCl_2$ anoxia was not able to regulate any of the mentioned genes at the time point of the measurement. In turn, anoxia caused an induction in expression of mRNA coding for cyclins D3 an E1 (13-fold induction for both genes) and the regulation was HIF-1α-dependent.

Oxidative stress, which was shown to be induced in HDMEC after $CoCl_2$ treatment, can often lead to the adaptive increase in the expression of antioxidant enzymes. Of interest, therefore, was $Co^{2+}$-induced expression of a group of mRNAs coding for GSTs (GSTM4, GSTO1 and GSTT2; 2.3-, 4.9- and 4.8-fold induction, respectively) and Trx-related proteins TXNDC6 and TXNDC10 (thioredoxin domain containing 6 and 10; 12.3- and 5.7-fold elevation, respectively). Regulation of all of these genes was HIF-1α-dependent, since siRNA to HIF-1α efficiently abrogated $CoCl_2$-induced gene expression to the levels, which were even slightly lower than in control cells. Interestingly, in response to anoxia only GSTT2 mRNA was up-regulated and this event was also HIF-1α-dependent.

Another group of genes regulated by $CoCl_2$ and anoxia consisted of HSP and DNAJ chaperones. HDMEC treated with 0.7 mM $CoCl_2$ for 18 h displayed elevated expression of mRNAs for HSPA1A, HSPA8 and HSPA14 (2.3-, 3.2- and 14.8- fold increase, respectively). HSPs up-regulation in HDMEC treated with $CoCl_2$ could be abrogated by siRNA against HIF-1α. In contrast, anoxia induced the expression of other chaperones, HSPA4 and DNAJA3 (correspondingly, 60- and 6-fold), although the expression was still HIF-1α-dependent. HIF-1α-dependent regulation of HSPA8 expression was opposite in case of $CoCl_2$ and anoxia. While $CoCl_2$ induced HSPA8 mRNA and its expression was decreased by HIF-1α siRNA,

anoxia itself did not change HSPA8 mRNA expression but was able to induce the expression together with HIF-1α knock-down.

Altogether, the data pointed to the distinct effects of $CoCl_2$ and anoxia on gene expression in HDMEC, although some of the changes induced by both treatments overlapped. Moreover, both HIF-1α-dependent and independent gene regulation was observed for both $CoCl_2$ and anoxia. However, to conclude on the HIF-1α-dependent and independent molecular pathways induced by different agents, more rigorous computational analysis of microarray data will be necessary. Furthermore, the changes caused by transfection of siRNA against HIF-1α should be confirmed using other siRNAs with the same specificity, mRNA expression should be confirmed with other methods and correlated to the changes at protein level. Nevertheless, the data provide a good basis for the further dissection of $Co^{2+}$- and anoxia-induced signalling.

# 4. Discussion

## 4.1. Response of endothelial cells to Ti6Al4V alloy

### 4.1.1. Ti6Al4V-induced oxidative stress

Titanium and titanium alloys are materials of choice for many medical applications. Apart from their excellent mechanical properties, widely accepted titanium corrosion resistance and biocompatibility are the main reasons for wide use of titanium-based biomaterials. The surface of Ti6Al4V, the titanium alloy used in this study, as well as other titanium-based materials, is normally covered with a $TiO_2$ layer that is held responsible for their biocompatibility (Williams 1981). However, several facts point to the reactivity of titanium surfaces. Bikondoa et al. (Bikondoa et al 2006) showed that defects such as oxygen vacancies in a model oxide surface, rutile $TiO_2$ (110), mediate the dissociation of water. Another indication for titanium alloy reactivity is an elevated concentration of titanium in the serum of patients after implantation. Dramatic increase in titanium serum concentration was demonstrated in patients with failed knee implants (Hallab et al 2000, Jacobs et al 1999). Titanium release is a result of the anodic corrosion process, which takes place at the sites of defects in the $TiO_2$-layer. Wear particles formed at the interface bone/implant or implant/cement (used for the fixation of the implant) can disrupt the protective $TiO_2$ film, thus further inducing corrosion and leading to the synergistic fretting-wear process. Metal ions are released from the metal implants as well as from its wear debris and can reach significant concentrations in peri-implant tissues and blood. Ti-ion concentration in tissues surrounding hip prosthesis can reach 0.6 mM (Blumenthal et al 1994). It is important that normally only Ti ion elevation is detected in patients with implants made of titanium alloys. Hence, the concentration of Al showed no differences between patients with failed and stable Ti6Al4V alloys, while the concentration of V remained low (Jacobs et al 1991). An increased metal ion concentration can be detected even in individuals with no complications after implantation of Ti-based prostheses, suggesting that metal corrosion occurs even in the absence of metal wear debris formation (Jacobs et al 1998b).

The cathodic part of the corrosion process, in contrast, results in the reduction of oxygen at physiological pH with the formation of ROS and $H_2O_2$ as intermediate products (Mentus 2004). Thickening of the $TiO_2$-layer in biological solutions substantiates the fact that

corrosion processes permanently occur at titanium implant surfaces (Lin & Bumgardner 2004, Pan et al 1998). Besides the possible formation of ROS by the titanium(-alloy) itself as the result of cathodic corrosion, titanium may be subjected to the ROS produced by inflammatory cells coming into contact with titanium(-alloy) surfaces directly after implantation. One of the mediators is $H_2O_2$ released by monocytes, macrophages and granulocytes. The $TiO_2$ layer may interact with $H_2O_2$ leading to formation of hydroxyl radicals (Lee et al 2005). Altogether, these facts led to the hypothesis that endothelial cells that take part in the wound healing early after implantation, might be permanently subjected to ROS formed at the titanium implant surface, which exeeds physiological protection mechanisms and can thus be referred to as oxidative stress. To confirm this hypothesis the reactions of endothelial cells to the Ti6Al4V alloy in the presence of the oxidative stress inducer $H_2O_2$ in comparison to the reactions elicited in endothelial cells grown on cell culture PS were studied.

The quantification of HDMEC growing on Ti6Al4V and PS revealed the dose-dependent reduction of cell number to the same extent on PS and Ti6Al4V alloy 24 h after $H_2O_2$ treatment compared to the untreated control, with no significant differences between the materials. In contrast, expression of Ki67, a known proliferation marker, was lower in HDMEC grown on Ti6Al4V alloy compared to the cells grown on PS. This pointed to the possibility of higher $H_2O_2$ cytotoxicity on Ti6Al4V alloy. It has been shown in fibroblasts that $H_2O_2$ concentrations between 0.12 to 0.4 mM led to growth arrest, whereas higher $H_2O_2$-concentrations induced cell death via apoptosis (0.5 - 1.0 mM) or necrosis (5.0 - 10.0 mM) (reviewed in (Davies 1999)). Low $H_2O_2$ concentrations (< 0.05 mM) were also shown to inhibit proliferation in endothelial cells (de Bono & Yang 1995). The discrepancy in cell number and proliferation ability of HDMEC on Ti6Al4V could possibly be explained by the higher initial attachment of endothelial cells to Ti6Al4V alloy In fact, it was demonstrated that osteoblasts attach to Ti6Al4V alloy in higher numbers compared to PS, which correlated to a better cell spreading (Sinha et al 1994). Another study, however, showed opposite results for epithelial cells (Shiraiwa et al 2002). The initially higher number of HDMEC on Ti6Al4V could gradually reduce due to slower proliferation and possible higher cytotoxicity leading to the equal cell amount on Ti6Al4V and PS at the measurement time point.

The LDH-release cytotoxicity assay revealed a concentration-dependent increase of LDH release from HDMEC after $H_2O_2$ treatment. The LDH release indicates damage of the cell membrane, a characteristic feature of necrotic cell death. Moreover, the LDH release was higher in cells grown on Ti6Al4V alloy compared to those in contact with PS. Another indication for a higher degree of cytotoxicity, the reduction of cellular metabolic activity

(determined by the MTS viability assay which mirrors the energy metabolic state, e.g. the development of NADH) also occurred after $H_2O_2$-treatment. While the $H_2O_2$ concentrations tested did not induce major changes in the metabolic activity of HDMEC grown on PS, they significantly decreased MTS conversion in the cells grown on the Ti6Al4V alloy. Importantly, even the basic MTS conversion rates (i.e. in cells not treated with $H_2O_2$) were lower in the cells grown on Ti6Al4V alloy compared to the cells grown on PS. It has been shown that oxidative stress induced by $H_2O_2$ treatment can lead to a rapid depletion of NADH and ATP due to an increased catabolic rate (Schraufstatter et al 1986). Thus, the reduction of metabolic activity in cells grown on Ti6Al4V could be a result of $H_2O_2$-induced oxidative stress. However, this does not explain the absence of metabolic reduction of cells in contact with PS. It is possible that compensatory mechanisms in HDMEC on PS prevent changes in metabolic activity after $H_2O_2$ treatment, while Ti6Al4V itself and $H_2O_2$ induce cumulative effects which result in reduced adaptive potential of the cells.

As already mentioned, $H_2O_2$ can induce oxidative stress in endothelial cells by promoting ROS formation. This is achieved by several mechanisms including activation of ROS production by mitochondria, NADPH oxidases, xanthine oxidase, uncoupled eNOS etc. (Cai 2005). $H_2O_2$ in the cell can also undergo the Fenton reaction in the presence of metal ions, resulting in the formation of highly toxic hydroxyl radicals. Using the DCF-assay higher levels of ROS was observed in endothelial cells grown on Ti6Al4V alloy 1 h after $H_2O_2$ addition compared to the cells on PS. DCF is the resulting oxidation product from DCDHF, which is oxidized by peroxyl radical, peroxynitrite and also $H_2O_2$ (Gomes et al 2005). Therefore, increases in DCF-fluorescence shown in this study can be explained through oxidation by $H_2O_2$, which enters the cell. However, since the $H_2O_2$-concentration remaining in the medium 1 h after its addition is nearly similar on both materials the higher DCF-fluorescence in cells grown on Ti6Al4V alloy might reflect further ROS production. One possible explanation for this could be the formation of ROS due to the reactivity of $H_2O_2$ with the $TiO_2$-layer. A study by Lee et al. (Lee et al 2005) showed that $^{\cdot}OH$ were formed during the interaction of $TiO_2$ and $H_2O_2$ *in vitro,* while irradiated $TiO_2$ reacting with $H_2O_2$ could produce $^{\cdot}O_2$-. Other studies, on the contrary, demonstrate no formation of $^{\cdot}OH$ in the reaction between $H_2O_2$ and $TiO_2$ (Tengvall et al 1989a, Tengvall et al 1989b). Tengvall et al. suggested that a Ti-peroxy gel is formed as a result of the interaction of Ti with $H_2O_2$ (Tengvall et al 1989b). This gel is believed to trap $^{\cdot}O_2$- (Tengvall et al 1989a). Interestingly, in the absence of serum, Ti-peroxy gels could decrease ROS production by activated leukocytes (Larsson et al 2004). Opposite effects of Ti-peroxy gel were also reported. Thus, while the $TiO_2$ layer was

acting as a scavenger for ˙OH, the Ti-peroxy gel could amplify detrimental effects of ˙OH on ECM proteins, as well as cause these effects alone *in vitro* (Taylor et al 1996). High amounts of $H_2O_2$ are needed to produce Ti-peroxy gel *in vitro*. Such conditions are probably unachievable *in vivo*, although the formation of Ti-peroxy gel and trapping of radicals could hypothetically contribute to the tissue reactions to the implant over longer time periods. This may also be a reason for a relatively better performance of Ti materials compared to other metal materials. However, higher ROS formation in HDMEC on Ti6Al4V alloy shown in this study favours the interaction of $H_2O_2$ with the $TiO_2$ layer on the alloy surface. It is also known that traces of iron are present in titanium alloys (according to ASTM F136 Ti6Al4V is allowed to have up to 0.2% Fe). The presence of iron in titanium alloy surface could also lead to the formation of ROS due to the Fenton reaction upon $H_2O_2$ exposure.

Cells have several mechanisms to protect themselves against oxidative stress. SOD, catalase and GSH system are the central defence players in enzymatic ROS detoxification. The balance between GSH and its oxidised form (GSSG) is critical for protecting cells against oxidants. Excessive formation of GSSG and glutathione conjugates with organic molecules during prolonged oxidative stress leads to the depletion of the GSH pool (Dickinson et al 2003). Thus, the reduced GSH-concentrations in endothelial cells grown on Ti6Al4V alloy compared to the cells grown on PS could reflect a state of permanent oxidative stress in cells in contact with Ti6Al4V alloy due to ROS formation on the titanium surface. This is supported by the fact that the GSH-concentration in endothelial cells on Ti6Al4V was reduced by $H_2O_2$-treatment, whereas in cells grown on PS the $H_2O_2$-treatment induced an elevation of GSH-level. The effects of $H_2O_2$-treatment on PS are in agreement with reports of adaptive increase in GSH concentration after exposure to $H_2O_2$, a fact that can be explained by the onset of GSH *de novo* synthesis and $H_2O_2$-induced up-regulation of the expression of GSH synthesis enzymes (γ-glutamylcysteine synthetase and GSH synthetase) by these temporary oxidative stimuli (Lu 2000, Rahman et al 1996).

Additional evidence for permanent oxidative stress on Ti6Al4V is based on the analysis of enzymatic activities of catalase and SOD. Cells grown on Ti6Al4V alloy showed significantly lower SOD activities than cells grown on PS. This could be explained by a persistent ROS-formation in cells on the Ti6Al4V-surface resulting in the exhaustion of enzyme activity, e.g. due to protein oxidation by ROS (Davies 1987). Catalase activity in endothelial cells grown on Ti6Al4V was only slightly reduced compared to cells cultured on PS. Moreover, $H_2O_2$ treatment of endothelial cells grown on PS elevated catalase and SOD activity. It is known that oxidative stress may increase the activity of antioxidant enzymes. The mecha-

nism of this induction may include changes in enzymatic activity of existing proteins and *de novo* enzyme synthesis (Meilhac et al 2000). Interestingly, 0.5 mM $H_2O_2$ did not change catalase activity, whereas this $H_2O_2$ concentration induced an increase in SOD activity suggesting an uncoupled regulation of catalase and SOD activity. In contrast, $H_2O_2$-exposure on Ti6Al4V led to a decrease in SOD activity in endothelial cells. This reduction in SOD activity could be caused by a cumulative effect of the temporary $H_2O_2$-induced and the permanent Ti6Al4V-induced oxidative stress. Consequently, the facts demonstrated above indicated an elevated sensitivity of endothelial cells to oxidative stress when growing in contact with Ti6Al4V and thus a reduced antioxidant defence potential.

An animal study by Ozmen et al. (Ozmen et al 2005) indicated a similar effect *in vivo*: it was shown that 1 month after the insertion of titanium implants in rabbits an increase in lipid peroxidation (a possible result of oxidative stress) in the tissues surrounding the titanium implants occurred, whereas there was a decrease in the activities of antioxidant enzymes (e. g. catalase, SOD, GPX). The same reactions, though to a lesser extent, were seen in the tissues around implanted stainless steel but were minimal in the case of implanted polyethylene. These observations indicate a state of permanent oxidative stress at the surface of titanium implants, leading to exhaustion of antioxidant enzymes in the surrounding tissues. In another study, increased oxidative stress was observed in patients in the tissue surrounding stable and loose total hip implants (Kinov et al 2006). It was manifested by a low GSH/GSSH ratio and elevated levels of MDA, a known product of lipid peroxidation, in patients compared to control individuals. Increased $H_2O_2$ concentrations and decreased catalase activity were also detected in the fibrotic capsule from a failed joint implant (Tucci et al 2000). Endothelial cells were also shown to undergo oxidative stress when growing in contact with a NiTi alloy. However, this was attributed to the presence of the transition metal Ni in the $TiO_2$ layer (Plant et al 2005). Vanadium, which is a component of the alloy used in this study, is known to be toxic and to induce formation of ROS via Fenton and Haber-Weiss reactions (Zhang et al 2001). However, on analysis of the surface oxide film of the Ti6Al4V alloy using X-ray photoelectron spectroscopy vanadium oxide was not detected (Milosev et al 2000), but the presence of traces of vanadium on the surface of titanium alloy cannot be completely excluded.

The occurrence of permanent oxidative stress on Ti6Al4V alloy in the present study was further substantiated by the positive effect of external GSH on the metabolic activity of endothelial cells. HDMEC grown on Ti6Al4V in the presence of GSH-MEE displayed significantly higher metabolic activity as compared to the cells incubated without GSH-MEE.

Importantly, MTS conversion in GSH-MEE-treated cells was higher than in HDMEC grown on PS. GSH-MEE also had a stimulating effect on the cells grown on cell culture plastic. Although the increase in metabolic activity caused by the addition of external GSH was higher in HDMEC on Ti6Al4V alloy, a general stimulating effect of GSH on cellular metabolism cannot be excluded. However, it is likely that cells on PS are protected by GSH-MEE from ROS that are continually formed in the cells during normal metabolism. On Ti6Al4V, on the other hand, at least part of the GSH-MEE stimulating effect could be attributed to the protection against $H_2O_2$ and ROS formed at the titanium surface or induced in the cell by the growth on Ti6Al4V. Interestingly, another ROS scavenger, DMTU, showed no visible effect on the metabolic activity of HDMEC grown on Ti6Al4V, while the cells on PS were slightly stimulated. DMTU is known to bind to $^{\cdot}OH$ (Wasil et al 1987), while GSH can directly detoxify $H_2O_2$. GSH-MEE is membrane permeable, so it can decompose $H_2O_2$ both inside the cells as well as during possible $H_2O_2$ formation on the titanium alloy surface. However, the specificity of ROS scavengers has been questioned, thus making the issue of the exact ROS responsible for oxidative stress on Ti6Al4V alloy difficult to unravel.

In conclusion, a permanent state of oxidative stress appears to exist in endothelial cells grown in direct contact with Ti6Al4V surfaces. Although the nature of the stressor is unknown, it is possible that corrosion might take place at the interface of titanium alloy, since ROS formation is expected to occur as a result of the cathodic partial reaction of corrosion.

### 4.1.2. Cathodic half-reaction of corrosion as the possible source of oxidative stress on Ti6Al4V alloy

Only very few studies have addressed the problem of the cathodic partial reaction of corrosion simulation *in vitro* toi investigate its effects on the cells involved in the implant integration process. It was found in electrochemical studies that oxygen reduction reactions, the main event during cathodic partial reaction of corrosion, can lead to the formation of $H_2O_2$ on $TiO_2$ surfaces (Clark & Johnson 1997, Clechet et al 1979). The study by Mentus et al. (Mentus 2004) provided evidence that this process is driven by a pH-dependent transition from $2e^-$ to $4e^-$ reduction of oxygen on anodically formed $TiO_2$ in an electrochemical cell that led to the formation of $H_2O_2$ and other oxygen radicals as intermediate products. It also showed that oxygen reduction reactions can occur on $TiO_2$ at any pH value without any particular activation.

To examine the effects of cathodic polarisation products on cellular functions an experimental setup was developed in which Ti6Al4V disks with cultivated cells were cathodically polarised by applying electrical current to the system (Kalbacova et al 2007). It was demonstrated that endothelial cells grown on Ti6Al4V alloy display the reduction of metabolic activity with increasing current densities applied to Ti6Al4V samples. This was in agreement with lower metabolic activity of HDMEC grown on Ti6Al4V compared to the cells on PS and the further decrease induced by $H_2O_2$. While lower current densities had no visible effects, higher current densities induced adverse effects. This was also true for cathodic polarisation-induced rearrangements of actin cytoskeleton and loss of intercellular contacts, this being important for the regulation of endothelial permeability during inflammation, at the higher current densities as well as for cell nuclear condensation. This indicated that cathodic corrosion could induce changes in viability and pro-inflammatory phenotype of endothelial cells, thus potentially exerting negative effects on wound healing and stability of an implant. It was also shown that cathodic polarisation of Ti6Al4V alloy induced drastic elevation in fluorescence of DCF that was given to the cells prior to the treatment. This can result from DCDHF oxidation by $H_2O_2$ formed during the cathodic partial reaction and freely diffusing through the cell membrane or by ROS induced in the cells by $H_2O_2$.

Apart from $H_2O_2$ and ROS formation cathodic half-reaction of corrosion may result in few additional events. First of all hydroxyl ions are formed in oxygen reduction reactions, which might lead to the change in pH. However, the experiments were performed in a buffered system ruling out the possibility of pH effect. Secondly, oxygen deficiency may occur locally due to oxygen consumption in the cathodic half-reaction. In fact, decreased oxygen concentrations were detected in close proximity to the surface of polarised titanium (Gilbert et al 1998). This effect correlated with the reduced spreading of osteoblasts on polarised titanium. However, the authors did not take into consideration other events occuring during cathodic half-reactions. Finally, hydrogen might be formed as a result of the cathodic half-reaction. However, this reaction is prevalent at acidic pH or when higher current densities are applied. This could be excluded, since the current densities used in this study where below oxygen diffusion current density, which is approximately -30 µA/cm² in unstirred air-saturated aqueous electrolytes (Song et al 2002a). Additionally, interactions of the electric field occurring during polarisation with electric properties of cell membranes and electric field-induced changes in the conformation of proteins absorbed to the polarised surface are poorly studied phenomena and can also play their role in the reduction of cell viability in the

used model. Electric fields have been shown to direct cell migration during wound healing processes (Zhao et al 2006).

Interestingly, similar results were obtained in the same model of cathodic polarisation with osteoblastic and macrophage cell lines. Cathodic polarisation of Ti6Al4V alloy induced current density-dependent reduction in cellular metabolic activity that coincided with increased ROS formation and changes in cell morphology. The reactions of osteoblasts and macrophages were comparable to $H_2O_2$ treatment on Ti6Al4V alloy done in parallel (Kalbacova et al 2007).

This *in vitro* model, that allows the exposure of cultivated cells to cathodic corrosion products, offers the possibility to study direct influence of ROS formed at the metal surface on cellular viability and functions. Using current densities that induce production of ROS amounts similar to the *in vivo* situation could deepen our knowledge about the contribution of the cathodic partial reaction of corrosion to metal-induced adverse tissue reactions. However, the origin and nature of oxidative stress at the metal implant surface has to be considered as a multifactorial process, in which the effects of $H_2O_2$ and ROS formed on titanium alloy surface may be augmented by ROS derived from inflammatory cells. The possibility of $H_2O_2$ interaction with $TiO_2$ layer leading to the formation of further ROS makes the process even more complicated. Upon metal debris formation damage to the $TiO_2$ layer occurs, which can amplify the corrosion process. All of these factors point to the contribution of the cathodic half-reaction of corrosion to adverse tissue reactions, leading eventually to aseptic loosening of implants.

### 4.1.3. Oxidative stress on Ti6Al4V alloy and pro-inflammatory response of endothelial cells

Inflammatory reactions are often observed in patients with failed metal implants. A typical sign of this is accumulation of inflammatory cells often seen in the close proximity of metal implants (Voggenreiter et al 2003). Furthermore, transient production of pro-inflammatory cytokines, such as IL-1β, IL-6 and TNF-α, can be observed around titanium devices in *in vivo* studies (Giudiceandrea et al 1998, Suska et al 2003). In most of the *in vivo* animal studies, however, the inflammation induced by metal bulk material is rather mild and transient and could be ascribed to the foreign body reaction. The presence of metal degradation products usually correlates to a much more pronounced inflammatory response.

Particles of Ti and CoCr alloys detected around loosened total joint replacement prostheses were found to induce the production of pro-inflammatory factors such as IL-1 and prostaglandin E2 (PGE2) in the tissues surrounding the implant (Thornhill et al 1990). These effects of metal particles were ascribed e.g. to the activation of inflammatory cells. Thus, particles of cpTi and Ti alloy particles retrieved at revision arthroplasty induced the release of PGE2, IL-1β, IL-6 and TNF-α by macrophages in *in vitro* studies (Garrigues et al 2005, Gonzales et al 1996, Maloney et al 1996, Rolf et al 2005). Metal ions, that are known to be released from metal implants during corrosion, have also been shown to affect different aspects of the inflammatory response. For instance, Ti, Cr and Co ions to a different extent could induce the release of IL-1β, TNF-α and IL-6 by macrophages (Wang et al 1996).

Less is known about the contribution of endothelial cells to the inflammation induced by metal implants and their degradation products. In *in vivo* experiments Ti6Al4V was shown to induce only a transient inflammatory response regarding increased leukocyte-endothelial cell interaction, leukocyte transmigration and vascular permeability (Pennekamp et al 2006). In contrast to Ti6Al4V, these parameters were markedly higher in the case of CoCrMo implantation (Kraft et al 2005). Importantly, inflammatory reactions induced by Ti particulate wear debris have been shown to be more drastic compared to the respective bulk material (Kraft et al 2003, Zysk et al 2004). Endothelial cells could also release IL-8 in response to Co and to a much lesser extent $TiO_2$ particles (Peters et al 2004).

Furthermore, a number of reports suggest that the presence of bacterial endotoxins on metal particulate wear debris due to lack of endotoxin removal steps in the preparation and sterilization of metal implants or due to accumulation of circulating endotoxin from intestinal flora or infections could be responsible for the pro-inflammatory properties of the bulk metal materials and particles and is the main cause for aseptic loosening of implants (reviewed in (Greenfield et al 2005)). In the study by Akisue et al. (Akisue et al 2002) Ti alloy particles retrieved from the soft tissue around a failed hip implant did not induce the release of TNF-α and IL-1β by monocyte/macrophage cell line, while bacterial endotoxin LPS and LPS-treated particles did induce release of cytokines. In another report cpTi particles free of endotoxin showed only half of the osteolytic reaction induced by particles with adherent endotoxin (Bunn & Poyton 1996).

Although the direct induction of an inflammatory response in endothelial cells by Ti6Al4V alloy is unclear, it is possible that endothelial cells are stimulated by inflammatory cytokines derived from macrophages and other inflammatory cells activated by metal implant degradation products or during the course of the normal wound healing process. Endothelial

cells in close proximity to Ti6Al4V alloy might be exposed to oxidative stress that could alter their response to pro-inflammatory stimuli. Therefore, the pro-inflammatory response to a known pro-inflammatory cytokine, TNF-α, and bacterial endotoxin (LPS) was compared in endothelial cells grown on Ti6Al4V or PS. TNF-α and LPS are known to bind to different receptors, but the signalling induced by these molecules leads to the activation of NF-κB and AP-1 transcription factors, which are thought to induce the transcription of pro-inflammatory genes (Dauphinee & Karsan 2006, Guha & Mackman 2001).

Actin and CD31 distribution in endothelial cells on Ti6Al4V alloy pointed to the possibility of a pro-inflammatory reaction. More stress fibres, less uniform intercellular contacts and a stronger reaction to $H_2O_2$ in HDMEC grown on Ti6Al4V alloy compared to the cells on PS were reminiscent of the pattern observed upon pro-inflammatory stimulation with TNF-α (Peters et al 2008). Oxidative stress is well known to induce actin stress fibres and increased vascular permeability, which can be in part reflected by alterations in intercellular contact distribution (Liu & Sundqvist 1995). Actin stress fibre formation was shown to be induced by $H_2O_2$ and mediated by p38 MAPK (mitogen-activated protein kinase) phosphorylation of actin binding protein HSP27 (Marceau et al 1998, Pouteau et al 1998). $H_2O_2$ was also shown to induce the translocation of filamin, a cross-linking actin binding protein that connects actin microfilaments, from membrane to cytosol, followed by rearrangement of the actin cytoskeleton (Hastie et al 1998). $H_2O_2$-induced increase in leukocyte extravasation was shown to be CD31 dependent (Scalia & Lefer 1998). CD31 can also undergo tyrosine phosphorylation following $H_2O_2$ treatment, a critical event for the regulation of its activity (Maas et al 2003). It is plausible, therefore, that oxidative stress on Ti6Al4V alloy is involved in the signalling which leads to redistribution of actin and CD31.

Although actin and CD31 rearrangements on Ti6Al4V alloy could indicate pro-inflammatory activation of HDMEC, E-selectin and ICAM-1 expression and IL-8 release by endothelial cells grown on Ti6Al4V were not induced compared to the cells on PS. In fact, these parameters were lower on Ti6Al4V than on PS. Importantly, however, expression of adhesion molecules on cell surface and release of cytokines were at least 10-fold lower on both materials compared to the cells stimulated with TNF-α. The data are in disagreement with the report by Bruni et al. (Bruni et al 2005), where higher ICAM-1 expression was detected in human umbilical cord endothelial cells grown on Ti6Al4V alloy compared to the control cells on tissue culture plastic, although ICAM-1 expression induced by alloy contact was much lower than in the case of stimulation with TNF-α. These divergencies might be

explained by differences in endothelial cell origin or by variations in Ti6Al4V surface characteristics.

Divergent reactions to $H_2O_2$ were observed in the HDMEC cultured on different materials. While on Ti6Al4V the amount of all studied pro-inflammatory molecules decreased, IL-8 release did not change and ICAM-1 expression was slightly up-regulated in HDMEC on PS. It is possible that the differences observed on PS and Ti6Al4V might be induced by ROS production on the titanium surface. ROS and $H_2O_2$ are known regulators of the inflammatory response, although the data obtained in studies with different cells and different experimental conditions are ambiguous. $H_2O_2$ treatment has been shown to induce ICAM-1 expression in endothelial cells (Lakshminarayanan et al 1997, Lo et al 1993, Roebuck 1999), while other reports showed no induction (True et al 2000). There is also some controversy about the effect of $H_2O_2$ on the production of cytokines by endothelial cells. An increase in MCP-1 mRNA (Lakshminarayanan et al 2001) and IL-8 release (Shono et al 1996) was observed upon $H_2O_2$ treatment of endothelial cells, whereas in another study $H_2O_2$ did not induce an elevation of IL-8 mRNA expression (Lakshminarayanan et al 1997). Oxidative stress has been shown to increase vascular permeability and leukocyte transmigration (Lum & Roebuck 2001)), and is therefore involved in the inflammatory response. Although some of the differences observed in cells on Ti6Al4V and PS were significant, they were rather small and it is difficult to say if these slight differences could be relevant for the *in vivo* situation. It was shown, however, that even small changes in the ICAM-1 expression in endothelial cells had an effect on the adhesion of neutrophils to endothelial cells (Gasic et al 1991, Lo et al 1993).

Importantly, the difference in the expression of E-selectin and ICAM-1 on the cell surface and IL-8 release were detected in HDMEC grown on Ti6Al4V and stimulated with TNF-α or LPS. For both treatments the induction of pro-inflammatory molecules was lower in the cells grown on Ti6Al4V alloy compared to the cells on PS. This correlated with the reduced metabolic activity of HDMEC on Ti6Al4V alloy, although no significant differences were observed in cell number on Ti6Al4V and PS under the same treatments. Oxidative stress on Ti6Al4V alloy could be responsible for a less effective response of HDMEC to TNF-α or LPS. Interestingly, pre-treatment of endothelial cells with $H_2O_2$ has been shown to reduce TNF-α-induced expression of E-selectin and ICAM-1, as well as IL-8 release and correlated with decreased NF-κB translocation (Zahler et al 2000). In this study, however, $H_2O_2$ treatment in the presence of TNF-α induced further increase in ICAM-1 expression and IL-8 release. By contrast this effect was absent in HDMEC grown on Ti6Al4V alloy. Interestingly,

the effects of $H_2O_2$ on TNF-α-induced NF-κB activation have been shown to be concentration-dependent: while lower doses (up to 25 μM) had a stimulatory effect, higher doses led to the inhibition of TNF-α-induced NF-κB nuclear translocation (de Oliveira-Marques et al 2007). It was demonstrated, however, that while TNF-α induction of ICAM-1 is NF-κB-dependent, regulation by $H_2O_2$ can proceed through AP-1 activation (Roebuck et al 1995). Therefore, there might be differences in the separate and simultaneous modes of $H_2O_2$ and TNF-α action. It is known that ROS are involved in TNF-α-induced NF-κB signalling (Bubici et al 2006). This could possibly explain the cumulative effect of $H_2O_2$ (that is rapidly decomposed in cell culture medium) and TNF-α on ICAM-1 expression and IL-8 release. In contrast, endothelial cells on Ti6Al4V that are exposed to a permanent oxidative stress respond in a less pronounced way to TNF-α and LPS. Synergistic effects of LPS and $H_2O_2$ treatment were not observed, indicating that ROS might have different roles in TNF-α and LPS-induced signalling, although ROS formation has also been shown to be induced by LPS (Dauphinee & Karsan 2006). Reduced pro-inflammatory response could, therefore, be due to the interference of Ti6Al4V-induced $H_2O_2$ and ROS with NF-κB and AP-1 signalling, but could also be explained by modulated cellular metabolic activity.

To study if the less efficient endothelial cell response to TNF-α on Ti6Al4V alloy is regulated at the transcriptional level the mRNA expression of pro-inflammatory genes was assessed on both materials. Surprisingly, TNF-α-induced E-selectin, ICAM-1 and IL-8 mRNA expression showed the opposite pattern. TNF-α-induced mRNA expression in all cases was higher in HDMEC grown on Ti6Al4V alloy compared to the cells on PS. In addition, a $H_2O_2$ synergistic effect was observed in HDMEC on Ti6Al4V alloy. In fact, it was higher (except for IL-8) than in the cells grown on PS. This could indicate that during oxidative stress on Ti6Al4V, TNF-α and $H_2O_2$ can interact in the induction of pro-inflammatory mRNAs in HDMEC on Ti alloy. As shown before, this increase is not reflected by the protein expression. Interestingly, the ROS scavenger DMTU had a stimulating effect on the expression of E-selectin, ICAM-1 and IL-8 mRNA on both materials. However, the effect of DMTU on TNF-α-induced expression of mRNA for pro-inflammatory proteins studied was more pronounced in HDMEC grown on Ti6Al4V alloy compared to the cells on PS. In contrast, GSH-MEE did not cause additional increase in TNF-α-induced response to either of the materials. ROS have been shown to be able to both stimulate and inhibit NF-κB signalling. ROS are believed to be involved at the I-κB degradation step at IKK activation level, but the exact mechanism of their action is still elusive. ROS can also inhibit NF-κB DNA binding activity via oxidation of a particular cysteine residue of the p50 subunit of NF-

κB (Bubici et al 2006). ROS scavengers have been shown to exert different effects on NF-κB and AP-1signalling. Hence, NAC (N-acetyl-L-cysteine) and PDTC (pyrrolidine dithiocarbamate) have been shown to inhibit TNF-α-induced NF-κB activation (Schreck et al 1992). Also DMTU was shown to inhibit TNF-α-induced ICAM-1 expression in epithelial cells (Krunkosky et al 2003). In contrast, DNA-binding activity of NF-κB has been shown to be inhibited by oxidation and could be restored by Trx. Importantly, high levels of GSSG also inhibited NF-κB pointing to redox sensitivity of this transcription factor (Galter et al 1994, Toledano & Leonard 1991). AP-1 has also been shown to be redox sensitive and GSH depletion has been demonstrated to inhibit AP-1 DNA binding (Rokutan et al 1998). In fact, modulation of GSH/GSSH ratio in endothelial cells permitted regulation of neutrophil binding via expression of adhesion molecules (Kokura et al 1999). NF-κB and AP-1signalling is therefore a complex process that can be modulated by both ROS and antioxidants. This could possibly explain why both $H_2O_2$ and DMTU were able to increase ICAM-1 and IL-8 mRNA induction by TNF-α on PS. It is also possible that oxidative stress on Ti6Al4V, which also results in decreased amounts of GSH, can have both stimulatory and inhibitory effects on different aspects of TNF-α–induced expression of pro-inflammatory mRNAs. Interestingly, however, addition of external GSH did not have a stimulatory effect on the pro-inflammatory phenotype of endothelial cells in this study, thus further pointing to the complexity of oxidative stress-induced events on Ti6Al4V alloy.

The discrepancy between protein and mRNA expression after TNF-α stimulation in HDMEC on Ti6Al4V points to the deregulation of mRNA to protein transition. This could possibly be explained by inhibition of mRNA translation. One of the mechanisms involved in translation repression is driven by microRNA (miRNA) (Carthew & Sontheimer 2009). miRNAs have been shown to regulate the expression of pro-inflammatory molecules. Thus, miRNAs were demonstrated to inhibit the expression of VCAM-1 in endothelial (Harris et al 2008) and IL-8 release in epithelial cells (Perry et al 2008). In turn, miRNAs expression can be up-regulated by oxidative stress induced with sodium arsenite (Leung et al 2006, Marsit et al 2006). In addition TNF-α and LPS were also shown to regulate the expression of particular miRNAs in macrophages (Tili et al 2007). Altogether, these reports provide a possible mechanism for the disparity of pro-inflammatory molecule regulation in endothelial cells on Ti6Al4V alloy at protein and mRNA levels.

A stimulating effect of DMTU on ICAM-1 expression on the cell surface after TNF-α stimulation was also observed in HDMEC grown on PS. DMTU caused only a minor increase in TNF-α-induced ICAM-1 up-regulation in the cells grown on Ti6Al4V alloy and

this effect was not statistically significant. No stimulatory effect of DMTU was observed for IL-8, and GSH-MEE was ineffective for both proteins. This further pointed to a possible deregulation of mRNA translation in HDMEC exposed to oxidative stress on Ti6Al4V alloy. Another possible explanation for the different regulation at mRNA and protein levels could be defective transport of synthesised protein to the cell membrane in HDMEC on Ti6Al4V alloy. As a possible indication for this process the amount of ICAM-1 in total cell extracts was quantified. Indeed, TNF-α-induced ICAM-1 expression was slightly higher in HDMEC on Ti6Al4V alloy compared to the cells grown on PS. Importantly, DMTU treatment significantly increased ICAM-1 expression induced by TNF-α in HDMEC on Ti6Al4V and the increase was higher than in the cells on PS. A similar disparity in the induction of pro-inflammatory molecules at the mRNA and protein levels was observed in a system in which intracellular ROS formation could be induced in endothelial cells (Volanti et al 2004). While this led to NF-κB activation and the induction of ICAM-1 and VCAM-1 transcription, the expression of the respective proteins was not detected. The system was also able to reduce ICAM-1 and E-selectin expression, induced by TNF-α and LPS. This was shown to be the result of the degradation of ICAM-1 and VCAM-1 in lysosomes. As ROS scavengers were able to restore ICAM-1 expression oxidative stress-induced lipid peroxidation was suggested to be responsible for incorrect ICAM-1 plasma membrane targeting (Volanti et al 2004). Matrix metalloproteinase 9 (MMP9) that is induced by $H_2O_2$ (Kolev et al 2003) has been also shown to cleave ICAM-1 (Fiore et al 2002). In the present study the difference in ICAM-1 level in the whole cell lysates of HDMEC grown on PS and Ti6Al4V alloy was still not as pronounced as at the mRNA level. It is possible, therefore, that both mechanisms, inhibition of mRNA translation and protein transport to the cell membrane, could be responsible for the reduced response of endothelial cells on Ti6Al4V alloy to pro-inflammatory stimuli.

The reduced response of endothelial cells to pro-inflammatory stimulation shown in this study could be of relevance for the *in vivo* situation. It is unclear, however, if this could have a positive or negative effect on the wound healing around metal implants. From one point of view a reduced inflammatory response could be beneficial to avoid the chronic inflammation situation around the implants and could contribute to the overall good biocompatibility of titanium prostheses. From another point of view the inability to effectively respond to pro-inflammatory stimuli could have a negative effect on the implant integration due to an affected wound healing process. However, since endothelial cells on Ti6A4V alloy express higher amounts of mRNA for pro-inflammatory genes than on PS this could under some circumstances induce the higher protein expression. Therefore, the role which the

observed reduced pro-inflammatory response of endothelial cells plays *in vivo*, would depend on the extent of titanium alloy corrosion and interaction with other cell types. There is, however, a discussion about the necessity of inflammation for successful wound healing. Antisera depletion of neutrophils did not disturb wound healing in sterile conditions (Simpson & Ross 1972) and could even speed up tissue repair (Dovi et al 2003). The studies in knockout mice deficient for neutrophils and macrophages due to disruption of certain genes showed enhanced wound healing in the absence of infection (Martin et al 2003, Martin & Leibovich 2005). These observations are in line with the fact that fetal wounds show no or little inflammatory response (Szpaderska & DiPietro 2005). Altogether, this could open a perspective of anti-inflammatory therapy for enhanced healing, which can hypothetically be applied for the treatment of metal implant debris-induced inflammation. However, the fact that sterile conditions are rare during the normal course of wound healing points to the requirement for further studies on the role of inflammation in wound healing.

### 4.1.4. Angiogenesis on Ti6Al4V alloy

Another important function of endothelial cells is their role as the driving cell type in angiogenesis. The influence of titanium degradation products on angiogenic potential of endothelial cells has not yet been examined. In this study there were no differences seen in angiogenic potential of HDMEC in an *in vitro* assay performed on PS or Ti6Al4V. It has to be stated, however, that the cells were not growing on the metal surface. Thus, the effects of oxidative stress on Ti6Al4V could be masked by collagen and fibrin used in the assay. Addition of 0.5 mM $H_2O_2$, however, reduced the formation of tube-like structures on both materials. There are contradictory reports in the literature regarding the effects of $H_2O_2$ on endothelial cells. In one study the low doses of $H_2O_2$ (0.1 or 1 µM) induced proliferative activity of endothelial cells and increased tube formation in an *in vitro* angiogenesis assay. A higher concentration of $H_2O_2$ (10 µM), in turn, reduced the angiogenic potential of endothelial cells (Yasuda et al 1999). In contrast, in another study treatment of microvascular endothelial cells with much higher $H_2O_2$ concentrations (0.1 to 0.5 mM for 15 min) induced tubular morphogenesis in type I collagen gel (Shono et al 1996). The differences between the reports could possibly be explained by different cell types and cell culture media.

The situation *in vivo* might be even more complicated, since other cell types can modulate angiogenesis in response to oxidative stress. Thus, in *in vitro* studies exogenous $H_2O_2$ has been shown to induce VEGF expression in vascular smooth muscle cells (Ruef et al

1997), keratinocytes (Brauchle et al 1996), as well as endothelial cells (Gonzalez-Pacheco et al 2006). This was also observed for metal ions. $Co^{2+}$ has been shown to induce VEGF mRNA expression in osteoblasts (Steinbrech et al 2000) and VEGF release by fibroblasts (Trompezinski et al 2000). Metal ions can also be involved in the regulation of other growth factors with angiogenic activity. Thus, macrophages exposed to $CoCl_2$ secrete bFGF and PDGF (Kuwabara et al 1995). Metal ions have the ability to modulate angiogenesis directly *in vitro.* In the same *in vitro* system as in this study $CoCl_2$ significantly reduced angiogenic potential of endothelial cells (Peters et al 2002).

Altogether, it is unclear if oxidative stress on Ti6Al4V alloy has an influence on angiogenesis. Studies on the effect of cathodically polarised Ti6Al4V on the formation of *in vitro* capillaries by HDMEC could provide an answer to this question.

## 4.2. Effects of Co28Cr6Mo alloy and Co-ions on endothelial cells

CoCrMo-based alloys are considered to be less biocompatible than Ti-based materials. This is mostly due to a higher corrosion rate and release of toxic Co and Cr ions. An 8-fold increase in the serum concentration of Cr was detected in the patients with well functioning Co-Cr-based prosthesis compared to the serum of control individuals (Jacobs et al 1998b). In the long term study of Jacobs et al. (Jacobs et al 1996) a nine-fold elevation of Cr and at least three-fold increase in Co serum concentration was registered in the patients with Co-Cr-based total hip implant 20 years after implantation. Co-ion concentration was shown to reach up to 0.9 mM in the peri-prosthetic tissue (Blumenthal et al 1994).

As already mentioned, in *in vivo* studies CoCrMo samples induced a higher and persistent inflammatory response than Ti6Al4V alloy when implanted into animals (Kraft et al 2005). Also CoCr particles injected into knee joints of mice induced higher leukocyte adhesion to endothelial cells than particles from cpTi (Zysk et al 2004). Co particles provoked higher cytokine release by endothelial cells than $TiO_2$ particles *in vitro* (Peters et al 2004). Elevated levels of metal ions in blood and peri-implant tissues may result from implant metal release that happens permanently during the lifetime of the prosthesis. *In vitro* results indicate that metal ions can induce inflammatory reactions. Thus, $CoCl_2$ induced adhesion of neutrophils to endothelial cells (Klein et al 1994) as well as the expression of ICAM-1 and E-selectin and production of IL-6 and IL-8 by endothelial cells, which coincides with the activation of the transcription factors, NF-κB and AP-1 (Kim et al 2006, Wagner et al 1997,

Wagner et al 1998). Metal ion-induced inflammation can amplify responses induced by metal wear debris, contributing therefore to bone resorption and implant aseptic loosening.

Therefore, in this study the effect of Co28Cr6Mo alloy on endothelial cells *in vitro* was studied in the context of possible $Co^{2+}$ release and alloy biocompatibility was improved by $TiO_2$ coating. Furthermore, the effects of $Co^{2+}$ on endothelial cells were studied in the context of HIF-1α-dependent and independent reactions.

### 4.2.1. $TiO_2$ coating improves biocompatibility of Co28Cr6Mo alloy to endothelial cells

According to previous reports (Peters et al 2008) endothelial cells grown on Co28Cr6Mo alloy displayed an activated phenotype regarding the actin cytoskeleton and the phenotype of their intercellular contacts (e.g.distribution of CD31) compared to the control cells grown on glass. HDMEC on Co28Cr6Mo had more actin stress fibres in the cytoplasm and non-uniform CD31 distribution. Interestingly, $CoCl_2$ could also induce striking changes in actin and CD31 patterns in endothelial cells (Peters et al 2008). Importantly, $TiO_2$-coating reduced the changes caused by Co28Cr6Mo in actin and CD31 distribution in HDMEC. To study the response of HDMEC to Co28Cr6Mo and the effect of $TiO_2$-coating in more detail microarray analysis of mRNA expression was performed. Of 1308 genes examined 247 genes were differentially expressed in HDMEC on Co28Cr6Mo compared to the glass control (125 genes were up- and 122 genes down-regulated). The $TiO_2$-coating of Co28Cr6Mo markedly reduced the number of differentially expressed genes. After $TiO_2$-coating only 34 genes were differentially expressed (13 were up- and 21 down-regulated) in HDMEC grown on this material. Importantly, the gene regulation patterns on different materials overlapped almost completely, i.e. $TiO_2$-coating reduced the number of genes regulated in HDMEC by the contact to Co28Cr6Mo and did not seem to induce considerable changes in gene expression on its own. It is tempting to speculate that $TiO_2$-coating reduces the corrosion of Co28Cr6Mo alloy and $Co^{2+}$ release, decreasing, therefore, the changes in gene expression observed in HDMEC on Co28Cr6Mo. Indeed, the decrease in $Co^{2+}$ release was observed after coating Co28Cr6Mo alloy with $TiO_2$ layer (Hoffmann et al 2007, Hoffmann et al 2005). It is possible, however, that the products of the cathodic half-reaction of corrosion have their role in Co28Cr6Mo-induced changes in HDMEC gene expression profile. $TiO_2$-coating has been shown to reduce the release of Co, Cr and Mo ions from Co28Cr6Mo alloy at least two-fold

in PBS and cell culture medium. Such a sealing effect of $TiO_2$ was responsible for the increased metabolic activity and cell number of osteoblasts growing on $TiO_2$-coated material compared to uncoated Co28Cr6Mo (Hoffmann et al 2007, Hoffmann et al 2005).

#### *4.2.1.1. Effects of $TiO_2$-coating on Co28Cr6Mo-induced changes in proliferation*

Among the genes regulated in HDMEC grown on Co28Cr6Mo a group of cell cycle-related genes was apparent. It included replication accessory proteins (Ki67, PCNA, RCF, RPA), cyclins (A2, B2, D1, E1) and cyclin-dependent kinases (CDK1 and CDK2). Both interphase CDK2 and mitotic CDK1 were down-regulated in HDMEC grown on Co28Cr6Mo, compared to the glass control. This correlated with the lower expression level of cyclin mRNAs in HDMEC on Co28Cr6Mo alloy compared to glass; the expression was in general higher on $TiO_2$-coated Co28Cr6Mo than on uncoated material, but was still lower than in the cells grown on glass. This together could indicate the reduction in proliferation rate of HDMEC in contact with metal surfaces with uncoated Co28Cr6Mo inducing higher effects.

In line with these observations a number of CDK inhibitors (p21CIP1, p57KIP2 and p16-INK4A) were induced in HDMEC on Co28Cr6Mo but were, in turn, not regulated on $TiO_2$-coated material. The CDK inhibitors induced on Co28Cr6Mo are known to target mostly cyclin D/CDK4/6 complexes inducing, therefore, G1 block in the cell cycle (Besson et al 2008). Cyclin and CDK expression is known to be induced throughout cell cycle progression. Therefore, G1 block could explain the down-regulation of a group of these genes. In contrast to other cyclins cyclin G2 was up-regulated in HDMEC grown on Co28Cr6Mo alloy and was almost not regulated in the cells on $TiO_2$-coated material. Cyclin G2 is, however, an atypical cyclin, which has been shown to induce cell cycle arrest in the G1/S phase (Bennin et al 2002). This is, therefore, in line with the down-regulation of other cyclins and CDKs and up-regulation of CDK inhibitors. The expression of another CDK inhibitor, p27KIP1, was not regulated on either of the metallic materials, while p18-INK4, in contrast to other CDK inhibitors, was down-regulated. Although both p27KIP1 and p18-INK4 are involved in G1 cell cycle arrest and are known to cooperate in tumour suppression (Swarbrick et al 2000), it is possible that not all CDK inhibitors are involved in the growth arrest induced by Co28Cr6Mo alloy. In line with the growth arrest on Co28Cr6Mo alloy, the expression of PCNA, RCF, RPA, proteins, which act as components of the DNA replication complex (Masuda et al 2007), were also down-regulated in HDMEC on Co28Cr6Mo

compared to the glass control and were higher on $TiO_2$-coated alloy. Interestingly, p21 and p57 have been shown to bind to PCNA, therefore blocking DNA synthesis (Luo et al 1995, Watanabe et al 1998).

Reduced proliferation on Co28Cr6Mo was also indicated by expression of Ki67. Ki67 is widely used as a proliferative marker, although its exact function is still unclear (Brown & Gatter 2002). Cyclic change in its amount is observed during the cell cycle: Ki67 levels increase during S phase, reaching the maximum at mitosis and decreased in G1 phase (Lopez et al 1991). Reduced amounts of mRNA for the proliferative marker Ki67 correlated with the lower number of Ki-67 protein-positive cells on Co28Cr6Mo compared to glass and $TiO_2$-coated Co28Cr6Mo, although on the latter material Ki67 expression was still lower than on glass. This pointed to a decreased proliferation rate of HDMEC on Co28Cr6Mo and to a shielding effect of $TiO_2$-coating. In fact, the number of cells on both metal materials was lower than on glass at the time point of Ki67 quantification, although no difference was seen between coated and uncoated Co28Cr6Mo alloy. It is possible that $Co^{2+}$ released from Co28Cr6Mo alloy is responsible for the growth arrest of HDMEC. Indeed $CoCl_2$ has been shown to reduce Ki67 expression in HDMEC (Peters et al 2005). This is in agreement with the fact that $TiO_2$-coating increased cell proliferation (Ki67) and to some extent restored the Co28Cr6Mo-induced expression of cell cycle-related genes. $Co^{2+}$ can have a direct effect on the cell cycle or through ROS formation. Thus, $H_2O_2$ was shown to induce multiphase cell cycle arrest in fibroblasts, with down-regulation of cyclin D and induction of p21 expression (Barnouin et al 2002). $TiO_2$-coating, however, does not lead to a complete restoration of these values. This could be explained by the fact that small amounts of $Co^{2+}$ are still released from $TiO_2$-coated Co28Cr6Mo. The products of cathodic half-reaction of corrosion that might form on both surfaces could also be the reason for a partial effect of $TiO_2$-coating on growth arrest in endothelial cells.

#### *4.2.1.2. $TiO_2$-coating reduces the induction of stress response to Co28Cr6Mo alloy*

HDMEC grown on Co28Cr6Mo displayed signs of oxidative stress. A number of genes involved in antioxidant defence were regulated. Thus, SOD1, SOD2, GPX3, GST12 were up-regulated, while GPX1 and GSTT2 were down-regulated in HDMEC on Co28Cr6Mo compared to the cells on glass. No regulation of these genes was observed in HDMEC on $TiO_2$-coated Co28Cr6Mo compared to the cells on glass. In line with this, it was shown that GSH amounts in HDMEC on Co28Cr6Mo were significantly lower than in the

cells on glass. GSH amounts in HDMEC on $TiO_2$-coated Co28Cr6Mo, while lower than on glass, were higher than on uncoated Co28Cr6Mo. This points to the induction of oxidative stress in HDMEC on Co28Cr6Mo, possibly by $Co^{2+}$-mediated ROS formation. Reduced GSH levels in HDMEC on Co28Cr6Mo could therefore be a sign of GSH pool exhaustion. Regulation of gene expression of antioxidant enzymes in HDMEC on Co28Cr6Mo could indicate the adaptive response to oxidative stress. Indeed, mRNA expression of both SOD1 and SOD2 was elevated in HDMEC on Co28Cr6Mo. SOD2 up-regulation was shown in epithelial cells after $H_2O_2$ treatment, while SOD1 expression was not affected (Shull et al 1991). Interestingly, however, the total SOD activity was reduced in HDMEC on Co28Cr6Mo compared to the cells on glass, while it did not differ from controls in HDMEC on $TiO_2$-coated Co28Cr6Mo. Differences in the expression of SOD mRNAs and SOD activity could possibly be explained by a different time course of SOD reaction to oxidative stress. Adaptive responses on mRNA level were observed 30 h after seeding HDMEC on Co28Cr6Mo, while SOD activity was decreased after 40 h. Both reduced amounts of GSH and SOD activity in HDMEC grown on Co28Cr6Mo could indicate the exhaustion of antioxidant defence mechanisms caused by permanent exposure to ROS formed during the cathodic half-reaction of corrosion or induced by $Co^{2+}$. Importantly, $TiO_2$-coating restored most of the values measured, indicating that it can protect endothelial cells from Co28Cr6Mo-induced oxidative stress.

mRNAs for a number of heat shock proteins were up-regulated in HDMEC grown on Co28Cr6Mo compared to the glass control. Their expression could be decreased to an almost control level by $TiO_2$-coating. It is known that ROS induce protein oxidation resulting in changes of protein conformation and possibly unfolding (Martinez-Sanchez et al 2005). The function of heat shock proteins as chaperones points to a possibility of stress conditions on Co28Cr6Mo alloy that lead to the increased amount of unfolded proteins. $Co^{2+}$ was itself shown to induce the expression of HSPs. Thus, HSP70.1, which is highly induced on Co28Cr6Mo alloy, has been shown to be induced in keratinocytes exposed to $CoCl_2$ (Nordlind 2002). The HSP family and DnaJ subfamily of chaperones have also been shown to be regulated by $CoCl_2$ in endothelial cells in a recent study (Hang et al 2009). Interestingly, HSP70.1 and HSP105 induced in HDMEC on Co28Cr6Mo were also up-regulated by $CoCl_2$. Importantly, this effect can possibly be ROS-dependent, since ROS have been shown to induce the expression of HSP70.1 (Madamanchi et al 2001). Unfolded protein response pathways are a known mechanism that leads to the induction of HSP expression. Increased expression of mRNA for XBP1, one of the transcription factors involved in UPR could

indicate UPR activation on Co28Cr6Mo alloy. However, mRNA expression of GRP78 (glucose-regulated protein 78), another important regulator of UPR, was not affected in HDMEC on Co28Cr6Moalloy. No regulation of chaperones was observed on $TiO_2$-coated Co28Cr6Mo, again pointing to the reduction of $Co^{2+}$ release and protection against oxidative stress.

Growth on Co28Cr6Mo induced the expression of IL-8 mRNA, indicating the pro-inflammatory stimulation of endothelial cells by metal corrosion products. This is in agreement with the reports of $CoCl_2$ inducing IL-8 release by HDMEC (Kim et al 2006, Peters et al 2004). Importantly, $TiO_2$-coating reduced the expression of IL-8 mRNA in HDMEC. The expression of COX II, another inflammation-related molecule, was up-regulated in HDMEC grown on Co28Cr6Mo alloy at both mRNA and protein level, but practically unchanged on $TiO_2$-coated material. COX II is an inducible enzyme catalysing the conversion of arachidonic acid to prostaglandin H2, which is a precursor for the synthesis of other prostanoids. COX II has been shown to be up-regulated by inflammatory signals (Kuwano et al 2004) and COX II induction induces the expression of the cytokines IL-1β and IL-6 (Walch & Morris 2002). In fact, COX II inhibition has been shown to affect IL-8 induction (Singh et al 2006, Vij et al 2008). Therefore, COX II and IL-8 induction on Co28Cr6Mo alloy could be interconnected. Importantly, $CoCl_2$ has been demonstrated to induce COX II expression in astroglioma cells, ROS being involved in this process (Ahn et al 2007). Intracellular ROS formation (Barbieri et al 2003) and addition of exogenous $H_2O_2$ (Nakamura & Sakamoto 2001) have also been shown to induce COX II, indicating that both $Co^{2+}$ release and ROS formation on Co28Cr6Mo alloy could be responsible for COX II induction. Expression of another stress marker, HO-1, was induced on Co28Cr6Mo. Both HO-1 mRNA and protein were elevated in HDMEC on Co28Cr6Mo, compared to the cells grown on glass, and $TiO_2$-coating decreased their expression. HO-1 catalyses the degradation of heme to biliverdin, which is accompanied by the production of the important signalling molecule carbon monoxide (CO) and iron (Kutty & Maines 1987). Cobalt is known to induce HO-1 expression (Maines & Kappas 1976). Interestingly, $CoCl_2$-induced HO-1 up-regulation was associated with GSH depletion *in vivo* (Ewing & Maines 1993), which is in line with the reduced GSH amount in HDMEC on Co28Cr6Mo alloy in this study. HO-1 expression was also shown to be induced in response to ROS and $H_2O_2$ (Ryter et al 2006). The products of HO-1 catalysis exert a broad range of effects on cellular functions. Bilirubin, a product of biliverdin conversion, and CO were reported to have antioxidant properties and CO was shown to inhibit inflammation. This could indicate the adaptive response of HDMEC exposed

to the oxidative stress on Co28Cr6Mo alloy. Importantly, CO was also shown to inhibit proliferation. CO treatment induced p21 expression (Otterbein et al 2003) and decreased cyclin D1 level in smooth muscle cells (Song et al 2002b), which is reminiscent of the reactions observed in HDMEC grown on Co28Cr6Mo. However, further functional studies would be required to postulate the connection of HO-1 up-regulation and reduced proliferation rate on Co28Cr6Mo alloy.

In general, HDMEC grown on Co28Cr6Mo alloy showed a high number of differentially expressed genes when compared to the cells grown on glass. This included cell cycle and oxidative stress-related genes, inflammatory genes and chaperone genes. Some of these changes were also confirmed at protein level. These changes in gene expression are possibly triggered by released metal ions. Since, in particular, oxidative stress response genes are activated, reactive oxygen species (ROS) induced by metal ions or formed at the surface of the alloy during corrosion may contribute to the response of endothelial cells to Co28Cr6Mo. By $TiO_2$-coating of Co28Cr6Mo a marked reduction of differential gene expression was achieved. Thus, a layer of $TiO_2$, known to be relatively inert, reduces corrosion and release of metal ions from bulk material. This sealing effect of $TiO_2$ may explain the reduction of oxidative stress response of endothelial cells in comparison to unmodified Co28Cr6Mo. The increased biocompatibility of $TiO_2$-coated Co28Cr6Mo alloy to endothelial cells endorses the possibility of the use of such surface modification for production of implants.

### 4.2.2. Cobalt ion effects on the functions of endothelial cells

Metal ions are known to influence various cellular functions, including proliferation, differentiation, apoptosis, cell signalling and many other processes. It is suggested that regulation of cellular functions by metal ions is mediated by formation of ROS, although induction of ROS-independent effects by metals has also been reported (Harris & Shi 2003). $Co^{2+}$ is often used as an hypoxia-mimicking agent in biological experiments, since $Co^{2+}$ can induce activation of signalling pathways similar to hypoxia signalling by stabilisation of HIF-1α. However, a number of discrepancies between hypoxia and $Co^{2+}$ exist (Bunn & Poyton 1996). Therefore, in this study the response of endothelial cells to $CoCl_2$ was evaluated in the context of HIF-1α-dependency.

#### *4.2.2.1. Mechanisms of $Co^{2+}$ cytotoxicity in endothelial cells*

$CoCl_2$ treatment induced a dose- and time-dependent decrease in cellular metabolic activity and cell number. 0.7 mM $CoCl_2$, which is in a concentration range detected in patients with Co-based implants, caused 60% reduction in metabolic activity and 40% decline in cell number 24 h after treatment. Significantly, short-term $CoCl_2$ treatment induced much smaller changes in cellular metabolic activity and cell number indicating that the cells were able to repair the damage caused by $Co^{2+}$.

$CoCl_2$ cytotoxicity could at least in part be explained by ROS formation in HDMEC as observed 4 h after $CoCl_2$ treatment. Formation of ROS in the presence of metal ions proceeds among others through Fenton- and Haber-Weiss-type reactions to produce the extremely toxic $^{\cdot}OH$ (Harris & Shi 2003). Reaction of $Co^{2+}$ with $H_2O_2$ was also shown to result in $^{\cdot}O_2$- formation apart from $^{\cdot}OH$ (Hanna et al 1992, Kadiiska et al 1989, Leonard et al 1998). Other signs of oxidative stress were observed in HDMEC after $CoCl_2$ treatment. Hence, $CoCl_2$ induced the decrease of GSH amount in HDMEC 24 h after treatment. This was in contrast to a slight increase in GSH concentration induced by $H_2O_2$. $H_2O_2$ is rapidly decomposed in cell culture medium, making it a short-term treatment. Increase in GSH could, therefore be explained by induction of adaptive mechanisms (discussed above). On the contrary, ROS could be formed permanently in the presence of $Co^{2+}$ leading to the exhaustion in GSH pool. Decrease in GSH content was also reminiscent of GSH decline observed on Co28Cr6Mo. In contrast, however, $CoCl_2$ did not induce any significant changes either in SOD or in catalase activity. Also surprisingly DMTU, ROS scavengers known to bind $^{\cdot}OH$, did not have any protective effect on metabolic activity of HDMEC under $CoCl_2$ treatment. Addition of exogenous GSH (in the form of GSH-MEE) had only a slight effect on $CoCl_2$ cytotoxicity. Both ROS scavengers were highly effective against $H_2O_2$. The failure of ROS scavengers could be explained in a few ways. Firstly, it is possible that the ROS scavengers used in this study did not match the species of ROS induced by $CoCl_2$. Secondly, ROS scavengers could prove ineffective due to the permanent production of ROS in the presence of $Co^{2+}$ and gradual exhaustion of scavengers. Lastly, ROS-independent toxicity of $CoCl_2$ could be sufficient to cause reduction of metabolic activity and cell number. In another model, however, $CoCl_2$-induced apoptosis of a neuronal cell line could be blocked by the ROS scavengers, NAC and DTT (Zou et al 2001).

One of the possible $CoCl_2$ cytotoxicity mechanisms could be induction of oxidative DNA damage. Formation of the oxidative DNA lesion 8-oxoG was shown in HDMEC exposed to $CoCl_2$. DNA oxidation could result from $Co^{2+}$-induced ROS formation, in

particular $^{\cdot}OH$ produced during Fenton- and Haber-Weiss-type reactions. Indeed, $^{\cdot}OH$ were generated in the reaction between $Co^{2+}$ and $H_2O_2$ and were able to hydroxylate deoxyguanosine and induce strand breaks in DNA in a cell-free system (Mao et al 1996, Valavanidis et al 2005). $CoCl_2$-induced 8-oxoG formation also correlated with the increased AP-site formation in HDMEC treated with $CoCl_2$. $H_2O_2$ and anoxia were also shown to increase the amount of AP sites in DNA of HDMEC. AP sites are formed spontaneously during oxidation of DNA via hydrogen abstraction from deoxyribose (Breen & Murphy 1995) or in the course of repair of oxidised DNA aminobases. Importantly, AP sites have also been shown to be induced by the products of the Fenton reaction of $H_2O_2$ with $Fe^{2+}$ (Nakamura et al 2000). Therefore, it is possible that $CoCl_2$ directly induces AP sites via ROS formation or indirectly via repair of 8-oxoG and other oxidised base formation. The repair of ROS-induced AP sites has been shown to be inefficient (Nakamura et al 2000). $CoCl_2$ could inhibit nucleotide excision repair after DNA damage with ultraviolet (Kasten et al 1997). Binding to zinc finger domains of repair proteins has been suggested to be responsible for the inhibitory effect of $Co^{2+}$ (Asmuss et al 2000). Moreover, $CoCl_2$ has been shown to induce chromosome aberrations *in vivo* (Palit et al 1991). Altogether, the data point to persistent DNA damage of endothelial cells by $CoCl_2$.

p53 is known to be up-regulated by different types of DNA damage, although the role of p53 in the response to oxidative DNA damage is not clear as yet. It was shown, however, that p53 could interact with OGG1 and APE1, two enzymes involved in the removal of oxidative DNA damage, and enhance their activity, thus pointing to p53 role in sensing and removal of oxidised DNA bases (Achanta & Huang 2004). In the current study up-regulated p53 expression in the nuclei of HDMEC was noticed after $CoCl_2$ treatment; p53 levels increased with time. Conflicting effects of $CoCl_2$ on p53 stabilisation have been reported; HIF-1α-dependent p53 stabilisation was detected after $CoCl_2$ and hypoxia treatment (An et al 1998), $CoCl_2$ could also repress transcription of the p53 gene (Lee et al 2001) and inhibit p53 DNA binding activity (Palecek et al 1999). In contrast to $CoCl_2$, p53 was temporarily up-regulated shortly after placing HDMEC in an atmosphere without oxygen and returned to control levels later in the experiment. Interestingly, though almost the same levels of DNA damage (at least AP-sites) were detected in $CoCl_2$- and anoxia-treated cells and although p53 up-regulation could be induced by HIF-1α activation, different p53 activation patterns were observed. It is, therefore, possible, that p53 up-regulation is induced via different mechanisms by $CoCl_2$ and anoxia or that additional HIF-1α-independent mechanisms (possibly DNA damage-induced) of p53 regulation by $Co^{2+}$ exist. p53 is known to induce either apoptosis or

growth arrest depending on the type and strength of the stimuli. Indeed, prolonged exposure of HDMEC to $CoCl_2$ has been shown to induce apoptosis (Peters et al 2001). On the other hand, in the current study p53 up-regulation correlated with the elevation of p21 expression. As mentioned before, p21 is a CDK inhibitor and a known p53 target, so that its induction could point to the possibility of cell cycle arrest in HDMEC treated with $CoCl_2$. p21 expression patterns after $CoCl_2$ and anoxia treatment mirrored p53 expression under the respective treatment. While $CoCl_2$ induced time-dependent up-regulation of p21, its expression declined with time after initial elevation shortly after anoxia application. To explore if p21 up-regulation was DNA damage-dependent the DNA repair pathway responsible for oxidative damage repair was inhibited with the specific BER inhibitor known to selectively inhibit APE1 and to potentiate cytotoxicity of a number of DNA-base targeting compounds (Madhusudan et al 2005). BER inhibition led to a more pronounced induction of p21 by $CoCl_2$, suggesting DNA damage-dependence of this event. HIF-1α activation, however, was also shown to induce p21 (Pacary et al 2006) and could be a partial explanation for $CoCl_2$-induced p21 up-regulation in HDMEC (discussed below).

Possible cell cycle block induced by $CoCl_2$ could be interesting in the context of reduced cell proliferation, which could inhibit angiogenesis. A concentration-dependent inhibition of angiogenesis *in vitro* even at $CoCl_2$ concentrations that induced no or only minor effects on cell viability was demonstrated (Peters et al 2002). Interestingly, hypoxia exerted an opposite effect to $CoCl_2$ in a parallel study (Peters et al 2005). This points to a divergence between the signalling of $Co^{2+}$ and hypoxia and is also in agreement with different patterns of p21 regulation by $CoCl_2$ and lack of oxygen. Reduced angiogenesis potential could also be explained by p53-induced apoptosis of endothelial cells. Interestingly, p53 has also been shown to inhibit angiogenesis via transcriptional repression of proangiogenic and activation of antiangiogenic factors (Teodoro et al 2007). The data available do not provide enough information to postulate the exact mechanisms of angiogenesis inhibition; this will require additional functional studies. However, p53 and p21 induction and possible growth arrest or apoptosis of endothelial cells could be important with respect to the effects of $Co^{2+}$ released from cobalt-containing implants on endothelial cells in peri-implant tissue. It is important to consider, however, that *in vivo* the situation can differ significantly from *in vitro* experiments. Thus, in animal studies a stimulation of angiogenesis by $Co^{2+}$ was demonstrated. Infusion of the bladder in rats with $CoCl_2$ solution led to the formation of numerous microvessels in the bladder wall not apparent in bladders of control animals. The expression of HIF-1α and VEGF was higher in $CoCl_2$-infused bladders (Buttyan et al 2003). In another study,

administration of $CoCl_2$ to rats with a partly removed kidney induced angiogenesis, which also correlated with the activation of HIF-1 and the expression of VEGF (Tanaka et al 2005). The difference between the results from *in vitro* and *in vivo* models could be explained by a $CoCl_2$-induced activation of other cell types (non-endothelial cells), which can be stimulated to produce pro-angiogenic molecules by metal ions. It is possible that both pro- and anti-angiogenic effects of metal ions coexist *in vivo* and depend on the tissue, local conditions and metal concentration. The subject of direct metal implant-induced influences on angiogenesis has not been largely addressed, although the fact that metal ions can modulate angiogenesis *in vitro* and *in vivo* points to the possible existence of such reactions around metal devices with potential effects on wound healing. The question as to whether these effects are detrimental or beneficial is unknown at this point and requires further investigation.

#### *4.2.2.2. HIF-1α-dependency of $CoCl_2$-induced effects in endothelial cells*

$CoCl_2$ is a well known inducer of HIF-1α stabilisation. HIF-1α level was induced rapidly after $CoCl_2$ treatment and remained increased over the whole experimental time due to the permanent $CoCl_2$ presence. HIF-1α induction by $CoCl_2$ was similar to HIF-1α stabilisation by anoxia. In the latter condition HIF-1α stability is regulated by PHD, enzymes responsible for HIF-1α degradation under normal conditions, while PHD activity is inhibited by the lack of oxygen, a cofactor important for PHD catalysis. $CoCl_2$ has also been shown to inhibit PHD activity. This could be mediated by the competitive occupation of $Fe^{2+}$ binding sites in the active centre of the enzyme or by ascorbate depletion, $Fe^{2+}$ and ascorbate being other important PHD cofactors (Epstein et al 2001, Huang et al 2002, Salnikow et al 2004). However, another study showed that cobalt was ineffective in inhibiting PHD, while it efficiently inhibited FIH, another enzyme, regulating HIF-1α activity (Hirsila et al 2005). Interestingly, cobalt was found to directly bind to HIF-2α and inhibit, therefore the interaction with pVHL, which normally targets HIF-α for degradation. It is significant that this inhibition was observed even when HIF-1α was hydroxylated (Yuan et al 2003). The ROS scavenger, NAC, was shown to inhibit $CoCl_2$-induced HIF-1α stabilisation, suggesting that $Co^{2+}$-induced ROS might also play a role in HIF-1α regulation (Chachami et al 2004). ROS might lead to the depletion of the $Fe^{2+}$ pool, thus inhibiting PHD activity and leading to HIF-1α stabilisation (Valko et al 2006). However, an up-regulation of HIF-1α synthesis through the effects of $CoCl_2$-induced ROS on the phosphatidylinositol 3-kinase (PI3K) signalling pathway, which is involved in translation regulation, was suggested (Chachami et al 2004). $Co^{2+}$ induced

stabilisation of HIF-1α is therefore a complex process that can proceed through several mechanisms.

$CoCl_2$ is often used as an hypoxia-mimicking agent and is known to induce similar cellular reactions. However, disparity in action of both agents has been shown (Peters et al 2005). This could be explained by possible effects of $Co^{2+}$ on various cellular functions independent of the HIF-1α pathway. To dissect HIF-1α-dependent and -independent effects of $CoCl_2$ HIF-1α expression was down-regulated in endothelial cells with siRNA and $CoCl_2$-induced changes in gene expression were compared to anoxia-induced effects. siRNAs to HIF-1α have been shown to effectively knock down HIF-1α mRNA expression and to inhibit $CoCl_2$ and anoxia-induced HIF-1α stabilisation. Importantly, HIF-1α knock down did not influence cell viability and did not have effects on cytotoxicity induced by $CoCl_2$ and other chemical agents. HIF-1α down-regulation also affected $CoCl_2$- and anoxia-induced expression of PHD2 and BNip3, known targets of HIF-1α, proving the feasibility of the used system.

Microarray analysis of mRNA expression in HDMEC showed that approximately equal numbers of genes were differentially expressed after $CoCl_2$ and anoxia treatment. Nevertheless, relatively few genes were regulated in the same way by both $CoCl_2$ and anoxia. Comparable results were obtained with microarray analysis of gene expression in $Co^{2+}$- and hypoxia-treated mouse embryonic fibroblasts, in which the patterns of gene regulation by both agents overlapped only partly (Vengellur et al 2003). Manual analysis of the microarray data in the current study revealed few functional groups of genes regulated by $CoCl_2$ and anoxia. However, certain genes in each group were regulated by either $CoCl_2$ or anoxia or by both agents simultaneously. The same was true for the HIF-1α-dependance of differentially expressed genes: for some genes transfection of endothelial cells with siRNA against HIF-1α abrogated $CoCl_2$ and anoxia-induced gene regulation, induction of other genes seemed to be HIF-1α-independent. Such HIF-1α-dependent and independent genes could be observed in the same functional group.

#### 4.2.2.2.1. Regulation of transcription factors by $Co^{2+}$

$CoCl_2$ induced the expression of mRNAs coding for transcription factors. Among others ATF2, STAT3, RELA, and VEZF1 were strongly induced 18 h after starting $CoCl_2$ treatment and the up-regulation was HIF-1α-dependent. ATF2 encodes a transcriptional factor that regulates the expression of various proteins involved in cell cycle regulation, inflammation and protein degradation (Bhoumik et al 2007). It also possesses histone acetylase activity, important for a direct DNA damage response. Active ATF2 dimerises with

other transcription factors, such as ATF1 and the members of the Fos and Jun families of AP-1 transcription factors. Interestingly, ATF2 has been shown to be responsible for the expression of a subset of genes induced by hypoxia (Maekawa et al 2007). It was not related to HIF-1α before; thus, it is difficult to address the issue of different ATF2 regulation by $CoCl_2$ and anoxia. Another transcription factor, expression of which was induced by $CoCl_2$, is STAT3. STAT3 has been shown to regulate the expression of genes involved in angiogenesis, e.g. VEGF (Chen & Han 2008). Other effects of STAT3 through its interaction with different proteins in cytosol were demonstrated (Sehgal 2008). The fact that STAT3 up-regulation could be restored by HIF-1α siRNA is interesting in the context of the report on HIF-1α and STAT3 interaction at the VEGF promoter after $CoCl_2$ treatment (Gray et al 2005). Inhibition of HIF-1α degradation by direct binding to STAT3 (Jung et al 2008) further points to the crosstalk between these two transcription factors. However, reciprocal regulation of HIF-1α and STAT3 might be complex, since down-regulation of STAT3 with siRNA in tumour cells reduced both basal and growth signal-induced HIF-1α expression (Xu et al 2005).

The NF-κB subunit, RELA, which was also induced by $CoCl_2$ at the mRNA level, is known to be involved in the activation of inflammatory responses and could, therefore, mediate known $Co^{2+}$ effects on the expression of inflammatory molecules. A crosstalk between HIF-1α and NF-κB has also been reported, although, the mechanism of the mutual regulation seems to be complex. While HIF-1α up-regulation at mRNA level has been shown to be NF-κB-dependent (Taylor 2008), NF-κB, in turn, has also been shown to be the target of HIF-1α (Walmsley et al 2005). It is important to note that the activity of the mentioned transcription factors is usually regulated at posttranslational level, although the regulation on the transcriptional level has also been demonstrated (Senyuk et al 2009, Song et al 2007, Tsutsumi et al 2006).

Finally, VEZF1, induced in HDMEC incubated with $CoCl_2$, belongs to the family of zinc finger domain-containing transcription factors. VEZF1 is expressed solely in endothelial cells (Xiong et al 1999), where it is involved in the regulation of angiogenesis-related genes (Aitsebaomo et al 2001, Miyashita et al 2004). VEZF1 up-regulation was abrogated by siRNA against HIF-1α. HIF-1α-dependancy of this transcription factor has not been reported before. Importantly, a lot of other zinc finger proteins, some with unknown functions, were induced by $CoCl_2$ in a HIF-1α-dependent way. Altogether, the induction of transcription factors could explain the broad range of $Co^{2+}$ action and also underlines the differences compared with the events induced by the lack of oxygen, since none of the discussed transcription factors was regulated by anoxia. Although the regulation of the above mentioned transcription factors by

$CoCl_2$ was HIF-1α-dependent it does not necessarily imply that they are direct transcriptional targets of HIF-1α, as their expression can be regulated via additional intermediate steps. The same is true for other genes, induction of which by $CoCl_2$ is HIF-1α dependent. Thus, they can be regulated either by HIF-1α itself or by other transcription factors induced by $CoCl_2$. Furthermore, since a large number of HIF-1α binding partners have been described, abolishment of the interaction in the cells with HIF-1α knock-down might inactivate certain proteins eventually leading to the lack of gene expression regulation.

#### 4.2.2.2.2. Effects of $Co^{2+}$ on the expression of growth factors

Another group of genes regulated by $CoCl_2$ and anoxia contained growth factors and their receptors. Interestingly, both $CoCl_2$ and anoxia induced the expression of mRNA for TGFβ and FGFRL1 in a HIF-1α-dependent way. While various effects of TGFβ1 have been described, including its contribution to angiogenesis (Goumans et al 2009), FGFRL1 is less studied. It has been shown, however, that apart from FGFRL1 function in the response to growth factors with possible negative effect on cell proliferation (Trueb et al 2003), it can form homodimers, which directly promote cell adhesion (Rieckmann et al 2008). In addition, TGFβ1-induced VEGF expression as well as a number of other effects were HIF-1α-dependent (Jeon et al 2007). In turn, HIF-1α-dependent induction of TGFβ1 and FGFRL1, however, have not yet been demonstrated.

In contrast, Ang1 mRNA expression was induced by $CoCl_2$ only and the gene regulation was independent of HIF-1α. Ang1 is a growth factor that is known to act through binding to the Tie2 receptor and to promote angiogenesis (Morisada et al 2006). Interestingly, $CoCl_2$ has been shown to induce Tie2 expression in endothelial cells (Willam et al 2000), but similar effects for its ligands have not yet been described. Moreover, certain effects of Ang1 were shown to induce HIF-1α stabilisation (Chen & Stinnett 2008), although, in the current study Ang1 mRNA induction did not require HIF-1α. Significantly, Ang2 has been shown to be induced by hypoxia in a HIF-1α-dependent way due to the presence of hypoxia-responsive elements in the promoter of Ang2 (Simon et al 2008). It is known, however, that Ang2 is an antagonist of Ang1, which could explain the existence of different regulatory mechanisms in the control of expression of these related molecules.

HIF-1α-dependent induction of FGF5 mRNA in the present study was anoxia specific. FGF5 has been shown to be expressed in endothelial cells (Antoine et al 2005). It also had an autocrine and paracrine activity in human glioblastoma, with a stimulatory effect on angiogenic behaviour of endothelial cells in vitro (Allerstorfer et al 2008). FGF5

regulation by oxygen deficiency and HIF-1α has not been described. In contrast to the above mentioned molecules, the expression of proangiogenic FGF2 (bFGF) mRNA was not regulated by either $CoCl_2$ or by anoxia but was elevated in cells with HIF-1α knock-down after both treatments, thus pointing to a possible negative regulation of bFGF expression by HIF-1α. Hypoxia was also reported to induce bFGF expression in macrophages and cancer cells and this induction was associated with HIF-1α activation. (Bos et al 2005, Kuwabara et al 1995). Such discrepancy could be attributed to different regulation mechanisms specific to different cell types and to the possible difference in cellular response to partial reduction of oxygen concentration and complete lack of oxygen. Overall, the data show the induction of growth factors and their receptors in endothelial cells exposed to $CoCl_2$ and anoxia. HIF-1α-dependency of these effects might reflect a direct involvement of HIF-1α in the transcription of growth factor genes, but might also point to the existence of intermediary regulatory steps exerted by HIF-1α targets.

#### 4.2.2.2.3. DNA-damage response and cell cycle-related gene regulation by $Co^{2+}$

DNA damage and signs of cell cycle arrest, observed in HDMEC treated with $CoCl_2$ correlated with the regulation of the genes involved in the cellular response to DNA damage and cell cycle control. Significantly, the expression of OGG1 mRNA was induced in HDMEC by $CoCl_2$ treatment. OGG1 is a DNA repair enzyme, involved in the repair of 8-oxoG, which was shown to be elevated by $CoCl_2$. OGG1 was demonstrated to be inducible, and its expression was increased in mouse lung cells upon exposure to oxidative stress induced by X-rays (Risom et al 2003). OGG1 mRNA expression has been shown to be regulated on a transcriptional level (Lee et al 2004, Youn et al 2005). In the current study OGG1 induction was shown to be HIF-1α-dependent, and this has not been described before. However, further studies will be required to establish whether OGG1 is a direct target of HIF-1α or if it is regulated by other HIF-1α-induced proteins.

As mentioned before DNA damage often leads to p53 activation. Thus, it is of interest that $CoCl_2$ induced the expression of mRNA coding for MDM2, a p53 interaction partner, which negatively regulates its stability and is known as a transcription target of p53. No changes in p53 mRNA expression were observed in HDMEC treated with $CoCl_2$. This, however, is due to the prevalent regulation of p53 activity at protein level. Other known p53 targets, p21, regulating the cell cycle arrest in G1, and GAD45A and GADD45B, involved in the G2/M cell cycle block induction, were also induced at the mRNA level in HDMEC exposed to $CoCl_2$. However, the induction of all these mRNAs was abrogated by HIF-1α

down-regulation with siRNA, indicating a the possible role of HIF-1α in the regulation of these genes. HIF-1α has been shown to interact with the p53 pathway. In fact, a direct binding of p53 and HIF-1α has been demonstrated (Sanchez-Puig et al 2005). It was suggested that p53 could attenuate HIF-1α signalling by competing for binding with the common interaction partner p300. Moreover, HIF-1α has also been shown to directly bind to MDM2, which had a positive effect on p53 stability and activated p53-mediated transcription (Chen et al 2003). Since $Co^{2+}$ seems to induce stabilisation of both p53 and HIF-1α and both transcription factors interact with each other, it is possible that some aspects of p53-induced responses are regulated by HIF-1α and vice versa. On the other hand HIF-1α might exert p53-independent regulation of cell cycle-related genes. In fact, HIF-1α has been shown to be involved in p21 induction even in p53-deficient cells (Goda et al 2003). Surprisingly, neither HIF-1α transcription activity nor its DNA binding was essential for p21 up-regulation (Koshiji et al 2004). The regulation proceeded via functional counteraction of HIF-1α with c-Myc, which normally represses p21 expression by binding to its promoter and can be displaced by HIF-1α upon certain stimuli (Koshiji et al 2004). This HIF-1α-dependent p21 induction was shown to be additionally regulated by inhibiting the activity of another protein, β-catenin, via direct interaction with HIF-1α (Kaidi et al 2007). Interaction of β-catenin with HIF-1-α enhanced HIF-1-mediated transcription thus promoting cell survival during hypoxia. Thus, it is of interest that the expression of β-catenin mRNA was induced by $CoCl_2$ in HDMEC in a HIF-1α-dependent way. Therefore, p21 induction in HDMEC exposed to $CoCl_2$, which was shown to be DNA damage-dependent (discussed above), could possibly be regulated by $Co^{2+}$ via multiple mechanisms, one of them being HIF-1α pathway. The expression of GADD45 proteins has not been shown to be regulated by HIF-1α before. Therefore, it will be of interest to investigate if the mechanisms of GADD45 induction are common with p21.

Anoxia did not regulate the expression of any of the mentioned genes. This difference might result from the differences in the formation of DNA damage or in DNA damage response and is reminiscent of only temporal up-regulation of p53 protein in HDMEC exposed to anoxia and the lack of p21 induction in these conditions. On the contrary, anoxia treatment induced the expression of mRNAs for cyclins D2 and E1, this being HIF-1α-dependent. Contradictory reports on the effects of hypoxia on the cell cycle and cyclin expression exist in the literature (Box & Demetrick 2004, Kook et al 2008, Lin et al 2008) depending on the cell type and the type of hypoxic stimuli. This makes it difficult to explain cell cycle regulation by anoxia in HDMEC without further investigations.

#### 4.2.2.2.4. Induction of oxidative stress-related genes and chaperones by $Co^{2+}$

$Co^{2+}$ leads to ROS production, as was shown in HDMEC treated with $CoCl_2$. Oxidative stress is known to induce an adaptive response that might include the regulation of antioxidant enzyme activity, the increase of nonenzymatic antioxidant synthesis and elevated transcription of the genes involved in ROS detoxification, such as antioxidant enzymes. The induction of antioxidant-related genes in HDMEC by $CoCl_2$ could therefore be attributed to such adaptive responses. $CoCl_2$ treatment induced mRNA expression of the enzymes GSTM4, GSTO1 and GSTT2 and Trx-related TXNDC6 and TXNDC10. It is significant that the induction of all these genes was dependent on the presence of HIF-1α and could be abrogated by HIF-1α siRNA. GSTs are known to be involved in detoxification of xenobiotics and endoperoxides, the products of biomacromolecular oxidation. The induction of GSTs, therefore, might be important for cells to cope with the oxidative stress induced by $Co^{2+}$. However, due to the overlapping specificity of GSTs (Awasthi et al 1994) it is difficult to speculate on the exact functions of particular GSTs in $CoCl_2$-treated HDMEC. GSTs induction by oxidative stress is well known (Hayes & Pulford 1995), but liver GST activity regulation by $CoCl_2$ was also shown in *in vivo* experiments, where it could be abrogated by inhibitors of protein synthesis. This suggests that GST expression regulation is involved in the response to $CoCl_2$ (Daido & Aniya 1994). GST mRNA expression has not been related to HIF-1α activation until now. Although the exact function of TXNDC6 and TXNDC10 is also unknown, their homology with Trx points to the possibility of their involvement in the defence of endothelial cells against $Co^{2+}$-provoked ROS formation. In addition, a function of TXNDC10 has been described in the disulfide bond formation during protein folding in endoplasmatic reticulum (Haugstetter et al 2005). Interestingly, only GSTT2 was induced in HDMEC by anoxia, although to a lower extent than $CoCl_2$. This indicates clear differences in the cellular response to the oxidative stress that is induced via different mechanisms by $Co^{2+}$ or by the lack of oxygen.

Oxidation of proteins is a known result of oxidative stress. Induction of chaperones is a common cellular response to the conditions that lead to unfolding and misfolding of proteins, oxidative stress being one of such conditions. UPR, a mechanism of chaperone expression regulation, has been shown to be induced by S-glutathionylation of proteins and this is catalysed by GSTs (Townsend 2007), which were regulated in HDMEC treated with $CoCl_2$. In line with this HSPs were induced in HDMEC exposed to $CoCl_2$ and anoxia. However, no uniform pattern of HSPs regulation was observed. $CoCl_2$ could induce the mRNA expression of HSPA1A, HSPA8 and HSPA14 in a HIF-1α-dependent way. In turn,

anoxia treatment caused an increase in the amount of mRNA for HSPA4 and DNAJA3, and this was also HIF-1α-dependent. The regulation of HSPA8 by anoxia was different, as it only induced HSPA8 mRNA in the cells with down-regulated HIF-1α. As mentioned before, $Co^{2+}$ has been shown to induce the expression of HSPs (Hang et al 2009). Up-regulation of HSP mRNAs by hypoxia was also demonstrated and, importantly, it was shown to be HIF-1α-dependent (Huang et al 2009). It is difficult, however, to explain why particular chaperones are induced by $CoCl_2$ or anoxia exclusively. Moreover, the HIF-1α pathway can modulate UPR (van den Beucken et al 2006), suggesting the presence of both direct and indirect involvement of HIF-1α in the regulation of transcription of mRNAs coding for chaperones.

Overall, microarray data provide information about partly unknown HIF-1α-dependent and independent gene expression regulation. It is too early, however, to perform a definite dissection of the molecular pathways which are regulated by HIF-1α following $CoCl_2$ exposure and those which are induced by HIF-1α-independent effects of $Co^{2+}$. It is also possible that different genes in the same pathway are regulated differently and therefore no pathway could be ascribed as HIF-1α-dependent or independent. Therefore, more detailed analysis with clustering of the genes and grouping depending on the gene ontology will be required to elucidate HIF-1α-dependency of $CoCl_2$- and anoxia-induced gene regulation. The discrepancy in gene expression changes induced by both agents is difficult to explain at this point but could depend on diverse modes of action of the two agents at molecular level, different time courses of gene regulation by both treatments or the existence of other pathways involved in $CoCl_2$- and anoxia-induced signalling besides HIF-1α. Furthermore, since siRNA does not reduce HIF-1α mRNA level completely the differences in $CoCl_2$- and anoxia-induced changes in gene expression might be explained by the different threshold level of HIF-1α protein required by different agents to efficiently induce differential expression.

Nevertheless, the issue of HIF-1α-dependancy of $Co^{2+}$-induced effects might be of relevance in the context of diverse tissue reactions to $Co^{2+}$ released from metal implants and metal implant degradation products. The effects of metal particles and metal ions that can be amplified by ROS production include the induction of acute and chronic inflammatory responses in the tissues around metal prostheses. Permanent activation of inflammatory cells leads to degradation of ECM, induction of osteoclast differentiation and peri-prosthetic bone loss, eventually culminating in aseptic implant loosening. Therefore, the reduction of wear formation is certainly important in the prevention of aseptic loosening. This can be achieved

by changes in implant design, the use of improved wear- and corrosion-resistant metallic biomaterials, implant surface modifications, correct implant fixation and loading. In this respect knowledge of the mechanisms of metal implant-induced effects on inflammation and wound healing might prove to be useful for the production of materials with improved mechanical properties and minimized adverse effects. Though complete reduction of wear formation is probably an unachievable goal, even a small improvement of metal implant performance could be crucial with respect to reduction of pain and chronic inflammatory reactions, prolongation of implant lifetime and decline of metal failure incidence. The reduction of adverse effects of Co28Cr6Mo alloy by $TiO_2$-coating in this study could be one of the potential surface modifications for the production of metallic materials for medical applications. Furthermore, knowledge about molecular mechanisms of the action of metal degradation products could prove useful for therapeutic intervention against undesirable reactions of the human body to metallic materials. HIF-1α activation may, therefore, be one of the pathways whose regulation could be used in the future to modify tissue reactions to metal implants.

# 5. Summary

Aseptic loosening of metal implants is mainly attributed to the formation of metal degradation products. These include particulate debris and corrosion products, such as metal ions (anodic half-reaction) and ROS (cathodic half-reaction). While numerous clinical studies describe various adverse effects of metal degradation products, detailed knowledge of metal-induced cellular reactions, which might be important for possible therapeutic intervention, is not comprehensive. Since endothelial cells are involved in inflammation and angiogenesis, two processes which are critical for wound healing and integration of metal implants, the effects of different metal alloys and their degradation products on these cells were investigated. Endothelial cells on Ti6Al4V alloy showed signs of oxidative stress, which was similar to the response of endothelial cells to cathodic partial reaction of corrosion induced directly on Ti6Al4V surfaces. Furthermore, oxidative stress on Ti6Al4V alloy reduced the pro-inflammatory stimulation of endothelial cells by TNF-α and LPS. Oxidative stress and other stress-related responses were observed in endothelial cells in contact with Co28Cr6Mo alloy. Importantly, these features could be reduced by coating Co28Cr6Mo with a $TiO_2$ layer, thus favouring the use of such surface modification in the development of medical devices for orthopaedic surgery. The reaction of endothelial cells to Co28Cr6Mo alloy was partially similar to the effects exerted by $Co^{2+}$, which is known to be released from metal implants. $Co^{2+}$ also induced ROS formation and DNA damage in endothelial cells. This correlated with p53 and p21 up-regulation, indicating the possibility of cell cycle arrest. Since $CoCl_2$ is used as an hypoxia-mimicking agent, HIF-1α-dependence of cellular responses to $Co^{2+}$ was studied in comparison to anoxia-induced effects. Although important HIF-1α-dependent genes were identified, a more detailed analysis of microarray data will be required to provide additional information about the mechanisms of $Co^{2+}$ action. All these reactions of endothelial cells to metal degradation products might play their role in the complex processes taking place in the body following metal device implantation. In the worst case this can lead to aseptic loosening of the implant and requirement for revision surgery. Knowledge of molecular mechanisms of metal-induced responses will hopefully provide the possibility to interfere with undesirable processes at the implant/tissue interface, thus extending the life-time of the implant and the overall success of metal implant applications.

## 6. References

Achanta G, Huang P. 2004. Role of p53 in sensing oxidative DNA damage in response to reactive oxygen species-generating agents. *Cancer Res* 64: 6233-9

Adams RH, Alitalo K. 2007. Molecular regulation of angiogenesis and lymphangiogenesis. *Nat Rev Mol Cell Biol* 8: 464-78

Ahn BH, Park MH, Lee YH, Kwon TK, Min do S. 2007. Up-regulation of cyclooxygenase-2 by cobalt chloride-induced hypoxia is mediated by phospholipase D isozymes in human astroglioma cells. *Biochim Biophys Acta* 1773: 1721-31

Aitsebaomo J, Kingsley-Kallesen ML, Wu Y, Quertermous T, Patterson C. 2001. Vezf1/DB1 is an endothelial cell-specific transcription factor that regulates expression of the endothelin-1 promoter. *J Biol Chem* 276: 39197-205

Akisue T, Bauer TW, Farver CF, Mochida Y. 2002. The effect of particle wear debris on NFkappaB activation and pro-inflammatory cytokine release in differentiated THP-1 cells. *J Biomed Mater Res* 59: 507-15

Albina JE, Mastrofrancesco B, Vessella JA, Louis CA, Henry WL, Jr., Reichner JS. 2001. HIF-1 expression in healing wounds: HIF-1alpha induction in primary inflammatory cells by TNF-alpha. *Am J Physiol Cell Physiol* 281: C1971-7

Allerstorfer S, Sonvilla G, Fischer H, Spiegl-Kreinecker S, Gauglhofer C, et al. 2008. FGF5 as an oncogenic factor in human glioblastoma multiforme: autocrine and paracrine activities. *Oncogene* 27: 4180-90

An WG, Kanekal M, Simon MC, Maltepe E, Blagosklonny MV, Neckers LM. 1998. Stabilization of wild-type p53 by hypoxia-inducible factor 1alpha. *Nature* 392: 405-8

Antoine M, Wirz W, Tag CG, Mavituna M, Emans N, et al. 2005. Expression pattern of fibroblast growth factors (FGFs), their receptors and antagonists in primary endothelial cells and vascular smooth muscle cells. *Growth Factors* 23: 87-95

Appella E, Anderson CW. 2001. Post-translational modifications and activation of p53 by genotoxic stresses. *Eur J Biochem* 268: 2764-72

Asmuss M, Mullenders LH, Hartwig A. 2000. Interference by toxic metal compounds with isolated zinc finger DNA repair proteins. *Toxicol Lett* 112-113: 227-31

Awasthi YC, Sharma R, Singhal SS. 1994. Human glutathione S-transferases. *Int J Biochem* 26: 295-308

Barbieri SS, Eligini S, Brambilla M, Tremoli E, Colli S. 2003. Reactive oxygen species mediate cyclooxygenase-2 induction during monocyte to macrophage differentiation: critical role of NADPH oxidase. *Cardiovasc Res* 60: 187-97

Barnouin K, Dubuisson ML, Child ES, Fernandez de Mattos S, Glassford J, et al. 2002. H2O2 induces a transient multi-phase cell cycle arrest in mouse fibroblasts through modulating cyclin D and p21Cip1 expression. *J Biol Chem* 277: 13761-70

Bauer TW, Schils J. 1999. The pathology of total joint arthroplasty.II. Mechanisms of implant failure. *Skeletal Radiol* 28: 483-97

Bennin DA, Don AS, Brake T, McKenzie JL, Rosenbaum H, et al. 2002. Cyclin G2 associates with protein phosphatase 2A catalytic and regulatory B' subunits in active complexes and induces nuclear aberrations and a G1/S phase cell cycle arrest. *J Biol Chem* 277: 27449-67

Berra E, Ginouves A, Pouyssegur J. 2006. The hypoxia-inducible-factor hydroxylases bring fresh air into hypoxia signalling. *EMBO Rep* 7: 41-5

Besson A, Dowdy SF, Roberts JM. 2008. CDK inhibitors: cell cycle regulators and beyond. *Dev Cell* 14: 159-69

Bhoumik A, Lopez-Bergami P, Ronai Z. 2007. ATF2 on the double - activating transcription factor and DNA damage response protein. *Pigment Cell Res* 20: 498-506

Bikondoa O, Pang CL, Ithinin R, Muryn CA, Onishi H, Thornton G. 2006. Direct visualization of defect-mediated dissociation of water on TiO2(110) *Nat Mater* 5: 189–92

Blair IA. 2008. DNA adducts with lipid peroxidation products. *J Biol Chem* 283: 15545-9

Blumenthal NC, Cosma V, Jaffe W, Stuchin S. 1994. A new technique for quantitation of metal particulates and metal reaction products in tissues near implants. *J Appl Biomater* 5: 191-3

Bockris JOM, Reddy AKN, Gamboa-Aldeco M. 1998. *Modern electrochemistry*. New York: Plenum Press. 3 v. (liv, 2053 p.) pp.

Bos R, van Diest PJ, de Jong JS, van der Groep P, van der Valk P, van der Wall E. 2005. Hypoxia-inducible factor-1alpha is associated with angiogenesis, and expression of bFGF, PDGF-BB, and EGFR in invasive breast cancer. *Histopathology* 46: 31-6

Box AH, Demetrick DJ. 2004. Cell cycle kinase inhibitor expression and hypoxia-induced cell cycle arrest in human cancer cell lines. *Carcinogenesis* 25: 2325-35

Bradford MM. 1976. A rapid and sensitive method for the quantitation of microgram quantities of protein utilizing the principle of protein-dye binding. *Anal Biochem* 72: 248-54

Brauchle M, Funk JO, Kind P, Werner S. 1996. Ultraviolet B and H2O2 are potent inducers of vascular endothelial growth factor expression in cultured keratinocytes. *J Biol Chem* 271: 21793-7

Breen AP, Murphy JA. 1995. Reactions of oxyl radicals with DNA. *Free Radic Biol Med* 18: 1033-77

Brown DC, Gatter KC. 2002. Ki67 protein: the immaculate deception? *Histopathology* 40: 2-11

Bruni S, Martinesi M, Stio M, Treves C, Bacci T, Borgioli F. 2005. Effects of surface treatment of Ti-6Al-4V titanium alloy on biocompatibility in cultured human umbilical vein endothelial cells. *Acta Biomater* 1: 223-34

Bubici C, Papa S, Dean K, Franzoso G. 2006. Mutual cross-talk between reactive oxygen species and nuclear factor-kappa B: molecular basis and biological significance. *Oncogene* 25: 6731-48

Bunn HF, Poyton RO. 1996. Oxygen sensing and molecular adaptation to hypoxia. *Physiol Rev* 76: 839-85

Buttyan R, Chichester P, Stisser B, Matsumoto S, Ghafar MA, Levin RM. 2003. Acute intravesical infusion of a cobalt solution stimulates a hypoxia response, growth and angiogenesis in the rat bladder. *J Urol* 169: 2402-6

Cai H. 2005. Hydrogen peroxide regulation of endothelial function: origins, mechanisms, and consequences. *Cardiovasc Res* 68: 26-36

Carroll VA, Ashcroft M. 2005. Targeting the molecular basis for tumour hypoxia. *Expert Rev Mol Med* 7: 1-16

Carthew RW, Sontheimer EJ. 2009. Origins and Mechanisms of miRNAs and siRNAs. *Cell* 136: 642-55

Case CP, Langkamer VG, James C, Palmer MR, Kemp AJ, et al. 1994. Widespread dissemination of metal debris from implants. *J Bone Joint Surg Br* 76: 701-12

Chachami G, Simos G, Hatziefthimiou A, Bonanou S, Molyvdas PA, Paraskeva E. 2004. Cobalt induces hypoxia-inducible factor-1alpha expression in airway smooth muscle cells by a reactive oxygen species- and PI3K-dependent mechanism. *Am J Respir Cell Mol Biol* 31: 544-51

Chen D, Li M, Luo J, Gu W. 2003. Direct interactions between HIF-1 alpha and Mdm2 modulate p53 function. *J Biol Chem* 278: 13595-8

Chen JX, Stinnett A. 2008. Ang-1 gene therapy inhibits hypoxia-inducible factor-1alpha (HIF-1alpha)-prolyl-4-hydroxylase-2, stabilizes HIF-1alpha expression, and normalizes immature vasculature in db/db mice. *Diabetes* 57: 3335-43

Chen Z, Han ZC. 2008. STAT3: a critical transcription activator in angiogenesis. *Med Res Rev* 28: 185-200

Christmann M, Tomicic MT, Roos WP, Kaina B. 2003. Mechanisms of human DNA repair: an update. *Toxicology* 193: 3-34

Cimprich KA, Cortez D. 2008. ATR: an essential regulator of genome integrity. *Nat Rev Mol Cell Biol* 9: 616-27

Clark T, Johnson D. 1997. Activation of titanium electrodes for voltammetric detection of oxygen and hydrogen peroxide in alkaline media. *Electroanalysis* 9: 273-8

Clechet P, Martelet C, Martin JR, Olier R. 1979. Photoelectrochemical behaviour of TiO2 and formation of hydrogen-peroxyde. *Electrochim Acta* 24: 457-61

D'Autreaux B, Toledano MB. 2007. ROS as signalling molecules: mechanisms that generate specificity in ROS homeostasis. *Nat Rev Mol Cell Biol* 8: 813-24

Daido A, Aniya Y. 1994. Alteration of liver glutathione S-transferase and protease activities by cobalt chloride treatment of rats. *Jpn J Pharmacol* 66: 357-62

Dauphinee SM, Karsan A. 2006. Lipopolysaccharide signaling in endothelial cells. *Lab Invest* 86: 9-22

David SS, O'Shea VL, Kundu S. 2007. Base-excision repair of oxidative DNA damage. *Nature* 447: 941-50

Davies KJ. 1987. Protein damage and degradation by oxygen radicals. I. general aspects. *J Biol Chem* 262: 9895-901

Davies KJ. 1999. The broad spectrum of responses to oxidants in proliferating cells: a new paradigm for oxidative stress. *IUBMB Life* 48: 41-7

Davies KJ. 2000. Oxidative stress, antioxidant defenses, and damage removal, repair, and replacement systems. *IUBMB Life* 50: 279-89

de Bono DP, Yang WD. 1995. Exposure to low concentrations of hydrogen peroxide causes delayed endothelial cell death and inhibits proliferation of surviving cells. *Atherosclerosis* 114: 235-45

de Oliveira-Marques V, Cyrne L, Marinho HS, Antunes F. 2007. A quantitative study of NF-kappaB activation by H2O2: relevance in inflammation and synergy with TNF-alpha. *J Immunol* 178: 3893-902

Dhalla NS, Temsah RM, Netticadan T. 2000. Role of oxidative stress in cardiovascular diseases. *J Hypertens* 18: 655-73

Dianov G, Bischoff C, Piotrowski J, Bohr VA. 1998. Repair pathways for processing of 8-oxoguanine in DNA by mammalian cell extracts. *J Biol Chem* 273: 33811-6

Dianova, II, Bohr VA, Dianov GL. 2001. Interaction of human AP endonuclease 1 with flap endonuclease 1 and proliferating cell nuclear antigen involved in long-patch base excision repair. *Biochemistry* 40: 12639-44

Dickinson DA, Moellering DR, Iles KE, Patel RP, Levonen AL, et al. 2003. Cytoprotection against oxidative stress and the regulation of glutathione synthesis. *Biol Chem* 384: 527-37

Diegelmann RF, Evans MC. 2004. Wound healing: an overview of acute, fibrotic and delayed healing. *Front Biosci* 9: 283-9

Disegi JA. 2000. Titanium alloys for fracture fixation implants. *Injury* 31 Suppl 4: 14-7

Donovan J, Slingerland J. 2000. Transforming growth factor-beta and breast cancer: Cell cycle arrest by transforming growth factor-beta and its disruption in cancer. *Breast Cancer Res* 2: 116-24

Doorn PF, Campbell PA, Amstutz HC. 1996. Metal versus polyethylene wear particles in total hip replacements. A review. *Clin Orthop Relat Res*: S206-16

Dovi JV, He LK, DiPietro LA. 2003. Accelerated wound closure in neutrophil-depleted mice. *J Leukoc Biol* 73: 448-55

Droge W. 2002. Free radicals in the physiological control of cell function. *Physiol Rev* 82: 47-95

Epstein AC, Gleadle JM, McNeill LA, Hewitson KS, O'Rourke J, et al. 2001. C. elegans EGL-9 and mammalian homologs define a family of dioxygenases that regulate HIF by prolyl hydroxylation. *Cell* 107: 43-54

Espinosa JM, Verdun RE, Emerson BM. 2003. p53 functions through stress- and promoter-specific recruitment of transcription initiation components before and after DNA damage. *Mol Cell* 12: 1015-27

Ewing JF, Maines MD. 1993. Glutathione depletion induces heme oxygenase-1 (HSP32) mRNA and protein in rat brain. *J Neurochem* 60: 1512-9

Finkel T. 2003. Oxidant signals and oxidative stress. *Curr Opin Cell Biol* 15: 247-54

Fiore E, Fusco C, Romero P, Stamenkovic I. 2002. Matrix metalloproteinase 9 (MMP-9/gelatinase B) proteolytically cleaves ICAM-1 and participates in tumor cell resistance to natural killer cell-mediated cytotoxicity. *Oncogene* 21: 5213-23

Forman HJ, Torres M. 2002. Reactive oxygen species and cell signaling: respiratory burst in macrophage signaling. *Am J Respir Crit Care Med* 166: S4-8

Fraisl P, Mazzone M, Schmidt T, Carmeliet P. 2009. Regulation of angiogenesis by oxygen and metabolism. *Dev Cell* 16: 167-79

Frolov MV, Dyson NJ. 2004. Molecular mechanisms of E2F-dependent activation and pRB-mediated repression. *J Cell Sci* 117: 2173-81

Fujikawa K, Kamiya H, Yakushiji H, Fujii Y, Nakabeppu Y, Kasai H. 1999. The oxidized forms of dATP are substrates for the human MutT homologue, the hMTH1 protein. *J Biol Chem* 274: 18201-5

Galli F, Piroddi M, Annetti C, Aisa C, Floridi E, Floridi A. 2005. Oxidative stress and reactive oxygen species. *Contrib Nephrol* 149: 240-60

Galter D, Mihm S, Droge W. 1994. Distinct effects of glutathione disulphide on the nuclear transcription factor kappa B and the activator protein-1. *Eur J Biochem* 221: 639-48

Garrigues GE, Cho DR, Rubash HE, Goldring SR, Herndon JH, Shanbhag AS. 2005. Gene expression clustering using self-organizing maps: analysis of the macrophage response to particulate biomaterials. *Biomaterials* 26: 2933-45

Gasic AC, McGuire G, Krater S, Farhood AI, Goldstein MA, et al. 1991. Hydrogen peroxide pretreatment of perfused canine vessels induces ICAM-1 and CD18-dependent neutrophil adherence. *Circulation* 84: 2154-66

Gerald D, Berra E, Frapart YM, Chan DA, Giaccia AJ, et al. 2004. JunD reduces tumor angiogenesis by protecting cells from oxidative stress. *Cell* 118: 781-94

Ghosh S, Hayden MS. 2008. New regulators of NF-kappaB in inflammation. *Nat Rev Immunol* 8: 837-48

Gilbert JL, Zarka L, Chang E, Thomas CH. 1998. The reduction half cell in biomaterials corrosion: oxygen diffusion profiles near and cell response to polarized titanium surfaces. *J Biomed Mater Res* 42: 321-30

Gilmore TD. 2006. Introduction to NF-kappaB: players, pathways, perspectives. *Oncogene* 25: 6680-4

Giudiceandrea F, Iacona A, Cervelli G, Grimaldi M, Maggiulli G, et al. 1998. Mechanisms of bone resorption: analysis of proinflammatory cytokines in peritoneal macrophages from titanium implant--an experimental design. *J Craniofac Surg* 9: 254-9

Goda N, Ryan HE, Khadivi B, McNulty W, Rickert RC, Johnson RS. 2003. Hypoxia-inducible factor 1alpha is essential for cell cycle arrest during hypoxia. *Mol Cell Biol* 23: 359-69

Gomes A, Fernandes E, Lima JL. 2005. Fluorescence probes used for detection of reactive oxygen species. *J Biochem Biophys Methods* 65: 45-80

Gonzales JB, Purdon MA, Horowitz SM. 1996. In vitro studies on the role of titanium in aseptic loosening. *Clin Orthop Relat Res*: 244-50

Gonzalez-Pacheco FR, Deudero JJ, Castellanos MC, Castilla MA, Alvarez-Arroyo MV, et al. 2006. Mechanisms of endothelial response to oxidative aggression: protective role of autologous VEGF and induction of VEGFR2 by H2O2. *Am J Physiol Heart Circ Physiol* 291: H1395-401

Goodman SB. 1994. The effects of micromotion and particulate materials on tissue differentiation. Bone chamber studies in rabbits. *Acta Orthop Scand Suppl* 258: 1-43

Goumans MJ, Liu Z, ten Dijke P. 2009. TGF-beta signaling in vascular biology and dysfunction. *Cell Res* 19: 116-27

Gray MJ, Zhang J, Ellis LM, Semenza GL, Evans DB, et al. 2005. HIF-1alpha, STAT3, CBP/p300 and Ref-1/APE are components of a transcriptional complex that regulates Src-dependent hypoxia-induced expression of VEGF in pancreatic and prostate carcinomas. *Oncogene* 24: 3110-20

Greenfield EM, Bi Y, Ragab AA, Goldberg VM, Nalepka JL, Seabold JM. 2005. Does endotoxin contribute to aseptic loosening of orthopedic implants? *J Biomed Mater Res B Appl Biomater* 72: 179-85

Guha M, Mackman N. 2001. LPS induction of gene expression in human monocytes. *Cell Signal* 13: 85-94

Gurtner GC, Werner S, Barrandon Y, Longaker MT. 2008. Wound repair and regeneration. *Nature* 453: 314-21

Hallab NJ, Jacobs JJ, Skipor A, Black J, Mikecz K, Galante JO. 2000. Systemic metal-protein binding associated with total joint replacement arthroplasty. *J Biomed Mater Res* 49: 353-61

Hang X, Li P, Li Z, Qu W, Yu Y, et al. 2009. Transcription and splicing regulation in human umbilical vein endothelial cells under hypoxic stress conditions by exon array. *BMC Genomics* 10: 126

Hanna PM, Kadiiska MB, Mason RP. 1992. Oxygen-derived free radical and active oxygen complex formation from cobalt(II) chelates in vitro. *Chem Res Toxicol* 5: 109-15

Harris ED. 1992. Regulation of antioxidant enzymes. *FASEB J* 6: 2675-83

Harris GK, Shi X. 2003. Signaling by carcinogenic metals and metal-induced reactive oxygen species. *Mutat Res* 533: 183-200

Harris TA, Yamakuchi M, Ferlito M, Mendell JT, Lowenstein CJ. 2008. MicroRNA-126 regulates endothelial expression of vascular cell adhesion molecule 1. *Proc Natl Acad Sci U S A* 105: 1516-21

Harris WH, Schiller AL, Scholler JM, Freiberg RA, Scott R. 1976. Extensive localized bone resorption in the femur following total hip replacement. *J Bone Joint Surg Am* 58: 612-8

Hashimoto K, Tominaga Y, Nakabeppu Y, Moriya M. 2004. Futile short-patch DNA base excision repair of adenine:8-oxoguanine mispair. *Nucleic Acids Res* 32: 5928-34

Hastie LE, Patton WF, Hechtman HB, Shepro D. 1998. Metabolites of the phospholipase D pathway regulate H2O2-induced filamin redistribution in endothelial cells. *J Cell Biochem* 68: 511-24

Haugstetter J, Blicher T, Ellgaard L. 2005. Identification and characterization of a novel thioredoxin-related transmembrane protein of the endoplasmic reticulum. *J Biol Chem* 280: 8371-80

Hayes JD, Pulford DJ. 1995. The glutathione S-transferase supergene family: regulation of GST and the contribution of the isoenzymes to cancer chemoprotection and drug resistance. *Crit Rev Biochem Mol Biol* 30: 445-600

Hazra TK, Izumi T, Maidt L, Floyd RA, Mitra S. 1998. The presence of two distinct 8-oxoguanine repair enzymes in human cells: their potential complementary roles in preventing mutation. *Nucleic Acids Res* 26: 5116-22

He L, He X, Lim LP, de Stanchina E, Xuan Z, et al. 2007a. A microRNA component of the p53 tumour suppressor network. *Nature* 447: 1130-4

He L, He X, Lowe SW, Hannon GJ. 2007b. microRNAs join the p53 network--another piece in the tumour-suppression puzzle. *Nat Rev Cancer* 7: 819-22

Hirsila M, Koivunen P, Xu L, Seeley T, Kivirikko KI, Myllyharju J. 2005. Effect of desferrioxamine and metals on the hydroxylases in the oxygen sensing pathway. *FASEB J* 19: 1308-10

Hoffmann B, Feldmann M, Ziegler G. 2007. Sol-gel and precursor-derived coatings with cover function on medical alloys. *J Mater Chem* 17: 4034-40

Hoffmann B, Kokott A, Shafranska O, Detsch R, Winter S, et al. 2005. [Corrosion behaviour, metal release and biocompatibility of implant materials coated by TiO2-sol gel chemistry]. *Biomed Tech (Berl)* 50: 320-9

Holmgren A. 1995. Thioredoxin structure and mechanism: conformational changes on oxidation of the active-site sulfhydryls to a disulfide. *Structure* 3: 239-43

Huang J, Zhao Q, Mooney SM, Lee FS. 2002. Sequence determinants in hypoxia-inducible factor-1alpha for hydroxylation by the prolyl hydroxylases PHD1, PHD2, and PHD3. *J Biol Chem* 277: 39792-800

Huang WJ, Xia LM, Zhu F, Huang B, Zhou C, et al. 2009. Transcriptional upregulation of HSP70-2 by HIF-1 in cancer cells in response to hypoxia. *Int J Cancer* 124: 298-305

Ivan M, Kondo K, Yang H, Kim W, Valiando J, et al. 2001. HIFalpha targeted for VHL-mediated destruction by proline hydroxylation: implications for O2 sensing. *Science* 292: 464-8

Jaakkola P, Mole DR, Tian YM, Wilson MI, Gielbert J, et al. 2001. Targeting of HIF-alpha to the von Hippel-Lindau ubiquitylation complex by O2-regulated prolyl hydroxylation. *Science* 292: 468-72

Jacobs JJ, Gilbert JL, Urban RM. 1998a. Corrosion of metal orthopaedic implants. *J Bone Joint Surg Am* 80: 268-82

Jacobs JJ, Hallab NJ, Skipor AK, Urban RM. 2003. Metal degradation products: a cause for concern in metal-metal bearings? *Clin Orthop Relat Res*: 139-47

Jacobs JJ, Silverton C, Hallab NJ, Skipor AK, Patterson L, et al. 1999. Metal release and excretion from cementless titanium alloy total knee replacements. *Clin Orthop Relat Res*: 173-80

Jacobs JJ, Skipor AK, Black J, Urban R, Galante JO. 1991. Release and excretion of metal in patients who have a total hip-replacement component made of titanium-base alloy. *J Bone Joint Surg Am* 73: 1475-86

Jacobs JJ, Skipor AK, Doorn PF, Campbell P, Schmalzried TP, et al. 1996. Cobalt and chromium concentrations in patients with metal on metal total hip replacements. *Clin Orthop Relat Res*: S256-63

Jacobs JJ, Skipor AK, Patterson LM, Hallab NJ, Paprosky WG, et al. 1998b. Metal release in patients who have had a primary total hip arthroplasty. A prospective, controlled, longitudinal study. *J Bone Joint Surg Am* 80: 1447-58

Jefferies H, Coster J, Khalil A, Bot J, McCauley RD, Hall JC. 2003. Glutathione. *ANZ J Surg* 73: 517-22

Jegga AG, Inga A, Menendez D, Aronow BJ, Resnick MA. 2008. Functional evolution of the p53 regulatory network through its target response elements. *Proc Natl Acad Sci U S A* 105: 944-9

Jeon SH, Chae BC, Kim HA, Seo GY, Seo DW, et al. 2007. Mechanisms underlying TGF-beta1-induced expression of VEGF and Flk-1 in mouse macrophages and their implications for angiogenesis. *J Leukoc Biol* 81: 557-66

Johnson-Leger C, Aurrand-Lions M, Imhof BA. 2000. The parting of the endothelium: miracle, or simply a junctional affair? *J Cell Sci* 113 ( Pt 6): 921-33

Jung JE, Kim HS, Lee CS, Shin YJ, Kim YN, et al. 2008. STAT3 inhibits the degradation of HIF-1alpha by pVHL-mediated ubiquitination. *Exp Mol Med* 40: 479-85

Kadiiska MB, Maples KR, Mason RP. 1989. A comparison of cobalt(II) and iron(II) hydroxyl and superoxide free radical formation. *Arch Biochem Biophys* 275: 98-111

Kaelin WG, Jr., Ratcliffe PJ. 2008. Oxygen sensing by metazoans: the central role of the HIF hydroxylase pathway. *Mol Cell* 30: 393-402

Kaidi A, Williams AC, Paraskeva C. 2007. Interaction between beta-catenin and HIF-1 promotes cellular adaptation to hypoxia. *Nat Cell Biol* 9: 210-7

Kalbacova M, Roessler S, Hempel U, Tsaryk R, Peters K, et al. 2007. The effect of electrochemically simulated titanium cathodic corrosion products on ROS production and metabolic activity of osteoblasts and monocytes/macrophages. *Biomaterials* 28: 3263-72

Kasten U, Mullenders LH, Hartwig A. 1997. Cobalt(II) inhibits the incision and the polymerization step of nucleotide excision repair in human fibroblasts. *Mutat Res* 383: 81-9

Kim KS, Rajagopal V, Gonsalves C, Johnson C, Kalra VK. 2006. A novel role of hypoxia-inducible factor in cobalt chloride- and hypoxia-mediated expression of IL-8 chemokine in human endothelial cells. *J Immunol* 177: 7211-24

Kinov P, Leithner A, Radl R, Bodo K, Khoschsorur GA, et al. 2006. Role of free radicals in aseptic loosening of hip arthroplasty. *J Orthop Res* 24: 55-62

Kirkpatrick CJ, Barth S, Gerdes T, Krump-Konvalinkova V, Peters K. 2002. [Pathomechanisms of impaired wound healing by metallic corrosion products]. *Mund Kiefer Gesichtschir* 6: 183-90

Klein CL, Kohler H, Kirkpatrick CJ. 1994. Increased adhesion and activation of polymorphonuclear neutrophil granulocytes to endothelial cells under heavy metal exposure in vitro. *Pathobiology* 62: 90-8

Kokura S, Wolf RE, Yoshikawa T, Granger DN, Aw TY. 1999. Molecular mechanisms of neutrophil-endothelial cell adhesion induced by redox imbalance. *Circ Res* 84: 516-24

Kolev K, Skopal J, Simon L, Csonka E, Machovich R, Nagy Z. 2003. Matrix metalloproteinase-9 expression in post-hypoxic human brain capillary endothelial cells: H2O2 as a trigger and NF-kappaB as a signal transducer. *Thromb Haemost* 90: 528-37

Konttinen YT, Zhao D, Beklen A, Ma G, Takagi M, et al. 2005. The microenvironment around total hip replacement prostheses. *Clin Orthop Relat Res*: 28-38

Kook SH, Son YO, Lee KY, Lee HJ, Chung WT, et al. 2008. Hypoxia affects positively the proliferation of bovine satellite cells and their myogenic differentiation through up-regulation of MyoD. *Cell Biol Int* 32: 871-8

Koshiji M, Kageyama Y, Pete EA, Horikawa I, Barrett JC, Huang LE. 2004. HIF-1alpha induces cell cycle arrest by functionally counteracting Myc. *EMBO J* 23: 1949-56

Kraft CN, Burian B, Diedrich O, Gessmann J, Wimmer MA, Pennekamp PH. 2005. Microvascular response of striated muscle to common arthroplasty-alloys: A comparative in vivo study with CoCrMo, Ti-6Al-4V, and Ti-6Al-7Nb. *J Biomed Mater Res A* 75: 31-40

Kraft CN, Diedrich O, Burian B, Schmitt O, Wimmer MA. 2003. Microvascular response of striated muscle to metal debris. A comparative in vivo study with titanium and stainless steel. *J Bone Joint Surg Br* 85: 133-41

Krunkosky TM, Martin LD, Fischer BM, Voynow JA, Adler KB. 2003. Effects of TNFalpha on expression of ICAM-1 in human airway epithelial cells in vitro: oxidant-mediated pathways and transcription factors. *Free Radic Biol Med* 35: 1158-67

Kruse JP, Gu W. 2008. SnapShot: p53 posttranslational modifications. *Cell* 133: 930-30 e1

Kutty RK, Maines MD. 1987. Characterization of an NADH-dependent haem-degrading system in ox heart mitochondria. *Biochem J* 246: 467-74

Kuwabara K, Ogawa S, Matsumoto M, Koga S, Clauss M, et al. 1995. Hypoxia-mediated induction of acidic/basic fibroblast growth factor and platelet-derived growth factor in mononuclear phagocytes stimulates growth of hypoxic endothelial cells. *Proc Natl Acad Sci U S A* 92: 4606-10

Kuwano T, Nakao S, Yamamoto H, Tsuneyoshi M, Yamamoto T, et al. 2004. Cyclooxygenase 2 is a key enzyme for inflammatory cytokine-induced angiogenesis. *FASEB J* 18: 300-10

Laemmli UK. 1970. Cleavage of structural proteins during the assembly of the head of bacteriophage T4. *Nature* 227: 680-5

Lakshminarayanan V, Beno DW, Costa RH, Roebuck KA. 1997. Differential regulation of interleukin-8 and intercellular adhesion molecule-1 by H2O2 and tumor necrosis factor-alpha in endothelial and epithelial cells. *J Biol Chem* 272: 32910-8

Lakshminarayanan V, Lewallen M, Frangogiannis NG, Evans AJ, Wedin KE, et al. 2001. Reactive oxygen intermediates induce monocyte chemotactic protein-1 in vascular endothelium after brief ischemia. *Am J Pathol* 159: 1301-11

Larsson J, Persson C, Tengvall P, Lundqvist-Gustafsson H. 2004. Anti-inflammatory effects of a titanium-peroxy gel: role of oxygen metabolites and apoptosis. *J Biomed Mater Res A* 68: 448-57

Lavin MF. 2008. Ataxia-telangiectasia: from a rare disorder to a paradigm for cell signalling and cancer. *Nat Rev Mol Cell Biol* 9: 759-69

Lee MC, Yoshino F, Shoji H, Takahashi S, Todoki K, et al. 2005. Characterization by electron spin resonance spectroscopy of reactive oxygen species generated by titanium dioxide and hydrogen peroxide. *J Dent Res* 84: 178-82

Lee MR, Kim SH, Cho HJ, Lee KY, Moon AR, et al. 2004. Transcription factors NF-YA regulate the induction of human OGG1 following DNA-alkylating agent methylmethane sulfonate (MMS) treatment. *J Biol Chem* 279: 9857-66

Lee SG, Lee H, Rho HM. 2001. Transcriptional repression of the human p53 gene by cobalt chloride mimicking hypoxia. *FEBS Lett* 507: 259-63

Lee SR, Kwon KS, Kim SR, Rhee SG. 1998. Reversible inactivation of protein-tyrosine phosphatase 1B in A431 cells stimulated with epidermal growth factor. *J Biol Chem* 273: 15366-72

Lee TM, Chang E, Yang CY. 2000. A comparison of the surface characteristics and ion release of Ti6Al4V and heat-treated Ti6Al4V. *J Biomed Mater Res* 50: 499-511

Leonard S, Gannett PM, Rojanasakul Y, Schwegler-Berry D, Castranova V, et al. 1998. Cobalt-mediated generation of reactive oxygen species and its possible mechanism. *J Inorg Biochem* 70: 239-44

Leung AK, Calabrese JM, Sharp PA. 2006. Quantitative analysis of Argonaute protein reveals microRNA-dependent localization to stress granules. *Proc Natl Acad Sci U S A* 103: 18125-30

Ley K, Laudanna C, Cybulsky MI, Nourshargh S. 2007. Getting to the site of inflammation: the leukocyte adhesion cascade updated. *Nat Rev Immunol* 7: 678-89

Li J, Zhang YP, Kirsner RS. 2003. Angiogenesis in wound repair: angiogenic growth factors and the extracellular matrix. *Microsc Res Tech* 60: 107-14

Lin HY, Bumgardner JD. 2004. In vitro biocorrosion of Ti-6Al-4V implant alloy by a mouse macrophage cell line. *J Biomed Mater Res A* 68: 717-24

Lin YM, Huang SK, Wang HF, Chen LM, Tsai FJ, et al. 2008. Short-term versus long-term intermittent hypobaric hypoxia on cardiac fibrosis and Fas death receptor dependent apoptotic pathway in rat hearts. *Chin J Physiol* 51: 308-16

Liu SM, Sundqvist T. 1995. Effects of hydrogen peroxide and phorbol myristate acetate on endothelial transport and F-actin distribution. *Exp Cell Res* 217: 1-7

Lo SK, Janakidevi K, Lai L, Malik AB. 1993. Hydrogen peroxide-induced increase in endothelial adhesiveness is dependent on ICAM-1 activation. *Am J Physiol* 264: L406-12

Loboda A, Jazwa A, Wegiel B, Jozkowicz A, Dulak J. 2005. Heme oxygenase-1-dependent and -independent regulation of angiogenic genes expression: effect of cobalt protoporphyrin and cobalt chloride on VEGF and IL-8 synthesis in human microvascular endothelial cells. *Cell Mol Biol (Noisy-le-grand)* 51: 347-55

Long M, Rack HJ. 1998. Titanium alloys in total joint replacement--a materials science perspective. *Biomaterials* 19: 1621-39

Lopez F, Belloc F, Lacombe F, Dumain P, Reiffers J, et al. 1991. Modalities of synthesis of Ki67 antigen during the stimulation of lymphocytes. *Cytometry* 12: 42-9

Lu SC. 2000. Regulation of glutathione synthesis. *Curr Top Cell Regul* 36: 95-116

Lum H, Roebuck KA. 2001. Oxidant stress and endothelial cell dysfunction. *Am J Physiol Cell Physiol* 280: C719-41

Luo Y, Hurwitz J, Massague J. 1995. Cell-cycle inhibition by independent CDK and PCNA binding domains in p21Cip1. *Nature* 375: 159-61

Maas M, Wang R, Paddock C, Kotamraju S, Kalyanaraman B, et al. 2003. Reactive oxygen species induce reversible PECAM-1 tyrosine phosphorylation and SHP-2 binding. *Am J Physiol Heart Circ Physiol* 285: H2336-44

MacCallum DE, Hupp TR, Midgley CA, Stuart D, Campbell SJ, et al. 1996. The p53 response to ionising radiation in adult and developing murine tissues. *Oncogene* 13: 2575-87

MacDonald SJ. 2004. Metal-on-metal total hip arthroplasty: the concerns. *Clin Orthop Relat Res*: 86-93

Madamanchi NR, Li S, Patterson C, Runge MS. 2001. Reactive oxygen species regulate heat-shock protein 70 via the JAK/STAT pathway. *Arterioscler Thromb Vasc Biol* 21: 321-6

Madhusudan S, Smart F, Shrimpton P, Parsons JL, Gardiner L, et al. 2005. Isolation of a small molecule inhibitor of DNA base excision repair. *Nucleic Acids Res* 33: 4711-24

Maekawa T, Shinagawa T, Sano Y, Sakuma T, Nomura S, et al. 2007. Reduced levels of ATF-2 predispose mice to mammary tumors. *Mol Cell Biol* 27: 1730-44

Maines MD, Kappas A. 1976. The induction of heme oxidation in various tissues by trace metals: evidence for the catabolism of endogenous heme by hepatic heme oxygenase. *Ann Clin Res* 8 Suppl 17: 39-46

Mak SK, Kultz D. 2004. Gadd45 proteins induce G2/M arrest and modulate apoptosis in kidney cells exposed to hyperosmotic stress. *J Biol Chem* 279: 39075-84

Malhotra JD, Miao H, Zhang K, Wolfson A, Pennathur S, et al. 2008. Antioxidants reduce endoplasmic reticulum stress and improve protein secretion. *Proc Natl Acad Sci U S A* 105: 18525-30

Maloney WJ, James RE, Smith RL. 1996. Human macrophage response to retrieved titanium alloy particles in vitro. *Clin Orthop Relat Res*: 268-78

Malumbres M, Barbacid M. 2009. Cell cycle, CDKs and cancer: a changing paradigm. *Nat Rev Cancer* 9: 153-66

Mandelin J, Li TF, Liljestrom M, Kroon ME, Hanemaaijer R, et al. 2003. Imbalance of RANKL/RANK/OPG system in interface tissue in loosening of total hip replacement. *J Bone Joint Surg Br* 85: 1196-201

Mao Y, Liu KJ, Jiang JJ, Shi X. 1996. Generation of reactive oxygen species by Co(II) from H2O2 in the presence of chelators in relation to DNA damage and 2'-deoxyguanosine hydroxylation. *J Toxicol Environ Health* 47: 61-75

Marceau M, Kouame N, Lacourciere Y, Cleroux J. 1998. Vascular structure in the forearm and calf after 6 months of angiotensin converting enzyme inhibition in elderly hypertensive subjects with left ventricular hypertrophy. *J Hypertens* 16: 673-9

Marsit CJ, Eddy K, Kelsey KT. 2006. MicroRNA responses to cellular stress. *Cancer Res* 66: 10843-8

Marti A. 2000. Cobalt-base alloys used in bone surgery. *Injury* 31 Suppl 4: 18-21

Martin P, D'Souza D, Martin J, Grose R, Cooper L, et al. 2003. Wound healing in the PU.1 null mouse--tissue repair is not dependent on inflammatory cells. *Curr Biol* 13: 1122-8

Martin P, Leibovich SJ. 2005. Inflammatory cells during wound repair: the good, the bad and the ugly. *Trends Cell Biol* 15: 599-607

Martinez-Sanchez G, Giuliani A, Perez-Davison G, Leon-Fernandez OS. 2005. Oxidized proteins and their contribution to redox homeostasis. *Redox Rep* 10: 175-85

Masuda Y, Suzuki M, Piao J, Gu Y, Tsurimoto T, Kamiya K. 2007. Dynamics of human replication factors in the elongation phase of DNA replication. *Nucleic Acids Res* 35: 6904-16

Meek DW. 2004. The p53 response to DNA damage. *DNA Repair (Amst)* 3: 1049-56

Meilhac O, Zhou M, Santanam N, Parthasarathy S. 2000. Lipid peroxides induce expression of catalase in cultured vascular cells. *J Lipid Res* 41: 1205-13

Menon SG, Goswami PC. 2007. A redox cycle within the cell cycle: ring in the old with the new. *Oncogene* 26: 1101-9

Mentus SV. 2004. Oxygen reduction on anodically formed titanium dioxide. *Electrochimica Acta* 50: 27-32

Midwood KS, Williams LV, Schwarzbauer JE. 2004. Tissue repair and the dynamics of the extracellular matrix. *Int J Biochem Cell Biol* 36: 1031-7

Millan J, Hewlett L, Glyn M, Toomre D, Clark P, Ridley AJ. 2006. Lymphocyte transcellular migration occurs through recruitment of endothelial ICAM-1 to caveola- and F-actin-rich domains. *Nat Cell Biol* 8: 113-23

Milosev I, Metikos-Hukovic M, Strehblow HH. 2000. Passive film on orthopaedic TiAlV alloy formed in physiological solution investigated by X-ray photoelectron spectroscopy. *Biomaterials* 21: 2103-13

Mitra S, Boldogh I, Izumi T, Hazra TK. 2001. Complexities of the DNA base excision repair pathway for repair of oxidative DNA damage. *Environ Mol Mutagen* 38: 180-90

Miyashita H, Kanemura M, Yamazaki T, Abe M, Sato Y. 2004. Vascular endothelial zinc finger 1 is involved in the regulation of angiogenesis: possible contribution of stathmin/OP18 as a downstream target gene. *Arterioscler Thromb Vasc Biol* 24: 878-84

Morisada T, Kubota Y, Urano T, Suda T, Oike Y. 2006. Angiopoietins and angiopoietin-like proteins in angiogenesis. *Endothelium* 13: 71-9

Mu Y, Kobayashi T, Sumita M, Yamamoto A, Hanawa T. 2000. Metal ion release from titanium with active oxygen species generated by rat macrophages in vitro. *J Biomed Mater Res* 49: 238-43

Murphy RC, Johnson KM. 2008. Cholesterol, reactive oxygen species, and the formation of biologically active mediators. *J Biol Chem* 283: 15521-5

Murray-Zmijewski F, Slee EA, Lu X. 2008. A complex barcode underlies the heterogeneous response of p53 to stress. *Nat Rev Mol Cell Biol* 9: 702-12

Nakamura J, La DK, Swenberg JA. 2000. 5'-nicked apurinic/apyrimidinic sites are resistant to beta-elimination by beta-polymerase and are persistent in human cultured cells after oxidative stress. *J Biol Chem* 275: 5323-8

Nakamura T, Sakamoto K. 2001. Reactive oxygen species up-regulates cyclooxygenase-2, p53, and Bax mRNA expression in bovine luteal cells. *Biochem Biophys Res Commun* 284: 203-10

Ni M, Lee AS. 2007. ER chaperones in mammalian development and human diseases. *FEBS Lett* 581: 3641-51

Nordlind K. 2002. Expression of heat shock proteins in heavy metal-provoked inflamed human skin. *Immunopharmacol Immunotoxicol* 24: 383-94

Otterbein LE, Zuckerbraun BS, Haga M, Liu F, Song R, et al. 2003. Carbon monoxide suppresses arteriosclerotic lesions associated with chronic graft rejection and with balloon injury. *Nat Med* 9: 183-90

Ozmen I, Naziroglu M, Okutan R. 2005. Comparative study of antioxidant enzymes in tissues surrounding implant in rabbits. *Cell Biochem Funct* 24: 275-81

Pacary E, Legros H, Valable S, Duchatelle P, Lecocq M, et al. 2006. Synergistic effects of CoCl(2) and ROCK inhibition on mesenchymal stem cell differentiation into neuron-like cells. *J Cell Sci* 119: 2667-78

Palecek E, Brazdova M, Cernocka H, Vlk D, Brazda V, Vojtesek B. 1999. Effect of transition metals on binding of p53 protein to supercoiled DNA and to consensus sequence in DNA fragments. *Oncogene* 18: 3617-25

Palit S, Sharma A, Talukder G. 1991. Chromosomal aberrations induced by cobaltous chloride in mice in vivo. *Biol Trace Elem Res* 29: 139-45

Pan J, Liao H, Leygraf C, Thierry D, Li J. 1998. Variation of oxide films on titanium induced by osteoblast-like cell culture and the influence of an H2O2 pretreatment. *J Biomed Mater Res* 40: 244-56

Patel SA, Simon MC. 2008. Biology of hypoxia-inducible factor-2alpha in development and disease. *Cell Death Differ* 15: 628-34

Pennekamp PH, Gessmann J, Diedrich O, Burian B, Wimmer MA, et al. 2006. Short-term microvascular response of striated muscle to cp-Ti, Ti-6Al-4V, and Ti-6Al-7Nb. *J Orthop Res* 24: 531-40

Perry MM, Moschos SA, Williams AE, Shepherd NJ, Larner-Svensson HM, Lindsay MA. 2008. Rapid changes in microRNA-146a expression negatively regulate the IL-1beta-induced inflammatory response in human lung alveolar epithelial cells. *J Immunol* 180: 5689-98

Peters K, Schmidt H, Unger RE, Kamp G, Prols F, et al. 2005. Paradoxical effects of hypoxia-mimicking divalent cobalt ions in human endothelial cells in vitro. *Mol Cell Biochem* 270: 157-66

Peters K, Schmidt H, Unger RE, Otto M, Kamp G, Kirkpatrick CJ. 2002. Software-supported image quantification of angiogenesis in an in vitro culture system: application to studies of biocompatibility. *Biomaterials* 23: 3413-9

Peters K, Unger RE, Barth S, Gerdes T, Kirkpatrick CJ. 2001. Induction of apoptosis in human microvascular endothelial cells by divalent cobalt ions. Evidence for integrin-mediated signaling via the cytoskeleton. *J Mater Sci Mater Med* 12: 955-8

Peters K, Unger RE, Brunner J, Kirkpatrick CJ. 2003. Molecular basis of endothelial dysfunction in sepsis. *Cardiovasc Res* 60: 49-57

Peters K, Unger RE, Kirkpatrick CJ, Gatti AM, Monari E. 2004. Effects of nano-scaled particles on endothelial cell function in vitro: studies on viability, proliferation and inflammation. *J Mater Sci Mater Med* 15: 321-5

Peters K, Unger RE, Stumpf S, Schafer J, Tsaryk R, et al. 2008. Cell type-specific aspects in biocompatibility testing: the intercellular contact in vitro as an indicator for endothelial cell compatibility. *J Mater Sci Mater Med* 19: 1637-44

Pfaffl MW, Horgan GW, Dempfle L. 2002. Relative expression software tool (REST) for group-wise comparison and statistical analysis of relative expression results in real-time PCR. *Nucleic Acids Res* 30: e36

Plant SD, Grant DM, Leach L. 2005. Behaviour of human endothelial cells on surface modified NiTi alloy. *Biomaterials* 26: 5359-67

Pohler OE. 2000. Unalloyed titanium for implants in bone surgery. *Injury* 31 Suppl 4: 7-13

Polager S, Ginsberg D. 2008. E2F - at the crossroads of life and death. *Trends Cell Biol* 18: 528-35

Pouteau E, Dumon H, Biourge V, Krempf M, Nguyen P. 1998. Hydrogen production in dogs adapts to addition of lactulose and to a meat and rice diet. *J Nutr* 128: 2666S-8S

Rahman I, Bel A, Mulier B, Lawson MF, Harrison DJ, et al. 1996. Transcriptional regulation of gamma-glutamylcysteine synthetase-heavy subunit by oxidants in human alveolar epithelial cells. *Biochem Biophys Res Commun* 229: 832-7

Ramakers C, Ruijter JM, Deprez RH, Moorman AF. 2003. Assumption-free analysis of quantitative real-time polymerase chain reaction (PCR) data. *Neurosci Lett* 339: 62-6

Rhee SG, Chang TS, Bae YS, Lee SR, Kang SW. 2003. Cellular regulation by hydrogen peroxide. *J Am Soc Nephrol* 14: S211-5

Rieckmann T, Kotevic I, Trueb B. 2008. The cell surface receptor FGFRL1 forms constitutive dimers that promote cell adhesion. *Exp Cell Res* 314: 1071-81

Riley T, Sontag E, Chen P, Levine A. 2008. Transcriptional control of human p53-regulated genes. *Nat Rev Mol Cell Biol* 9: 402-12

Risom L, Moller P, Vogel U, Kristjansen PE, Loft S. 2003. X-ray-induced oxidative stress: DNA damage and gene expression of HO-1, ERCC1 and OGG1 in mouse lung. *Free Radic Res* 37: 957-66

Roebuck KA. 1999. Oxidant stress regulation of IL-8 and ICAM-1 gene expression: differential activation and binding of the transcription factors AP-1 and NF-kappaB (Review). *Int J Mol Med* 4: 223-30

Roebuck KA, Rahman A, Lakshminarayanan V, Janakidevi K, Malik AB. 1995. H2O2 and tumor necrosis factor-alpha activate intercellular adhesion molecule 1 (ICAM-1) gene transcription through distinct cis-regulatory elements within the ICAM-1 promoter. *J Biol Chem* 270: 18966-74

Rokutan K, Teshima S, Miyoshi M, Kawai T, Nikawa T, Kishi K. 1998. Glutathione depletion inhibits oxidant-induced activation of nuclear factor-kappa B, AP-1, and c-Jun/ATF-2 in cultured guinea-pig gastric epithelial cells. *J Gastroenterol* 33: 646-55

Rolf O, Baumann B, Sterner T, Schutze N, Jakob F, et al. 2005. Characterization of mode II-wear particles and cytokine response in a human macrophage-like cell culture. *Biomed Tech (Berl)* 50: 25-9

Ruef J, Hu ZY, Yin LY, Wu Y, Hanson SR, et al. 1997. Induction of vascular endothelial growth factor in balloon-injured baboon arteries. A novel role for reactive oxygen species in atherosclerosis. *Circ Res* 81: 24-33

Ryter SW, Alam J, Choi AM. 2006. Heme oxygenase-1/carbon monoxide: from basic science to therapeutic applications. *Physiol Rev* 86: 583-650

Sabokbar A, Pandey R, Quinn JM, Athanasou NA. 1998. Osteoclastic differentiation by mononuclear phagocytes containing biomaterial particles. *Arch Orthop Trauma Surg* 117: 136-40

Saito S, Yamaguchi H, Higashimoto Y, Chao C, Xu Y, et al. 2003. Phosphorylation site interdependence of human p53 post-translational modifications in response to stress. *J Biol Chem* 278: 37536-44

Salnikow K, Donald SP, Bruick RK, Zhitkovich A, Phang JM, Kasprzak KS. 2004. Depletion of intracellular ascorbate by the carcinogenic metals nickel and cobalt results in the induction of hypoxic stress. *J Biol Chem* 279: 40337-44

Samuels-Lev Y, O'Connor DJ, Bergamaschi D, Trigiante G, Hsieh JK, et al. 2001. ASPP proteins specifically stimulate the apoptotic function of p53. *Mol Cell* 8: 781-94

Sanchez-Puig N, Veprintsev DB, Fersht AR. 2005. Binding of natively unfolded HIF-1alpha ODD domain to p53. *Mol Cell* 17: 11-21

Scalia R, Lefer AM. 1998. In vivo regulation of PECAM-1 activity during acute endothelial dysfunction in the rat mesenteric microvasculature. *J Leukoc Biol* 64: 163-9

Schraufstatter IU, Hinshaw DB, Hyslop PA, Spragg RG, Cochrane CG. 1986. Oxidant injury of cells. DNA strand-breaks activate polyadenosine diphosphate-ribose polymerase and lead to depletion of nicotinamide adenine dinucleotide. *J Clin Invest* 77: 1312-20

Schreck R, Albermann K, Baeuerle PA. 1992. Nuclear factor kappa B: an oxidative stress-responsive transcription factor of eukaryotic cells (a review). *Free Radic Res Commun* 17: 221-37

Schroder M, Kaufman RJ. 2005. ER stress and the unfolded protein response. *Mutat Res* 569: 29-63

Sehgal PB. 2008. Paradigm shifts in the cell biology of STAT signaling. *Semin Cell Dev Biol* 19: 329-40

Senderowicz AM. 2003. Small-molecule cyclin-dependent kinase modulators. *Oncogene* 22: 6609-20

Senyuk V, Rinaldi CR, Li D, Cattaneo F, Stojanovic A, et al. 2009. Consistent up-regulation of Stat3 Independently of Jak2 mutations in a new murine model of essential thrombocythemia. *Cancer Res* 69: 262-71

Sherr CJ. 2006. Divorcing ARF and p53: an unsettled case. *Nat Rev Cancer* 6: 663-73

Shiraiwa M, Goto T, Yoshinari M, Koyano K, Tanaka T. 2002. A study of the initial attachment and subsequent behavior of rat oral epithelial cells cultured on titanium. *J Periodontol* 73: 852-60

Shono T, Ono M, Izumi H, Jimi SI, Matsushima K, et al. 1996. Involvement of the transcription factor NF-kappaB in tubular morphogenesis of human microvascular endothelial cells by oxidative stress. *Mol Cell Biol* 16: 4231-9

Shull S, Heintz NH, Periasamy M, Manohar M, Janssen YM, et al. 1991. Differential regulation of antioxidant enzymes in response to oxidants. *J Biol Chem* 266: 24398-403

Simon MP, Tournaire R, Pouyssegur J. 2008. The angiopoietin-2 gene of endothelial cells is up-regulated in hypoxia by a HIF binding site located in its first intron and by the central factors GATA-2 and Ets-1. *J Cell Physiol* 217: 809-18

Simpson DM, Ross R. 1972. The neutrophilic leukocyte in wound repair a study with antineutrophil serum. *J Clin Invest* 51: 2009-23

Singh A, Jayaraman A, Hahn J. 2006. Modeling regulatory mechanisms in IL-6 signal transduction in hepatocytes. *Biotechnol Bioeng* 95: 850-62

Sinha RK, Morris F, Shah SA, Tuan RS. 1994. Surface composition of orthopaedic implant metals regulates cell attachment, spreading, and cytoskeletal organization of primary human osteoblasts in vitro. *Clin Orthop Relat Res*: 258-72

Slupphaug G, Kavli B, Krokan HE. 2003. The interacting pathways for prevention and repair of oxidative DNA damage. *Mutat Res* 531: 231-51

Sobol RW, Horton JK, Kuhn R, Gu H, Singhal RK, et al. 1996. Requirement of mammalian DNA polymerase-beta in base-excision repair. *Nature* 379: 183-6

Sobol RW, Prasad R, Evenski A, Baker A, Yang XP, et al. 2000. The lyase activity of the DNA repair protein beta-polymerase protects from DNA-damage-induced cytotoxicity. *Nature* 405: 807-10

Song FM, Kirk DW, Graydon JW, Cormack DE. 2002a. CO2 corrosion of bare steel under an aqueous boundary layer with oxygen. *Journal of the Electrochemical Society* 149: 479-86

Song R, Mahidhara RS, Liu F, Ning W, Otterbein LE, Choi AM. 2002b. Carbon monoxide inhibits human airway smooth muscle cell proliferation via mitogen-activated protein kinase pathway. *Am J Respir Cell Mol Biol* 27: 603-10

Song YS, Lee YS, Narasimhan P, Chan PH. 2007. Reduced oxidative stress promotes NF-kappaB-mediated neuroprotective gene expression after transient focal cerebral ischemia: lymphocytotrophic cytokines and antiapoptotic factors. *J Cereb Blood Flow Metab* 27: 764-75

Spurgers KB, Gold DL, Coombes KR, Bohnenstiehl NL, Mullins B, et al. 2006. Identification of cell cycle regulatory genes as principal targets of p53-mediated transcriptional repression. *J Biol Chem* 281: 25134-42

Steinbrech DS, Mehrara BJ, Saadeh PB, Greenwald JA, Spector JA, et al. 2000. VEGF expression in an osteoblast-like cell line is regulated by a hypoxia response mechanism. *Am J Physiol Cell Physiol* 278: C853-60

Stucki M, Pascucci B, Parlanti E, Fortini P, Wilson SH, et al. 1998. Mammalian base excision repair by DNA polymerases delta and epsilon. *Oncogene* 17: 835-43

Sundfeldt M, Carlsson LV, Johansson CB, Thomsen P, Gretzer C. 2006. Aseptic loosening, not only a question of wear: a review of different theories. *Acta Orthop* 77: 177-97

Suska F, Esposito M, Gretzer C, Kalltorp M, Tengvall P, Thomsen P. 2003. IL-1alpha, IL-1beta and TNF-alpha secretion during in vivo/ex vivo cellular interactions with titanium and copper. *Biomaterials* 24: 461-8

Swarbrick A, Lee CS, Sutherland RL, Musgrove EA. 2000. Cooperation of p27(Kip1) and p18(INK4c) in progestin-mediated cell cycle arrest in T-47D breast cancer cells. *Mol Cell Biol* 20: 2581-91

Szpaderska AM, DiPietro LA. 2005. Inflammation in surgical wound healing: friend or foe? *Surgery* 137: 571-3

Tanaka T, Kojima I, Ohse T, Ingelfinger JR, Adler S, et al. 2005. Cobalt promotes angiogenesis via hypoxia-inducible factor and protects tubulointerstitium in the remnant kidney model. *Lab Invest* 85: 1292-307

Taylor CT. 2008. Interdependent roles for hypoxia inducible factor and nuclear factor-kappaB in hypoxic inflammation. *J Physiol* 586: 4055-9

Taylor GC, Waddington RJ, Moseley R, Williams KR, Embery G. 1996. Influence of titanium oxide and titanium peroxy gel on the breakdown of hyaluronan by reactive oxygen species. *Biomaterials* 17: 1313-9

Tengvall P, Elwing H, Sjoqvist L, Lundstrom I, Bjursten LM. 1989a. Interaction between hydrogen peroxide and titanium: a possible role in the biocompatibility of titanium. *Biomaterials* 10: 118-20

Tengvall P, Lundstrom I, Sjoqvist L, Elwing H, Bjursten LM. 1989b. Titanium-hydrogen peroxide interaction: model studies of the influence of the inflammatory response on titanium implants. *Biomaterials* 10: 166-75

Teodoro JG, Evans SK, Green MR. 2007. Inhibition of tumor angiogenesis by p53: a new role for the guardian of the genome. *J Mol Med* 85: 1175-86

Thornhill TS, Ozuna RM, Shortkroff S, Keller K, Sledge CB, Spector M. 1990. Biochemical and histological evaluation of the synovial-like tissue around failed (loose) total joint replacement prostheses in human subjects and a canine model. *Biomaterials* 11: 69-72

Tili E, Michaille JJ, Cimino A, Costinean S, Dumitru CD, et al. 2007. Modulation of miR-155 and miR-125b levels following lipopolysaccharide/TNF-alpha stimulation and their possible roles in regulating the response to endotoxin shock. *J Immunol* 179: 5082-9

Toledano MB, Leonard WJ. 1991. Modulation of transcription factor NF-kappa B binding activity by oxidation-reduction in vitro. *Proc Natl Acad Sci U S A* 88: 4328-32

Toledo F, Wahl GM. 2006. Regulating the p53 pathway: in vitro hypotheses, in vivo veritas. *Nat Rev Cancer* 6: 909-23

Tomkinson AE, Chen L, Dong Z, Leppard JB, Levin DS, et al. 2001. Completion of base excision repair by mammalian DNA ligases. *Prog Nucleic Acid Res Mol Biol* 68: 151-64

Townsend DM. 2007. S-glutathionylation: indicator of cell stress and regulator of the unfolded protein response. *Mol Interv* 7: 313-24

Trompezinski S, Pernet I, Mayoux C, Schmitt D, Viac J. 2000. Transforming growth factor-beta1 and ultraviolet A1 radiation increase production of vascular endothelial growth factor but not endothelin-1 in human dermal fibroblasts. *Br J Dermatol* 143: 539-45

True AL, Rahman A, Malik AB. 2000. Activation of NF-kappaB induced by H(2)O(2) and TNF-alpha and its effects on ICAM-1 expression in endothelial cells. *Am J Physiol Lung Cell Mol Physiol* 279: L302-11

Trueb B, Zhuang L, Taeschler S, Wiedemann M. 2003. Characterization of FGFRL1, a novel fibroblast growth factor (FGF) receptor preferentially expressed in skeletal tissues. *J Biol Chem* 278: 33857-65

Tsutsumi S, Namba T, Tanaka KI, Arai Y, Ishihara T, et al. 2006. Celecoxib upregulates endoplasmic reticulum chaperones that inhibit celecoxib-induced apoptosis in human gastric cells. *Oncogene* 25: 1018-29

Tucci M, Baker R, Benghuzzi H, Hughes J. 2000. Levels of hydrogen peroxide in tissues adjacent to failing implantable devices may play an active role in cytokine production. *Biomed Sci Instrum* 36: 215-20

Ushio-Fukai M, Alexander RW. 2004. Reactive oxygen species as mediators of angiogenesis signaling: role of NAD(P)H oxidase. *Mol Cell Biochem* 264: 85-97

Valavanidis A, Vlahoyianni T, Fiotakis K. 2005. Comparative study of the formation of oxidative damage marker 8-hydroxy-2'-deoxyguanosine (8-OHdG) adduct from the nucleoside 2'-deoxyguanosine by transition metals and suspensions of particulate matter in relation to metal content and redox reactivity. *Free Radic Res* 39: 1071-81

Valko M, Rhodes CJ, Moncol J, Izakovic M, Mazur M. 2006. Free radicals, metals and antioxidants in oxidative stress-induced cancer. *Chem Biol Interact* 160: 1-40

van den Beucken T, Koritzinsky M, Wouters BG. 2006. Translational control of gene expression during hypoxia. *Cancer Biol Ther* 5: 749-55

Veal EA, Day AM, Morgan BA. 2007. Hydrogen peroxide sensing and signaling. *Mol Cell* 26: 1-14

Vengellur A, Woods BG, Ryan HE, Johnson RS, LaPres JJ. 2003. Gene expression profiling of the hypoxia signaling pathway in hypoxia-inducible factor 1alpha null mouse embryonic fibroblasts. *Gene Expr* 11: 181-97

Vij N, Amoako MO, Mazur S, Zeitlin PL. 2008. CHOP transcription factor mediates IL-8 signaling in cystic fibrosis bronchial epithelial cells. *Am J Respir Cell Mol Biol* 38: 176-84

Voggenreiter G, Leiting S, Brauer H, Leiting P, Majetschak M, et al. 2003. Immuno-inflammatory tissue reaction to stainless-steel and titanium plates used for internal fixation of long bones. *Biomaterials* 24: 247-54

Volanti C, Gloire G, Vanderplasschen A, Jacobs N, Habraken Y, Piette J. 2004. Downregulation of ICAM-1 and VCAM-1 expression in endothelial cells treated by photodynamic therapy. *Oncogene* 23: 8649-58

Wagner M, Klein CL, Kleinert H, Euchenhofer C, Forstermann U, Kirkpatrick CJ. 1997. Heavy metal ion induction of adhesion molecules and cytokines in human endothelial cells: the role of NF-kappaB, I kappaB-alpha and AP-1. *Pathobiology* 65: 241-52

Wagner M, Klein CL, van Kooten TG, Kirkpatrick CJ. 1998. Mechanisms of cell activation by heavy metal ions. *J Biomed Mater Res* 42: 443-52

Walch L, Morris PL. 2002. Cyclooxygenase 2 pathway mediates IL-1beta regulation of IL-1alpha, -1beta, and IL-6 mRNA levels in Leydig cell progenitors. *Endocrinology* 143: 3276-83

Walmsley SR, Print C, Farahi N, Peyssonnaux C, Johnson RS, et al. 2005. Hypoxia-induced neutrophil survival is mediated by HIF-1alpha-dependent NF-kappaB activity. *J Exp Med* 201: 105-15

Wang JY, Wicklund BH, Gustilo RB, Tsukayama DT. 1996. Titanium, chromium and cobalt ions modulate the release of bone-associated cytokines by human monocytes/macrophages in vitro. *Biomaterials* 17: 2233-40

Wasil M, Halliwell B, Grootveld M, Moorhouse CP, Hutchison DC, Baum H. 1987. The specificity of thiourea, dimethylthiourea and dimethyl sulphoxide as scavengers of hydroxyl radicals. Their protection of alpha 1-antiproteinase against inactivation by hypochlorous acid. *Biochem J* 243: 867-70

Watanabe H, Pan ZQ, Schreiber-Agus N, DePinho RA, Hurwitz J, Xiong Y. 1998. Suppression of cell transformation by the cyclin-dependent kinase inhibitor p57KIP2 requires binding to proliferating cell nuclear antigen. *Proc Natl Acad Sci U S A* 95: 1392-7

Weidemann A, Johnson RS. 2008. Biology of HIF-1alpha. *Cell Death Differ* 15: 621-7

Weinberg RL, Veprintsev DB, Bycroft M, Fersht AR. 2005. Comparative binding of p53 to its promoter and DNA recognition elements. *J Mol Biol* 348: 589-96

Werner S, Grose R. 2003. Regulation of wound healing by growth factors and cytokines. *Physiol Rev* 83: 835-70

Willam C, Koehne P, Jurgensen JS, Grafe M, Wagner KD, et al. 2000. Tie2 receptor expression is stimulated by hypoxia and proinflammatory cytokines in human endothelial cells. *Circ Res* 87: 370-7

Williams DF. 1981. Titanium and titanium alloys. In *Biocompatibility of clinical implant materials*, ed. DF Williams, pp. 9-44. Boca Raton, Florida: CRC Press

Winterbourn CC. 2008. Reconciling the chemistry and biology of reactive oxygen species. *Nat Chem Biol* 4: 278-86

Wooley PH, Schwarz EM. 2004. Aseptic loosening. *Gene Ther* 11: 402-7

Wu G, Fang YZ, Yang S, Lupton JR, Turner ND. 2004. Glutathione metabolism and its implications for health. *J Nutr* 134: 489-92

Xiong JW, Leahy A, Lee HH, Stuhlmann H. 1999. Vezf1: A Zn finger transcription factor restricted to endothelial cells and their precursors. *Dev Biol* 206: 123-41

Xu Q, Briggs J, Park S, Niu G, Kortylewski M, et al. 2005. Targeting Stat3 blocks both HIF-1 and VEGF expression induced by multiple oncogenic growth signaling pathways. *Oncogene* 24: 5552-60

Yasuda M, Ohzeki Y, Shimizu S, Naito S, Ohtsuru A, et al. 1999. Stimulation of in vitro angiogenesis by hydrogen peroxide and the relation with ETS-1 in endothelial cells. *Life Sci* 64: 249-58

Youn CK, Kim SH, Lee DY, Song SH, Chang IY, et al. 2005. Cadmium down-regulates human OGG1 through suppression of Sp1 activity. *J Biol Chem* 280: 25185-95

Yuan JS, Reed A, Chen F, Stewart CN, Jr. 2006. Statistical analysis of real-time PCR data. *BMC Bioinformatics* 7: 85

Yuan Y, Hilliard G, Ferguson T, Millhorn DE. 2003. Cobalt inhibits the interaction between hypoxia-inducible factor-alpha and von Hippel-Lindau protein by direct binding to hypoxia-inducible factor-alpha. *J Biol Chem* 278: 15911-6

Zahler S, Kupatt C, Becker BF. 2000. Endothelial preconditioning by transient oxidative stress reduces inflammatory responses of cultured endothelial cells to TNF-alpha. *Faseb J* 14: 555-64

Zhang Z, Huang C, Li J, Leonard SS, Lanciotti R, et al. 2001. Vanadate-induced cell growth regulation and the role of reactive oxygen species. *Arch Biochem Biophys* 392: 311-20

Zhao M, Song B, Pu J, Wada T, Reid B, et al. 2006. Electrical signals control wound healing through phosphatidylinositol-3-OH kinase-gamma and PTEN. *Nature* 442: 457-60

Zou W, Yan M, Xu W, Huo H, Sun L, et al. 2001. Cobalt chloride induces PC12 cells apoptosis through reactive oxygen species and accompanied by AP-1 activation. *J Neurosci Res* 64: 646-53

Zumdahl S. 2007. *Chemical Principles*: Brooks Cole. 1073 pp.

Zysk SP, Gebhard H, Plitz W, Buchhorn GH, Sprecher CM, et al. 2004. Influence of orthopedic particulate biomaterials on inflammation and synovial microcirculation in the murine knee joint. *J Biomed Mater Res B Appl Biomater* 71: 108-15

## Publications

**Tsaryk, R**., M. Kalbacova, U. Hempel, D. Scharnweber, R.E. Unger, P. Dieter, C.J. Kirkpatrick, and K. Peters. 2007a. Response of human endothelial cells to oxidative stress on Ti6Al4V alloy. *Biomaterials*. 28:806-13.

**Tsaryk, R**., K. Peters, R.E. Unger, D. Scharnweber, and C.J. Kirkpatrick. 2007b. The effects of metal implants on inflammatory and healing processes. *International Journal of Materials Research*. 98:622-629.

Kalbacova, M., S. Roessler, U. Hempel, **R. Tsaryk**, K. Peters, D. Scharnweber, J.C. Kirkpatrick, and P. Dieter. 2007. The effect of electrochemically simulated titanium cathodic corrosion products on ROS production and metabolic activity of osteoblasts and monocytes/macrophages. *Biomaterials*. 28:3263-72.

Peters, K., R.E. Unger, A.M. Gatti, E. Sabbioni, **R. Tsaryk**, and C.J. Kirkpatrick. 2007. Metallic nanoparticles exhibit paradoxical effects on oxidative stress and pro-inflammatory response in endothelial cells in vitro. *Int J Immunopathol Pharmacol*. 20:685-95.

Peters, K., R.E. Unger, S. Stumpf, J. Schafer, **R. Tsaryk**, B. Hoffmann, E. Eisenbarth, J. Breme, G. Ziegler, and C.J. Kirkpatrick. 2008. Cell type-specific aspects in biocompatibility testing: the intercellular contact in vitro as an indicator for endothelial cell compatibility. *J Mater Sci Mater Med*. 19:1637-44.

## Conference contributions

### Oral presentations:

R. Tsaryk, K. Peters, M. Fischer, R.E. Unger, C.J. Kirkpatrick. $Co^{2+}$ induces oxidative stress and DNA damage in endothelial cells. 21st European Conference on Biomaterials. Brighton, UK. September 9-13, 2007.

R. Tsaryk, K. Peters, R. Unger, M. Feldmann, B. Hoffmann, F. Heidenau, G. Ziegler, C.J. Kirkpatrick. $TiO_2$-coating improves biocompatibility of Co28Cr6Mo alloy to endothelial Cells. 21nd European Conference on Biomaterials. Lausanne, Switzerland. September 7-11, 2009.

### Poster presentations:

Tsaryk R., Kalbacova M., Hempel U., Scharnweber D., Unger R.E., Kirkpatrick C.J., Peters, K. Analysis of oxidative stress in endothelial cells grown on Ti6Al4V. 2nd International Symposium “Interface Biology of Implants”. Rostock, Germany. May 17-19, 2006.

Tsaryk R., Kalbacova M., Hempel U., Scharnweber D., Unger R.E., Kirkpatrick C.J., Peters K. Comparison of Pro-Inflammatory Effects of Oxidative Stress in Human Endothelial Cells Grown on Ti6Al4V and Polystyrene. 20th European Conference on Biomaterials. Nantes, France. September 27 – October 1, 2006.

Tsaryk R., Kalbacova M., Hempel U., Scharnweber D., Unger R.E., Kirkpatrick C.J., Peters K. Study on oxidative stress and pro-inflammatory response of endothelial cells *in vitro* in direct contact to Ti6Al4V. International Symposium Essen 2006. September 5-8, 2006.
R. Tsaryk, K. Peters, R.E. Unger, F. Pröls and C.J Kirkpatrick. Effects of different oxidative stress inducers on unfolded protein response in endothelial cells in vitro. ELSO 2007 Meeting. Dresden, Germany. September 1-4, 2007.

R. Tsaryk, K. Peters, R.E. Unger, D. Scharnweber, C.J. Kirkpatrick. Oxidative stress on Ti6Al4V alloy reduces inflammatory response of endothelial cells. 8$^{th}$ World Biomaterials Congress. Amsterdam, Netherlands. May 28 – June 1, 2008.

R. Tsaryk, K. Peters, R. Unger, M. Feldmann, B. Hoffmann, F. Heidenau, G. Ziegler, C.J. Kirkpatrick. $TiO_2$-coating increases endothelial cell compatibility of Co28Cr6Mo alloy. Jahrestagung der Deutschen Gesellschaft für Biomaterialien. Hamburg, Germany. November 20-22 2008

R. Tsaryk, K. Peters, M. Kalbacova, S. Rössler, U. Hempel, D. Scharnweber, R.E. Unger, C.J. Kirkpatrick. Response of human endothelial cells to cathodic partial reaction of corrosion on Ti6Al4V alloy. 3$^{rd}$ International Symposium "Interface Biology of Implants". Rostock, Germany. May 13-15, 2009.

R. Tsaryk, K. Peters, R. Unger, M. Feldmann, B. Hoffmann, F. Heidenau, G. Ziegler, C. J. Kirkpatrick. Mechanisms of $Co^{2+}$-induced cytotoxicity in endothelial cells in vitro. Jahrestagung der Deutschen Gesellschaft für Biomaterialien. Tübingen, Germany. October 8-10, 2009.